Identification of proviral and host restriction factors that impact the *Flaviviridae* lifecycle

Byron Shue, B.Sc. (Hons)

Department of Molecular and Biomedical Science

School of Biological Sciences

The University of Adelaide

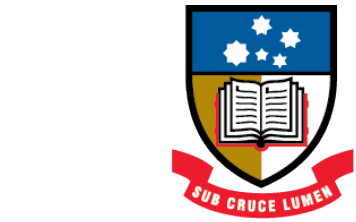

THE UNIVERSITY of ADELAIDE

A dissertation submitted to The University of Adelaide

In candidature for the degree of

Doctor of Philosophy in the Faculty of Sciences

February 2021

Table of Contents

List of Figures and Tables

Thesis Summary

The complex interplay between virus and host is an often overlooked key determinant to the outcome of infection. Host factors are instrumental in supporting the entire virus lifecycle, where a majority have been implicated in the virus replication, especially for the formation of replication organelles. Simultaneously, the innate immune response confers a rapid non-specific defence against invading flaviviruses, where interferon (IFNs) and subsequently interferon stimulated genes (ISGs) are upregulated to directly inhibit virus replication and induction of an antiviral state within a cellular population. Although numerous host factors have been identified and characterised to be critical for the flaviviridae lifecycle through the usage of both RNAi and CRISPR genome-wide screens, limitations with RNAi technology combined with modifications of screening methodology may allow elucidation of novel host factors for virus infection. This thesis aims to identify and characterise novel host factors which positively and negatively influence the flaviviridae lifecycle, using in part genome wide CRISPR knockout (KO) technology.

Hepatitis C Virus (HCV) is a medically important member of the flaviviridae family and thus chosen as a model virus to search for pan-flaviviridae novel host factors. The first aim explores the generation of multiple HCV sub-genomic (SGR) cell lines with mCherry, GFP and thymidine kinase (TK) reporter genes and their compatibility with our chosen screening platform, the GeCKO LentiCRISPRv2 library. Proof of concept experiments with the LentiCRISPRv2 system were performed via simplistic KO of EGFP or Cluster of Differentiation 81 (CD81), demonstrating the effectiveness of CRISPR in targeting both exogenous and endogenous genes. Furthermore, issues which surface upon attempting the genome-wide CRISPR screen with the HCV SGR are addressed and future directions proposed.

The second aim repurposes the optimised GeCKO LentiCRISPRv2 library with an altered screening methodology to identify novel host factors important for ZIKV infection which may also be important for cell survival. Our top hits include previously identified host factors from the endoplasmic reticulum membrane protein complex (EMC) complex in addition to novel host factors Bcl-2-associated X protein 2 (BAX2) and Receptor for Activated C Kinase 1 (RACK1). We show that RACK1 is an important

pro-viral host factor for both mosquito and tick-borne flaviviruses. Furthermore, it plays a critical role in the construction of replication organelles early in the virus lifecycle. Furthermore, flavivirus non-structural protein 1 (NS1) which is important for the biogenesis of vesicle packets (VPs) is able to interact with RACK1 within the ER lumen. Collectively this aim reinforces the utility of CRISPR/Cas9 genome-wide KO screens in the identification of viral host dependency factors and identifies RACK1 as a scaffold protein for the recruitment of viral NS proteins that are essential to the biogenesis of the replication complex.

The third aim investigates the cellular innate immune response to Zika Virus (ZIKV) infection. We show that biologically relevant transformed and primary cells infected with ZIKV have abrogated upregulation of IFN-β and associated ISGs. In addition, we have identified that ZIKV attenuates the RIG-I-like Receptors (RLR) signalling pathway, required for the efficient induction of ISGs. Expression of the highly characterised multifunctional ISG viperin inhibits the ZIKV lifecycle and this observation is complemented by the usage of ZIKV infected viperin-/- mouse embryonic fibroblasts (MEFs). Finally, we show that the C-terminus of viperin is critical for ZIKV antiviral activity, an observation which is supported in future publications by collaborators.

Collectively, this thesis not only enhances our understanding of the flavivirus lifecycle and their complex relationship with the host but also may guide towards the development of effective novel therapeutics against flavivirus infection.

Declaration

I certify that this work contains no material which has been accepted for the award of any other degree or diploma in my name, in any university or other tertiary institution and, to the best of my knowledge and belief, contains no material previously published or written by another person, except where due reference has been made in the text. In addition, I certify that no part of this work will, in the future, be used in a submission in my name, for any other degree or diploma in any university or other tertiary institution without the prior approval of the University of Adelaide and where applicable, any partner institution responsible for the joint-award of this degree.

I give consent to this copy of my thesis when deposited in the University Library, being made available for loan and photocopying subject to the provisions of the Copyright Act 1968.

The author acknowledges that copyright of published work contained within this thesis resides with the copyright holder(s) of those works.

I give permission for the digital version of my thesis to be made available on the web, via the University's digital research repository, the Library Search and also through web search engines, unless permission has been granted by the University to restrict access for a period of time.

Byron Shue

Acknowledgements

#adventureisoutthere!

This quote from the Disney Pixar movie UP is what inspires and motivates me to try new things. Although the destination is often the reward at the end of the adventure, half of the adventure is the journey itself. Throughout my PhD journey, I am both lucky and grateful to have made buddies along the way to what has made the past 6 years unforgettable.

I would like to first thank my supervisor Prof. Michael Beard for the opportunity to conduct my PhD in the Viral Pathogenesis Research Laboratory. I appreciate all the support, confidence (even when it ended badly) and wisdom you provided and also the friendly banter and eye rolls we gave each other when someone did or said something stupid. Also, thanks for helping me fix my bike every time it blew out.

I would also like to thank my co-supervisor Assoc. Prof. Karla Helbig, who supervised me during honours, where both the good and ~~bad~~ habits you taught me are the foundations I needed to complete my PhD. Thank you for all the support you provided from afar, especially when I needed a second opinion.

Thank you to my unofficial co-supervisors Dr. Nick Eyre and Dr. Kylie Van der Hoek (Lab Mum). You guys were always there to hear out my crazy experimental ideas and listen to my frustrations when something didn't work (mainly because I screwed up). Will miss all the yummy muffins and cupcakes you bring in.

I would also like to thank everyone past and present in the lab. I would like to especially thank the following people in no particular order:

- Rosa – our venting sessions, making sure we don't forget the beers on Friday arvos and also helping me with controls for my experiments
- Chuan – for being an excellent across the bench lab mate and also as our resident MD for when I'm too lazy to go to Horace Lamb. Also, thanks for fixing my bike time and time again (I swear that bike is bad luck…).

- Yulee – for teaching me the basics when I was a newbie back in 2014. Sorry, I took too long in TC at 5pm and you had to wait 2 hours for me to finish. Also, I will go to Thailand to visit you one day, that's a pinky promise…
- Emily - honestly, the most ah-mazing lab mate ever (I'm sorry you didn't get 2 sentences, but I think it sums it up nicely).
- Ornella – bringing a super positive vibe into the lab (Top of the morning!). Also dealing with stuff that I didn't wanna touch (mainly ordering, been there – never want to do it again)
- Tom – finally someone who also appreciates the joys of a bargain
- Brandon – for all the friendly chats when there were waiting times for experiments – also believing in FAT FRIDAYS…
- Colt – thanks for teaching me all the cool stuff you learnt in the US. Appreciate that you would go all out to fix my experiments that didn't work, even when I had already given up on them
- Matt – sorry for being your supervisor when you were in honours, where most of your project didn't work… and to never voluntary do it again... but appreciate all the banter and getting me back onto coffee again
- Dave – thanks for introducing me to gym to relieve the stress from lab work… also sorry you took the fall for when Michael found out we were playing broforce in the lab…
- Brooke – for bringing unnecessary stress into my life…. Thanks for tolerating all the endless vocab and sentence grammar during thesis writing and how important it is to have a diary (it's still not gonna happen). Also the queen of strawberry daiquiris and espresso martinis…

Thanks to everyone at MLS who have supported me throughout the years, especially the Peet/Whitelaw Labs (Alexis, Jo, Cam, Ice, Josh, Timmy), the Shearwin Lab (Andrew, Jia), the Bruning Lab (Bec, Steph, Dan), the Grutzner Lab (Eunice, Tahlia, Tash), the Thomas Lab (Chan) and the chemists (BJ, Kat, Henry, Ruth, Joel). Honestly, without all of you guys, the fond memories I have of MLS just wouldn't be the same. Also, thanks to my second lab, the Helbig Lab @ Latrobe (Ebony, Keaton, Monique). Will never forget the conferences we went on together and the number of times we saw our supervisors with a little too much alcohol.

Thanks to all my non-science mates who make sure I'm not spending my entire life in the lab. I would like to especially thank my best bud of 20 years Abhi for all the support he has given me throughout the years. Thank you to all my ex-KFC mates (Radhe, Chris, Ellise, Spring, Vaishali, Denise), my badminton/camping buddies (Cindy, Michelle), my third wheeling gym buddies (Dave, Kristi, Chris, Dharsh), my undergrad buddies (Jesse, Alex, Lillian, Lenna, Nhan, Thu) and my childhood pals from NZ (Sam, Eugene, Beau, Anuj).

And finally, I'll like to thank my family (Mum, Dad, Stella, Han) for their continued love, support and encouragement throughout my PhD. Although our family doesn't say I love you all that much (it's an Asian thing), I'll always cherish the phone calls at 5pm asking when I'll be home for dinner (Wei…) and making sure that even if my day in the lab has been disastrous and frustrating, you guys would always know how to make it better. Don't worry mum, I got a job!!!

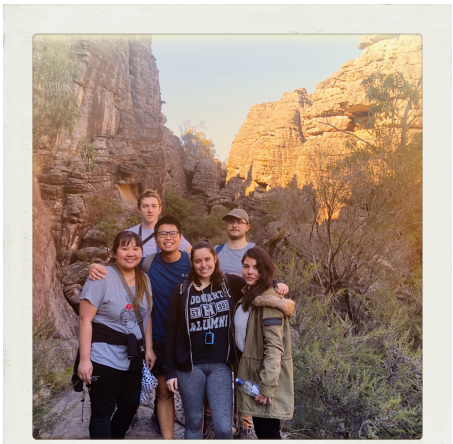

Presentations

Van der Hoek KH, Eyre NS, **Shue B,** Khantisitthiporn O, Glab-ampai K, Jankovic-Karasoulos T, Roberts C, Jolly L, Carr JM, Helbig KJ and Beard MR. Attenuation of the host innate reponse to ZIKV in placental trophoblasts and neural progenitor cells, Lorne, Australia, 2016. (poster presentation)

Shue B, Eyre NS, Helbig KJ and Beard MR. Identification of novel host factors critical for HCV replication using a CRISPR/Cas9 genome-wide KO screen. Australian Centre for Hepatitis Virology and HIV virology interest group, Barossa Valley, Australia, 2017. (poster presentation)

Shue B, Eyre NS, Pederson S and Beard MR. CRISPR/Cas9 genome-wide KO screen approach to identify novel host factors for ZIKV replication. 9th Australasian Virology Society Meeting, Adelaide, Australia, 2017. (oral presentation)

Shue B, Eyre NS, Pederson S and Beard MR. CRISPR/Cas9 genome-wide KO screen reveals RACK1 as a critical pan-flavivirus host factor for virus replication. Adelaide Protein Group Meeting, Adelaide, Australia, 2018. (oral presentation) – Finalist for best student presentation

Shue B, Eyre NS, Thu H, Pederson SM, Helbig KJ, Best SM and Beard MR. CRISPR/Cas9 Genome-wide KO screen reveals RACK1 as a critical host factor for Flavivirus replication, 37th American Society for Virology meeting, University of Maryland, USA, 2018. (poster presentation) – ASV 2018 Student Travel Award

Shue B, Eyre NS, Thu H, Pederson S, Chiramel A, Broeckel R, Best S and Beard M. CRISPR/Cas9 genome-wide KO screen reveals RACK1 as a critical flavivirus host

factor for virus replication, 25th International Symposium on Hepatitis C Virus and Related Viruses, Dublin, Ireland 2018. (oral presentation)

Shue B, Eyre NS, Thu H, Pederson S and Beard MR. RACK1, flexible storage for all your Flavivirus replication needs. Adelaide Protein Group Meeting, Adelaide, Australia, 2019. (oral presentation) - Finalist for best student presentation

Shue B, Eyre NS, Thu H, Pederson S and Beard MR. CRISPR/Cas9 genome-wide KO screen reveals RACK1 as a critical pan-flavivirus host factor for virus replication. The Australian Society for Microbiology 2019 Meeting, Adelaide, Australia 2019. (oral presentation)

Shue B, Eyre NS, Thu H, Lim CK, Chiramel A, Pederson SM, Best SM and Beard MR. Screening for the "CRISPR" perspective of RACK1 as a critical pan-flavivirus host factor for virus infection. 10th Australasian Virology Society Meeting, Queenstown, New Zealand, 2019. (oral presentation) – AIDRC Student Presentation Award

Publications

Van Der Hoek KH, Eyre NS, **Shue B**, Khantisitthiporn O, Glab-Ampi K, Carr JM, Gartner MJ, Jolly LA, Thomas PQ, Adikusuma F, Jankovic-Karasoulos T, Roberts CT, Helbig KJ & Beard MR, Viperin is an important host restriction factor in control of Zika virus infection. Sci Rep, 7, 4475. 2017

Shue B, Chiramel AI, Cerikan B, To T-H, Pederson SM, Eyre NS, Bartenschlager RFW, Best SM and Beard MR. Genome-wide CRISPR KO screen identifies RACK1 as a critical host factor for flavivirus replication – manuscript submitted

Publications in addition to this thesis

Coldbeck-Shackley RC, Tate MD, Rosli S, Gearing LJ, Gould JA, Lim SS, Van der Hoek KH, Eyre NS, **Shue B**, Robertson SA, Best SM, Hertzog PJ and Beard MR. IFN-epsilon is a distinct constitutively expressed type-I IFN in the female reproductive tract that protects against ZIKV infection – manuscript submitted

Khantisitthiporn O, **Shue B**, Eyre NS, Nash CW, Turnbull L, Whitchurch CB, Van der Hoek KH, Helbig KJ and Beard MR. Viperin interacts with PEX19 to mediate peroxisomal augmentation of the innate antiviral response – manuscript accepted into Life Science Alliance.

Materials Providers

Abcam	Cambridge, UK
Addgene	Massachusetts, USA
AGRF	Adelaide, Australia
Ambion	Texas, USA
Applied Biosystems	Massachusetts, USA
ATCC	Virginia, USA
BD Biosciences	New Jersey, USA
Beckman Coulter	Miami, FL, USA
Bioline	Sydney, Australia
Bio-Rad Laboratories	California, USA
Cell Signaling	Massachusetts, USA
Chem-Supply	Adelaide, Australia
Corning Life Sciences	New York, USA
Dharmacon Inc	Colorado, USA
Eppendorf	Hamburg, Germany
GenScript	New Jersey, USA
Gibco	New York, USA
GraphPad Software Inc.	California, USA
Implen GmbH	Munich, Germany
iNtRON Biotechnology	Seoul, South Korea
Illumina Inc	California, USA
Invitrogen	California, USA
Life Technologies	California, USA
Livingstone	Sydney, Australia
Lucigen	Wisconsin, USA
Macherey Nagel	Düren, Germany
Merck Millipore	Massachusetts, USA
Nalge Nunc International	New York, USA
New England Biolabs	Massachusetts, USA
Nikon	Tokyo, Japan
Olink	Uppsala, Sweden
Olympus	Tokyo, Japan

Panasonic Healthcare	Tokyo, Japan
Perkin Elmer	Massachusetts, USA
Promega	Wisconsin, USA
Qiagen	Hilden, Germany
Santa Cruz Biotechnology	Texas, USA
Sigma Aldrich	Missouri, USA
SnapGene	California, USA
STEMCELL Technologies	Vancouver, Canada
Stratagene	California, USA
Thermo Fisher Scientific	Massachusetts, USA
Toolgen	Seoul, South Korea
UVP Inc	California, USA
Vector Laboratories	California, USA

Abbreviations used

Abbreviation or Symbol	Term
× *g*	Acceleration gravity
°C	Degree(s) Celsius
5’ppp	5’ triphosphate
μg	Microgram(s)
μl	Microliter(s)
μm	Micrometer(s)
μM	Micromoles
A	Adenine
aa	Amino acids
ADE	Antibody-dependent enhancement
ATP	Adenosine triphosphate
bp	Base pair(s)
BSA	Bovine serum albumin
C	Cytosine
CARD	caspase recruitment and activation domains
cccDNA	Covalently closed circular DNA
CD81	Cluster of Differentiation 81
cDNA	Complementary deoxyribonucleic acid
cGAS	Cyclic-GMP-AMP synthase
cGAMP	2’3’-cyclic GMP-AMP
CHC	Chronic hepatitis C
CLDN	Claudin
CMV	Cytomegalovirus
CPE	Cytopathic effect
CRISPR	Clustered Regularly Interspaced Short Palindromic Repeats
crRNA	CRISPR targeting RNA
CTD	C-terminal domain
CypA	Cyclophilin A
CZS	Congenital ZIKV syndrome

DAA	Direct acting antiviral
DAPI	4', 6-Diamidino-2-pheylinodole
dATP	Deoxyadenosine triphosphate
dCas9	Dead Cas9
DC-SIGN	Dendritic cell-specific intercellular adhesion molecule-3-Grabbing non-integrin
dCTP	Deoxycytosine tripshosphate
ddhCTP	3'-deoxy-3',4'-didehydro-CTP
DENV	Dengue Virus
DF	Dengue Fever
dGTP	Deoxyguanosine triphosphate
dH_2O	Deionised water
DHF	Dengue Hemorrhagic Fever
DMEM	Dulbecco's Modified Eagle Medium with HEPES
DMSO	Dimethyl sulfoxide
DMV	Double-membrane vesicle
DNA	Deoxyribonucleic acid
dNTP	Deoxynucleotide triphosphate
DSB	Double strand break
dsRNA	Double stranded RNA
DSS	Dengue Shock Syndrome
DTT	Dithiothreitol
dTTP	Deoxythymidine triphosphate
E	Envelope
EBV	Epstein-Barr Virus
ECMV	Encephalomyocarditis virus
EDTA	Ethylenediamine tetraacetic acid
eIF	E74-like factor
ER	Endoplasmic reticulum
FACS	Fluorescence-activated cell sorting
FASN	Fatty acid synthase
FCS	Foetal calf serum

ffu	Focus forming units
G	Guanosine
g	Gram(s)
GAGs	Glycosaminoglycans
GBS	Guillan-Barré syndrome
GBF1	Golgi brefeldin A-resistant guanine nucleotide exchange factor 1
GeCKO	Genome-scale CRISPR knock-out
GFP	Green fluorescent protein
gRNA	Genomic RNA
HCC	Hepatocellular carcinoma
HCEC	Human primary corneal epithelial cells
HCV	Hepatitis C virus
HCVcc	Cell-culture propagated hepatitis C virus
HEPES	4-(2-hydroxyethyl)-1-piperazineethanesulfonic acid
HIV	Human immunodeficiency virus
hr	Hour(s)
HRP	Horse radish peroxidase
Huh	Human hepatoma
IFI6	IFN-inducible protein 6
IFITM	IFN-inducible transmembrane
IFN	Interferon
IFN-γ	Interferon gamma
IFN-α	Interferon alpha
IFN-β	Interferon beta
IFN-λ	Interferon lambda
IFNAR	Interferon-alpha/beta receptor
Ig	Immunoglobulin(s)
IKKε	Iκβ kinase-ε
IL	Interleukin
IRES	Internal ribosome entry site
IRF	Interferon regulatory factor

ISRE	Interferon stimulated response element
ISGs	Interferon stimulated genes
ISG15	IFN stimulated gene 15
ISGF3	IFN stimulated gene factor 3
IVDU	Intravenous drug use
JAK	Janus kinase
JEV	Japanese Encephalitis Virus
JFH-1	Japanese patient with fulminant hepatitis
kb	Kilobase
kDa	Kilodalton(s)
KFDV	Kyasanur Forest disease virus
kg(s)	Kilogram(s)
KO	Knock out
L-Agar	LB + agar
LB	Luria Bertani broth
LD	Lipid droplet
LDL-R	Low-density lipoprotein receptor
LGP2	Laboratory of genetics and physiology 2
LGTV	Langat virus
LIV	Louping ill virus
Luc	Luciferase
M	Mole
mA	Milliampere(s)
MAVS	Mitochondrial antiviral-signaling protein
MCS	multiple cloning site
MDA5	Melanoma differentiation associated factor 5
MEM	Minimum Essential Medium
mg	Milligram(s)
MHC	Major Histocompatibility Complex
min	Minute(s)
miR122	Micro-RNA 122
ml	Milliliter(s)
mM	Millimolar(s)

MMV	Multi-membrane vesicle
MOI	Multiplicity of infection
mRNA	Messenger ribonucleic acid
MTase	Methyltransferase
MuV	Mumps Virus
MW	Molecular weight
Mx1	MX Dynamin Like GTPase 1
N/A	Not applicable
NANBH	Non-A, non-B hepatitis
NF-κB	Nuclear factor kappa-light-chain-enhancer of activated B cells
ng	Nanogram(s)
NHEJ	Non-homologous end joining
nM	Nanomolar
NS	Non-structural
nt (s)	Nucleotide (s)
OAS	2'-5'-Oligoadenylate Synthetase
OCLN	Occludin
OHFV	Omsk hemorrhagic fever virus
ORF	Open reading frame
OSBP	Oxysterol-binding protein
OST	Oligosaccharyltransferase
PAM	Protospacer adjacent motif
PAMPS	Pathogen associated molecular patterns
PBMCs	Peripheral blood mononuclear cells
PBS	Phosphate buffered saline
PCR	Polymerase chain reaction
pDCs	Plasmacytoid dendritic cells
PEG	Polyethylene glycol
pg	Picograms
pH	Negative logarithm of hydrogen ion activity
PI4KA	Phosphatidylinositol 4-kinase III alpha
PI4P	Phosphatidylinositol 4-phosphate

PKR	Protein kinase R
pmol	Picomolar
POWV	Powassan virus
prM	Pre-membrane
PRRs	Pattern recognition receptors
Rab	Ras-associated binding
RC	Replication complex
RdRp	RNA-dependent RNA polymerase
RIG-I	Retinoic acid-induced gene-I
RISC	RNA-induced silencing complex
RLR	RIG-I like receptors
RNA	Ribonucleic acid
RNAi	RNA interference
RNase	Ribonuclease
rpm	Revolutions per minute
RT	Reverse transcriptase or Room Temperature
RT-PCR	Reverse transcriptase polymerase chain reaction
SDS	Sodium dodecyl sulfate
SDS-PAGE	Sodium dodecyl sulfate polyacrylamide gel electrophoresis
sec	Second(s)
SGR	Sub-genomic replicon
sgRNA	Single guide RNA
shRNA	Short hairpin RNA
siRNA	Short interfering RNA
SLA	Stem-loop A
SLB	Stem-loop B
SMV	Single-membrane vesicle
sNS1	Secreted NS1
SOC	Super optimal broth with catabolite repression
SRB1	Scavenger receptor class B1
ss	Single stranded

STAT	Signal transducer and activator of transcription
STING	Stimulator of Interferon Genes
T	Thymidine
TAE	Tris, acetic acid, EDTA (TAE) buffer
TALEN	Transcription activator-like effector nuclease
TAM	TYRO3, AXL and MERTK
TBEV	Tick-borne encephalitis virus
TBFV	Tick-borne flaviviruses
TBK1	TANK-binding kinase 1
TEMED	N,N,N',N'-tetramethylethylenediamine
TIM	T-cell Ig mucin
TLR	Toll-like receptor
TNF-α	Tumor necrosis factor alpha
tracRNA	Trans-acting RNA
TRIF	TIR-domain-containing adapter-inducing interferon-β
TRIM	Tripartite motif
TYK2	Tyrosine kinase 2
U/μl	Unit(s) per microliter
UTR	Untranslated region
UV	Ultraviolet
V	Volt(s)
v/v	Volume per volume
VAPA	Vesicle-associated membrane protein-associated protein A
Viperin	Virus inhibitory endoplasmic reticulum associated interferon inducible protein
VLDL	Very low density lipoprotein
VP	Vesicle packet
w/v	Weight per volume
WNV	West Nile Virus
WHO	World Health Organization
WT	Wild-type

x g	Acceleration gravity
X-α-gal	5-bromo-4-chloro-3-indolyl-α-D-galactopyranoside
YFV	Yellow Fever Virus
ZIKV	Zika Virus

Chapter 1 - Introduction

1.1 The Flaviviridae family

The *flaviviridae* family consists of a group of enveloped viruses with a positive sense RNA genome. Viruses in this family are grouped, according to similarities in their genome structure and canonical lifecycle of replication, into multiple genera. The two most prominent are the *hepacivirus* and *flaviviruses*. Viruses from these genera, such as Hepatitis C virus (HCV) and Dengue virus (DENV) and Zika virus (ZIKV) respectively, are classified as major human pathogens that inflict a worldwide burden on society. As obligate intracellular parasites, viruses have evolved multiple strategies to manipulate infected cells to support their own replication. However, research indicates that the subtle differences in how these viruses manipulate the cell allows them each to flourish in their unique niches.

1.2 Discovery and Epidemiology

The flaviviridae family consists of four genera; *Flavivirus, Hepacivirus, Pegivirus and Pestivirus* (Fig. 1.1). The *Flavivirus* genus is named after the Yellow Fever virus (YFV), where the Latin word for "yellow" is *flavus*, describing yellowing of the skin as a visible symptom of liver damage caused by virus infection. This genus is composed of over 80 viruses of which several with high medical importance will be discussed below (Kuno et al. 1998; King et al. 2012).

YFV has had a huge impact historically, with epidemics recorded in the 18th and 19th century in North and Central America and Europe, likely introduced via ships originating from Africa (Cathey and Marr 2014). Flaviviruses were originally categorised into the Togaviridae family which include Chikungunya virus, Rubella virus and Ross River virus based on early serological assessment but in 1984 they were re-classified into the flaviviridae family when research made it apparent that these viruses differ to other Togaviridae significantly in both virion structure and virus lifecycle.

The earliest official Dengue virus (DENV) infection was recorded in 1779 in Java, Indonesia by David Bylon after centuries of etiological confusion between the former

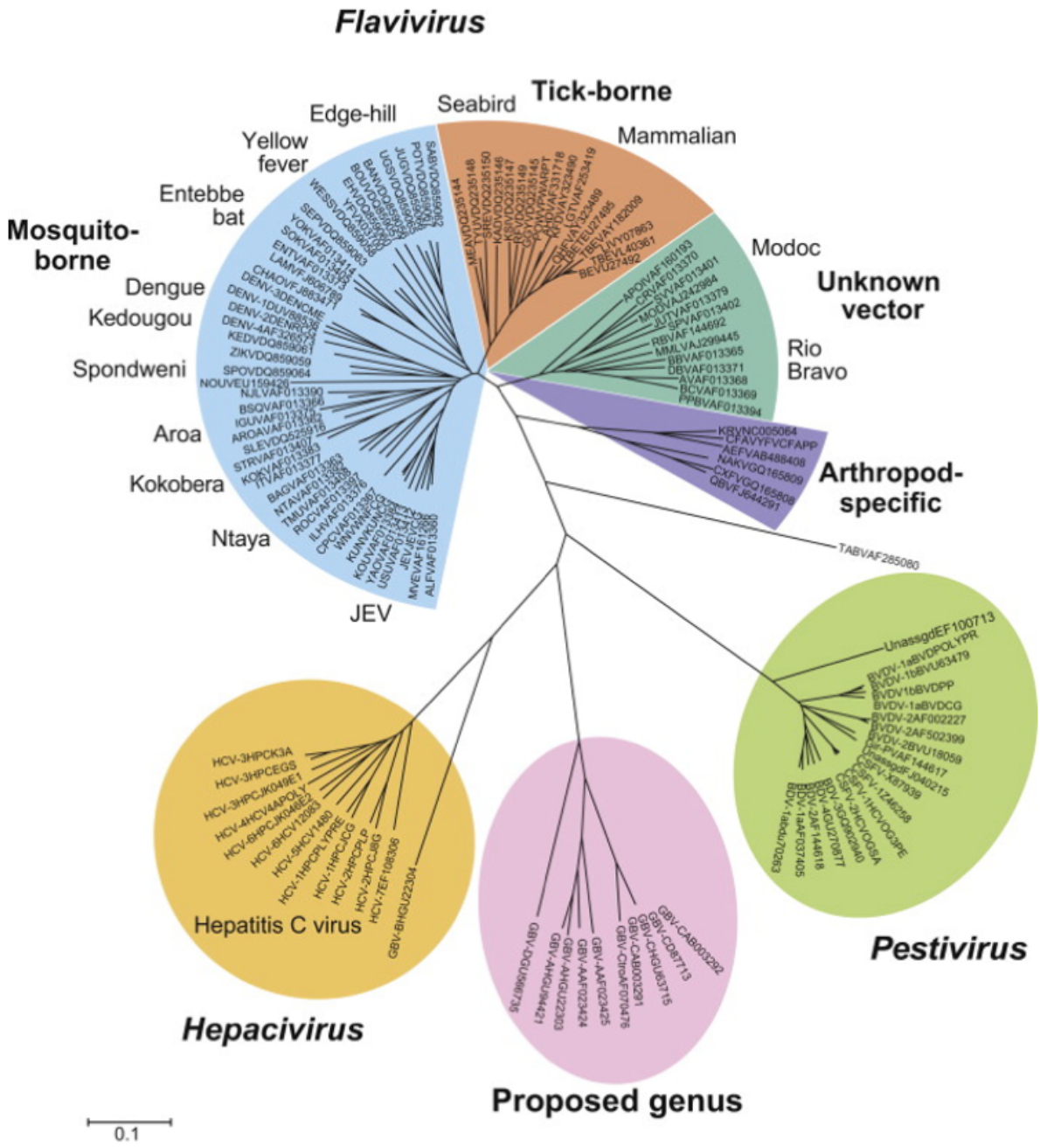

Figure 1.1: Phylogeny of the *flaviviridae* family based on genetic analysis of the NS5 (NS5B) RdRp

The *flaviviridae* family is composed of 4 genera; flaviviruses, hepaciviruses, pestiviruses and pegiviruses (King *et al.* 2012).

and Chikungunya virus due to their similarities in pathogenesis in causing arthritis in patients (Halstead 2015). DENV is currently endemic in at least 100 countries located within the Asia-Pacific, African and American regions, where annually approximately one million infected individuals display symptoms of dengue fever or dengue haemorrhagic fever and approximately 5% succumb to infection (Fig. 1.2). In contrast, ZIKV was first identified in 1947 in a sentinel rhesus macaque in Uganda with little impact on public health systems until 2005, where the first outbreak outside of Africa and Asia occurred on Yap state in the Federated states of Micronesia, resulting in approximately 72% of the population infected (Musso et al. 2014). Another outbreak in 2013 in French Polynesia identified a possible link between ZIKV and Guillan-Barré syndrome (GBS) where an increase in severe neurological manifestations were reported (Musso et al. 2014). Global attention to ZIKV increased dramatically in 2015, when spread of the ZIKV infection skyrocketed to upwards of 1.3 million cases in Brazil following increased population movement due to the 2015 FIFA world cup and 2016 Rio Olympic games. To date, at least 87 countries and territories have recorded evidence of mosquito-borne transmission of ZIKV (WHO).

Transmission of the above flaviviruses is highly dependent on the activity and geographic distribution of arthropod vectors (Fig. 1.2). Rapid urbanisation, increased international travel and ongoing climate change are all factors that increase the range of the Aedes (DENV/ZIKV) and Culex (West Nile Virus (WNV) and Japanese Encephalitis Virus (JEV)) species of mosquitoes which in turn greatly expands the areas these viruses are now endemic (Daep et al. 2014).

Unlike flaviviruses, HCV was classified as non-A and non-B hepatitis virus (NANBH) until 1989 when the viral genome was isolated from NANBH patient serum (Choo et al. 1989). 170 million people are now infected worldwide with HCV, with 500,000 patients succumbing to HCV-related liver disease each year (Fig. 1.3) (Thomas 2013; Messina et al. 2015). In Australia, it is estimated that 264,000 are infected with HCV and it is the most common cause of clinically significant liver disease as a result of virus induced liver cirrhosis and hepatocellular carcinoma (HCC) (Razali et al. 2009). However, in contrast to the above mentioned flaviviruses, we now have efficacious therapeutics for HCV that is further discussed below.

1.3 Transmission

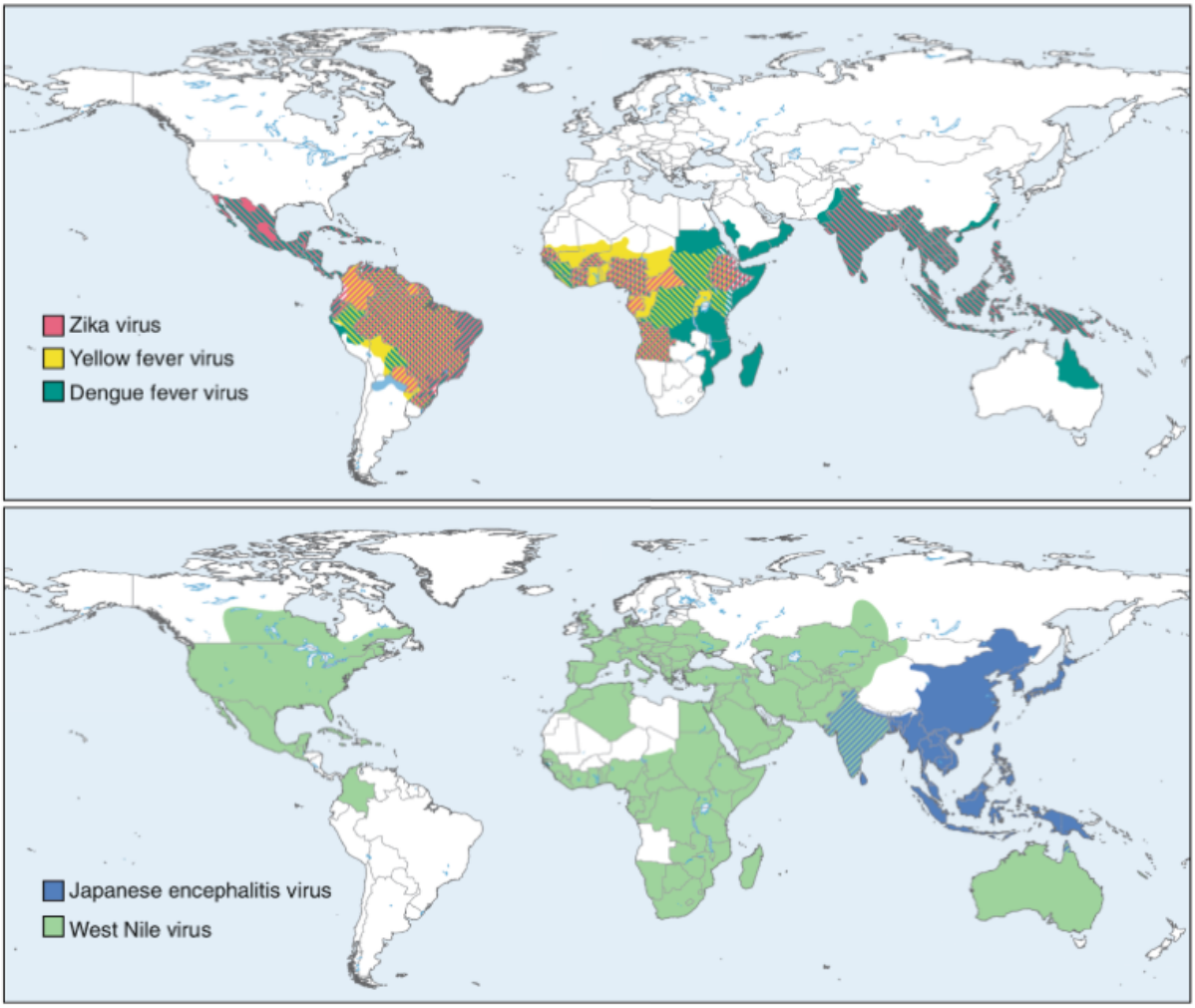

Figure 1.2: Global distribution of flavivirus infection.

Worldwide distribution of flaviviruses varies in geographical area, dependent on the habitual area of the mosquito vector. West Nile Virus, Zika Virus and Dengue virus are distributed worldwide whereas Japanese Encephalitis Virus and Yellow Fever are endemic in specific areas (Pierson & Diamond 2020).

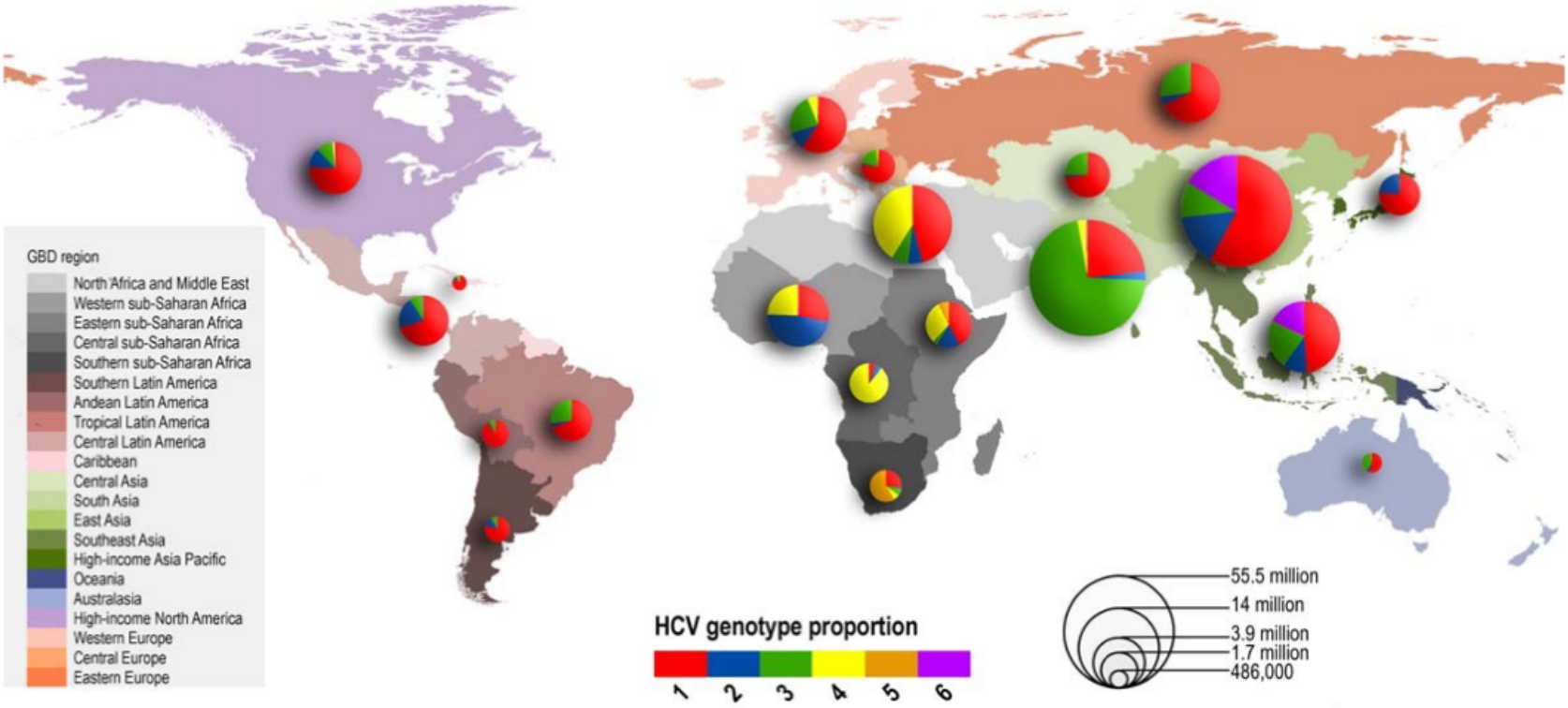

Figure 1.3: Global distribution of HCV genotypes.

Worldwide distribution of HCV varies in geographical area where genotypes 1-3 are widely distributed across the world and genotypes 4-6 are endemic to specific areas (Messina et al. 2015)

Members of the *flaviviridae* family are split into two groups when considering transmission of virions from one host to another: arthropod dependent or arthropod independent transmission.

1.3.1 Arthropod dependent transmission

Arthropod-dependant flaviviruses are generally categorised into two groups defined by the arthropods that carry them, mosquito-borne and tick-borne.

1.3.1.1 Mosquito-borne transmission

Historically, the link between the role of mosquitos in transmitting agents that result in flavivirus disease, such as yellow fever was first reported in 1881, while in Cuba in 1900 Major Walter Reed deduced that yellow fever was a filterable agent responsible for the outbreak of yellow fever (Brès 1986; Clements and Harbach 2017). Since then, multiple viruses within the flaviviridae family, especially in the flavivirus genus have been found to utilise the mosquito as the primary arthropod for transmission. The mosquito (namely *Aedes aegypti and Aedes albopictus)* is able to transmit virions via a blood meal of an infected host. In the case of flaviviruses, the natural reservoir (host) is often wild birds and domesticated animals, where infection of the former results in negligible pathogenesis despite high viremic load. The consensus is that high viremic load is critical for efficiency of transmission for not only flaviviruses, but other viruses as well. This is the main reason why humans are often a dead end for most flaviviruses, as transmission from one human to another is inefficient due to low viremia during infection. One exception to this rule is Dengue virus, where high viremia in humans means they can act as a reservoir for epidemics to spread. Vector control of mosquitoes is utilised in developing countries to prevent flavivirus transmission. This primarily involves the usage of insecticide treated nets and sprays. Mosquitoes have however adapted to develop resistance to insecticides and also changes in feeding schedules (Liu 2015). To bypass the need for insecticides trials involving the introduction of the bacteria Wolbachia into *Aedes aegypti* to not only control population levels of flavivirus carrying mosquitoes but also directly block virus transmission are ongoing (Ford et al. 2019). As a naturally existing gram-negative bacterium, Wolbachia is harmless to humans but transmitted vertically in mosquitoes. Infection distorts sex ratio phenotypes of progeny mosquitoes through a number of mechanisms,

including feminisation of genetic males, parthenogenetic induction, the killing of male progeny from infected females and cytoplasmic incompatibility (Werren et al. 2008). In addition, *aedes aegypti* mosquitoes harbouring Wolbachia are highly resistant to infection of circulating ZIKV strains and therefore also prevent viral transmission (Dutra et al. 2016). Although innovative vector control strategies utilising Wolbachia shows great promise to supress transmission of flaviviruses, antivirals and vaccines will still be required to control virus infection.

1.3.1.2 Tick-borne transmission

Although ticks carry multiple pathogens including bacteria, protozoa and viruses, the tick-borne flaviviruses (TBFV) are considered major pathogens worldwide. Ioxdidae (hard ticks) and Argasidae (soft ticks) are the main families of ticks that transmit flaviviruses. Unlike mosquitoes where multiple species such as *Aedes aegypti* have a global distribution in transmitting flaviviruses, TBFV are transmitted by ticks which reside in specific geographical locations (Grabowski and Hill 2017). Currently, there are seven mammalian TBFV of known or putative (implicit) medical importance; Kyasanur Forest disease virus (KFDV), Karshi virus, Langat virus (LGTV), Louping ill virus (LIV), Omsk hemorrhagic fever virus (OHFV), Powassan virus (POWV) and Tick borne encephalitis virus (TBEV) (Kemenesi and Bányai 2019). TBEV and LIV are endemic in both Europe and Asia whereas OHFV, LGTV, KFDV and Karshi virus are present only in the latter. POWV is the only known member of the TBFV family endemic across North America, where transmission rates have been increasing annually and the fatality rate of virus induced encephalitis exceeds 30% in some cases (Hinten et al. 2008; Hermance and Thangamani 2017). Other TBFVs that cause meningitis and encephalitis in humans include, TBEV, LIV, LGTV and Karshi virus while OFHV and KFDV induce haemorrhagic fever in infected patients (Kemenesi and Bányai 2019).

1.3.2 Arthropod independent transmission

The main vector-independent virus in the flaviviridae family is the hepacivirus Hepatitis C virus (HCV). This virus is transmitted via entry of contaminated infected blood directly into blood stream. Blood transfusion was the main mode of infection until 1992, when improvements in blood screening technology eliminated HCV contamination in

donor blood. However, in developing countries inappropriate medical procedures combined with inadequate blood screening technology means this type of transmission remains prevalent. In developed countries HCV is now predominately transmitted by intravenous drug use (IVDU) particularly through sharing virus-contaminated needles and syringes (Ng et al. 2015). Other modes for transmission of HCV include tattooing, piercing, sexual intercourse or vertical transmission from mother to baby during pregnancy (S. L. Thomas et al. 1998; Fauteux-Daniel et al. 2017). Although flaviviruses were thought to be only transmitted by mosquitoes, there is evidence that DENV can be vertically transmitted, although this is a rare event most likely due to the short duration of viremia (Yin et al. 2016). In addition, during the outbreak of ZIKV in the Americas in 2015, it was found ZIKV can be readily transmitted vertically due to the virus's ability to infect the reproductive organs of both sexes and cross the placental barrier during pregnancy, resulting in congenital Zika syndrome in the foetus (Chan et al. 2016; Krauer et al. 2017).

1.4 Pathogenesis

Due to the diverse nature of members of the *flaviviridae* family, pathogenesis of disease differs significantly. As members of the *flaviviridae* family do not integrate their genome into host cell genetic material, clinical outcomes of infection are mediated either directly through viral factors or indirectly through interaction with the immune response of the infected individual.

Our understanding of the intricacies of flavivirus pathogenesis is still limited in part due to the lack of a suitable models of disease progression. Immuno-compromised mice that cannot respond to type I IFN ($IFNAR^{-/-}$) are widely used as an animal model for DENV, WNV and ZIKV infection, as they support replication of clinical isolates (Wong and Qiu 2018). However, the clinical symptoms arising in these mouse models do not mirror those seen in humans. Although non-human primates do not present clinical disease, the onset of viremia and the production of humoral immune responses against flaviviruses is similar to that seen in humans indicating non-human primates can be utilised for vaccine testing (Estes et al. 2018).

Flaviviruses can be categorised into two groups defined by the clinical outcomes the infection produces, one being vascular leakage and haemorrhage (DENV and YFV)

and the other encephalitis (JEV and WNV). Flaviviruses such as DENV, JEV, WNV and ZIKV all induce cytopathic effects (CPE) on the infected cell type during replication. However, the mechanism by which CPE is induced by each flavivirus is unique. Most infections (up to 80%) by flaviviruses are asymptomatic or result in mild flu-like symptoms, however failure to clear flavivirus infection in an individual may progress to more severe clinical outcomes.

Although is still not possible to predict which individuals will progress to severe clinical disease post infection, epidemiological studies have shown that there are several risks factors including age (younger for DENV and JEV/older for WNV), high body mass index, viral strain, gender, genetic variation in genes involved in innate immune response (MHC class I/TNF-α) and receptors for viral entry (DC-SIGN), environmental conditions, such as mosquito spread and temperature, and previous exposure to flavivirus infection (Daep et al. 2014). Although HCV, DENV and ZIKV are all viruses within the *flaviviridae* family and thus have similar replication strategies, each cause unique pathological disease during virus infection which will be discussed below.

1.4.1 Dengue Virus

The numerous symptoms which are collectively referred to as Dengue Fever (DF) have been identified by various observations of both natural and experimental origins since the 1920s. These symptoms often occur after an incubation period of 3-15 days with the first of these including the onset of fever, chills and breakbone headaches. Young children can often present with respiratory symptoms as well as maculopapular rash of the trunks and/or limbs. Although young children often experience less severe disease from primary DENV infection compared to adults, they are more susceptible to severe outcomes from secondary infection in endemic areas via antibody dependent enhancement (ADE). Other symptoms which arise from Dengue Fever include nausea and vomiting, lymphadenopathy, leukopenia and insufficient coagulation complications (Fig. 1.4) (Chuang et al. 2013). Viremia duration ranges from 1-7 days post infection and is often absent approximately the same time the fever dissipates.

Dengue Haemorrhagic Fever (DHF) is primarily physiologically distinguished from Dengue Fever by the leakage of plasma, termed vascular leakage, and is often the

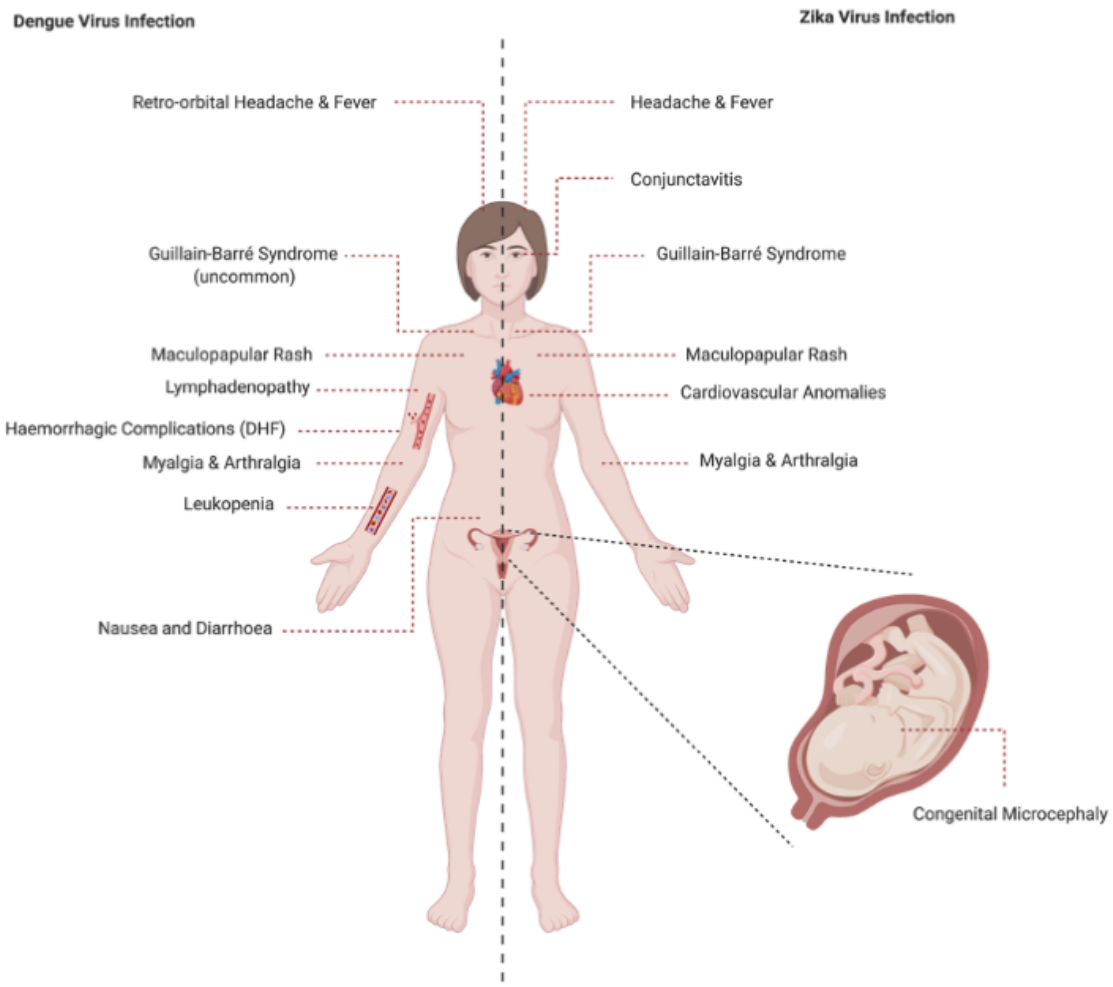

Figure 1.4: Clinical symptoms of Dengue (DENV) and Zika (ZIKV) Virus infection. Symptoms for DENV and ZIKV infections are similar in the acute phase, resulting in headaches, rash, myalgia and arthralgia. However, patients with DENV infection can progress to Dengue Haemorrhagic Fever (DHF), resulting in organ haemorrhage and vascular leakage. Pregnant women infected with ZIKV can vertically transmit the virus to the foetus, resulting in congenital microcephaly.

determinant of severity of disease (Fig. 1.4) (Chuansumrit and Chaiyaratana 2014).

There are four grades of disease for patients diagnosed with DHF as outlined by the World Health Organisation. Grade I is classified as high fever accompanied by symptoms which resemble DF, whereas Grade II includes spontaneous haemorrhagic manifestations which results in positive tourniquet tests, measuring both capillary fragility and thrombocytopenia (Chuansumrit and Chaiyaratana 2014). Grade III and IV are classified as Dengue Shock Syndrome (DSS) where the condition of patients deteriorates rapidly, resulting in circulatory failure brought on low blood pressure and characterised by rapid weak pulse with, cold skin and restlessness (Chuansumrit and Chaiyaratana 2014).

There is also the potential complication of ADE upon DENV re-infection. Pre-existing antibodies that develop against one serotype of DENV bind to a DENV virion of a different serotype and aid viral entry in a subsequent infection. The antibody-virion complex that forms is able to bind Fcγ receptors present on the cell surface of macrophages, promoting fusion and entry of viral particles as well as enhancing DENV infection (Flipse et al. 2016). In addition, an extensive cross-reactive antibody response is observed between DENV and ZIKV due to the high similarity of the envelope protein of both viruses (Priyamvada et al. 2016). Thus, antibodies from a previous DENV infection have been shown to confer either protective (cross-neutralisation) or inhibitory ADE effects on a sequential ZIKV infection (Dejnirattisai et al. 2016; Paul et al. 2016; Robbiani et al. 2017; Pantoja et al. 2017).

1.4.2 Zika Virus

Patients infected with ZIKV present with febrile disease consisting of flu-like symptoms in about 20% of individuals and most fully recover within days. These symptoms are similar to that of DENV but may include arthralgia, rash and cardiovascular complications (Fig. 1.4). However, a rare subset of patients may develop Guillain-Barré Syndrome (GBS), an autoimmune condition where the patient's immune response attacks the peripheral nerve myelin proteins. These patients can die from complications arising from blood infections and paralysis of muscles critical for breathing (Krauer et al. 2017). The link between ZIKV infection and its ability to cause microcephaly in infants born to ZIKV infected mothers only became evident as the

2015 epidemic in Brazil progressed. ZIKV infected infants may develop Congenital ZIKV Syndrome (CZS), which encompasses a unique spectrum of congenital defects including microcephaly, ocular abnormalities, delays in neurological development and arthrogryposis (Fig. 1.4) (Del Campo et al. 2017). In addition, neurodevelopment abnormalities were observed in children without ZIKV induced CZS at birth and thus further follow up on infants with *in utero* exposure is required to assess the impacts of congenital infection on adulthood (Mulkey et al. 2020). To date, this is the only flavivirus that can cross the placental barrier and infect the developing foetus, furthermore the mechanisms by which ZIKV is able to cross the placental barrier and induce CZS remain poorly understood.

1.4.3 Hepatitis C Virus

Due to cell specificity of infection, pathogenesis of HCV is limited mainly to the liver. As HCV is a non-cytopathic virus, liver disease as a result of infection occurs slowly and is primarily driven by both innate and adaptive immune responses to HCV infected hepatocytes, leading to immune-mediated cytolysis. Although hepatocytes are the main target during HCV infection, HCV RNA has been reported in other cell types including macrophages, monocytes and dendritic cells (Liu et al. 2019). However, this is somewhat controversial and its relevance in the clinical outcome during infection is unknown. Acute HCV infection is asymptomatic in most individuals, where 20% will successfully clear the virus while the remaining 80% of patients develop a chronic lifelong infection due to ineffective host antiviral responses. Twenty % of patients who develop chronic HCV infection will progress to liver cirrhosis within 25-30 years, where long term hepatic inflammation results in extensive scarring of liver tissue (Fig. 1.5) (Conde et al. 2017; Lingala & Ghany 2015). Two percent of individuals with liver cirrhosis progress to HCC. Co-factors that drive progression to chronic liver disease include alcohol consumption and co-infection with other viruses including HIV and HBV.

1.5 Treatment

Current treatments for the majority of flaviviruses are limited to supportive care, which include analgesics, fluid replacements and bedrest. There are no effective specific therapies for disease caused by the flaviviruses, despite highly successful drug

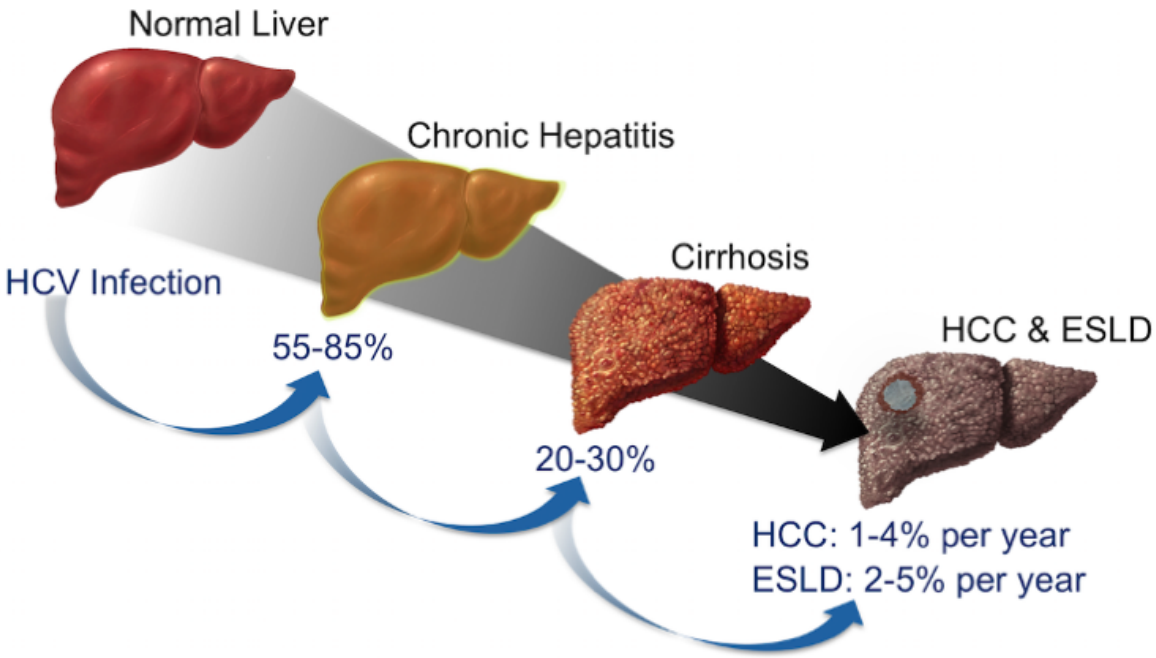

Figure 1.5: Clinical progression of HCV infection.

Following initial infection with HCV, ~55-85% of patients will develop chronic HCV infection where 20-30% go on to develop cirrhosis. Patients with HCV-induced cirrhosis have a 1-4% risk per year of developing hepatocellular carcinoma (HCC) or 2-5% risk per year developing end-stage liver disease (ESLD) (Lingala and Ghany 2015).

discoveries in treating the hepacivirus HCV where the cure rate is now upwards of 95%. There are several reasons for the failure thus far to produce antivirals to treat flavivirus infections (Grebely et al. 2018). Flaviviruses have been previously regarded as neglected pathogens, due to prevalent spread in developing tropical countries with high variability in symptoms during infection. In addition, there are efficient vaccines to combat a subset of flaviviruses, including YFV, JEV and TBEV. More recently, significant progress has been made in the development of antivirals for flaviviruses, including repurposing drugs with known antiviral activity to non-flaviviruses to screening compound libraries to identify molecules which disrupt virus replication (Botta et al. 2018; Eyre et al. 2020). Antivirals targeting both the structural and non-structural proteins are currently undergoing clinical trials, with significant focus on NS3 and NS5 due to their essential roles in virus replication and the success of direct acting antivirals that target the proteases and polymerases of other viruses, including HIV and HCV. However, challenges still remain during development and testing of candidate antivirals due to limited efficacy *in vivo* and the need to target multiple genotypes of certain flaviviruses such as DENV to prevent ADE by a single drug candidate. In addition, the differentiation of patients who may progress to severe dengue fever from the thousands of patients with febrile illness during an outbreak combined with a reduced window of opportunity for treatment with patients upon late presentation to the clinic complicates the challenges involved in the implementation of effective antivirals for flavivirus infection.

The first vaccine produced for flaviviruses, YFV-17D was developed in 1937 through 176 passages in chicken embryo tissue to produce a live attenuated stain which lost its neurotropic phenotype (Theiler and Smith 1937). Since then, YFV-17D has been utilised to produce chimeric live attenuated vaccines to target both the pre-membrane and envelope proteins, the major antigen of the virion, of other flaviviruses with varying results. IMOJEV, a vaccine in which the JEV pre-membrane and envelope proteins replaced the endogenous YFV pre-membrane and envelope proteins has high efficacy with regards to JEV infection and was approved for use in Australia in 2010 (Feroldi et al. 2012). Development of vaccines which target DENV has been inherently difficult due to the need to protect against all four serotypes, as cross protection is poor between serotypes of DENV and the risk of development of DHF, due to ADE, is 15-80x higher following secondary infection. The only approved vaccines are tetravalent

by the replacement of prM/E proteins from each of the four serotypes into the YFV-17D backbone. Clinical trials demonstrated strong neutralising antibody responses against all serotypes despite variances in serotypes (DENV3=78.4%, DENV2=35%) with genetically and phenotypically stable and non-hepatropic properties (Guy et al. 2015). However, the efficacy in children was dependent on age, with a reported efficacy of 33.7% in children aged 2-5 years old. In addition, manufacturer of Dengvaxia, Sanofi, discovered that vaccination actually resulted in increased risk of developing severe DF/DHF post DENV infection compared to naïve infection. This ultimately resulted in a permanent ban of Dengvaxia by the department of health in the Philippines after approximately 600 people died after receiving the vaccination, although the link hasn't been medically confirmed (Fatima and Syed 2018).

1.6 Lifecycle

Despite differences in transmission, cell tropism and pathogenesis, there is a conserved lifecycle for viruses within the *flaviviridae* family with distinct differences and is outlined below (Fig. 1.6 & 1.7)

1.6.1 *Flaviviridae* binding and entry:

Viruses from the flaviviridae family are grouped according to their similar viral lifecycles and replication strategies despite differences in cell tropism, transmission and pathogenesis.

Due to the broad cell tropism of flaviviruses, DENV and ZIKV interact with myriad of receptors in a cell-candidate manner to allow for entry into permissive cells. Despite identification of multiple receptors for both DENV and ZIKV, the key receptors required exclusively for entry remains a contentious issue. Common receptors extensively characterised important for entry of both DENV and ZIKV include mannose specific C-type lectins DC-SIGN and phosphatidyl serines receptors families TIM and TAM (Tassaneetrithep et al. 2003; Meertens et al. 2012; Hamel et al. 2015). Not only are these receptors important for viral attachment and internalisation, some also play a role in priming an optimal environment for viral replication to occur via triggering of internal signalling cascades which prevent apoptosis, induction of autophagy, downregulation of innate immune signalling or enhance binding of viral particles

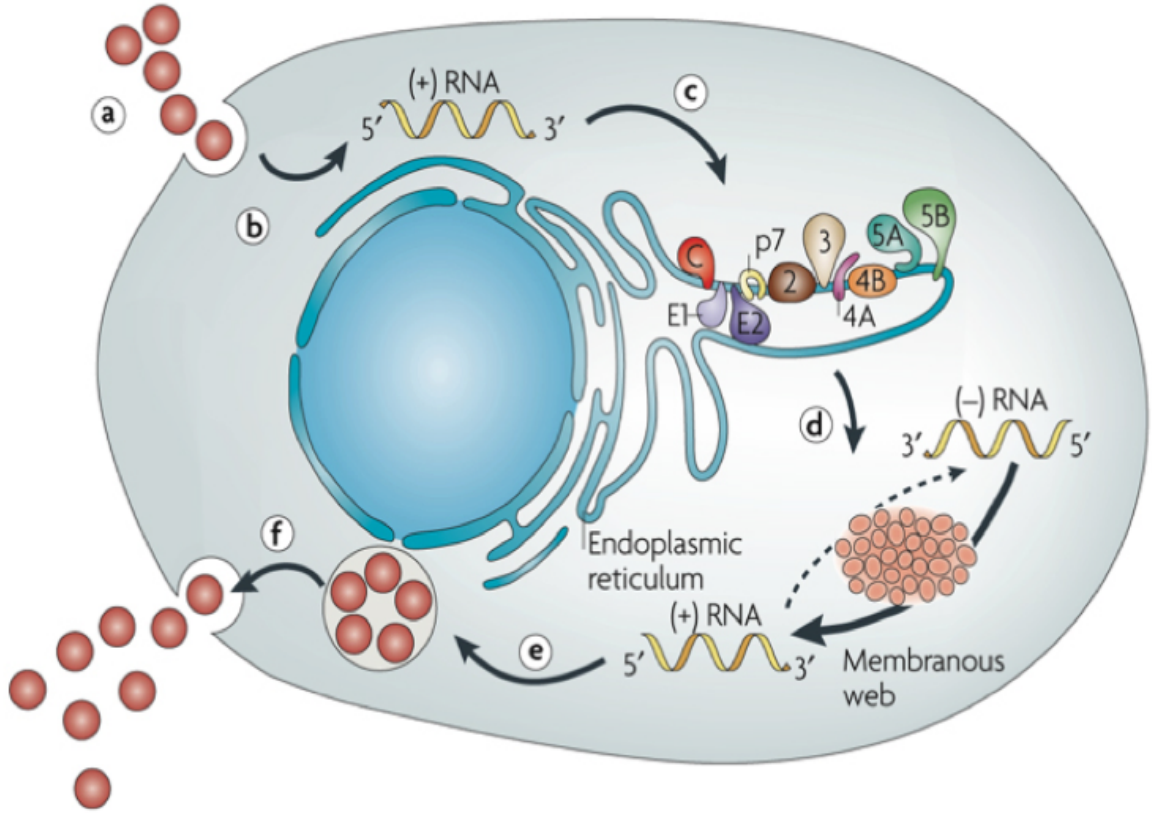

Figure 1.6: Schematic representation of the HCV lifecycle.

The HCV lifecycle consists of multiple phases, where the (a) virus attaches on a cell and internalised, (b) viral uncoating, (c) IRES mediated translation and polypeptide processing which (d) results in the establishment of HCV replication and replication complex formation. The virus is (e) packaged into progeny virions to be (f) released by exocytosis (Moradpour et al. 2007).

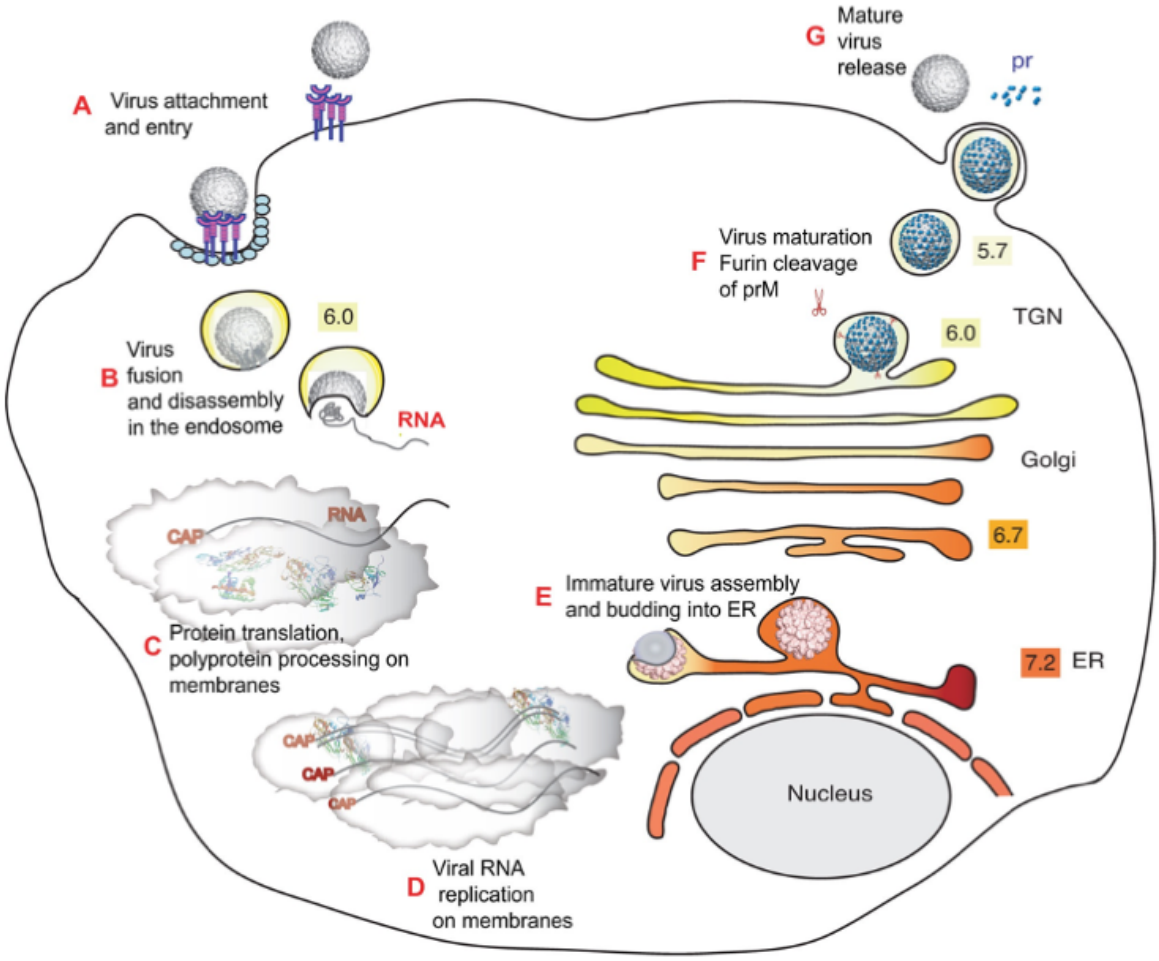

Figure 1.7: Schematic representation of the flavivirus lifecycle.

The flavivirus lifecycle consists of multiple phases, where the (a) virus attaches on a cell and internalised, (b) membrane fusion and release of the viral RNA genome, (c) cap-mediated translation and polypeptide processing which (d) results in the establishment of flavivirus replication and replication complex formation. The virus is (e) packaged into progeny virions to (f) mature during golgi transport and (g) released by exocytosis (Perera et al. 2008).

(Lee et al. 2005; Best 2013; Aid et al. 2017; Dejarnac et al. 2018; Chu et al. 2019). HCV enters the host hepatocytes via receptor mediated endocytosis by a highly orchestrated process involving several cellular receptors (CD81, scavenger receptor class B type 1 (SRB1), claudin-1 and occludin), attachment molecules (apolipoprotein E) and HCV glycoprotein E1 and E2 (Fig. 1.8) (Cerikan et al. 2020).

1.6.2 *Flaviviridae* internalisation and viral genomic RNA (gRNA) release:

There are several routes of entry for DENV and to a certain extent ZIKV. The canonical route of entry requires flavivirus virions to form complexes with receptors and/or co-receptors followed by fusion of the cell membrane and direct release of the nucleocapsid without the formation of vesicles (Hase et al. 1989). The ectodomains of the viral envelope protein play a critical role during this stage of the virus lifecycle. Clathrin-mediated endocytosis is the primary accepted model for entry of DENV, where DENV virion/receptor complexes are internalised within a pre-existing clathrin-coated pit where the virion particle is delivered to Rab5-positive early endosomes (van der Schaar et al. 2008). Maturation of the early endosomes via the accumulation of Rab7 and loss of Rab5 in addition to acidification signals the beginning of the fusion between endosomal and viral membranes (Acosta et al. 2012). Insertion of the dissociated envelope homodimers into the endosomal membrane results in formation of DENV envelope trimers. A fusion pore is constructed by conformational changes induced by the DENV envelope trimers, resulting in the release of the DENV viral nucleocapsid. Uncoating of the viral genome requires ubiquitination, where the capsid protein is degraded in a proteasome mediated manner (Byk et al. 2016). How the flavivirus nucleoprotein folds and renders itself susceptible to ribosomal translation remains speculative due to the lack of a solved flaviviral capsid-RNA crystal structure. Similar to flaviviruses, HCV virions are transported with Rab5a positive early endosomes where acidification induce virus uncoating and allowing release of the viral gRNA into the cytosol for translation (Coller et al. 2009; Farquhar et al. 2012).

1.6.3 *Flaviviridae* viral gRNA translation:

The flavivirus gRNA contains all the genetic information required to initiate and facilitate virus replication, is released into the host cell cytoplasm. Through a multi-coordinated effort between the viral gRNA flanking 5’ and 3’ untranslated regions (UTR)

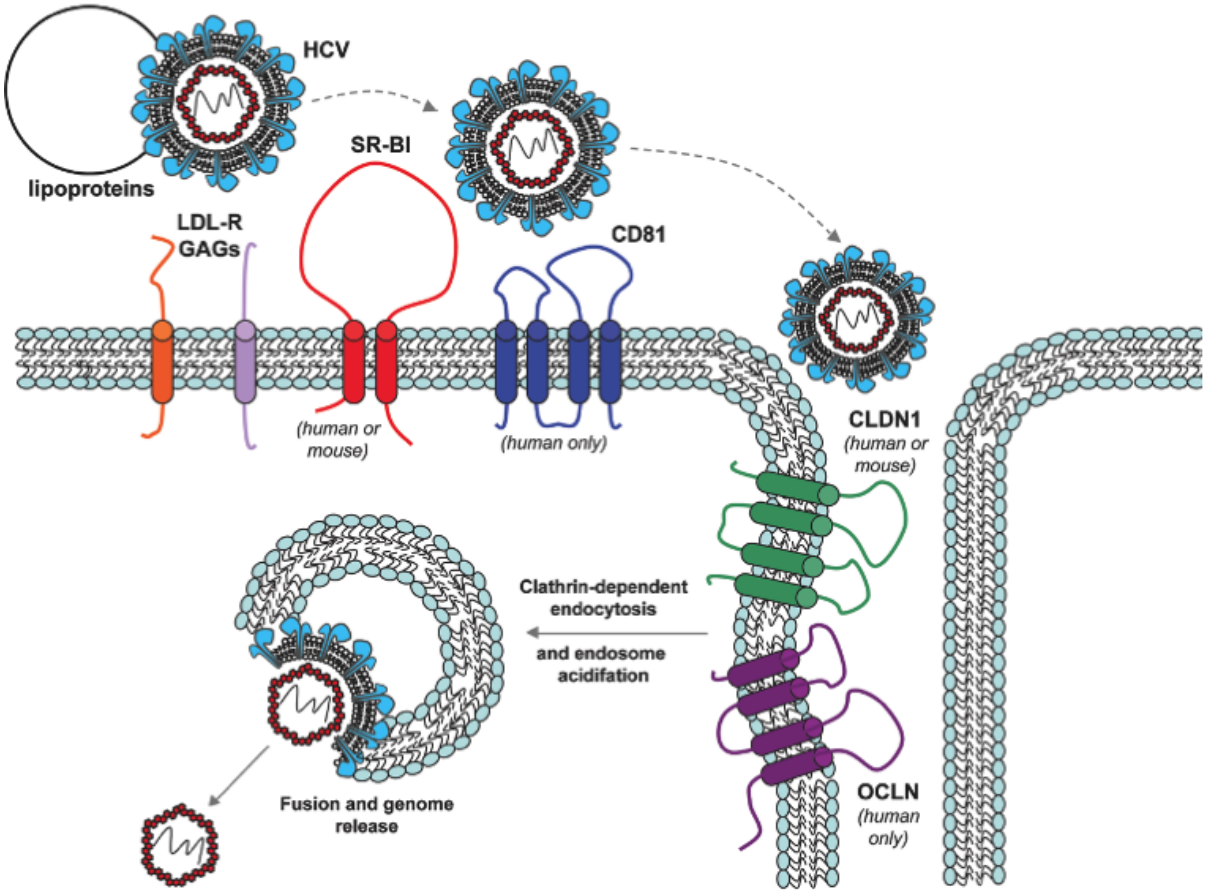

Figure 1.8: Entry and attachment of HCV virions.

HCV infects hepatocytes via clathrin mediated endocytosis, mediated by a highly orchestrated process which involves multiple host receptors including low-density lipoprotein receptor (LDL-R), glycosaminoglycans (GAGs), tetraspanin (CD81), scavenger receptor class B type 1 (SR-B1), claudin-1 (CLDN1) and occludin (OCLN) (McCartney et al. 2011).

and host cellular proteins, the RNA is circularised to achieve efficient canonical cap-dependent translation of the gRNA on the surface of the ER (Holden and Harris 2004; Chiu et al. 2005). DENV gRNA can also be cap-independent translated, leading to establishment of replication and the production of virus progeny (Edgil et al. 2006). It is thought that cap-independent translation is regulated through the 5' and 3' UTR, however the mechanism by which translation of the gRNA is achieved is unclear, especially due to the lack of IRES which is present in other viruses in the *flaviviridae* family such as HCV. The HCV internal ribosome entry site (IRES) present within the 5' UTR is a highly structured RNA element, which can directly recruit the 40S ribosomal subunit to the start AUG codon without scanning (Otto and Puglisi 2004). Recruitment of additional ribosomal subunits ultimately results in the formation of the 60S IRES-preinitiation complex and the commencement of translation and elongation (Kieft et al. 2001; Fraser et al. 2009).

1.6.4 *Flaviviridae* polyprotein processing:

Translation of both HCV and flavivirus viral gRNA results in the production of a transmembrane polyprotein that is highly associated with the endoplasmic reticulum (ER). The polyprotein is subsequently cleaved by host proteases such as signal peptidases, allowing the release of the structural proteins (capsid, pre-membrane and envelope for flaviviruses and core, E1 and E2 for HCV) from the rest of the polypeptide (Fig. 1.9 & 1.10) (Markoff 1989). Cleavage by viral proteases (NS2B-3 in flaviviruses and NS2/3 and NS3-4A in HCV) allow release of all the remaining NS proteins (Fig. 1.9 & 1.10) (Preugschat et al. 1990; Khumthong et al. 2002). Introduction of constraints within the efficiency of viral protein processing is a tool both flaviviruses and HCV utilise to regulate lifecycle kinetics and/or the expression levels of viral proteins (Stocks and Lobigs 1998; Carrère-Kremer et al. 2004; Welbourn et al. 2005).

1.6.5 *Flaviviridae* replication complex formation and viral gRNA generation:

Spatiotemporal regulation of virus replication and encapsulation is required in order to allow for efficient completion of the virus lifecycle. Thus, compartmentalisation of each process is achieved through the remodelling of ER membranes to allow the construction of a micro-environment favourable to virus replication, commonly called the replication complex or replication organelles for both flaviviruses and HCV.

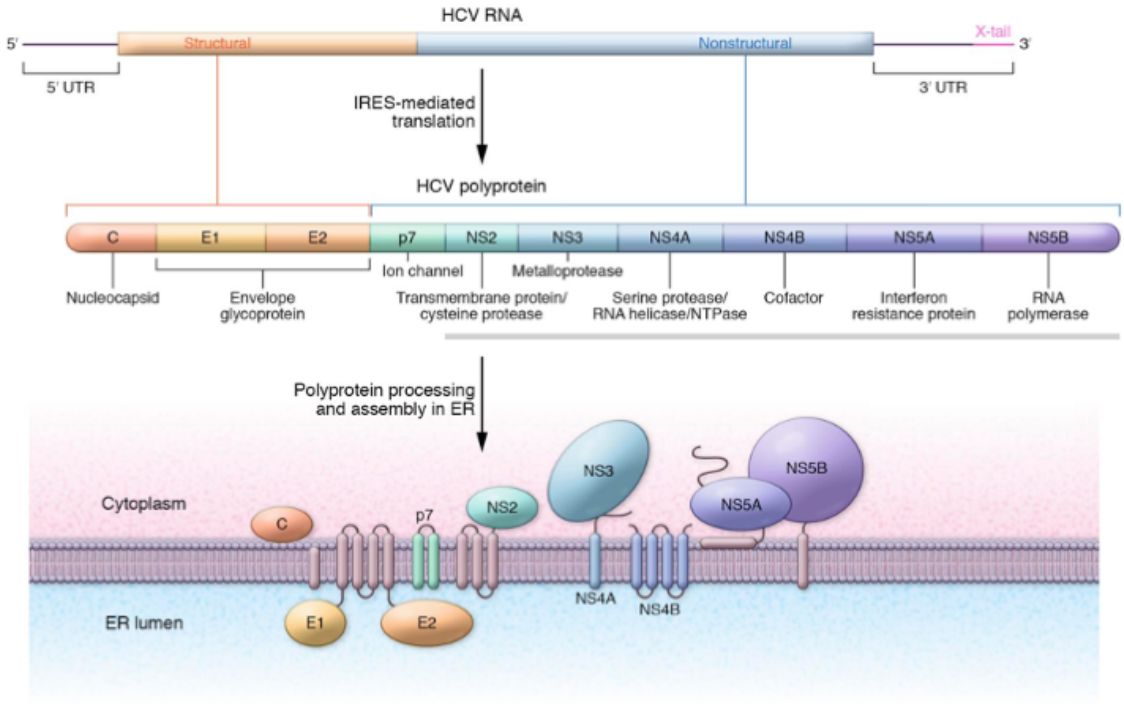

Figure 1.9: HCV genome organisation and polypeptide processing.

HCV is a 9.6kb positive-strand RNA genome with 5' and 3' UTRs important for translation and replication of the viral RNA. Translation and processing by viral and host proteases of the polypeptide yields the structural proteins (core, envelope glycoproteins E1 and E2), transmembrane protein p7 and non-structural proteins (NS2, NS3, NS4A, NS4B, NS5A and NS5B) (adapted from (Williams 2016).

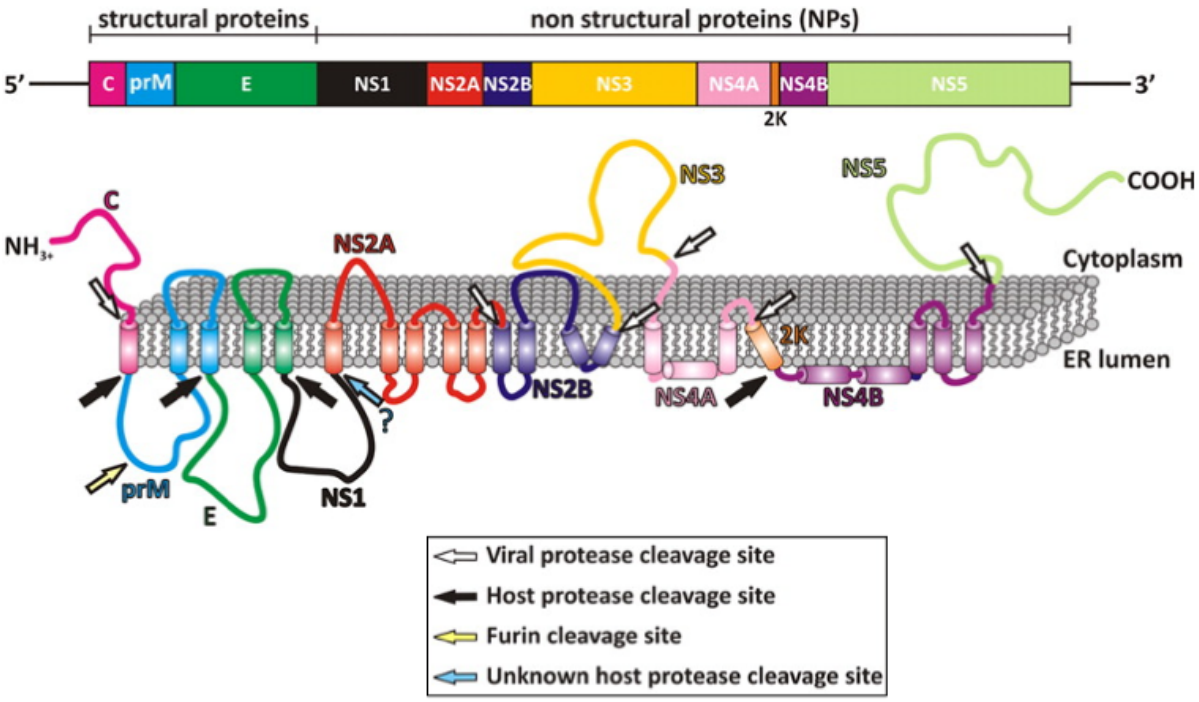

Figure 1.10: Flavivirus genome organisation and polypeptide processing.
Flaviviruses consist of a ~11kb positive-strand RNA genome that encodes one large open reading frame flanked by 5' and and 3' UTRs, critical for viral genome translation and replication. Translation and processing by viral and host proteases of the polypeptide yields the structural proteins (capsid (C), pre-membrane (prM) and envelope (E)) and non-structural proteins (NS1, NS2A, NS2B, NS3, NS4A, 2K-NS4B and NS5) (adapted from (Assenberg et al. 2009).

Formation of the replication complex in flaviviruses is a co-ordinated process involving all non-structural proteins and numerous host factors (Mackenzie et al. 1998; Uchil and Satchidanandam 2003; Gillespie et al. 2010; Muller and Young 2013). Within the flavivirus replication complex, electron microscopy coupled with immunogold labelling has identified dsRNA (the replication intermediate) as well as non-structural proteins within ~90nm wide vesicles, which are grouped together within vesicle packets (VP), a sub-structure within the replication complex and is thought to be the primary location of active virus replication (Fig. 1.11) (Welsch et al. 2009; Chatel-Chaix and Bartenschlager 2014). In contrast to this, HCV induces formation of the membranous web, which includes ~150nm wide ER membrane derived double membrane vesicles (DMV) during the peak level of viral replication, and is primarily driven by NS5A with secondary roles played other HCV NS proteins, especially NS4B (Fig. 1.11) (Paul et al. 2011; Romero-Brey et al. 2012). Host cell lipids are present within the membranous web (Alvisi et al. 2011) and multiple membrane vesicles (MMV) are also found at latter stages of HCV infection (Fig. 1.11) (Chatel-Chaix and Bartenschlager 2014). In addition, virus replication within the VP or DMV allows for protection of the viral genome and its dsRNA replication intermediates from the hosts defensive cytosolic nucleases and pathogen sensors, that would degrade gRNA and trigger an innate immune response respectively. Further research into *flaviviridae*-driven biogenesis of replication complexes and the host factors required has been directed by the construction of plasmid viral constructs that generate membranous webs (HCV) or VPs (DENV/ZIKV) indistinguishable from natural infection. For example, HCV membranous web formation can be generated solely by expression of HCV NS3-5B controlled by the T7 promoter (Tai and Salloum 2011) while both the flavivirus NS1-NS5 proteins and RNA elements within the 3'UTR contribute to VPs biogenesis for both DENV and ZIKV (Cerikan et al. 2020).

Amplification of viral RNA occurs within the replication complex, where a pool of viral RNAs is generated for either, translation of the polyprotein to form additional replication complexes, or assembly of genome into new virus progeny. This is possible via the RNA dependent RNA polymerase (RdRp) activity of the flavivirus NS5 protein in concert with other NS proteins, where binding to the secondary structures within the 5'UTR known as stem loop A (SLA) result in the production of a complementary

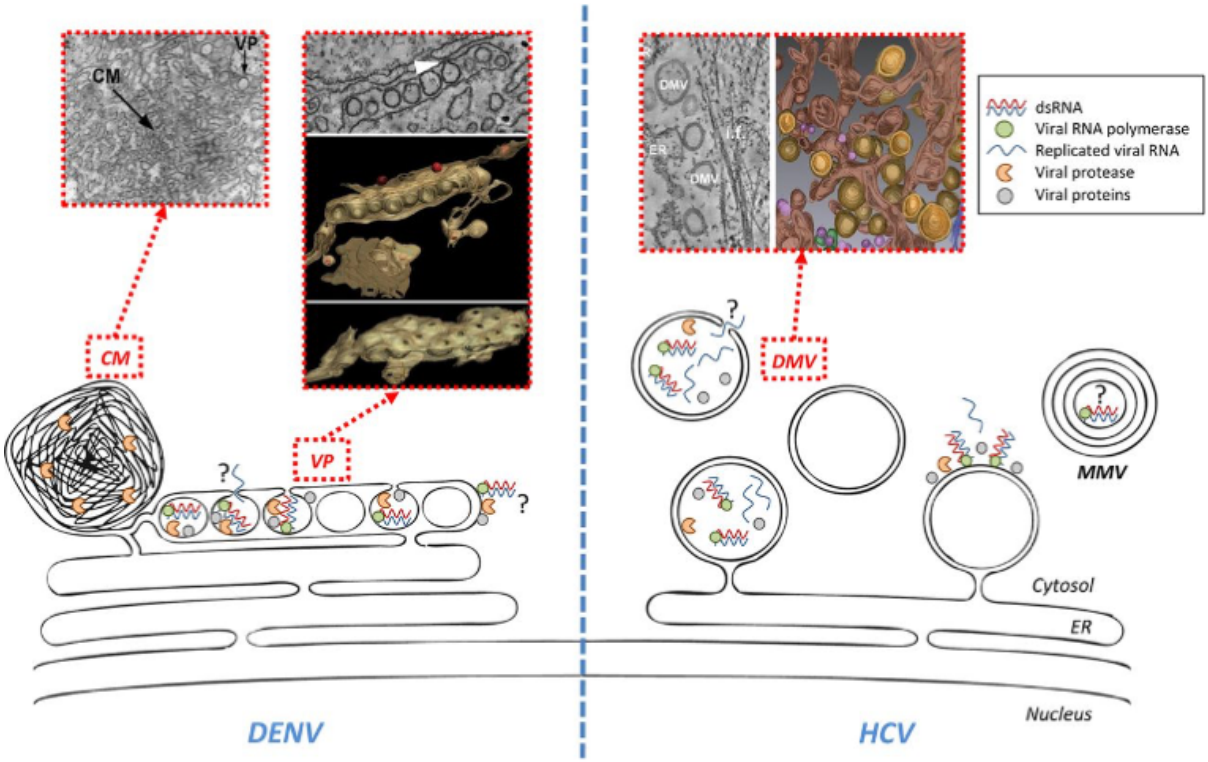

Figure 1.11: Replication complex morphology of DENV and HCV.

DENV induce remodelling of endoplasmic reticulum (ER) membranes to produce vesicle packets (VP) and convoluted membranes (CM), which is the location of active viral replication. In contrast, although HCV also re-arranges ER membranes to form replication complexes, double membrane vesicles (DMV) are present at the peak of viral replication, where multi membrane vesicles (MMV) are observed at later stages of infection (Chatel-Chaix and Bartenschlager 2014).

intermediate negative sense RNA (Lodeiro et al. 2009). The NS5B protein of HCV is the RdRp required for *de novo* synthesis of complementary intermediate negative sense RNA (Lohmann et al. 1997). This intermediate template is then utilised to generate additional copies of the positive sense stranded RNA to be translated or associated with capsid (flavivirus) or core (HCV) to be assembled into virus progeny.

1.6.6 *Flaviviridae* assembly and release:

Assembly of the virion is tightly coupled with replication and thus occurs adjacent to the replication complex for both flaviviruses and HCV. This is a highly orchestrated process involving the binding of only the negatively charged viral RNA to the basic capsid protein, likely through a non-specific mechanism despite the risk of cellular mRNA or viral intermediates contaminating the new viral progeny. Co-ordination of packaging and assembly of the virion is mediated by the NS proteins including NS1 and NS2A in flaviviruses (Scaturro et al. 2015; Xie et al. 2019b). Although the precise roles of assembly for each NS proteins is unclear, there is evidence that NS proteins may shuttle RNA from replication complexes into new particles through direct binding of the viral genomic RNA. This potentially provides temporal and spatial control of viral replication dynamics, allowing the switch from active RNA replication to a later stage of the viral lifecycle. In contrast, HCV assembly is closely associated with lipids, where the matured core protein translocates from the ER membrane to the surface of lipid droplets and interactions with NS5A result in the recruitment of replication complexes to this site (Miyanari et al. 2007; Masaki et al. 2008; Counihan et al. 2011).

After packaging of nascent viral genomes with core (HCV) or capsid (flavivirus) proteins, viral nucleocapsids bud into the ER lumen. Although the entry stages of *flaviviridae* are similar through the usage of pH and subsequent fusion of the viral and endosomal membranes, divergent secretory pathways exist for both HCV and flaviviruses where the former protects envelope proteins from pH through the construction of the p7 ion channel and the latter allows for additional processing and maturation of prM by host protease furin during passage through the golgi network (Wengler 1989; Steinmann et al. 2007; Atoom et al. 2014). Infectious viral particles are released from the cell through exocytosis, enabling the virus lifecycle to repeat.

1.7 *Flaviviridae* genome and proteins

The *flaviviridae* family are classified according to their positive sense single stranded RNA genomes that can range from 9.6kb (HCV) to 12kb (flaviviruses) in size. The genome consists of single open reading frame (ORF) flanked by highly structured non-coding 5' and 3' untranslated regions (UTR) (Fig 1.9 & 1.10). The flavivirus 5'UTR of approximately 100bp in size is highly conserved which contains a m^7GpppAmpN1 cap, which allows for translation of the polyprotein by host translational machinery in addition to providing protection from cellular exonucleases. Downstream of the m^7GpppAmpN1 cap are the SLA and SLB regions, important for flavivirus virus replication through recruitment and initiation of RNA synthesis via NS5 (Lodeiro et al. 2009). In contrast, the 3'UTR is more variable but still contains highly structured regions. It is likely that interactions between the highly structured 5'UTR and the 3'UTR are critical to allow for circularisation of the RNA genome required to promote initiation of viral synthesis of the complementary negative sense RNA (Khromykh et al. 2001; Alvarez et al. 2005). In comparison, the HCV 5'UTR contains four highly structured domains in addition to the internal ribosomal entry site (IRES), a highly structured RNA complex which can directly initiate cap-independent translation through high affinity recruitment and binding to the host 40S ribosomal subunit and translation initiation factor eIF3 (Otto and Puglisi 2004; Pérard et al. 2009). The HCV 3'UTR is essential for viral replication, consisting of a variable region, a long poly (U/UC) stretch and a highly conserved X region (Niepmann 2013). The 3'UTR is thought to facilitate efficient translation of the polyprotein through retention of the 40S ribosomal subunit post translation termination (Bai et al. 2013).

Following polyprotein translation of the HCV genome and processing by cellular and viral proteases, 10 viral proteins are produced: three structural proteins (core, envelope glycoproteins E1 and E2) and seven non-structural proteins (p7, NS2, NS3, NS4A, NS4B, NS5A and NS5B) (Fig. 1.9). In comparison, the flavivirus polyprotein following processing allows release of three structural proteins (capsid, pre-membrane and envelope) and seven non-structural proteins (NS1, NS2A, NS2B, NS3, NS4A, NS4B and NS5) (Fig. 1.10). The structural proteins are instrumental to the formation of the virion while the non-structural proteins are critical in the establishment of viral replication and immune evasion. Crosstalk between the structural and non-structural proteins is crucial in many stages within the virus lifecycle to allow for spatiotemporal

regulation, particularly during assembly of viral progeny. A brief summary of the functions of these proteins is provided below.

1.7.1 Flavivirus Structural Proteins

The flavivirus capsid is a highly basic protein, composed of four main alpha helices (α1 to α4) (Jones et al. 2003). Forming homodimers with asymmetric charge distribution, the top hydrophobic layer pre-α1 is thought to interact with lipid droplets and bind to membranes at sites of virus assembly (Martins et al. 2012; Faustino et al. 2019). The bottom layer formed by α4 is positively charged and interacts with the viral RNA to form the nucleocapsid, the core of the mature virion particle (Shang et al. 2018). Although classically defined as a structural protein, the flavivirus capsid protein has additional roles outside the virus assembly process including entry into the nucleus to possibly regulate gene expression to favour a virus replication environment (Colpitts et al. 2011).

Precursor membrane (prM) is a ~20kDa protein which is critical for assembly of virion particles. Interaction of the envelope (E) protein with prM within the ER allows formation of prM-E complexes which form the key component of the immature virion (Li et al. 2008). During transportation of the immature virion through the trans-golgi network, maturation of prM is achieved through cleavage by furin or furin-like protease into the M protein (~9kDa) and release of the pr peptide which facilitates rearrangement of the E protein into homodimers (Murray et al. 1993; Zhang et al. 2003). prM is also critical for protection of the E protein to prevent premature fusion with membranes during passage through the low pH environment of the golgi network, allowing for release of functional viral progeny via exocytosis (Oliveira et al. 2017).

Envelope (E) protein is the primary component of the virion and is critical for multiple stages in the viral lifecycle including binding host cell receptors and internalisation during viral entry, virion assembly and release of the mature virus particle from the host cell. The flavivirus E monomer (53-60kDa dependent on glycosylation status) is composed of three main domains I, II and III (EDI, EDII and EDIII) and two transmembrane domains. Located at the N-terminus, EDI is the structural central domain linking EDII and EDIII and is responsible for the flexibility in the orientation of the E protein due to conformation changes in the virus assembly process (Zhang et

al. 2004). The fusion peptide is located within the EDII domain and is critical for virus mediated endosomal membrane fusion during viral entry (Allison et al. 2001). The EDIII participates in attachment of virions to host cells through binding to glycosaminoglycan (Watterson et al. 2012).

1.7.2 Flavivirus Non-structural Proteins

Flavivirus NS1 is a highly glycosylated protein with the molecular range of 46-55kDa, which can exist in various glycosolated states dependent on the stage of the viral lifecycle. The NS1 monomer is composed of the β-roll, wing and a β-sheet is translocated to the ER lumen post translation and cleaved from NS2A (Akey et al. 2015; Watterson et al. 2016). Conformational change within the NS1 monomer results in self-dimerisation, where the NS1 dimer is formed and predominately important for both viral replication and assembly (Winkler et al. 1989). NS1 colocalises with dsRNA and is thought to be critical for replication complex formation and viral protein maturation (Mackenzie et al. 1998; Płaszczyca et al. 2019). NS1 is co-immunoprecipitated with all the structural proteins and is hypothesised to play a critical role in infectious particle assembly (Scaturro et al. 2015). Hexameric NS1 is secreted (sNS1) from the infected cell and a significant contributor to the pathogenesis of DENV infection, where activation of multiple innate sensors including TLR4 results in development of proinflammatory cytokine storms, subsequent vascular leakage and increased endothelial permeability (Somnuke et al. 2011; Beatty et al. 2015; Modhiran et al. 2015).

Although the viruses within the *flaviviridae* family have a similar genome structure to HCV, flaviviruses do not encode a non-structural protein with auto-protease activity equivalent to HCV NS2. Downstream of NS1 are two non-structural transmembrane proteins (NS2A and NS2B) with hydrophobic properties localised to the ER (Xie et al. 2013). NS2A (~22kDa) is critical for both viral replication and assembly stages of the virus lifecycle (Xie et al. 2015; Xie et al. 2019b). Multifunctionality is achieved through interactions with not only viral RNA but also multiple viral proteins including prM, E and NS3 (Mackenzie et al. 1998). NS2A can also subvert the innate immune response through inhibition of interferon signalling pathways (Liu et al. 2004; Dalrymple et al. 2015).

Flavivirus NS3 (~70kDa) is a multifunctional protein critical for both replication and assembly stages of the virus lifecycle. NS3 possess serine proteolytic activities, with cofactor NS2B (~15kDa) to release the remaining NS proteins from the polypeptide (Assenberg et al. 2009). NS2B is responsible for the localisation of NS3 to the ER and also can inhibit the innate immune response with or without NS3 (Aguirre et al. 2017; Wu et al. 2019b; Xing et al. 2020). NS3 also has both RNA and nucleoside triphosphatase and helicase activities to support viral replication and particle formation (Li et al. 1999).

NS4A and NS4B (16kDa and 27kDa respectively) are both integral membrane bound proteins important for flavivirus replication which remain poorly characterised. A conserved signal peptide (2K) links both NS4A and NS4B and interaction with DENV NS1 is known to be important for viral RNA replication (Płaszczyca et al. 2019). NS4A and NS4B have multiple roles within the replication complex. WNV NS4A regulates ATPase activity of the NS3 helicase, similar to the role HCV NS4A plays (Shiryaev et al. 2009). However, DENV NS4B regulates NS3 helicase activity via dissociation of NS3 from single stranded RNA. Cleavage of 2K from DENV NS4A results in ER membrane rearrangements resembling virus replication complexes (Miller et al. 2007). In contrast, WNV_{KUN} NS4A retains 2K for membrane rearrangements indicating subtle differences in flavivirus replication complex construction strategies (Roosendaal et al. 2006). Both NS4A and NS4B are robust inhibitors of the innate immune signalling targeting multiple IFN signalling pathways (Castillo Ramirez and Urcuqui-Inchima 2015; Wu et al. 2017).

Flavivirus NS5 (~103kDa), the largest of all flaviviral encoded proteins is highly conserved among flaviviruses and is a critical component of the RNA replication complex. NS5 is composed of two domains, a N-terminal RNA methyltransferase domain (MTase domain) and a C-terminal RNA-dependent RNA polymerase (RdRp). The MTase domain is important for cap synthesis via methylation of the viral mRNA required for translation and also conceals the mRNA from innate immune sensors (Zhou et al. 2007; Daffis et al. 2010). The RdRp performs synthesis of *de novo* viral RNA from positive to negative polarity and vice versa with support from NS3 (Tay et al. 2015). NS5 is also a major inhibitor of innate immune signalling, primarily through

interactions with STAT2 or suppressing maturation of the IFNAR1 receptor (Grant et al. 2016; Best 2017).

1.7.3 HCV Structural Proteins

The immature core protein is located at the N-terminus of the HCV polyprotein. It is cleaved by an ER signal peptidase and undergoes further processing by intramembrane proteases and signal peptide peptidases to form the mature core protein (21kDa) that possess both RNA and lipid binding properties (McLauchlan et al. 2002). The core protein multimerizes with itself to form the viral nucleocapsid, the protective shell that encapsulates the RNA genome for packaging into new virions. In addition to its main role in viral replication, core has also been implicated as both, a gene regulatory protein since it associates with multiple host factors, and major factor in the development of HCC, the penultimate stage of HCV pathogenesis (Shi et al. 2002; Tsutsumi et al. 2002; Mahmoudvand et al. 2019).

The HCV envelope glycoproteins E1 and E2 (30-35kDa and 70-75kDa respectively) are highly glycosylated type 1 transmembrane proteins which form non-covalent heterodimers to become a key component of the HCV virion (Goffard and Dubuisson 2003). HCV E1 and E2 together mediate attachment and entry of the virion into a new target cell. E2 interacts with cellular host receptors including CD81 and SR-B1 while during the latter stages of the HCV entry process E1 facilitates the fusion between viral and cellular endosomes (Hsu et al. 2003; Zona et al. 2014).

1.7.4 HCV Non-structural Proteins

Immediately downstream of the structural proteins are the non-structural proteins, beginning with p7. The multifunctional p7 protein has roles in both viral assembly and ion channel activity, rendering it essential for infectious particle formation. Part of the viroporin family, p7 is also thought to orchestrate intracellular localisation of viral proteins with unclear interactions with NS2 (Ma et al. 2011). In addition, the amino terminus of p7 regulates cell secretory pathways to not only allow retention of intracellular E2 glycoproteins but also control the secretion of HCV particles and the infectivity of secreted virions (Denolly et al. 2017).

HCV NS2 (23kDa) like p7 is dispensable for HCV replication but is essential for infectious particle assembly. Localised to the ER with cysteine protease activity, NS2 is able to form complexes with multiple structural (E1, E2) and non-structural proteins (p7, NS3 and NS5A), driving localisation of these interacting partners to the lipid droplet to support virion assembly (Jirasko et al. 2010; Ma et al. 2011).

HCV NS3 is located at the ER membrane and replication complex and is a multifunctional protein critical for HCV replication. NS3 harbours serine protease activity at the N-terminus and helicase/NTPase activity at the C-terminal domain (Yao et al. 1999). In a stable, non-covalent complex with co-factor NS4A, NS3's serine protease activity is responsible for the cleavage and release of the remaining downstream NS proteins from the HCV polyprotein (Brass et al. 2008). Additionally, NS3 plays a significant role in viral immune evasion through cleavage of key innate signalling adaptor molecules including MAVS and TRIF (Li et al. 2005; Meylan et al. 2005; Ferreira et al. 2016).

HCV NS4B is an ER localised hydrophobic membrane protein with a primary role in the modification of ER membranes to induce membranous web formation, the key site for HCV RNA replication (Gouttenoire et al. 2010). NS4B interacts with other NS proteins including NS5A, where the former ensures proper localisation of the latter (Biswas et al. 2016). Additional roles for NS4B include viral assembly and evasion of immune response through degradation of TRIF (Liang et al. 2018).

HCV NS5A is a multifunctional zinc-metalloprotein that plays critical roles in the HCV lifecycle despite possessing no enzymatic activity. NS5A is able to interact with not only viral RNA but also a range of viral proteins including core, NS4A and NS5B to support both viral replication and assembly (Shimakami et al. 2004; Fiches et al. 2016; Biswas et al. 2016). Various states of serine phosphorylation within NS5A allows regulation of the level and stage of HCV replication within an infected cell (Appel et al. 2005). NS5A is also able to interact with numerous host proteins including PI4KA, Rab5a and VAP-A, which support membranous web formation, regulate trafficking of lipids and endosomes respectively (Berger et al. 2009; Berger et al. 2011; Eyre et al. 2014).

HCV NS5B is the RNA-dependent RNA polymerase (RdRp) critical for synthesis of viral RNA of both positive and negative polarity. NS5B is an ER membrane-bound protein via anchorage by the C-terminal transmembrane domain (Moradpour et al. 2004). Located within the replication complex, NS5B is able to interact with most, if not all non-structural proteins to allow for spatiotemporal regulation of virus replication (Tan et al. 2006). NS5B also interacts with multiple host proteins to support viral replication (Kyono et al. 2002; Goh et al. 2004; Kim et al. 2004). In contrast to flavivirus NS5, HCV NS5B activates innate signalling pathways, resulting in production of cytokines including type I interferons (IFN) and IL-6, likely triggering inflammation and inflicting damage to the liver (G.-Y. Yu et al. 2012; Gerold & Pietschmann 2013). As a crucial component of the HCV lifecycle, multiple direct acting antivirals (DAAs) have been developed to inhibit the polymerase activity of NS5 (Geddawy et al. 2017).

1.8 Infection model systems of *flaviviridae*

Historically, studies of the molecular virology and pathogenesis of *flaviviridae* especially HCV were limited due to the lack of efficient cell culture systems that supported the entire lifecycle. Establishment of the HCV sub-genomic replicon system in the human hepatocellular cell line (Huh-7), allowed for autonomous HCV replication and expression of the non-structural proteins to establish replication complexes (Lohmann et al. 1999). This was achieved through the replacement of the structural proteins with antibiotic resistance cassettes to select for cells with high levels of HCV replication and the introduction of an encephalomyocarditis (ECMV) IRES. Unfortunately, the lack of structural proteins results in no production of viral progeny and the inability to study the entire HCV lifecycle. However, this replicon system has been instrumental in elucidating key mechanisms of HCV replication. In 2005, the isolation of the genotype 2a HCV cDNA from a Japanese patient with fulminant hepatitis (JFH-1) led to efficient replication of HCV in cell culture and the production of infectious virus particles for the first time, enabling research into multiple stages within the HCV lifecycle (Wakita et al. 2005). Additional modifications have been introduced to improve usefulness of both these systems, including the introduction of reporter genes that express proteins with fluorescence and luminescence properties (Ikeda et al. 2005; Koutsoudakis et al. 2006; Schaller et al. 2007).

Flaviviruses including DENV generally replicate at high levels *in vitro* in a wider range of cell types and thus are less challenging to adapt to a cell culture model. Similar to HCV, replicons for flaviviruses including DENV and YFV have been generated with reporter tags to allow for more intricate study of virus replication and high-throughput screening of antiviral compounds (Pang et al. 2001; Patkar et al. 2009; Kato et al. 2019). The first infectious clone for a flavivirus was obtained from YFV in 1989, followed by DENV-4, JEV and Kunjun virus within three years (Rice et al. 1989; Lai et al. 1991; Sumiyoshi et al. 1992; Khromykh and Westaway 1994). Unlike HCV, flavivirus genomes are inherently unstable in *E.coli* during plasmid propagation, resulting in recombination. Thus, low copy number plasmids are utilised at the expense of plasmid yield. Like HCV, reporter genes have been inserted into flavivirus infectious clones as a tool to visualise and analyse viral infection (Schoggins et al. 2012; Eyre et al. 2017b).

1.9 Host Factors required for *flaviviridae* lifecycle

As the majority of viruses have a limited capacity to encode genetic information, they must exploit host factors to support replication and produce virus progeny and HCV is no exception. This is achieved through the secondment of host proteins, membrane structures, lipids and metabolites. An example of HCV's absolute requirement for host factors is exemplified by the virus's ability to remodel host intracellular membranes to generate sites of replication. This is facilitated by interactions of the viral non-structural proteins (NS3/4A, NS4B, NS5A and NS5B) with various target host factors. A common theme present in the currently characterised host factors for HCV replication is a role in protein trafficking or lipid biosynthesis and shuttling "supplies" into the replication complex (Fig. 1.12).

Probably the best characterised HCV proviral host factor is phosphatidylinositol 4-kinase III alpha (PI4KA). PI4KA is a host factor critical in HCV replication, identified by multiple small interfering RNA (siRNA) screens carried out to reveal co-factors of HCV replication. PI kinases are known to be essential for membrane trafficking and protein sorting and it is postulated that PI4KA, which predominately resides in the ER, helps in the remodelling of membranes required for the construction of the membranous web (Tai and Salloum 2011; Berger et al. 2011). This is accomplished via close association

of NS5A with PI4KA, where “hijacking” and subsequent enhancement of PI4KA enzymatic activity leads to local accumulation of PI4KA’s product PI(4)P, where it acts as a beacon in the recruitment of proteins with lipid binding motifs such as Oxysterol Binding Protein (OSBP) (Fig. 1.12) (Reiss et al. 2011; Berger et al. 2011). Through interactions with PI4KA, OSBP is able to regulate cholesterol trafficking to replication complexes, consistent with reports that cholesterol is required for the remodelling and integrity of cellular membranes during HCV replication (Fig. 1.12) (Wang et al. 2014). In addition, it is also postulated that together with NS5A, OSBP is able to assist in virus maturation (Amako et al. 2009)

Human vesicle-associated membrane protein-associated protein subtypes A and B (hVAP-A and hVAP-B) have been shown to interact with both NS5A and NS5B and be essential for HCV replication (Fig. 1.12) (Tu et al. 1999). Situated in lipid rafts, hVAP-A is required for formation of the replication complex and recruitment of NS5B after polyprotein cleavage (Gao et al. 2004). hVAP-B has been postulated to play an important role in HCV RNA synthesis, however the precise mechanism by which it achieves this via interaction with NS5A has yet to be elucidated (Hamamoto et al. 2005).

Cyclophilin A (CypA) is a molecular chaperone which harbours peptidyl prolyl isomerase activity, important for the regulation of protein trafficking and folding, and is essential for HCV replication. Although it has been shown that through interactions of CypA with NS5A, binding of the latter to 3’ UTR of HCV RNA is enhanced (Fig 1.12). The precise molecular mechanism by which CypA assists in HCV replication remains largely unknown (Kaul et al. 2009; Foster et al. 2011). CypA had initially shown promise as an effective host-targeting antiviral to treat chronic HCV infection, where three inhibitors of CypA (Alisporivir (Novartis), NIM-811 (Novartis) and SCY-635 (SCYNEXIS) progressed to phase I and II clinical trials with high efficacy and safety (Gallay 2012). Only Alisporivir which demonstrated efficacy against multiple HCV genotypes with an acceptable safety profile progressed to phase III clinical trials which are currently ongoing as of 2019 (Gallay 2012).

In addition to protein host factors, miRNAs have also been implicated in HCV replication. Micro-RNA 122 (miR122) is highly abundant in hepatocytes and has been

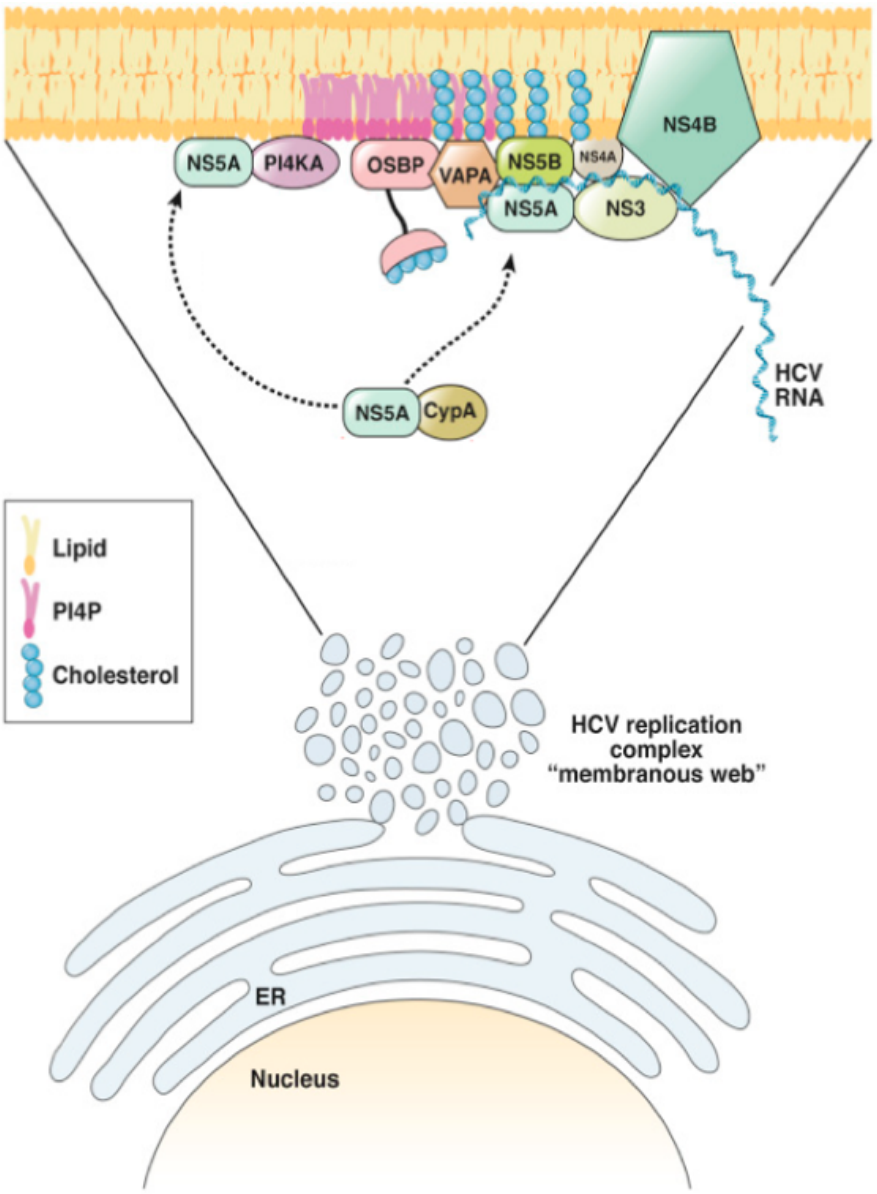

Figure 1.12: Host factors critical for the replication stage of the HCV lifecycle. HCV utilises multiple host factors for the biogenesis and maintenance of the replication complex. NS5A interacts with phosphatidylinositol-4-kinase-alpha (PI4KA) to allow for local accumulation of PI4P, which recruits oxysterol binding protein (OSBP) to enable transportation of cholesterol to the membranous web. OSBP and vesicle-associated membrane protein-associated protein A (VAPA) recruits NS proteins to the replication complex and interactions between cyclophilin A and NS5A is critical for membranous web biogenesis (Chukkapalli and Randall 2014).

implicated in multiple stages of the HCV lifecycle. Binding of miR122 to the 5'UTR of the HCV gRNA not only increases genome translation and initiation of replication but also confers resistance of degradation by host nucleases such as Xrn1 (Masaki et al. 2008; Niepmann 2009; Y. Li et al. 2013; Schult et al. 2018; Chang et al. 2008). Primarily through interaction with the 5' UTR, miR122 is able to protect the HCV RNA genome from host exonucleases and enhance binding of the 48S ribosome to HCV RNA, stimulating HCV translation (Henke et al. 2008; Li et al. 2013)Similar to HCV, host factors are also equally as important for flavivirus infection, often facilitated by interactions with multiple structural and non-structural viral proteins. Host factors identified usually have either direct roles in the virus lifecycle (i.e. entry of the virus into the cell or construction of membranous web through remodelling of ER membranes) or indirect roles, through alteration of the infected cell environment to favour virus replication (i.e. regulation of apoptosis and signalling cascades and immune evasion). Host factors required by flavivirus' have been identified by either the usage of genome-wide screening with RNAi and/or CRISPR technology or through proteomic approaches. SPCS1, a subunit within the signal peptidase complex was identified utilising a Huh7 cDNA library and the yeast 2 hybrid system utilising NS2 as the bait. Genome-wide screening identified that multiple subunits of the signal peptidase complex including SPCS1 was also important in flavivirus infection. However, the mechanism of action appears to be distinct, where SPCS1 is important in HCV assembly via interaction with NS2 and E2 compared to polyprotein processing for flaviviruses (R. Zhang et al. 2016; Suzuki et al. 2013).

Although each flavivirus recruits and exploits a unique set of host factors to support the virus lifecycle, functional and mechanistic studies suggest that these diverse host factors actually have common roles in establishing and facilitating flavivirus replication (Fig 1.13). Unlike HCV which utilises PI4KA and OSBP among others to remodel membranes to form replication complexes, flaviviruses including DENV and WNV utilise cholesterol, fatty acid synthase (FASN) and reticulon 3.1A for replication complex and vesicle packet formation (Heaton et al. 2010; Martín-Acebes et al. 2011; Aktepe et al. 2017). Genome-wide CRISPR screens have also identified host factors which are required for multiple flaviviruses including proteins belonging to the oligosaccharyltransferase (OST) complex, where DENV requires both OST isoforms SST3A and SST3B for virus replication, while WNV, YFV and ZIKV depend solely on

SST3A (Fig 1.13) (Marceau et al. 2016). Differences in the roles of host factors recruited by flaviviruses do however exist, for example, down-regulation of sphingolipid ceramide has contrary effects on WNV and DENV replication (Aktepe et al. 2015). However, cholesterol is utilised for multiple steps of the virus lifecycle for not only HCV, but also most flaviviruses including DENV and WNV (reviewed in (Felmlee et al. 2013; Osuna-Ramos et al. 2018)).

1.9.1 siRNA screens to identify host factors

The discovery of short hairpin RNA (shRNA) and small interfering RNA (siRNAs) followed by artificial exploitation of the RNA interference system led to the development of experimental inhibition of endogenous protein expression for the first time. This is accomplished via delivery of a single dsRNA oligonucleotide (siRNA) or shRNA expression vector utilising the drosha/dicer RNA interference system where endogenous protein expression is silenced by elimination of the target transcript RNA via sequence homology mediated by cytosolic argonaut proteins (Meister and Tuschl 2004).

Numerous shRNA/siRNAs screens have been performed in the past 10 years for HCV. These screens have been predominately limited to host kinases, cellular receptors and their appropriate signalling pathways, transcription factors and transporter proteins (Ng et al. 2007; Randall et al. 2007; Supekova et al. 2008; Vaillancourt et al. 2009; Berger et al. 2009; Borawski et al. 2009; Trotard et al. 2009; Reiss et al. 2011). It is theorised that these gene families mentioned above are most likely to have an impact on HCV replication and could likely targets for potential novel therapeutics. However, other gene families and genes with currently unexplored functions can't be discounted as these may play a vital role in HCV replication. To overcome this limitation, two genome wide screens (i.e. targeting the complete human genome) utilising siRNA have been published targeting host factors important for HCV replication, where one utilised the HCV sub-genomic replicon system and the other utilised the infectious JFH-1 HCV cell culture system (Tai et al. 2009; Q. Li et al. 2009). However, out of the 96 factors identified in the former screen utilising the replicon, only 15 hits overlapped with the latter utilising infectious virus, despite the necessity of both HCV model systems to enter the replication phase of the virus lifecycle.

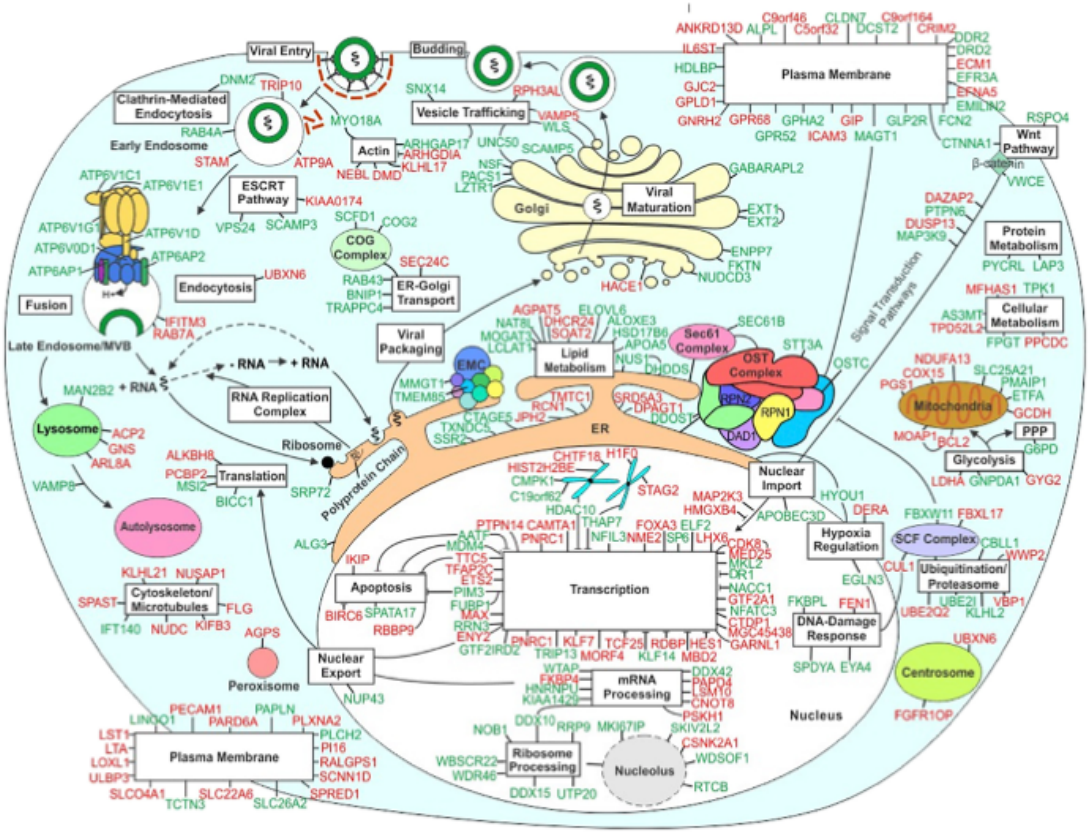

Figure 1.13: Host factors critical for the DENV lifecycle.

Host factors are critical to support the entire DENV lifecycle, where each gene is indicated in green text. In contrast, host factors indicated in red text are crucial in the innate immune response to subvert DENV virus entry and replication (Savidis et al. 2016a).

The discovery of short hairpin RNA (shRNA) and small interfering RNA (siRNAs) followed by artificial exploitation of the RNA interference system led to the development of experimental inhibition of endogenous protein expression for the first time. This is accomplished via delivery of a single dsRNA oligonucleotide (siRNA) or shRNA expression vector utilising the drosha/dicer RNA interference system where endogenous protein expression is silenced by elimination of the target transcript RNA via sequence homology mediated by cytosolic argonaut proteins (Meister and Tuschl 2004).

Numerous shRNA/siRNAs screens have been performed in the past 10 years for HCV. These screens have been predominately limited to host kinases, cellular receptors and their appropriate signalling pathways, transcription factors and transporter proteins (Ng et al. 2007; Randall et al. 2007; Supekova et al. 2008; Vaillancourt et al. 2009; Berger et al. 2009; Borawski et al. 2009; Trotard et al. 2009; Reiss et al. 2011). It is theorised that these gene families mentioned above are most likely to have an impact on HCV replication and could likely targets for potential novel therapeutics. However, other gene families and genes with currently unexplored functions can't be discounted as these may play a vital role in HCV replication. To overcome this limitation, two genome wide screens (i.e. targeting the complete human genome) utilising siRNA have been published targeting host factors important for HCV replication, where one utilised the HCV sub-genomic replicon system and the other utilised the infectious JFH-1 HCV cell culture system (Tai et al. 2009; Q. Li et al. 2009). However, out of the 96 factors identified in the former screen utilising the replicon, only 15 hits overlapped with the latter utilising infectious virus, despite the necessity of both HCV model systems to enter the replication phase of the virus lifecycle.

The majority of siRNA screens that have been performed on flaviviruses have utilised either DENV, WNV or YFV as their main virus during the screening process to identify novel host factors and deduce pan-flaviviral activity with confirmatory experiments. siRNA screening using a kinase subpool revealed 7 genes which inhibited DENV2 infection in excess of 40%, one hit (EIF2AK3) was present as a top hit in both genome-wide siRNA screens and AP2M1 was present in one, indicating that there is poor overlap despite use of the same strain of DENV2 (New Guinea C) and similar screening methodology (Kwon et al. 2014). TNFSF12 and SPHK12, which were both

present in the apoptosis siRNA screen was not present as top hits in both siRNA genome-wide screens (Savidis et al. 2016a; Barrows et al. 2019). However, given the output was measuring caspase-3 levels within DENV infected Huh-7 cells, poor overlap was expected and thus demonstrates that significant alteration of the screening protocol can have adverse effects on the top hits observed (Morchang et al. 2017).

Savidis *et al.* utilised multiple genome-wide siRNA libraries with not only the same strain of DENV2 (New Guinea C) but also similar screening methodology. Comparisons in the top hits from each siRNA library demonstrated that despite significant overlap of genes belonging to similar signalling pathways and gene clusters, exact gene overlap was poor and is reflective of the limitations that siRNA technology possess which is discussed below (Savidis et al. 2016a). Overlap between genome-wide screens with DENV2 performed by different groups is also poor, where the majority of genes were derived from the EMC complex (Savidis et al. 2016a; Barrows et al. 2019). In addition, proteins from the EMC complex were also present as top hits in genome-wide CRISPR screens performed with both DENV2 and ZIKV, demonstrating that usage of both siRNA and CRISPR technology concurrently can assist in validation of top hits and elimination of false positives. No ZIKV siRNA genome-wide screens have been performed to date as a result of the combination of low scientific interest of ZIKV biology prior to the pandemic within the Americas in 2015 and the concurrent rise of CRISPR technology and availability of associated genome-wide libraries. Despite the consensus that CRISPR has superseded siRNA technology to silence gene expression, performing a genome-wide siRNA screen would allow identification of host factors which are essential to cell survival.

Both subset and genome wide screens listed above each produce a unique set of results, where the top hits impact HCV replication with high efficacy but in most cases there is little overlap besides the host factors described previously, such as PI4KA and Cyclophilin A. This is primarily a result of the different siRNA sequences for each gene employed in each screen resulting in divergent off-target effects and knockdown efficiencies. The silencing efficiency of different siRNAs targeting the same gene can vary significantly (Kurreck 2006). Residual activity due to incomplete gene knockdown also makes it difficult to ascertain the degree of impact the host factor in question has

on HCV replication. Observation of high off-target rates observed in RNAi screens may also be attributed to (i) incomplete binding of siRNA onto the 3' UTR of mRNA which can facilitate miRNA-like inhibition, resulting in down-regulation of non-target genes and (ii) during the delivery of siRNA into the cell, the innate immune response can be activated by recognition of RNA in the endosome by TLR7 and TLR8 (Judge et al. 2005).

In addition, siRNA concentration and the associated method of transfection and subsequent duration of silencing may explain the variances observed between independent screens, where a shorter duration of silencing may bias proteins with a shorter half-life and vice versa, complicating data analysis. The presence of excess exogenous siRNA during transfection can also result in saturation of the endogenous RNAi machinery, where key components of the RNAi pathway, such as exportin 5 and the RISC complex have a limited capacity to bind siRNAs and pre-miRNA from shRNA, leading to a deficiency in gene knockdown (Hutvágner et al. 2004) Thus to ablate any concerns arising due to ineffective knockdown and high off-target effects commonly seen in siRNA screens, it would be beneficial to employ a novel screen where target genes are completely knocked out.

1.9.2 Clustered Regularly Interspaced Short Palindromic Repeats (CRISPR) Screens

Clustered regularly interspaced short palindromic repeats (CRISPR) technology as we know it today has been adapted from a naturally existing system by which prokaryotes defend against invading bacteriophages. To confer bacterial adaptive immunity via CRISPR, protospacers consisting of approximately 20bps of foreign DNA is inserted into the CRISPR array. A precursor CRISPR targeting RNA (crRNA) containing newly inserted protospacers is processed and individual crRNAs formed. Target recognition of crRNA to homologous sequences of foreign DNA results in recruitment of cas nucleases and subsequent cleavage and elimination of foreign DNA to prevent reinfection by the same bacteriophage (Barrangou and Marraffini 2014).

The basis of CRISPR editing technology as we know it today is derived from *Streptococcus pyogenes*, comprises of a single Cas9 protein complexed with an

engineered small guide RNA (sgRNA), which mimics the mature crRNA and a partially complementary trans-acting RNA (tracRNA) to allow RNA guided destruction of foreign nucleic acids. To facilitate cleavage and subsequent knockout of a target gene, a 20nt guide is designed complementary to the target site, flanked by a protospacer adjacent motif (PAM) sequence and in the case of *Streptococcus pyogenes* derived Cas9, 5' NGG (Fig. 1.14). The PAM sequence is recognised first by the Cas9 before the guide is scanned for complementarity. Once targeted to the DNA sequence in question, Cas9 induces a double stranded break (DSB) in the DNA 3-4bp upstream of the PAM sequence, which is repaired by host machinery primarily by non-homologous end joining (NHEJ) (Fig 1.14). The DSB ends are directly ligated back together, resulting in the introduction of insertion/deletion mutations at the repair site, and subsequently, a nonsense mutation in the coding sequence (reviewed in (Lieber 2010)). Using this methodology, it is now standard laboratory practice to knockout a gene of interest using CRISPR technology in an efficient cost-effective manner.

Most recently, mutation of both the critical RuvC and HNH nuclease domains in Cas9 results in an enzymatically inactive or "dead" cas9 (dCas9) that has lost the ability to cleave DNA but retains binding to sgRNA and targeting to specific DNA sites. This trait has been harnessed to target the dCas9 to specific DNA sequences with novel applications including activation and repressors of gene function and as a platform for dynamic fluorescence imaging of both DNA and RNA (Gilbert et al. 2013; Perez-Pinera et al. 2013; Chen et al. 2013; Nelles et al. 2016). In addition to genetic screening, CRISPR has also been instrumental to allow precise genetic engineering of both animals such as mice, mosquitos, pigs, chickens and ferrets (Kistler et al. 2015; Kou et al. 2015; Oishi et al. 2016; Lei et al. 2016). CRISPR is also a useful tool for the modification of large DNA viruses including EBV, vaccinia viruses and human pox viruses, where genomes range from 130kb-375kb in size, which has been challenging in the past to modify with conventional molecular cloning techniques (Bi et al. 2014; Yuan et al. 2015). CRISPR has also been considered as an antiviral strategy to combat persistent viral infection through cleavage of DNA, for example for cleaving the highly stable cccDNA in HBV infection or targeting of viral genes in EBV and HSV latent infection (Dong et al. 2015; van Diemen et al. 2016).

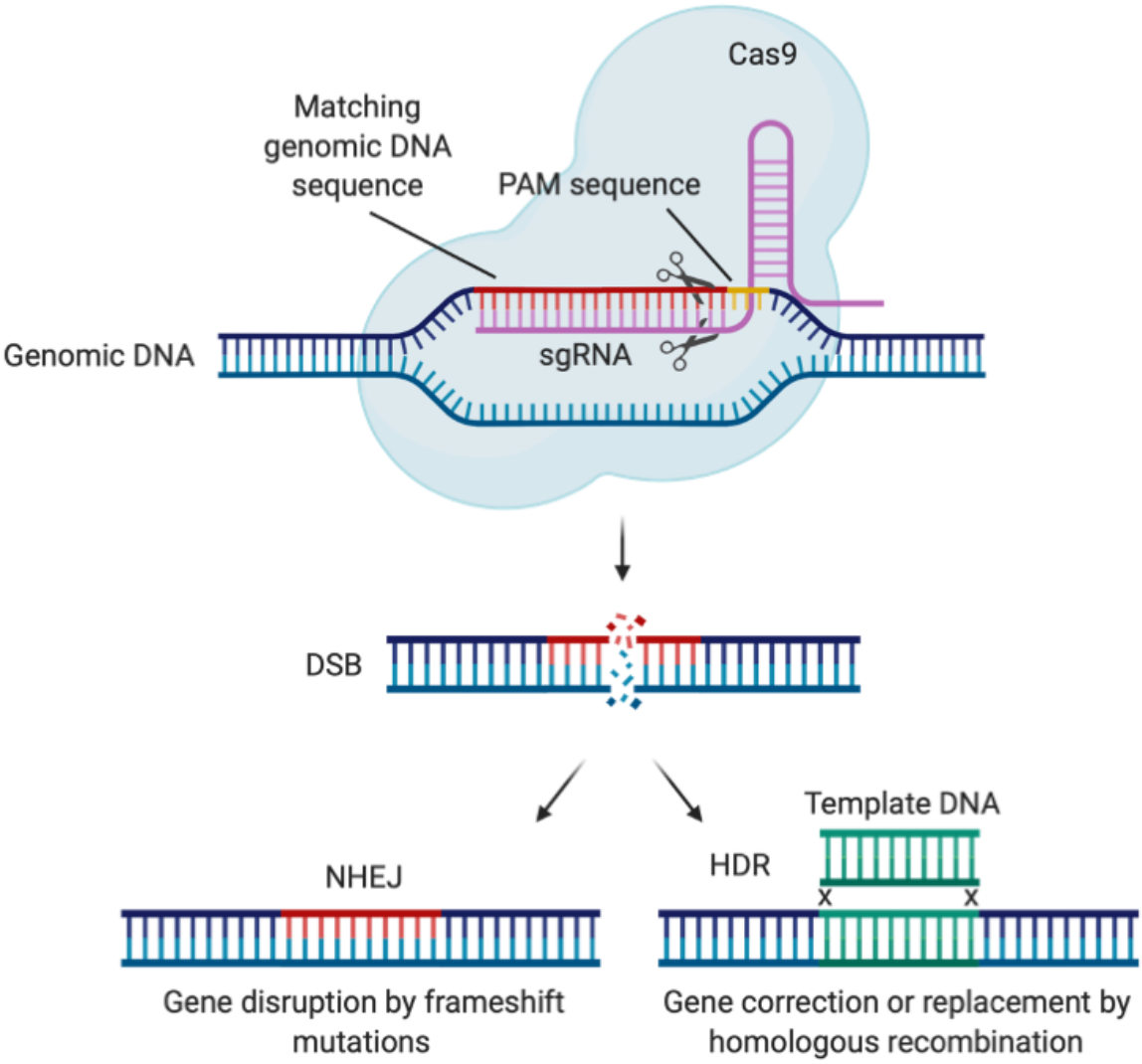

Figure 1.14: Canonical CRISPR editing technology.

The single guide RNA (sgRNA) hybridises to a 20nt DNA sequence directly upstream to the PAM sequence (NGG for Cas9 originating from *streptococcus pyogenes*). Cas9 cleavage is induced upon recognition of both the PAM sequence and sgRNA, resulting in double stranded breaks (DSB) within the target site of the genomic DNA. The genomic DNA can be repaired either through non-homologous end joining (NHEJ), resulting in frameshift mutations or homology directed repair (HDR) with the desired template DNA.

Genomic screens utilising CRISPR are feasible due to Cas9's ability to recognise a target site via specific DNA-RNA interactions. CRISPR is easily interchangeable from gene target to gene target by changing the sgRNA sequence and combined with the high efficiency of inducing DSBs, has resulted in an exponential rise of CRISPR driven genomic screens being performed in both human and murine cells. In these screens a pool of sgRNAs that target multiple genes in parallel is utilised (Shalem et al. 2014; Koike-Yusa et al. 2014; Konermann et al. 2015; Chen et al. 2015; Parnas et al. 2015). Results of CRISPR genomic screens mentioned above include analysis of phenotype resistant mutations from drug selection to pathogen invasion, to deduction of critical regulatory genes in multiple signalling pathways. Although on-target efficiencies between CRISPR and RNAi technology are similar, the latter is far less susceptible to systemic off-target effects (Smith et al. 2017). Screens utilising Cas9 (inducing DSBs) or dCas9 (with transcriptional activators/repressors) have both been performed, allowing complex gene expression patterns to be interrogated in a more flexible, accurate manner (Kweon and Kim 2018).

Numerous genome-wide CRISPR screens have been performed with both the traditional knockout cas9 and activator/repressor dCas9 systems in attempts to identify novel host factors critical in supporting viral replication. Novel host factors can be identified through either loss of function screens, where a knockout of a host factor will result in a permissive cell line resistant to virus infection, or gain of function screens, where overexpression of novel proteins in non-permissive cell line is made permissive to virus infection. CRISPR screens have high reproducibility, where multiple independent screens performing infection with the same virus have overlapping hits, while infecting multiple cell types with the same virus has also yielded overlapping hits in addition to some cell type specific novel host factors. Table 1.1 lists the genome-wide CRISPR screens which have been performed with regards to virus infection, where it is evident there are host factors which are important for numerous viruses within one viral family. However, it appears that slight modifications in screening technique and procedure can have a massive effect on the output of the sgRNA representation, and thus which novel host factors are present.

1.10 Innate Immunity

Virus	CRISPR screen	Host Factor class	Top Candidates Identified	Reference
Dengue Virus	KO	DF	EMC, OST complex (STT3A, SST3B), TRAP complex, ERAD (SEL1L, AUP1, DERL2)	Marceau *et al.* 2016, Lin *et al.* 2017
Epstein Barr Virus	KO	DF	CD81, CD19, CDK6, CCND2, IRF2, IRF4 CFLAR, BATF	Ma *et al.* 2017
Hepatitis C Virus	KO	DF	CD81, CLDN1, OCLN, miR-122, CYPA, ELAVL1, RFK, FLAD1	Marceau *et al.* 2016
Human Immunodeficiency Virus	KO	DF	CD4, CCR5, ALCAM, SLC35B2, TPST2	Park *et al.* 2017
Human Immunodeficiency Virus	Activation	IF	IFN pathway (IFNAR, STAT1), ZAP, TRIM25, N4BP1, MxB, IFITM1	OhAinle *et al.* 2018
Influenza A Virus	KO	DF	CMTR1, TMEM199, WDR7, CCDC115	Li *et al.* 2020
Influenza A Virus	Activation	IF	B4GALNT2	Heaton *et al.* 2017
Murine Novovirus	KO	DF	CD300LF, G3BP1, KMT2D, CD300LH	Orchard *et al.* 2016, Haga *et al.* 2016
Murine Novovirus	Activation	IF	TRIM7, MUC1, MX1	Orchard *et al.* 2018
Picornaviruses	KO	DF	PVR, GLI2, NTMT1, CD163, INPP4B	Kim *et al.* 2017
Severe Fever with Thrombocytopenia Syndrome Virus	KO	DF	SNX11, KRIT1, ZBTB6, AHR	Liu *et al.* 2019
West Nile Virus	KO	DF	SPCS1, SPCS3, EMC, OST complex (STT3A), TRAP complex, SEL1L, HRD1	Ma *et al.* 2015, Zhang *et al.* 2016
Yellow Fever Virus	Activation	IF	IFI6, IFN pathway (IFNAR, STAT2, JAK1), HSPA5	Richardson *et al.* 2018
Zika Virus	KO	DF	EMC, AXL, OST complex (STT3A), TRAP complex, ITGB5	Marceau *et al.* 2016, Savidis *et al.* 2016, Li *et al.* 2019, Wang *et al.* 2020
Zika Virus	Activation	IF	IFI6, ISG20, ZCCHC6, IFN-λ2, IRF1, MAVS, TRIM25	Dukhovny *et al.* 2019

Table 1.1: Host factors for virus infection identified utilising CRISPR screening technology.

Host factors which support or repress virus infection have been identified utilising either traditional CRISPR KO technology (KO) or the dCas9 activation systems (Activation). Dependency (DF) and Inhibitory (IF) Factors were present for multiple viruses and multiple screens have been performed on the same virus with varying cell types or experimental methodology.

The innate immune response is the crucial first line of defence against invading pathogens, where a rapid non-specific inflammatory response is initiated to subvert virus infection. The innate immune response is also critical in driving a robust adaptive immune response, resulting in not only the clearance of specific pathogens but also the development of long-lasting immunological memory (Iwasaki and Medzhitov 2015). Activation of the innate immune response relies on the detection of foreign microbial molecules known as pathogen associated molecular patterns (PAMPs) which accumulate within a cell during infection (Akira et al. 2006). PAMPs are recognised by pattern recognition receptors (PRRs) that are present in multiple compartments of the cell, including the cell surface, endosome and cytoplasm, where pathogens are likely to reside during infection (Saito and Gale 2007). Binding of PAMPs to PRRs results in the activation of multiple signalling cascades, culminating in the production of cytokines and the upregulation of multiple innate immune effector molecules (Brubaker et al. 2015). The interferons (IFN) are the most critical cytokines in combating viral infection and orchestrating an antiviral environment within infected and neighbouring uninfected cells, as well as regulation of immune cell activation and trafficking (Ivashkiv and Donlin 2014).

1.11 Recognition of DENV and ZIKV by RIG-I like Receptor (RLR) signalling pathways

During infection with either DENV or ZIKV, PAMPs such as single-stranded and double-stranded RNAs (ssRNA and dsRNA) are produced and can be readily recognised by the members of the DExD/H box RNA helicase family of cytoplasmic RIG-I like receptors (RLRs). The RLR family is currently composed of three members; retinoic acid-induced gene-I (RIG-I), melanoma differentiation associated factor 5 (MDA5) and laboratory of genetics and physiology 2 (LGP2) (Rehwinkel and Gack 2020) (Fig. 1.15). RIG-I and MDA5 have similar domain organisation, where an N-terminal tandem caspase recruitment and activation domains (CARD) is followed by a central RNA helicase domain (Yoneyama et al. 2005). The C-terminal domain (CTD) is multifunctional, allowing for both recognition of viral RNA, protein dimerisation and autoregulatory functions (Saito et al. 2007; Cui et al. 2008). In contrast, while LGP2 shares the conserved central RNA helicase domain and CTD, the N-terminal CARD domains are lost and therefore signalling incompetent. LGP2 is thought to possess

Figure 1.15: Structural representation of RLR family and adapter MAVS (IPS-1). Key domains critical for signalling include the CARD (caspase activation and recruitment domain), ATPase containing DEAD box helicase (DEAD Helicase) and a C-terminal domain (CTD). A repression domain (RD) within the CTD is present in RIG-I and MDA5 but not LGP2. MAVS (IPS-1) consists of a complimentary CARD domain, a proline rich region (Pro) and a c-terminal transmembrane domain (TM) (Loo and Gale 2011).

negative regulatory roles within RIG-I and MDA5 signalling (Rodriguez et al. 2014). Recognition of either short dsRNA or 5' triphosphate (5'ppp) uncapped ssRNA by RIG-I or long dsRNA by MDA5 results in multiple protein modifications (de-phosphorylation and K63-ubiqutiniation), ultimately resulting in conformation change via exposing the CARD domains (Loo and Gale 2011). The importance of RIG-I as a sensor for both DENV and ZIKV infection is exemplified by increased virus replication and subsequent apoptosis in A549 RIG-I$^{-/-}$ CRISPR KO infected cell lines (Schilling et al. 2020). Similarly, siRNA knockdown of either RIG-I or MDA5 resulted in increased DENV infection and both are required for the initiation of an effective IFN response (Nasirudeen et al. 2011). Shuttling of RIG-I/MDA5 to mitochondrial membranes is possible via interactions with translocation mediators TRIM25 and mitochondrial targeting chaperone 14-3-3ε (Gack et al. 2007; Liu et al. 2012a). Interaction with the complimentary CARD domains on the signalling intermediate mitochondrial antiviral signalling protein (MAVS) allows formation of the MAVS signalosome or innate immune synapse, where multiple cytosolic kinases including TANK-binding kinase 1 (TBK1) and Iκβ kinase-ε (IKKε) are activated and phosphorylate essential transcription factors in the RLR signalling pathway interferon regulatory factor 3 (IRF3) and interferon regulatory factor 7 (IRF7) (Kell and Gale 2015) (Fig. 1.16). CRISPR knockout of the signalling intermediate MAVS within human trophoblast cell lines resulted in both increased ZIKV virus infection and abolition of type I interferon signalling, further demonstrating the importance of MAVS within the RIG-I signalling pathway (Ma et al. 2018). The transcription factor NF-κB is also activated by the IKK complex (IKKα/β/γ), responsible for the upregulation of proinflammatory genes (Liu et al. 2017). Collectively, the RLR signalling pathway is crucial to both the detection and activation of the IFN response against flavivirus infection.

1.12 Recognition of DENV and ZIKV by Toll-like Receptors (TLRs)

Although the RLR pathway is the main driver for the activation of the innate immune response against DENV and ZIKV infection, secondary sensors including TLRs and cGAS-STING are also able to act synergistically with RLRs to induce an effective IFN response (Zevini et al. 2017). During viral entry, the accumulation of viral RNAs can activate TLR3/7 present within the endosomal membrane. TLRs are type I integral glycoprotein receptors where the transmembrane protein is flanked by a N-terminal

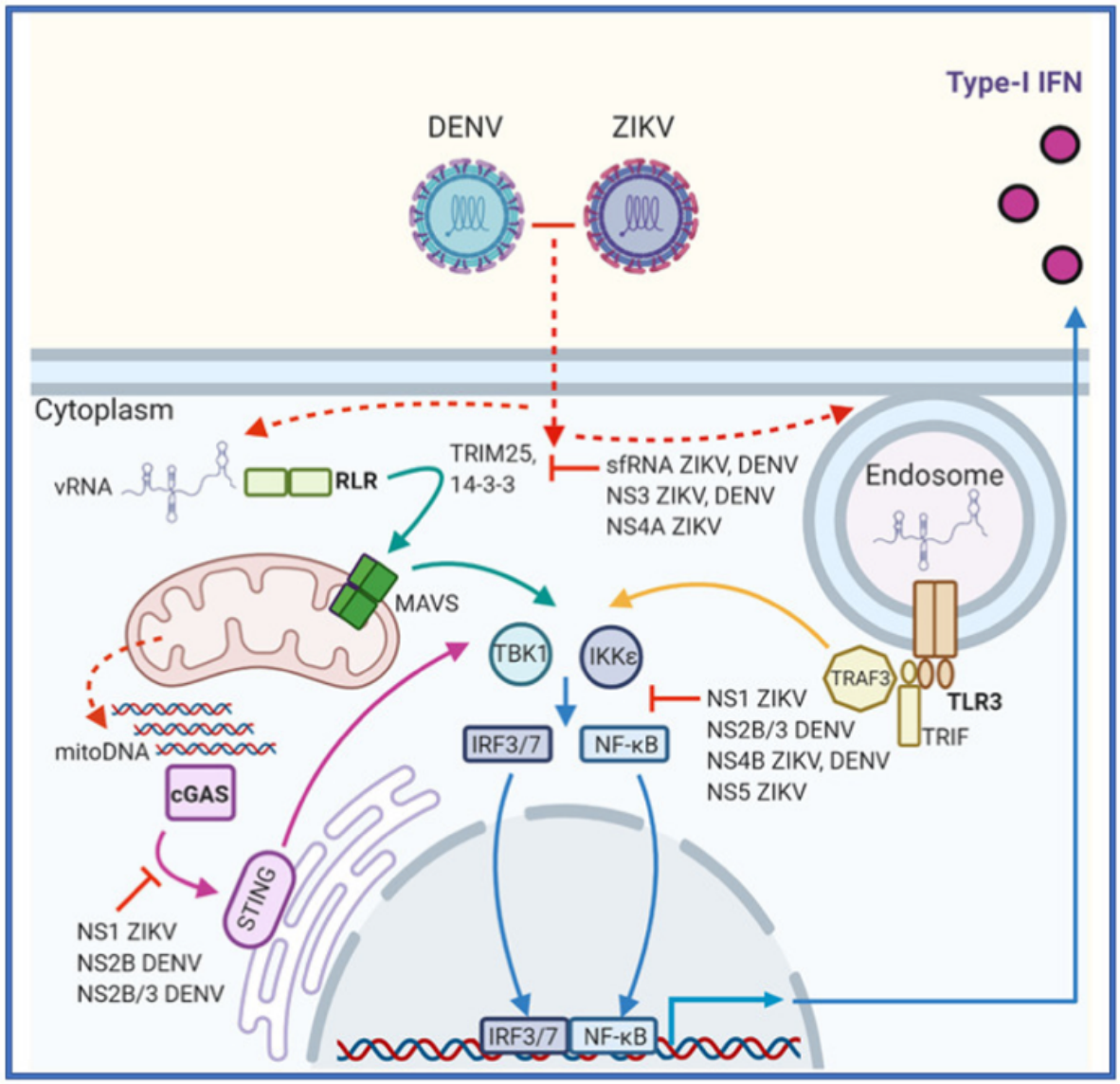

Figure 1.16: Recognition of DENV and ZIKV infection by the innate immune response and immune evasion by viral molecular components.

PAMPS such as viral RNA (vRNA) produced during virus replication can be recognised by PRRs (RLRs or TLR3). In addition, mitoDNA is released by the mitochondria within a stressed environment during flavivirus infection, resulting in the activation of the cGAS-STING pathway. These pathways culminate in the phosphorylation of TBK1 and IKKε which activate IRF3/7 and NF-κB to drive production of type I IFN. The importance of the pathways mentioned above is highlighted in red where both DENV and ZIKV have evolved mechanisms to inhibit multiple steps and prevent induction of type I IFN (Coldbeck-Shackley et al. 2020).

ligand binding ectodomain and a C-terminal cytoplasmic toll/interleukin-1 (TIR) domain (Botos et al. 2011). Expression of TLR3 is ubiquitous within multiple cell types in contrast to TLR7, which is present in specialised immune cells such as plasmacytoid dendritic cells (pDCs) (Takagi et al. 2016). Upon recognition of dsRNA by TLR3 or ssRNA by TLR7 and receptor dimerisation, two separate signalling pathways are activated both of which are dependent on further adapter binding (Fig. 1.16). Both CRISPR induced TLR3 KO macrophages and siRNA mediated TLR3 knockdown in fibroblast cell lines (HFF-1) are highly susceptible to DENV and ZIKV infection respectively (Nasirudeen et al. 2011; Hamel et al. 2015). Conversely, DENV infected HEK293 that were overexpressing TLR3 or TLR7 had elevated levels of cytokine production (Tsai et al. 2009). Activated TLR3 binds the TIR domain containing adapter inducing interferon-β protein (TRIF) resulting in upregulation of type I IFN by the TRIF dependent pathway (Yamamoto et al. 2003). In contrast, activated TLR7 forms a complex containing MyD88 with IRAK kinase family proteins, which are recruited to form the myddosome, where the MyD88 dependent pathway ultimately results in translocation of NF-κB and AP-1 to the nucleus to upregulate expression of both type I IFN and pro-inflammatory cytokines (Kawasaki and Kawai 2014). Flaviviruses can also activate TLR signalling pathways, resulting in elevated production of pro-inflammatory cytokines, leading to clinical manifestations (Thompson and Iwasaki 2008). For example, TLR3 is activated within human cerebral organoids by ZIKV infection, resulting in enhanced viral replication and hyper-activation of the innate immune response and transcriptional perturbation of neurodevelopment genes – a hallmark in the development of microcephaly (Hamel et al. 2015; Dang et al. 2016). Collectively, the TLRs pathways are an important innate sensor to detect and respond against flavivirus infection.

1.13 Recognition of DENV and ZIKV by cGAS-STING

Both DENV and ZIKV infection also impair mitochondrial function, where viral proteins can disrupt both mitochondrial membrane potential and homeostasis (Yu et al. 2015; Ledur et al. 2020). Following viral induced mitochondrial stress, mitoDNA is released into the cytoplasm and binds to the cytosolic sensor cyclic-GMP-AMP synthase (cGAS), resulting in a conformational change and allowing cGAS to convert ATP and GTP into 2’3’-cyclic GMP-AMP (cGAMP) (Sun et al. 2013). This molecule can then be

recognised by the ER-associated protein Stimulator of Interferon Genes (STING). Activation of STING results in phosphorylation of both TBK1 and IKKε to drive expression of type I IFN and pro-inflammatory cytokines (Motwani et al. 2019) (Fig. 1.16). Not only is ZIKV replication increased within infected cGAS$^{-/-}$ PBMCs, but IFN-β production is also reduced, highlighting the importance of cGAS-STING pathway in controlling ZIKV infection (Zheng et al. 2018). In addition, DENV replication is enhanced within cell lines which lack expression of the adapter molecule STING (Aguirre et al. 2012). Altogether, the RLR, TLR and cGAS innate signalling pathways are critical for the detection of both DENV and ZIKV infection, culminating in the production of type I IFNs and subsequent upregulation of ISGs.

1.14 Activation and signalling by type I IFNs

The downstream outcome of the recognition of viral components by PRRs described above results in the production of the Interferons (IFNs) and associated ISGs, that allow induction of an antiviral state within a cell. IFN are glycoproteins and are divided into three classes (I, II and III). Within a cluster located within chromosome 9, the type I IFN class consists of 14 subtypes of IFN-α and a single gene of IFN-β, IFN-ε, IFN-φ, IFN-τ, IFN-κ and IFN-ω (Hertzog and Williams 2013). Type II IFN is solely comprised of IFN-γ, while type III IFN consists of IFN-λ1, IFN-λ2 and IFN-λ3 (Platanias 2005; Iversen and Paludan 2010). Although all IFNs have function as antiviral agents, IFN-α and IFN-β are the main IFNs produced downstream of PRR activation.

Type I IFNs bind to the ubiquitously expressed heterodimer receptor composed of IFN-α receptor 1 (IFNAR1) and IFNAR2 subunits in an autocrine or paracrine manner (de Weerd and Nguyen 2012) (Fig. 1.17). Ligand binding results in heterodimerisation of the IFN-α receptor complex, where tyrosine kinase 2 (TYK2) and janus kinase 1 (JAK1) which are associated with IFNAR1 and IFNAR2 respectively are brought into close proximity and activated by trans-phosphorylation (Lamken et al. 2004). Following tyrosine phosphorylation of the intracellular domains of IFNAR by JAK1 and TYK2, signal transducer and activator of transcription 1 and 2 (STAT1 and STAT2) are recruited and docked on the receptor. STAT1 and STAT2 are phosphorylated at tyrosine residues 701 and 690 respectively, resulting in the formation of STAT1/STAT2 heterodimers to which IFN regulatory factor 9 (IRF9) binds to form the

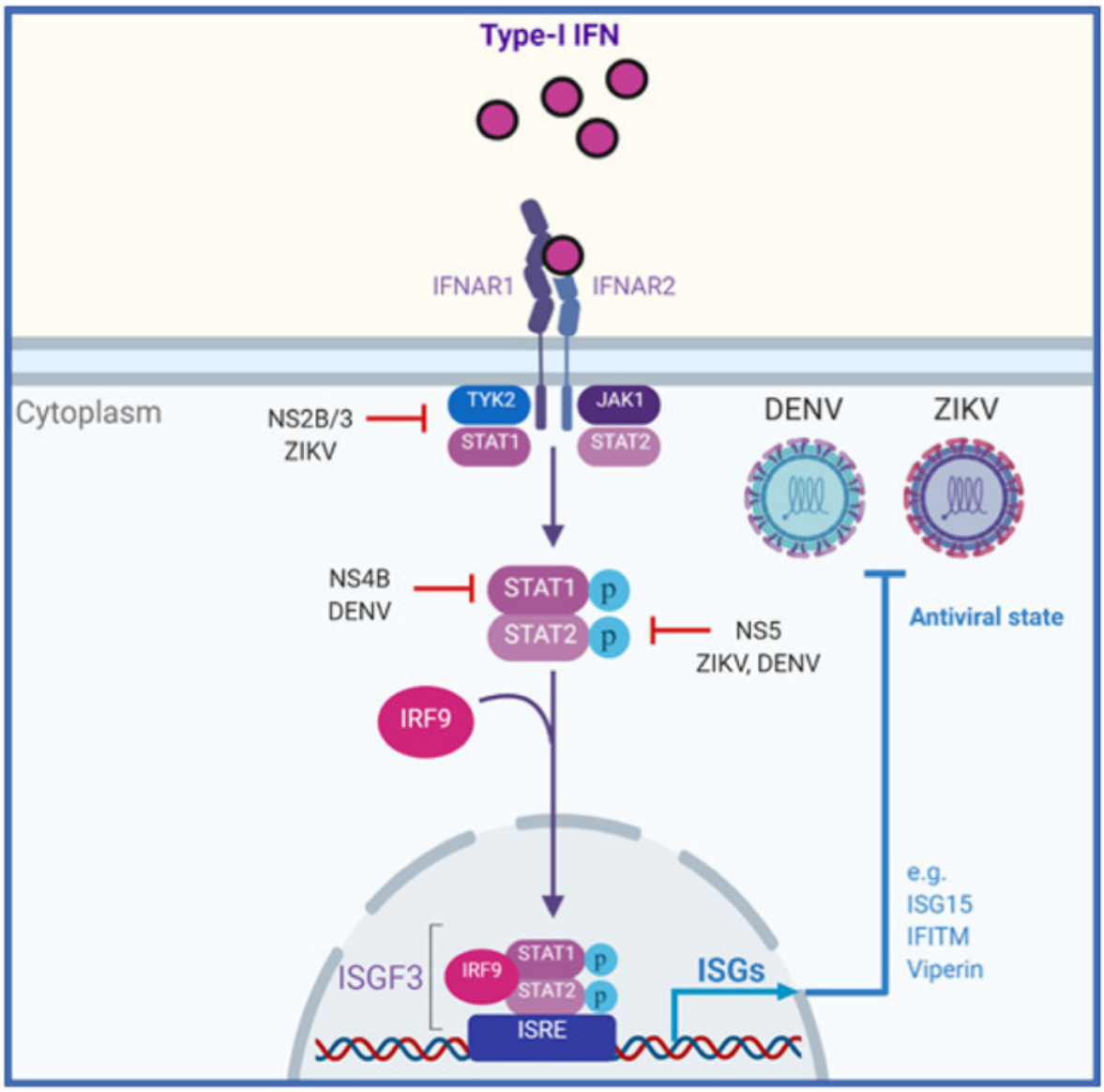

Figure 1.17: Upregulation of ISGs by the IFN pathway and subsequent inhibition mechanisms by DENV and ZIKV infection.

Type I IFN can bind their cognate receptors (IFNAR1 and IFNAR2) located on infected and neighbouring cells, activating the JAK-STAT pathway and culminating in the upregulation of hundreds of ISGs which induce an antiviral state within the cell. Both DENV and ZIKV have evolved mechanisms to inhibit multiple stages within the JAK-STAT pathway (Coldbeck-Shackley et al. 2020).

transcription complex IFN stimulated gene factor 3 (ISGF3) (Fig. 1.17) (Ivashkiv and Donlin 2014). This complex then translocates to the nucleus to bind IFN-stimulated response element (ISRE) present within the proximal promoter upstream of in excess of 300 ISGs, to initiate transcription and translation of proteins that control virus replication and activate the immune system (Kessler et al. 1990; Bluyssen et al. 1994).

1.15 Interferon Stimulated Genes (ISGs)

The definition of an ISG is a gene that is upregulated during an IFN response. They were first discovered more than 30 years ago (Knight and Korant 1979). Although a handful of classical ISGs such as PKR, OAS and Mx1 were initially thought to be the only genes displaying antiviral activity, subsequent microarray studies coupled with advances in RNA sequencing have shown that there are in excess of 300 ISGs, as approximately 10% of the human genome is subject to regulation by IFN (Schoggins et al. 2011; Shaw et al. 2017). In addition to upregulation of canonical ISGs that have direct acting antiviral activity, a small subset of ISGs can also be upregulated independently from IFN signalling by IRF or NF-κB transcription factors (Wang et al. 2017). Some ISGs are expressed basally and upregulated further by IFN while others are only induced in the presence of IFN stimulus. Although the main role of ISGs is to directly interfere with the virus lifecycle, others can augment activated innate signalling pathways, resulting in multiple mechanisms by which a single ISG can be upregulated (Fujita et al. 1989; Sato et al. 1998).

Numerous ISGs act in tandem to supress virus replication at multiple stages within the viral lifecycle (Fig. 1.18). The functions of many ISGs have been reviewed extensively elsewhere and therefore this section will be focused on ISGs which impact the DENV and ZIKV lifecycle due to their similar replication strategies (Schoggins 2019).

IFN stimulated gene 15 (ISG15) is a 15kDa ubiquitin like protein and has many roles within innate immunity that have been extensively reviewed (Perng and Lenschow 2018). The first ubiquitin-like protein to be discovered, ISG15 is a highly evolutionary conserved protein, consisting of a N-and C-terminal domain which are connected by a flexible polypeptide hinge (Dzimianski et al. 2019). The C-terminus of ISG15 also contains the LRLRGG motif, allowing for conjugation with target proteins (Lenschow

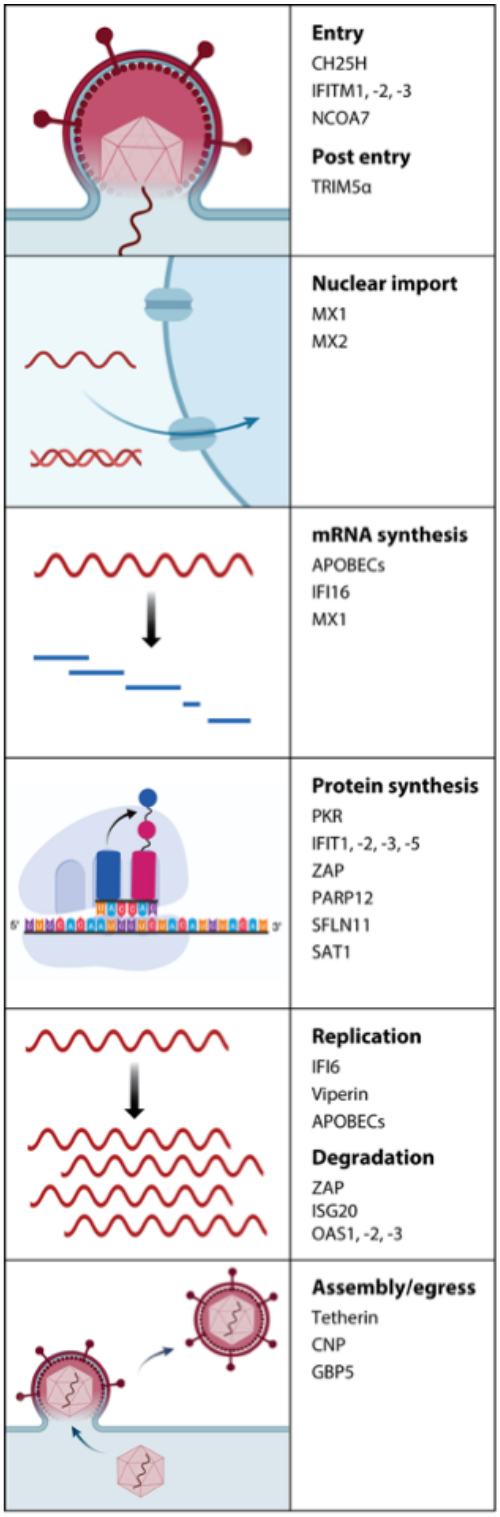

Figure 1.18 Function of ISGs

ISGs can inhibit multiple stages within a virus lifecycle (Schoggins 2019).

et al. 2005). One of the roles unique to ISG15 is its ability to conjugate with target protein (ISGylation) to disrupt localisation and interactions of the latter which may benefit virus replication. ISG15 can inhibit both the entry and replication stage of the ZIKV lifecycle while siRNA knockdown of ISG15 in infected human primary corneal epithelial cells (HCEC) results in elevated levels of DENV and ZIKV replication (Singh et al. 2019). This observation was mimicked in ISG15$^{-/-}$ mice following infection with ZIKV and also resulted in impaired expression of other ISGs such as RIG-I (which is also a PRR) and IFI6 (Singh et al. 2019).

Virus inhibitory endoplasmic reticulum associated interferon inducible protein (Viperin) is a 42kDa protein, which like ISG15, has diverse roles within the innate immune response and has direct antiviral activity against numerous viruses within multiple RNA and DNA viral families [reviewed in (Helbig and Beard 2014)] (Fig. 1.18). Viperin consists of 3 main structural elements; An evolutionary diverse N-terminal amphipathic helix and leucine zipper which allows tethering to ER membranes and association with lipid droplets, a highly conserved central domain which contains motifs belonging to the radical SAM enzyme family and a highly conserved C-terminal domain critical for antiviral activity against the *flaviviridae* family including HCV, DENV, TBEV and ZIKV, the latter which is explored in this thesis (Helbig et al. 2011; Helbig et al. 2013; Van der Hoek et al. 2017; Upadhyay et al. 2014). Viperin is one of the few ISGs which can be upregulated with or without IFN. It catalyses the conversion of cytidine triphosphate (CTP) to 3'-deoxy-3',4'-didehydro-CTP (ddhCTP), an antiviral ribonucleotide that inhibits flavivirus NS5 polymerases (DeFilippis et al. 2006; Gizzi et al. 2018). Viperin also affects the assembly of flavivirus virions by enhancing production of non-infectious capsid particles via interaction with Golgi brefeldin A-resistant guanine nucleotide exchange factor 1 (GBF1) (Vonderstein et al. 2018). During the course of this thesis, Viperin also interacts with ZIKV NS3 protein, resulting in proteasome dependent degradation of the latter and subsequently reduced virus replication, demonstrating the redundant functions present within one ISG (Panayiotou et al. 2018). In addition to its direct antiviral roles, Viperin can also augment innate signalling, through binding to STING and enhancing the type I IFN response following detection of virally derived dsDNA, resulting in an enhanced antiviral state (Crosse et al. 2020).

Proteins within the IFN-inducible transmembrane (IFITM) family are found within cellular membranes and exert their functions against virus infection via inhibition of viral membrane-endosomal fusion during the entry stage of the virus lifecycle (Bailey et al. 2014). The IFITM family consist of five proteins, three of which (IFITM1, IFITM2 and IFITM3) are inducible by both type I and II IFN (Fig. 1.18) (Lewin et al. 1991). The IFITM protein family have common structural topology, where short variable luminal N- and C-termini are separated by two anti-parallel transmembranes and connected with a conserved cytoplasmic region (Zhao et al. 2018). IFITM2 and IFITM3 have a 20aa and 21aa extension of the N-terminus compared to IFITIM1 respectively. Deletion of the 21aa extension within the N-terminus in IFITM3 resulted in impaired antiviral activity against DENV infection (John et al. 2013). In addition, siRNA knockdown of IFITM1 or IFITM3 within ZIKV infected cells resulted in elevated levels of virus replication whereas ectopically expression of IFITM2 or IFITM3 inhibited DENV replication (Jiang et al. 2010; Savidis et al. 2016b). Interestingly, all three IFITM proteins inhibit HCV replication, localising to both early and late endosomes (Narayana et al. 2015).

IFN-inducible protein 6 (IFI6) is a 13kDa is a recently discovered ISG which has been thrust into the spotlight as a top hit within genome-wide CRISPR activation screens against multiple flaviviruses (Fig. 1.18) (Richardson et al. 2018; Dukhovny et al. 2019). IFI6 is a mitochondrial targeted protein and delays apoptosis in DENV infection, potentially through the inhibition of release of cytochrome C from the mitochondria (Cheriyath et al. 2007; Qi et al. 2015). Infection of DENV and ZIKV in CRISPR KO IFI6 cells resulted in elevated levels of virus replication and that ectopic expression of IFI6 also prevented apoptosis in ZIKV infected Huh7 cells (Richardson et al. 2018). The mechanism of action is unclear but localisation of IFI6 to ZIKV replication complexes suggest that the former may disrupt virus replication or virion production (Dukhovny et al. 2019).

1.16 Immune evasion by the *flaviviridae* family

Given that viruses are obligate intracellular pathogens, viruses have evolved multiple mechanisms to subvert activation of innate immune signalling cascades. Viruses within the *flaviviridae* family can either passively conceal their viral molecules by

mimicking host cell components or directly antagonise or disrupt innate signalling pathways.

1.16.1 Passive mechanisms to hide from innate immune response

Upon release of the viral genomic RNA (gRNA) into the cytoplasm post entry, a 7-methylguanylate cap is present within the 5' end of the viral positive sense RNA genome (Decroly et al. 2011). This assists in the binding of host translation initiation factors required for production of the viral polyprotein and establishment of the replication complex. In addition, the gRNA mimics the appearance of host mRNA and prevents its degradation by cytoplasmic exonucleases (Saeedi and Geiss 2013). Furthermore, capping of flavivirus gRNA prevents recognition by both PRRs such as MDA5 and ISGs including IFIT1 which can bind and sequester gRNA of uncapped flavivirus genomes (Kimura et al. 2013). Flaviviruses can also 'hide' from the innate immune response through the construction of a replication complex (RC) during virus replication, here modified ER membranes act as a barrier between gRNA and cytoplasmic PRRs preventing recognition of both gRNA (Scutigliani and Kikkert 2017) and the forming viral nucleocapsid by the ISG MxA (Hoenen et al. 2007).

1.16.2 Direct antagonism of innate immune response by viral proteins

Although the main role of the NS proteins within the flavivirus lifecycle is to establish active virus replication and assembly of new progeny, these proteins also act to sever innate immune signalling pathways preventing the production of IFN and subsequent upregulation of ISGs. Viral NS proteins employ many diverse mechanisms to disrupt the PRR and IFN JAK STAT signalling pathways and these are summarised for DENV and ZIKV infection below.

Competitive binding is a common mechanism utilised by both DENV and ZIKV NS proteins to block innate signalling (Fig. 1.16). ZIKV NS4A is able to inhibit RLR signalling by both RIG-I and MDA5 via competitive binding to the N-terminal CARD domain of the common adapter protein MAVS, resulting in decreased IFN production (Ma et al. 2018; Ngueyen et al. 2019). ZIKV NS1 and NS4B also directly interact with TBK1, blocking phosphorylation and oligomerisation required for activation of IRF3 and subsequent IFN production (Wu et al. 2017). ZIKV NS5 is also able to interact

with not only the other prominent kinase required for IRF3 activation, IKKε but also IRF3 itself. ZIKV NS5-IKKε interactions result in both decreased protein levels and phosphorylation of IKKε, again preventing activation of IRF3 and subsequent IFN production (Xia et al. 2018; Lundberg et al. 2019). DENV NS2B/3 also interacts with IKKε and is predicted, via computational analysis, to mask the kinase domain of the latter inhibiting activation of downstream transcription factors (Angleró-Rodríguez et al. 2014).

In addition to above, ZIKV NS proteins are also able to bind to other innate immune signalling factors (Fig. 1.16). ZIKV NS3 interacts and competitively binds with members of the 14-3-3 family, where several (14-3-3ε and 14-3-3η) are mitochondria targeting chaperones allowing for translocation of activated RIG-I and MDA5 to MAVS anchored to the mitochondria membrane (Liu et al. 2012a; Lin et al. 2019b). This interaction is mediated by an aspartic acid residue located within a conserved binding motif present within ZIKV NS3 that when phosphorylated outcompetes binding of both 14-3-3ε and 14-3-3η to RIG-I and MDA5 (Riedl et al. 2019).

Another mechanism by which DENV and ZIKV NS proteins inhibit innate signalling is through the promotion of degradation of key signalling proteins. ZIKV NS1 possesses no de-ubiquitinase activity and therefore interacts with the host ubiquitinase USP8 to cleave K11-linked polyubiquitin chains from caspase-1. This conformational change confers stability to caspase-1 and results in proteolytic cleavage of cGAS and subsequent decreases in IFN production (Zheng et al. 2018). Both DENV and ZIKV NS5 is able to interact with STAT2, resulting in the degradation of the latter in a proteasome mediated manner (Fig. 1.17) (Ashour et al. 2009; Grant et al. 2016). This interaction is mediated by the RdRp domain of both DENV and ZIKV NS5 with the N-terminal domain of STAT2 (Wang et al. 2020). However, unlike ZIKV, DENV NS5 mediated degradation of STAT2 is dependent on the E3 ubiquitin ligase UBR4 (Morrison et al. 2013). ZIKV NS2B3 also induces proteasome mediated degradation of JAK1, resulting in deceased ISG expression (Wu et al. 2017). DENV NS2B induces degradation of cGAS by an autophagy-lysosome dependent mechanism to prevent activation of the latter by mitoDNA release during DENV infection (Fig. 1.16) (Aguirre et al. 2017). In addition, both DENV and ZIKV NS2B/3 are also able to cleave the adapter molecule of cGAS, STING. Two key residues (R78 and G79) in human STING

are crucial for cleavage by not only DENV and ZIKV NS2B3, but also JEV and WNV NS2B3. This evolutionary conserved mechanisms by which flaviviruses inhibit the cGAS-STING pathway highlight the importance of this innate signalling pathway for detection of this virus genus.

1.17 Hypothesis and Aims

Rationale

Viruses in general rely heavily on cellular host factors for efficient replication and spread. In contrast, following viral infection, activation of the innate immune response increases the expression of hundreds of genes that aim to not only limit viral replication but also shape the adaptive response. While our knowledge of proviral and antiviral cellular factors has expanded over recent years for the *flaviviridae* family of viruses, our understanding is not complete. The explosion of CRISPR technology has significantly enhanced our ability to modify cellular genomic sequences to efficiently knockout specific alleles. However, recent development of CRISPR technology now allows for genome-wide knockout screening for proviral host factors, which overcomes the limitations of widely used siRNA screens and may allow for the identification of novel proviral host factors for the *flaviviridae* life cycle. Identification of novel host factors will further our understanding of flavivirus biology and possibly identify novel targets for antiviral therapeutics. Moreover, identification of cellular antiviral strategies further enhances our understanding of the complex interplay between viral and host.

Hypothesis

The ability of viruses within the *flaviviridae* family to infect and establish replication involves numerous as yet, unidentified host factors which remain to be characterised. Furthermore, the interferon stimulated gene, Viperin, which has antiviral activity against numerous members of the *flaviviridae* family also negatively impacts ZIKV replication.

Aims

The overall aim of this thesis is to identify novel host factors which both positively and negatively influence *flaviviridae* replication.

1. To develop and optimise a CRISPR genome-wide knock out screening protocol (GeCKO LentiCRISPRv2) for the identification of novel proviral host factors for HCV (Chapter 3) and ZIKV and related flaviviruses (Chapter 4).
2. Determine the mechanism of action of novel proviral host factors identified from the genome-wide CRISPR screen (Chapter 4).
3. Characterise the cellular innate immune response to ZIKV infection in multiple relevant cell types and in particular, the antiviral activity against ZIKV by the ISG viperin (Chapter 5).

Chapter 2 - Materials and Methods

2.1 General Molecular Methods

2.1.1 Synthetic oligonucleotides

Synthetic oligonucleotides/primers to be used in PCR, Sanger sequencing or LentiCRISPRv2 cloning were ordered from Sigma at PCR/sequencing purity grade (see primer sequences in Appendix I). All primers were ordered resuspended in 100µm stock with TE buffer and stored at -20°C.

2.1.2 Bacterial transformation

The frozen α-Select Chemically Competent *E. coli* cells were purchased from Bioline for bacterial transformation for canonical plasmid construct generation. Competent cells were thawed on ice and 50µl aliquots per transformation placed within a pre-chilled microcentrifuge tube. Approximately 10ng of plasmid DNA or 5µl of ligation product was added to the competent cells and tube gently mixed by tapping and incubated on ice for 30 minutes. The mixture was heat shocked for 30 seconds prior to immediate incubation in ice for 2 minutes. 450µl of SOC medium (see Appendix II) was added to the transformation reaction and incubated at 37°C for 1 hour. To transform intact plasmid DNA, 50µl was added straight to an appropriate antibiotic coated agar plate and spread and incubated overnight at 37°C. If transformation the ligation product, cells were centrifuged at 2000 x g for 3 minutes, where 450µl of the SOC medium removed and the entire pellet resuspended and spread to an appropriate antibiotic coated agar plate and incubated overnight at 37°C.

2.1.3 Small scale plasmid DNA extraction (mini-preparation)

A single transformed bacterial colony was inoculated with 5ml of LB broth containing appropriate antibiotic prior to incubation with shaking at 200-250 rpm at 37°C overnight. Following centrifugation at 5,000 × g for 5 minutes, the LB broth was removed and the NucleoSpin Plasmid Kit (Macherey-Nagel) was used. Briefly, bacterial pellets were resuspended in 250µl containing ribonuclease A (*RNase*A). 250µl of buffer A2 was added to lyse the bacteria for 5 minutes prior to neutralisation with 300µl of buffer A3. All centrifugation steps were performed at 11,000 x g. The mixture was spun for 5

minutes and supernatant transferred to the mini spin column to be centrifuged for an additional 5 minutes. The column was washed with 600µl buffer A4 and centrifuged for 1 minute before further centrifugation for 2 minutes to dry the column. 50µl of buffer AE was added to the column and centrifuged for 1 minute to elute the plasmid DNA.

2.1.4 Large scale plasmid DNA extraction (maxi-preparation)

A single transformed bacterial colony was inoculated into 200ml of LB broth containing the appropriate antibiotic and the culture incubated with shaking at 37°C overnight. The bacterial culture was pelleted by centrifugation at 5,000 × g for 15 minutes using an AvantiTM J-25I Beckman Coulter JA-25.50 fixed-angle rotor. Plasmid DNA extraction was performed using a NucleoBond Xtra Maxi Kit (Macherey-Nagel) as per manufacturer's instructions. Briefly, bacterial pellets were resuspended in 12ml of RES buffer containing ribonuclease A (*RNase*A). The mixture was 12ml incubated with 12ml of LYS buffer and gently mixed by inverting the tube and incubated at room temperature (RT) for 5 minutes. 12ml of NEU buffer was added to the mixture and mixed by inverting 10-15 times before transferring to a pre-equilibrated NucleoBond Xtra column with filter. 15ml of EQU buffer was added to the column. The filter discarded prior to the addition of 25ml of WASH buffer. Plasmid DNA was eluted with 15ml of ELU buffer and subsequently precipitated with 10.5ml of cold isopropanol. The precipitated plasmid DNA was pelleted by centrifugation at 15,000 × g, 4°C for 30 minutes using an AvantiTM J-25I Beckman Coulter centrifuge (JA25.50 rotor). The pellet was washed with 70% ethanol and resuspended with an appropriate volume of TE buffer.

2.1.5 Restriction endonuclease digestion

Restriction enzymes were obtained from New England Biolabs (NEB). Restriction enzyme digestions were performed in a 20µl total volume, which contained 1µg of plasmid DNA or 5µl of ligation reaction (see section 2.1.7), 10 units of restriction enzyme(s) and 1× appropriate NEBuffer. The digestion reactions were incubated at 37°C overnight prior to visualisation on a 1% agarose gel (see section 2.1.6).

2.1.6 Agarose gel electrophoresis

Agarose gel electrophoresis was performed using 1% w/v agarose gel. The gels were prepared by dissolving molecular grade agarose (Bioline) in 1× TAE buffer (see Appendix II) and 3μl of Redsafe Nucleic Acid Staining Solution (iNtRON) per 100ml of 1% agarose solution. Gels were cast in a BioRad® Sub-Cell GT Minitank. DNA samples were mixed with 6× Loading dye (NEB) and loaded into wells on the agarose gel. Electrophoresis was performed at 100 Volts. To estimate product size, 0.5μg of 1 kb, 100 bp or 2log DNA marker (NEB) were run simultaneously dependent on the expected band size. Following electrophoresis, DNA bands were visualised under the UV Transilluminator (BioDoc-ItTM Imaging System, UVP) using Quantity One Version 4.6 Basic software (BioRad).

2.1.7 DNA ligation

Ligation reactions were performed using the Quick Ligation Kit (NEB). Ligation mixtures contained 50ng of digested plasmid, a 3-fold molar excess of the similarly digested insert DNA, 10μl of Quick Ligation Reaction Buffer (2×) and 1μl of Quick T4 DNA Ligase (2,000 Units/μl) and dH_2O to a final volume of 20μl. The reaction was incubated at RT for 5 minutes and chilled on ice before utilisation in bacterial transformation (see section 2.1.2).

2.1.8 Gibson Assembly

15μl of 2x Gibson Assembly reactions (see appendix II) were pre-aliquoted in PCR tubes and mixed with 50ng of digested plasmid, a 2-fold molar excess of each insert DNA and dH_2O to a final volume of 20μl. The reaction was incubated at 50°C for 30 minutes and chilled on ice before utilisation in bacterial transformation (see section 2.1.2).

2.1.9 DNA purification from agarose gel

DNA bands were purified from agarose gels using an ISOLATE II PCR and Gel Kit (Bioline) according to manufacturer's recommendations. Briefly, the DNA fragment was excised from the gel with a clean, sharp scalpel and gel slices mixed with 2 volumes of binding buffer CB (100mg of the gel slice was equal to 100μl) and the agar melted at 50°C for 5-10 minutes until the gel slice was completely dissolved. The

mixture was added to collection tubes and centrifuged at 11,000 x g for 30 seconds. After the flow-through was discarded, the collection tube was washed with 700μl of wash buffer CW and also centrifuged for 11,000 x g for 30 seconds. After an additional centrifugation of 11,000 x g for 1 minute to dry the membrane within the column, 15μl of elution buffer C was added to the collection tube and centrifuged at 11,000 x g for 1 minute to elute the DNA.

2.1.10 DNA sequencing

DNA sequencing (Sanger sequencing) was performed by the Australian Genome Research Facility (AGRF, Australia). Samples were prepared according to the sample submission guidelines, which consisted of 1μg of plasmid DNA, 9.6pmol of an appropriate forward or reverse primer and adjusted to 12 μl with dH_2O. DNA sequencing results were analysed using SnapGene and compared to sequences in the Genbank database using the Basic Local Alignment Search Tool (BLAST) from the National Center for Biotechnology Information website (http://www.ncbi.nlm.nih.gov/blast/Blast.cgi).

2.1.11 Total RNA extraction

Total cellular RNA was extracted using TRIzol Reagent (Life Technologies) and the manufacturer's protocol followed. Briefly, cells grown in a monolayer in 12-well or 24-well culture trays (Corning Life Sciences) were washed once with PBS and lysed by adding 0.5ml of TRIzol Reagent per well of a 12-well tray and adjusted accordingly for other tray sizes. Cell lysates were transferred to RNase-Free 1.5ml microcentrifuge tubes (Eppendorf). One-fifth volume of chloroform (0.1 ml for 0.5ml of TRIzol) was added to the preparation and incubated at RT for 2-3 minutes, and subsequently centrifuged at 12,000 × g at 4°C for 15 minutes. The top aqueous layer was transferred to a new tube. Total RNA was precipitated by adding 0.5 volume of cold isopropanol, mixed well and incubated at RT for 10 minutes. The RNA pellet was precipitated by centrifugation at 12,000 × g at 4°C for 10 minutes and washed with 1 volume of 75% (v/v) ethanol in RNase-free dH_2O. After centrifugation at 7,500 × g at 4°C for 5 minutes, the total RNA pellet was air-dried at RT. The RNA pellet was dissolved in 10μl of RNase-free dH_2O. RNA samples were kept at -80°C until use.

2.1.12 Nucleic acid quantification

DNA or RNA samples were quantified using the Nanophotometer (Implen GmbH). The absorbance at 260nm was read and concentrations of samples were calculated using the following formula:

$$Nucleic\ Acid\ (\mu g/ml) = A\_260nm \times dilution\ factor\ \times 50\ (DNA)\ \ or\ 40\ (RNA)$$

The purity of nucleic acids was determined by measuring the ratio of the absorbance at 260nm and 280nm (A_{260}/A_{280}). The DNA and RNA preparations used in this study generally had an A_{260nm}/A_{280nm} of 1.8 and 2.0, respectively.

2.1.13 First-strand cDNA synthesis

First-strand cDNA was produced from the total RNA using M-MLV Reverse Transcriptase RNase H minus, point mutant (Promega). The reaction was performed in a pre-chilled RNase-free microcentrifuge tube containing 1μg of total RNA, 50ng of random hexamer primer (IDT) or oligoDT primer (Invitrogen) and RNase-free dH_2O to a final volume of 14 μl. The mixture was incubated within the thermocycler (S1000TM, BioRad) at 70°C for 5 minutes. The tube was cooled down at 4°C for a further 5 minutes and the following mixture was added consisting of 5μl of 5× M-MLV RT Reaction Buffer (Promega), 1.25μl of 10mM each dNTP mix (Promega), 0.5μl of 40 Units/μl RNAsin RNase Inhibitor (Promega), 1μl of 200 Units M-MLV RT, RNase H (-) Point Mutant (Promega) and 3.25 μl dH_2O was added to the tube. Samples were incubated at RT for 10 minutes, then 42°C for 50 min within the thermocycler. Finally, samples were diluted to a final volume of 100 μl with dH_2O and stored at -20°C for PCR (see section 2.1.14) or qPCR (2.1.15).

To generate cDNA transcripts longer than 1kb, the Superscript III First-Strand Synthesis System (Thermo Fisher Scientific) was used and the manufacturer's recommended protocol followed. Briefly, 1μg of RNA was mixed with 1μl of 2μm gene-specific primer, 1μl of 10mM dNTP mix and RNase-free dH_2O to a total volume of 10μl in a RNase free PCR tube. The mixture was incubated at 65°C for 5 minutes and placed on ice for 1 minute before the addition of the cDNA synthesis mix which consisted of 2μl of 10x RT buffer, 4μl of 25mM $MgCl_2$, 2μl of 0.1M DTT, 1μl of 40U/μl

RNaseOUT and finally 1μl of 200U/μl SuperScript III RT. The mixture was incubated at 25°C for 10 minutes, 50°C for 50 minutes and reaction terminated at 85°C for 5 minutes. 1μl of RNase H was added and tubes incubated at 37°C for 20 minutes and stored at -20°C.

2.1.14 Polymerase Chain Reaction (PCR)

PCR reactions were performed using a thermal cycler (S1000TM, BioRad). Q5 High-Fidelity DNA polymerase enzymes (NEB) was mainly used for cloning purposes, due to the possession of high fidelity. The reactions were prepared in a PCR tube containing 12.5μl of Q5 High-Fidelity 2× Master Mix, 1.25μl each of 20μM forward and reverse primers, 1ng of DNA template and dH_2O to a final volume of 25 μl. PCR thermal cycling conditions consisted of initial denaturation at 98°C for 30 seconds, followed by 30 cycles of 98°C for 10 seconds, an appropriate annealing temperature for 30 seconds, 72°C for 20-30 seconds/kb and finally, a final extension at 72°C for 2 minutes. The PCR reactions were visualised by agarose gel electrophoresis (see section 2.1.6) or stored at 4°C.

2.1.15 Real-Time Quantitative PCR (qRT-PCR)

Quantitative real-time PCR was used to determine relative levels of the target RNA via the comparative CT method. qRT-PCR reactions were performed with the Luna Universal One-Step RT-qPCR Kit (NEB), where the manufacturer's recommended protocol was followed. Briefly, each reaction consisted of 5μl of 2x Luna Universal One-Step Reaction Mix, 0.2μl each of 20μM forward and reverse primers (see Appendix II), 1.6μl of nuclease free dH_2O and 0.5μl of Luna WarmStart RT Enzyme Mix. All samples were analysed in duplicate and also processed to quantify the RPLPO housekeeping gene in parallel to normalise input cDNA levels. An ABI StepOnePlus Real-Time PCR System (Applied Biosystems) coupled with the ABI PRISM 7000 SDS Software was used to control the reaction and cycling conditions consisted of reverse transcription at 55°C for 10 minutes prior to initial denaturation at 95°C for 1 minute followed by 40 cycles of 95°C for 10 seconds and 60°C for 1 minute. A final step of 95°C for 15 seconds, 60°C for 1 minute, followed by increasing the temperature by 0.5°C increments up to 95°C was performed to facilitate the melting curve. Data were

analysed using the StepOne v2.2 software and the threshold was set at 0.2 for all experiments.

2.1.16 Extraction of cellular proteins

Whole cell lysates were extracted from 80-90% confluent cell monolayers in 12-well trays. Culture media was first removed and cells washed with PBS prior to the addition of pre-chilled RIPA buffer or NP-40 buffer (200μl) (see Appendix II) containing protease inhibitor cocktail (Sigma Aldrich). Cell lysate was then transferred to a 1.5 ml microcentrifuge tube and placed on ice for 20 min. Whole cell lysates were centrifuged at 21,000 × g at 4°C for 10 minutes and the supernatant collected and used for further experiments or stored at -20°C.

To extract organelle fractionated whole cell lysates, cells were trypsinised (see section 2.3.2), resuspended with culture medium into microcentrifuge tubes and centrifuged at 500 x g for 5 minutes. The cell pellet was washed once with PBS by centrifugation prior to incubation with pre-chilled digitonin lysis buffer (see Appendix II) containing protease inhibitor cocktail (Sigma Aldrich) for 10 minutes. The whole cell lysates incubated with digitonin lysis buffer were centrifuged at 2,000 x g for 10 minutes and the cytosolic containing supernatant transferred to microcentrifuge tubes. The cellular pellet was washed once with PBS by centrifugation prior to incubation with pre-chilled NP-40 lysis buffer (see Appendix II) containing protease inhibitor cocktail (Sigma Aldrich) for 20 minutes. The whole cell lysates incubated with NP-40 lysis buffer were centrifuged at 2,000 x g for 10 minutes and the membranous organelle containing supernatant collected and used for western blot (see section 2.1.17) or stored at -20°C.

2.1.17 Western Blot

Protein samples were prepared by boiling for 5 min with 1× SDS PAGE sample buffer (see Appendix II) before loading onto the gel (Mini Protean 4-15% Precast Gels, Bio-Rad) alongside 5μl Precision Plus Protein Standards-Kaleidoscope (Bio-Rad). Gels were run in SDS-PAGE running buffer (see Appendix II) at 100 Volts for 90 minutes. Proteins were transferred onto nitrocellulose membrane via assembly with the Trans-Blot Turbo RTA Mini 0.2μm Nitrocellulose Transfer Kit (Bio-Rad) and utilisation of the Trans-Blot Turbo Transfer system (Bio-Rad) per manufacturer's instructions. The

transfer setting used was MINI-MIXED MW with 1.3 Amps, 25 Volts for 7 minutes. Following protein transfer, membranes were blocked with 5% skim milk in 0.1% TBS-T for 1 hour with gentle agitation prior to incubation with primary antibody at the appropriate dilution in 1% skim milk (see Appendix III) overnight at 4°C. Membranes were washed three times, each time for 5 minutes in 0.1% TBS-T with gentle agitation to remove unbound primary antibody before incubation with the appropriate horseradish peroxidase-conjugated secondary antibody for 1 hour and washed five times, each time for 10 minutes in 0.1% TBS-T with gentle agitation. HRP detection was carried out using the Clarity ECL Western Blotting Substrate (Bio-Rad) or the Supersignal West Femto Maximum Sensitivity Substrate detection kit (Thermo Fisher Scientific) with chemiluminescent detection as per manufacturer's instructions. Protein bands were visualised by a Chemi-DocTM MP Imaging System (Bio-Rad).

2.1.18 Co-immunoprecipitation

Whole cell lysate was harvested from cell monolayers as described in section 2.1.16. 0.5μg of the appropriate antibody was added to each sample and incubated overnight on a rotator at low speed at 4°C overnight. The Protein A MagBeads MX (GenScript) (50μl per sample) were washed with wash buffer (see Appendix II) twice with the MagnaRack (Invitrogen) and resuspended to the desired volume with wash buffer (50μl per sample). 50μl of Protein A MagBeads were added to each antibody bound whole cell lysate sample and placed on a rotator at low speed at RT for 1 hour. The beads were collected on the MagnaRack and the supernatant removed. Each sample was washed 5 times with wash buffer prior to incubation with 80μl of 2x SDS-PAGE loading buffer (see Appendix II) at 100°C for 10 minutes. The supernatant was collected utilising the MagnaRack followed by Western Blot analysis as per section 2.1.17.

2.1.19 Dual Luciferase Assay

Firefly and Renilla luciferase activity were measured using the Dual Luciferase Assay System (Promega). Cells were seeded into 24-well or 48-well trays, cultured overnight and co- transfected with the plasmid of interest (500 ng), ISRE-luc or IFN-β-Luc (500 ng) and pRL-TK (10 ng). Cells were treated with IFN-α (for ISRE-luc) or poly I:C (for IFN-β-Luc) at the indicated time points the following day and then washed once with

PBS. 5× Passive Lysis Buffer (Promega) was diluted to 1× lysis buffer with MilliQ water, and 80μl of 1x Passive Lysis Buffer was added to each well followed by a single freeze-thaw to harvest the cell lysate. 20μl of cell lysate was then added to an Opti-plate 96 (Perkin Elmer) and luciferase output measured on a GloMax Microplate Luminometer (Promega). Data were analysed using GraphPad Prism 6 software.

2.1.20 Nano-luciferase Assay

Nano-luciferase activity were measured using the Nano-Glo Luciferase Assay System (Promega). Cells were seeded into 48-well trays, cultured overnight and infected with DENV-NS1-NLuc (Eyre et al. 2017a) at the appropriate MOI for 3 hours at 37^{o}C and 5% CO_2. The culture medium was removed and cultured with fresh culture medium at the desired time point. To detect nano-luciferase activity within supernatant, 2x Passive Lysis Buffer (Promega) was added to the supernatant at a 2 Passive Lysis Buffer:3 supernatant ratio. To detect nano-luciferase activity within the cell monolayer, cells were washed once with PBS prior to the addition of 50μl of 1x Passive Lysis Buffer per well followed by a single freeze-thaw to harvest the cell lysate. 20μl of cell lysate was then added to an Opti-plate 96 (Perkin Elmer) and luciferase output measured on a GloMax Microplate Luminometer (Promega). Data were analysed using GraphPad Prism 6 software.

2.1.21 Duolink In-situ Proximity Ligation Assay

Cells were seeded into 48-well trays and cultured overnight prior to transient transfection with desired plasmids. Cells were fixed the following day with cold acetone:methanol (1:1) for 5 minutes and washed 3 times with PBS. Proximity ligation assays (PLA) were conducted using the Duolink in situ kit (Olink Biosciences) as per manufacturer's instructions. Briefly, cells were blocked with 5% BSA in PBS for 1 hour at RT and washed 3 times with PBS. A mixture of desired primary antibodies (different species such as mouse and rabbit) was added and the plate was incubated for 1 hour at RT before 5 washes with PBS. An isotype control for each primary antibody species was used as a negative control. PLA probe mixture (anti-mouse minus and anti-rabbit plus) in 1% BSA was added to the wells and the plate was incubated at 37°C in a humidity chamber for 1 hour. The humidity chamber was constructed by placing wet paper towels onto the bottom of a black container. Cells were washed with wash buffer

A (Olink Biosciences) 2 times for 5 minutes each. The ligation solution was prepared by mixing 8μl of 5× ligation stock, 31μl of dH_2O and 1μl of ligase. 40μl of ligation solution was added to wells and incubated at 37°C in humidity chamber for 30 minutes. The plate was washed 2 times with wash buffer A for 2 minutes each. An amplification step was performed by adding the mixture of 8μl of 5× amplification stock, 31.5μl of dH_2O and 0.5μl of polymerase to the wells and incubating at 37°C in a humidity chamber for 1 hour. The reaction was washed 2 times with wash buffer B (Olink Biosciences) for 10 minutes each, before a final wash with 0.01× wash buffer B for 1 min. Nuclear DAPI staining was performed after proximity ligation assay. The cells were visualised by fluorescence microscopy (see section 2.5.4) and a red dot indicated a protein-protein interaction.

2.1.22 *In vitro* RNA transcription

The HCV SGR RNA for transfection into Huh7.5 cells was synthesised using a T7 High Yield RNA Synthesis Kit (NEB) per manufacturer's recommended protocol. Prior to *in vitro* RNA transcription, the HCV pSGRm-JFH1-Bla was digested with *Pme*I overnight. The RNA synthesis mixture was prepared in a pre-chilled PCR tube and comprised of 2μl of each ATP, CTP, GTP, UTP, 2μl of 10× Reaction Buffer, 2μl of T7 RNA polymerase enzyme and 1μg of *Pme*I digested pSGRm-JFH1-Bla in a total volume of 20μl. The preparation was thoroughly mixed and incubated at 37°C for 3 hours. After incubation, samples were subsequently treated with 1μl (2 Units) of TURBO DNAseTM (Ambion®) for 15 minutes at 37°C. Reactions were transferred to pre-chilled RNAse free microcentrifuge tubes to perform RNA extraction (section 2.1.11). The concentration of RNA was measured using a UV spectrophotometer Nanophotometer® (Implen GmbH) and RNA integrity was checked by 1% agarose gel electrophoresis (section 2.1.6).

2.1.22 Plaque assay

Virus infectivity was determined by plaque assay as described previously (Van der Hoek et al. 2017). Briefly, Vero cells in 24-well plates were infected with 200 μl of serially-diluted virus-containing supernatants for 1 hour at 37 °C before the addition of 1ml overlay of complete media containing 1.5% (w/v) carboxymethylcellulose (CMC) (Sigma Aldrich) and cells returned to culture for various days dependent on the virus

(5 days for ZIKV and WNV_{KUN}, 2 days for HSV). The plate was flooded with 10% formalin for 1 hour before removal of the CMC overlay with PBS and crystal violet solution (see Appendix II) added to the well for 20 minutes. Wells were washed with dH_2O and plaques counted and virus infectivity expressed as plaque-forming units (PFU) per ml with the formula below:

$$\frac{number\ of\ plaques}{diution\ factor\ (10^x) \times volume\ added\ (0.2ml)}$$

2.1.23 Flow cytometry

Cells of interest were trypsinised and resuspended in complete cell medium prior to centrifugation at 1,000 x g for 5 minutes. All subsequent steps were incubated at 4°C. After 1 wash with PBS, cells were fixed in 100µl of 4% paraformaldehyde per sample for 20 minutes prior to centrifugation at 500 x g for 5 minutes. All subsequent centrifugation steps were performed at 500 x g for 5 minutes. The 4% paraformaldehyde was removed and 100µl of 0.1% Triton X-100 was added to permeabilise cells. After centrifugation, 100µl of 5% BSA in PBS was added prior to staining with the desired primary antibody (anti NS5A – 1/5 dilution/anti-CD81 1/100 dilution) for 1 hour and cells washed once with PBS. The desired secondary antibody (anti-mouse Alexa Fluor 488 – Life Technologies) was incubated with the cells for 1 hour and cells washed twice with PBS. The cell pellet was resuspended in 1% paraformaldehyde and run through a 70µm cell strainer (Corning Life Sciences) prior to flow cytometry. Stained cells were acquired on BD LSR II and FACSAria flow cytometer (BD Biosciences).

2.2 Construction of CRISPR lentiviral library

2.2.1 Expansion of CRISPR plasmid DNA library

The GeCKO LentiCRISPRv2 library was purchased from Addgene and delivered with the library dissolved in TE buffer. To expand the library, Endura Electrocompetent cells (Lucigen) were thawed on ice and 25µl aliquoted into pre-chilled microcentrifuge tubes. 2µl of 50ng/µl library A or B was added to electrocompetent cells and mixed gently before addition into a chilled 0.1cm Gene Pulser electroporation cuvette (Bio-Rad). The cuvette was quickly flicked downwards to deposit cells across the bottom of the

well. The plasmid/cell mixture was quickly pulsed with the following parameters: 10μF, 600 Ohms and 1800 Volts using a Gene Pulser XcellTM (Bio-Rad). 975μl of recovery medium was added directly to the cuvette and pipetted up and down three times to resuspend cells and transferred into microcentrifuge tubes. Tubes were incubated on an orbital shaker at 250rpm for 1 hour at 37^{o}C. Four electroporations were performed per half library and pooled together prior to spreading. The entire mixture was spread on 20 20cm ampicillin coated agar plates (400μl per plate) and plates incubated overnight at 32^{o}C to reduce plasmid recombination. 10μl of the mixture was diluted with 1ml of recovery media and 20μl spread onto a 10cm agar plate with ampicillin to deduce transformation efficiency. Transformation efficiency was calculated the following day and total colonies must exceed $3x10^{6}$ to enable complete representation of the library.

Colonies were scraped with the addition of 500μl of LB broth and a cell spreader and bacterial suspension collected into Falcon tubes (Thermo Fisher Scientific). After centrifugation at 5,000 x g for 15 minutes, the bacterial pellet was weighed and 0.45g of pellet transferred to one maxi-preparation column and plasmid extraction performed per section 2.1.4.

2.2.2 Generation of lentivirus from the CRISPR plasmid DNA library

To generate sufficient lentivirus to enable complete representation of the GeCKO LentiCRISPRv2 library, an upscaled version of section 2.3.8 was followed. Briefly, 10 20cm^{2} dishes consisting of HEK293T cells at 90% confluency were transfected with Lipofectamine 2000 per section 2.3.6. For each dish, Tube A consisted of 20μg of GeCKO LentiCRISPRv2 library A or B, 15μg of psPAX2 (Addgene) and 10μg of pMD2.G (Addgene) and 4ml of Opti-MEM (Gibco). Tube B consisted of 100μl of Lipofectamine 2000 and 4ml of Opti-MEM. After incubation for 5 minutes at RT, contents of tube B were added to tube A and mixed gently. After 20 minutes of incubation at RT, the transfection mixture was added to each dish and fresh culture media replaced the following day. Lentiviruses within the supernatant were harvested 72 hours post transfection and filtered through a 0.45μm filter membrane and stored at -20^{o}C.

2.2.3 Titration of the lentiviral GeCKO LentiCRISPRv2 library

To deduce the concentration of lentivirus generated in section 2.2.2, functional titration was performed utilising puromycin. Briefly, cells which will be transduced for genome-wide screening were seeded within a 12-well tray and transduced with a dilution series of lentivirus encoding the GeCKO LentiCRISPRv2 library. Cells were trypsinised the following day per section 2.3.2 and half of the cells were placed in one 12 well and the other in another 12 well. Following 3 days of incubation, puromycin was added only to half the cells at the appropriate dilution necessary to ensure cell death of un-transduced cells (3µg/ml for Huh7.5), leaving the duplicate well selection free. Following complete cell death of the mock transduced control cells, cells were trypsinised again and counted using a haemocytometer per section 2.3.3. The following formula was used and the closest dilution which yielded 0.3 was upscaled accordingly for genome-wide screening.

$$\frac{Cell\ count\ in\ puromycin\ treated\ well}{Cell\ count\ in\ non-puromcyin\ treated\ well}$$

2.3 Tissue Culture Techniques

2.3.1 Tissue culture medium

All mammalian cell lines excluding HTR8/SVneo were maintained in Dulbecco's Modified Eagle Medium (DMEM) containing 25 mM HEPES (Gibco). Standard DMEM was supplemented with 10% (w/v) foetal calf serum (Corning Life Sciences), Penicillin (Invitrogen; 100 U/ml) and Streptomycin (Invitrogen; 100µg/ml). Blasticidin-HCL 5µg/ml (Invitrogen), Puromycin 3µg/ml (Sigma-Aldrich) or Geneticin (G418) 800µg/ml (Invitrogen) were added for selection and maintenance of stable cell lines.

The HTR8/SVneo were maintained in Roswell Park Memorial Institute (RPMI) 1640 medium (Gibco) and supplemented with 10% (w/v) foetal calf serum (Corning Life Sciences), Penicillin (Invitrogen; 100 U/ml) and Streptomycin (Invitrogen; 100µg/ml).

The C6/36 *Aedes albopictus* cell line was maintained in Basal Medium Eagle (BME) medium (Gibco) supplemented with 1x MEM Non-Essential Amino Acids Solution (Gibco), 1mM Sodium Pyruvate (Gibco), 1% GlutaMAX Supplement (Gibco), 10% (w/v) foetal calf serum (Corning Life Sciences), Penicillin (Invitrogen; 100 U/ml) and Streptomycin (Invitrogen; 100µg/ml).

2.3.2 Cell maintenance

Cultured cell lines were maintained in sterile 0.2μm vented tissue culture flasks (25 cm^2, 75cm^2 or 175cm^2), tissue culture dishes (10cm^2 and 20 cm^2) or tissue culture trays (6, 12, 24, 48 or 96-well) (Corning Life Sciences). Near-confluent cells were passaged by removing culture medium, washing once with 1× PBS prior to the addition of a small volume of Trypsin-EDTA (see Appendix II). Cells were then placed in the CO_2 incubator at 37°C for 5 minutes or when cells are detached. Fresh culture medium was added to resuspend the cells. Cells were counted using a Neubauer Haemocytometer (Livingstone) with Trypan Blue (see section 2.3.3). Cells were grown at 37°C, 5% CO_2 in a humidified Panasonic CO_2 incubator (Panasonic Healthcare CO., Ltd). Cells were passaged every 2- 3 days depending on cell types and confluency. For the C6/36 cell line, cells were maintained as above but grown at 28°C with 5% CO_2.

2.3.3 Trypan blue exclusion

Cells were counted using a Neubauer Haemocytometer (Livingstone) and Trypan Blue Stain solution (prepared by the Tissue Culture Service Unit). Trypsinised cells were mixed with an equal volume of Trypan Blue and loaded into a haemocytometer. Cell concentration was then calculated using the following equation:

$$Cell\ concentration\ (cells/ml) = cell\ count\ per\ grid\ \times\ 2\ (dilution\ factor\ )\ \times\ 10^4$$

2.3.4 Cryopreservation of cells

Cells at 80-90% confluency were trypsinised, resuspended in fresh culture media and centrifuged at 1,000 × g for 5 minutes. Culture media was removed and cell pellets were resuspended in fresh culture media. An equal volume of 2× freezing media [50% media, 30% FCS, 20% DMSO (Sigma Aldrich)] was added to the cell suspension and mixed gently. Cells were aliquoted (1ml/vial) in sterile cryopreservation tubes (Corning Life Sciences). Cryotubes were transferred to a freezing chamber (Nalgene) containing fresh isopropanol and placed in a -80°C freezer. For long-term storage, vials were stored in a liquid nitrogen based cryopreservation system.

2.3.5 Resuscitation of cryopreserved cells

Cryopreserved vials containing frozen cell lines were thawed quickly in a 37°C water bath and transferred to T25cm^2 tissue culture flask containing pre- warmed standard tissue culture medium. Cells were incubated in the CO_2 incubator overnight. Fresh tissue culture medium containing an appropriate antibiotic (if necessary) was replaced the next day to remove dead cells.

2.3.6 Transient transfection of plasmid DNA and RNA

Cells were transiently transfected with expression plasmid DNA with either Lipofectamine 2000 or Lipofectamine 3000 (Life Technologies) to achieve protein overexpression following the manufacturers recommended protocol. Lipofectamine 3000 was also used to transfect *in vitro* transcribed SGR RNA or poly I:C into cells. Cells were seeded 24 hours prior to transfection and at approximately 80% confluency, either Lipofectamine 2000 or 3000 were incubated at RT for 15 minutes before usage. Transfection complexes for a single 12-well with Lipofectamine 2000 or 3000 consisted of two tubes, where tube A contained 1μg of plasmid DNA/RNA with 100μl of Opti-MEM media (Life Technologies) and tube B contained 3μl of Lipofectamine 2000 or 3000 with 100μl of Opti-MEM and incubated for 5 minutes at RT. Volumes were adjusted accordingly for trays with different well sizes. For Lipofectamine 3000, 3μl of P3000 was also added to tube A for only plasmid DNA transfections. Contents of Tube A were mixed directly into Tube B and after an additional 15 minutes incubation, mixture was added drop-wise to the cell monolayer. The plates were gently swirled and returned to normal tissue culture conditions.

2.3.7 Transient transfection of siRNA

Cells were transiently transfected with siRNA with Lipofectamine RNAiMAX Reagent (Life Technologies) per manufacturer's recommended protocol. Briefly, cells were seeded 24 hours prior to transfection and at approximately 80% confluency, Lipofectamine RNAiMAX Reagent incubated at RT for 5 minutes before usage. Transfection complexes for a single 12-well consisted of two tubes, where tube A contained 1μl of 20μm siRNA with 100μl of Opti-MEM media (Life Technologies) and tube B contained 3μl of Lipofectamine RNAiMAX Reagent with 100μl of Opti-MEM and

incubated for 5 minutes at RT. Contents of Tube A were mixed directly into Tube B and after an additional 5-minute incubation period, mixture was added drop-wise to the cell monolayer. The plates were gently swirled and returned to normal tissue culture conditions.

2.3.8 Lentiviral particle production

The lentiviral particles were produced in the 293T cell line due to their high transfection efficiency. 293T cells were seeded in a 6-well tray 24 hours prior to transfection. Cells were transfected with equal amounts of target plasmid DNA with the lentiviral packaging plasmids psPAX2 (a packaging plasmid, Addgene) and pMD2.G (VSV-G envelope expressing plasmid, Addgene) with Lipofectamine 2000 per section 2.3.6. Culture media were changed the following day and remove transfection reagent and plasmid present in the media. The supernatants from 293T cells were harvested 72 hr post-transfection and filtered through a 0.45μm filter membrane, aliquoted into vials and stored at -20°C.

To generate the stable cells, the cells were seeded in a 6-well tray prior to lentiviral transduction. The lentiviral aliquot was rapidly thawed, diluted 1:3 in complete media and added to the target cells. Culture media were replaced 5 hours post-transduction and cells returned to the incubator. The antibiotic selection was started 3 days post-transduction (Blasticidin at 5μg/ml and puromycin at 3μg/ml for Huh7 cells – adjusted accordingly for other cell types). Treatment of non-transduced cells was used as a negative control. The polyclonal cell line was considered as stable cells when the negative control culture was non-viable.

2.3.9 Generation of EGFP/CD81/PI4KA knockout (EGFP-KO/CD81-KO/PI4KA-KO) cell lines by CRISPR/Cas9 technology

20 nucleotides guide sequences (sgRNA) targeting the gene of interest (EGFP/CD81/PI4KA) were designed on Benchling and generated with *Bsm*BI overhangs as complementary DNA primers (see Appendix I). These primers were annealed and ligated into *Bsm*BI digested LentiCRISPRv2 plasmid (Addgene). Following transformation into competent cells (see section 2.1.2) and mini-preparation (see section 2.1.3), a diagnostic *Bsm*BI digestion was performed to deduce which

clones have the correct guide sequence. Lentivirus was generated and transduced as described previously in section 2.3.8. Monoclonal populations of each potential knockout colony were obtained by dilution (1:100-1:200) onto 150 mm dishes to separate the cellular population into single cell and once at a suitable size (approximately 4 weeks), colonies were isolated using a colony ring. Knockout cells were confirmed by immunofluorescence staining (see section 2.5.3) western blot analysis (see section 2.1.17) and FACS (section 2.1.24).

2.4 Cell lines

2.4.1 HeLa

The HeLa cell line is derived from cervical cancer cells taken from Henrietta Lacks (Scherer et al. 1953).

2.4.2 293T

The 293T cell line is derived from human embryonal kidney (HEK) cells transformed with the SV40 large T antigen.

2.4.3 Huh7

The Huh7 cell line is a human hepatocyte-derived carcinoma cell line, isolated from a liver tumour from a 57-year-old Japanese male (Nakabayashi et al. 1982).

2.4.4 Huh7.5

Derived from Huh7 cells, the Huh7.5 cell line used to harbour replication of an HCV sub-genomic replicon (SGR) but cured after IFN-α treatment. This cell line is highly permissive to HCV infection due to defective RIG-I signalling (Blight et al. 2002; Sumpter et al. 2005). These cells were kindly provided by Charles Rice (Rockefeller University, New York, USA).

2.4.5 Huh7-T7

The HuhT-T7 cell line is the Huh7 cell line with stable expression of the T7 bacteriophage RNA polymerase and maintained with puromycin selection.

2.4.6 Huh7-EGFP

The Huh7-EGFP cell line is the Huh7 cell line with stable expression of EGFP and maintained with blasticidin selection.

2.4.7 HTR8/SVneo

The HTR8/SVneo cell line was derived by chronic villi explant cells from human first trimester placenta transformed with the SV40 large T antigen.

2.4.8 JEG3

The JEG3 cell line are human choriocarcinoma cells derived and isolated from the Woods strain of the Erwin-Turner tumour (Kohler and Bridson 1971).

2.4.9 Vero

The Vero cell line are epithelial cells isolated from the kidney of a healthy adult African green monkey in Japan.

2.4.10 EGFP-KO Huh7 cells

EGFP-KO Huh7 cells are Huh7 cells that display a complete loss of EGFP expression generated by CRISPR/Cas9 editing technology.

2.4.11 CD81-KO Huh7.5 cells

CD81-KO Huh7 cells are Huh7 cells that display a complete loss of CD81 expression generated by CRISPR/Cas9 editing technology.

2.4.12 Sub-genomic replicon (SGR)

Huh7.5 cells were transfected with *in vitro* RNA transcribed from pSGRm-JFH1-BlaRL derived plasmids. Individual blasticidin-resistant colonies harbouring replication of the pSGRm-JFH1-BlaRL replicons were expanded and screened. Colonies displaying the desired phenotypes (NS5A expression) with functional reporter genes (mCherry, GFP, renilla luciferase or thymidine kinase expression) were chosen for further experiments.

2.4.13 Mouse embryonic fibroblasts (MEFs)

Viperin KO MEFs were derived from viperin deficient mice generated by CRISPR/Cas9 technology (Van der Hoek et al. 2017). PCR of the viperin locus from genomic DNA and sanger sequencing confirmed disruption of the viperin coding region. Wild type MEFs from the original inbred C57BL/6 mouse strain were used as a control.

2.5 Fluorescence Microscopy

2.5.1 Acetone/methanol fixation

To prepare acetone:methanol (1:1, v/v) fixative solution, an equal volume of Acetone (Chem-Supply) and Methanol (Chem-Supply) were mixed and stored at -20°C. Cell monolayers were washed with 1× PBS prior to the addition of cold acetone:methanol solution for 5 minutes at 4°C. Following removal of the fixation solution, cells were washed 3 times with PBS. Fixed cells were kept in PBS at 4°C before immunofluorescence labelling (see section 2.5.3).

2.5.2 4% Paraformaldehyde fixation

Cell monolayers were washed once with PBS prior to the addition of 4% paraformaldehyde solution (see Appendix II) for 20 minutes at RT. Following removal of the fixation solution, cells were washed 3 times with PBS. 0.1% Triton X-100 (Sigma Aldrich) was added to permeabilise cells for 10 minutes and washed twice with PBS before immunofluorescence labelling (see section 2.5.3).

2.5.3 Immunofluorescence labelling

Immunofluorescence labelling was performed after fixation with either acetone/methanol or 4% paraformaldehyde (see section 2.5.1 and 2.5.2). Fixed cells were first blocked with 5% BSA in PBS (see Appendix II) for 1 hour at RT before 2 washes with PBS. Cells were labelled with primary antibody (see Appendix III) diluted in 1% BSA in PBS (see Appendix II) for 1 hour at RT. After 3 washes with PBS, an appropriate dilution of fluorescence-conjugated secondary antibody (see Appendix III) was added to the wells and samples were incubated for 1 hour in the dark at RT.

Samples were washed 3 times with PBS prior to nuclear DAPI staining cells for 5 minutes in the dark. Cells were finally washed 2 times with PBS and samples stored in PBS at 4°C. Samples were visualised using a Nikon Eclipse TiE fluorescence inverted microscope and images were captured using NIS Elements software.

2.5.4 Confocal microscopy

Confocal microscopy was performed on the Olympus FV3000 at Adelaide Microscopy (Olympus Life Science). Cells were seeded on a 8-well chamber slide (μ-slide 8 well glass bottom – ibidi) and immunofluorescence labelling performed per section 2.5.3. Following DAPI staining, two drops of Vectashield PLUS Antifade Mounting Medium (Vector Laboratories) was added per well to prevent bleaching. Two drops of 60X immersion oil was placed on the objective lens before mounting the chamber slide. Images were captured with Fluoview software (Olympus Life Science) with line sequential scanning for each channel, which consisted of DAPI, Alexa Fluor 488 and Alexa Fluor 555.

2.6 Data analysis

All data was statistically analysed using GraphPad Prism 9.

Chapter 3 - Identification of novel host factors for HCV replication

3.1 Introduction

In general, viruses with RNA genomes, including the Hepatitis C Virus (HCV) have limited coding capacity and thus depend on host cellular components to support their entire lifecycle. A prime example are the cellular factors required for HCV entry, where the virus binds to host cell receptors including CD81, SRB1, Claudin-1 and occludin (see section 1.6.1). Additionally, cellular factors such as PI4KA and hVAP-A are instrumental to the formation of the membranous web required for HCV replication (see section 1.9). While we have a good understanding of HCV dependent host factors, it is likely that more remain to be identified and characterised. Identification of HCV proviral host factors has largely been dependent on RNAi technology, where both small-scale and genome-wide siRNA screens have uncovered the function of numerous cellular proteins which support the HCV lifecycle (Tai et al. 2009; Li et al. 2009). Although characterisation of these HCV proviral host factors has greatly contributed to the knowledge of the virus lifecycle and possible therapeutic interventions, limitations within RNAi technology which include incomplete knockout of protein expression, suggest that additional host factors remain to be discovered. However, the recent advent of CRISPR as a tool to allow for the possibility of genome-wide knockout screening and thus circumventing the limitations that RNAi poses, will allow for the elucidation of novel host factors that are essential for HCV replication. Therefore, the aim of this chapter was to optimise CRISPR technology to perform a genome-wide screen to identify additional host factors critical for the HCV lifecycle.

3.2 Proof of concept experiments using CRISPR technology to investigate proviral host factors

At the time this project was conceived, CRISPR genome-wide screen technology was in its infancy and the majority of studies to knockout targeted gene expression relied exclusively on transient transfection of plasmids encoding both the sgRNA and Cas9 (Yang et al. 2014). However, in contrast to above, the GeCKO LentiCRISPRv2 library that was used in this thesis, relies on lentiviral delivery of the CRISPR/Cas9 system and guides for genome-wide knockout across a population of cells (Sanjana et al. 2014). The use of the lentiviral delivery system overcomes any issues that may be

encountered when using lipid-based transfection protocols. These include control of delivery of Cas9 and sgRNAs on one plasmid and the lower cost associated with lentiviral transduction. Therefore, as a proof of concept before embarking on a large scale genome-wide screen, we used the LentiCRISPRv2 system to knockout a number of HCV proviral host factors and also EGFP expression in Huh7.5-EGFP stable cell lines.

3.2.1 Generation and validation of EGFP CRISPR KO cell line

We first evaluated LentiCRISPRv2's ability to knockout EGFP expression that had been ectopically stably introduced within the Huh7 genome. The EGFP coding region contained no intron/exons as the entire open reading frame was integrated within the genome, eliminating the possibility of unintentional alternative splicing during mRNA transcription, allowing for simple investigation of CRISPR/Cas9 knockout efficiency. Finally, we could monitor EGFP fluorescence levels in real time throughout the entire course of the process from the introduction of the Cas9 to isolation of monoclonal populations for further analysis.

Design of the sgRNA sequences that target EGFP mRNA was performed using the online tool Benchling (http://benchling.com), who have refined their sgRNA computational design rules to detect the optimum sequences ensuring effective Cas9 cleavage and maximum knockout efficiency (Hsu et al. 2013). Benchling arranges the potential sgRNA sequences based on on-target and off-target scores, and binding locations of sgRNAs, results are annotated in a simplistic manner (Doench et al. 2016). Two sets of oligonucleotides which bind within 100bp to the 5' end of the start codon for EGFP were designed and selected, where each bound on opposite strands of the EGFP coding DNA to determine if there was Cas9 knockout efficiency bias towards either sense strand. These oligos also contained *Bsm*BI overhangs to allow insertion into the LentiCRISPRv2 plasmid via traditional restriction enzyme cloning (see Appendix 1). These primers were annealed and ligated into *Bsm*BI digested LentiCRISPRv2 plasmid (see section 2.1.7). Following transformation and plasmid mini-preparation, a diagnostic *Bsm*BI digestion was performed to isolate clones which have successful integration of the sgRNA targeting EGFP (LCv2-EGFP.1 and LCv2-

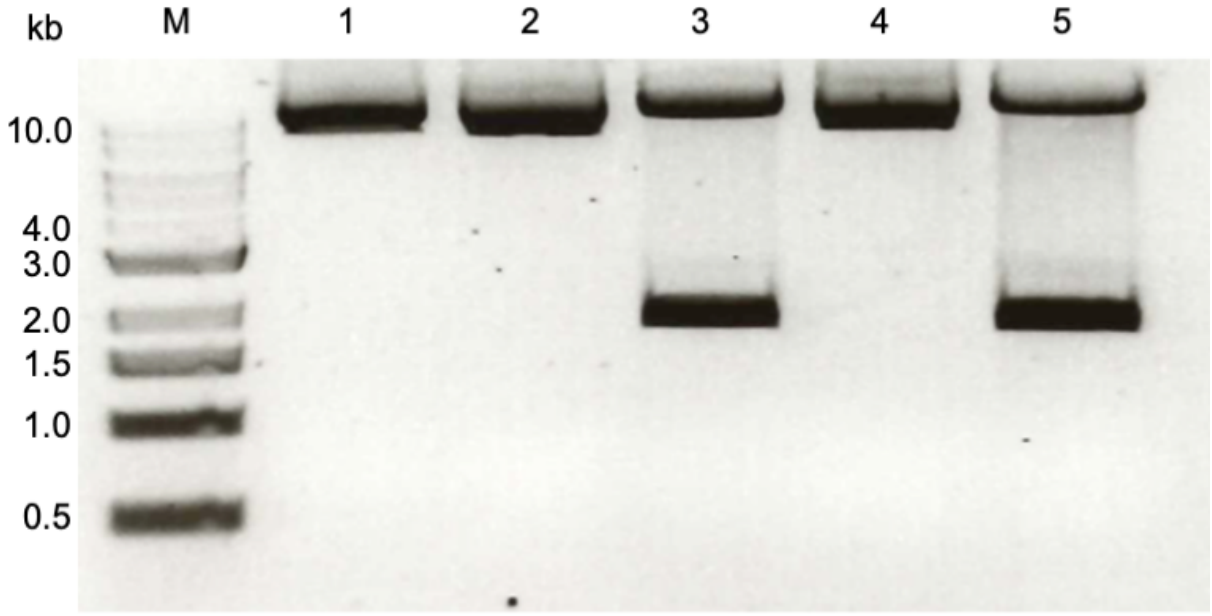

Figure 3.1: sgRNAs which target EGFP were successfully cloned into pLentiCRISPRv2.

To determine if the annealed sgRNAs which target EGFP were ligated into pLentiCRISPRv2, plasmid DNA was extracted from transformant clones and digested with Bsm*BI*. Lane M, 1kb DNA ladder, lanes 1-4, recombinant plasmid from transformant clones no. 1-4 respectively, lane 5, LCv2-WT plasmid.

EGFP.2) (see section 2.1.2 & 2.1.3) (Fig. 3.1). Lentivirus was generated (see section 2.3.8) with LCv2-EGFP.1 or LCv2-EGFP.2 and Huh7-EGFP stable cell lines were transduced with lentivirus, and puromycin selection of monoclonal populations of cells were isolated using cloning rings and expanded for analysis.

Immunofluorescence was first used to confirm EGFP knockout in the Huh7.5 EGFP stable cell lines. Transduction of the LentiCRISPRv2 wildtype (LCv2-WT), which contains a 2kb filler region instead of a 20nt sgRNA resulted in retention of EGFP fluorescence as expected (Fig. 3.2). In contrast, cells transduced with either LCv2-EGFP guide displayed complete loss of EGFP fluorescence, suggesting no influence was observed in polarity of binding by the sgRNA (Fig. 3.2). In addition, western blotting of EGFP indicated high levels of EGFP protein expression in the lysates of LCv2-WT cells but a complete loss of EGFP protein expression in cells transduced with either LCv2-EGFP guide, in multiple monoclonal populations (see section 2.1.17) (Fig. 3.3). Finally, flow cytometry was also used to investigate EGFP expression in LCv2-EGFP transduced KO cells (see section 2.1.24). Gated LCv2-WT cells had significant expression of EGFP as expected, however the loss of EGFP within the LCv2-EGFP transduced KO cells was similar to that of the negative control which had no EGFP expression (Fig. 3.4). Collectively, the data above indicates that the LentiCRISPRv2 system is able to knockout a specific gene of interest with high efficiency required for genome-wide screening.

3.2.2 Generation and validation of CD81 and PI4KA CRISPR KO cell lines

Following successful knockout of EGFP, we next determined whether LentiCRISPRv2 could knockout endogenous genes as efficiently. We therefore elected to knockout host factors that are critical for HCV replication. We selected CD81, one of the receptors required for HCV entry and PI4KA, an essential kinase for lipid metabolism and establishment of the HCV replication complex (see section 1.61 and 1.9).

Since we were now targeting an endogenous gene which contains multiple exons, we designed one sgRNA binding site within exon two (sgRNA, CD81.1) and the second within exon three (sgRNA, CD81.2) via Benchling with *Bsm*BI overhangs as described previously (see Appendix 1). This was done to improve the probability of CD81 frame shift mutations if alternative splicing occurs. Following ligation and transformation

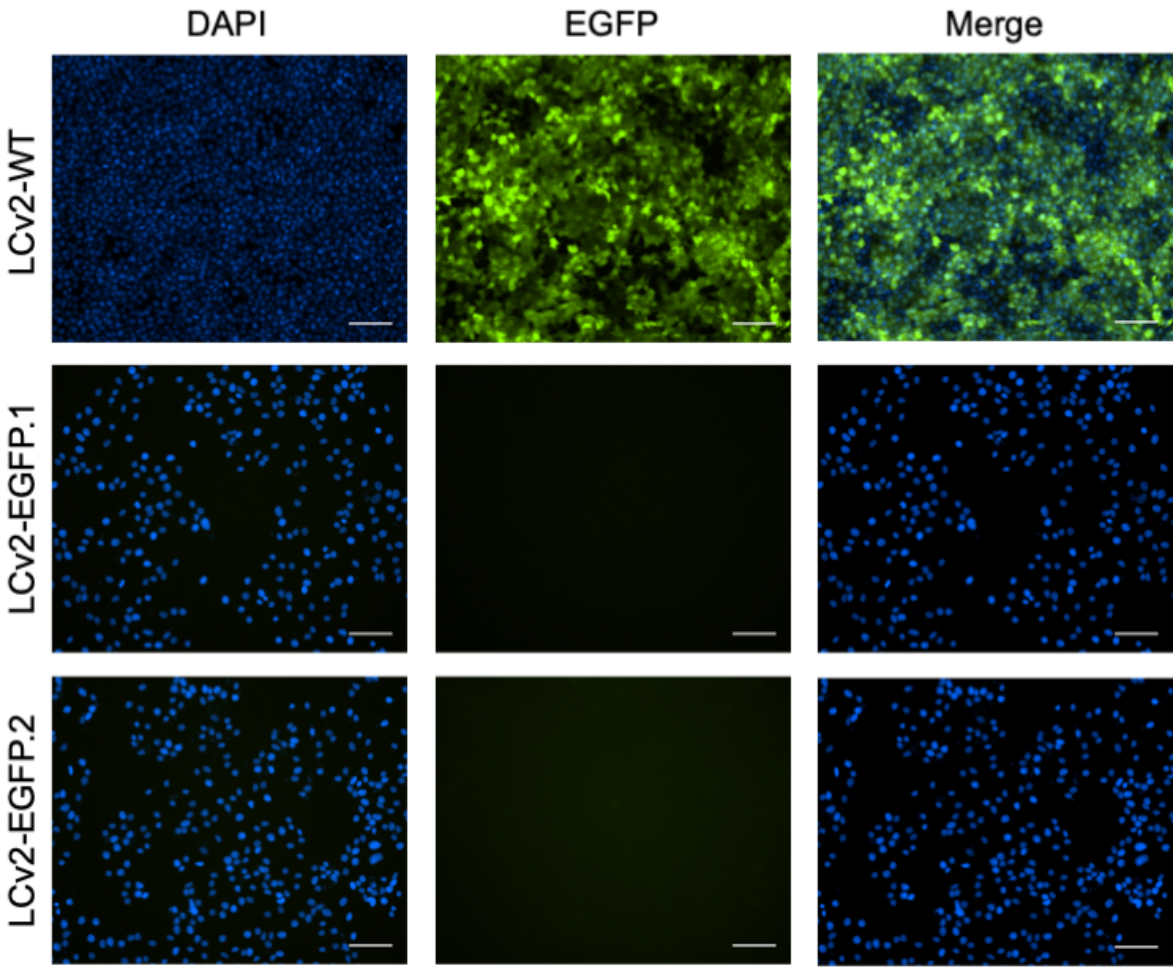

Figure 3.2: Transduction of LCv2-EGFP results in elimination of EGFP fluorescence in Huh7-EGFP stable cell line via immunofluorescence microscopy.

To evaluate LentiCRISPRv2 efficiency, we needed to determine if EGFP could be knocked out in a Huh-7 EGFP stable cell line. LentiCRISPRv2 wildtype control (LCv2-WT), LCv2-EGFP.1 and LCv2-EGFP.2 were stained with DAPI and endogenous EGFP expression visualised using a Nikon TiE inverted fluorescence microscope. Scale bars are 100μm. Representative of multiple monoclonal populations.

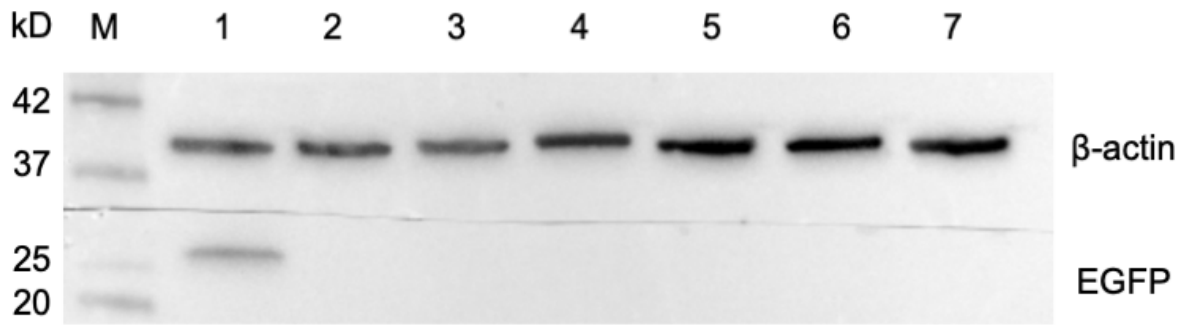

Figure 3.3: Transduction of LCv2-EGFP results in elimination of EGFP protein in Huh7-EGFP stable cell line via western blot.

To evaluate LentiCRISPRv2 efficiency, we needed to determine if EGFP could be knocked out in a Huh-7 EGFP stable cell line. Whole cell lysates of LentiCRISPRv2 wildtype control (LCv2-WT), LCv2-EGFP.1 and LCv2-EGFP.2 (where there are 3 individual monoclonal populations each) were harvested and western blot run, incubated with anti-EGFP and anti-β-actin antibodies. Lane M, Bio-Rad Kaleidoscope Ladder, lane 1 LCv2-WT, lane 2-4, three monoclonal populations of LCv2-EGFP.1, lane 5-7 three monoclonal populations of LCv2-EGFP.2.

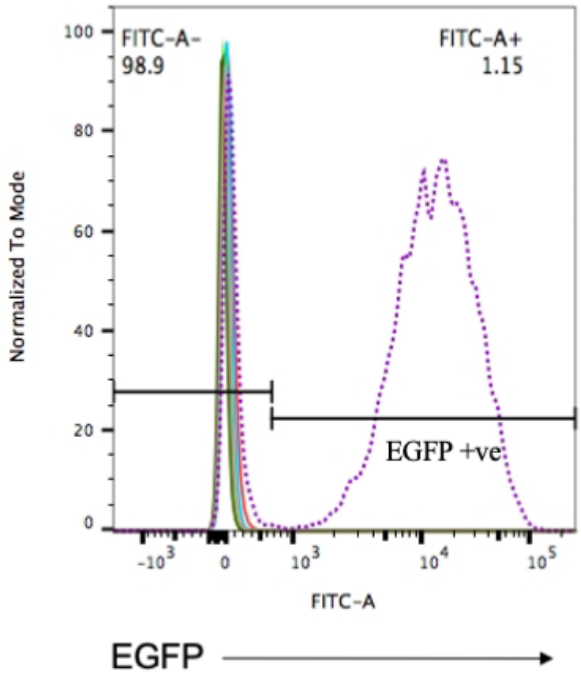

Sample Name	Count	Freq. of Parent
LCv2-WT	8948	71.2
LCv2-EGFP.1.1	8514	61.4
LCv2-EGFP.1.2	7596	50.2
LCv2-EGFP.1.3	8603	67.3
LCv2-EGFP.2.1	9089	70.9
LCv2-EGFP.2.2	9047	73.7
LCv2-EGFP.2.3	8919	65.1

Figure 3.4: Transduction of LCv2-EGFP results in elimination of EGFP fluorescence in Huh7-EGFP stable cell line via flow cytometry.

To evaluate LentiCRISPRv2 efficiency, we needed to determine if EGFP could be knocked out in a Huh-7 EGFP stable cell line. LCv2-WT, LCv2-EGFP.1 and LCv2-EGFP.2 (where there are 3 individual monoclonal populations each) were harvested and single cells analysed by flow cytometry.

of the annealing oligonucleotides into the *Bsm*BI digested LentiCRISPRv2 plasmid, colonies were diagnostically digested with *Bsm*BI to detect colonies that contained successful integration of the sgRNA targeting CD81 (LCv2-CD81) (Fig. 3.5). As described previously, lentivirus was generated using LCv2-CD81 and Huh7.5 cells were transduced and puromycin resistant monoclonal populations isolated using cloning rings and puromycin resistant colonies expanded for downstream experiments.

Immunofluorescence (see section 2.5.3) was employed to confirm CD81 knockout within the Huh7.5 monoclonal population. Cells transduced with LCv2-WT lentivirus revealed positive staining for CD81 as expected that was clearly present on the cell membrane and consistent with previous reports (Farquhar et al. 2012). In contrast, cells transduced with either LCv2-CD81 guide, resulted in complete loss of CD81 expression (Fig. 3.6). Flow cytometry was also used as a complementary method to ascertain CD81 expression in LCv2-CD81 cells. Gated LCv2-WT cells had high expression of CD81 as expected, while transduction with LCv2-CD81.1 resulted in complete loss of CD81 as shown by the lack of overlap between the two and indicating efficient knockout of CD81 expression (Fig. 3.7). Interestingly despite no visible CD81 immunofluorescence staining for LCv2-CD81.2, these cells had incomplete knockout of CD81 as is evidenced by a broader peak which overlaps with the LCv2-WT (Fig. 3.7). This implies that variable KO efficiency is observed with genes with multiple alleles and likely originates from the cancerous origins of the parental Huh7 cells, which possess between 55 and 63 chromosomes (Kasai et al. 2018). This would likely result in insufficient cleavage by Cas9, and incomplete knockout of CD81. This limitation may be rectified by repeating the transduction of LentiCRISPRv2 targeting CD81 and optimising time points prior to BSD selection.

To determine if the two LCv2-CD81 monoclonal populations were resistant to HCV infection due to the loss of CD81 expression, cells were infected with HCV JC1-GFP infectious virus at an approximate MOI of 2 for 48 hours prior to acetone/methanol fixation (see section 2.5.1) (Eyre et al. 2014). Immunofluorescence staining revealed high levels of NS5A staining in LCv2-WT cells when CD81 is present, indicative of efficient HCV replication. However, there was significantly reduced NS5A staining in both LCv2-CD81 monoclonal populations, indicating reduced HCV replication as a result of ablated CD81 expression (Fig. 3.8). qRT-PCR was also employed as a

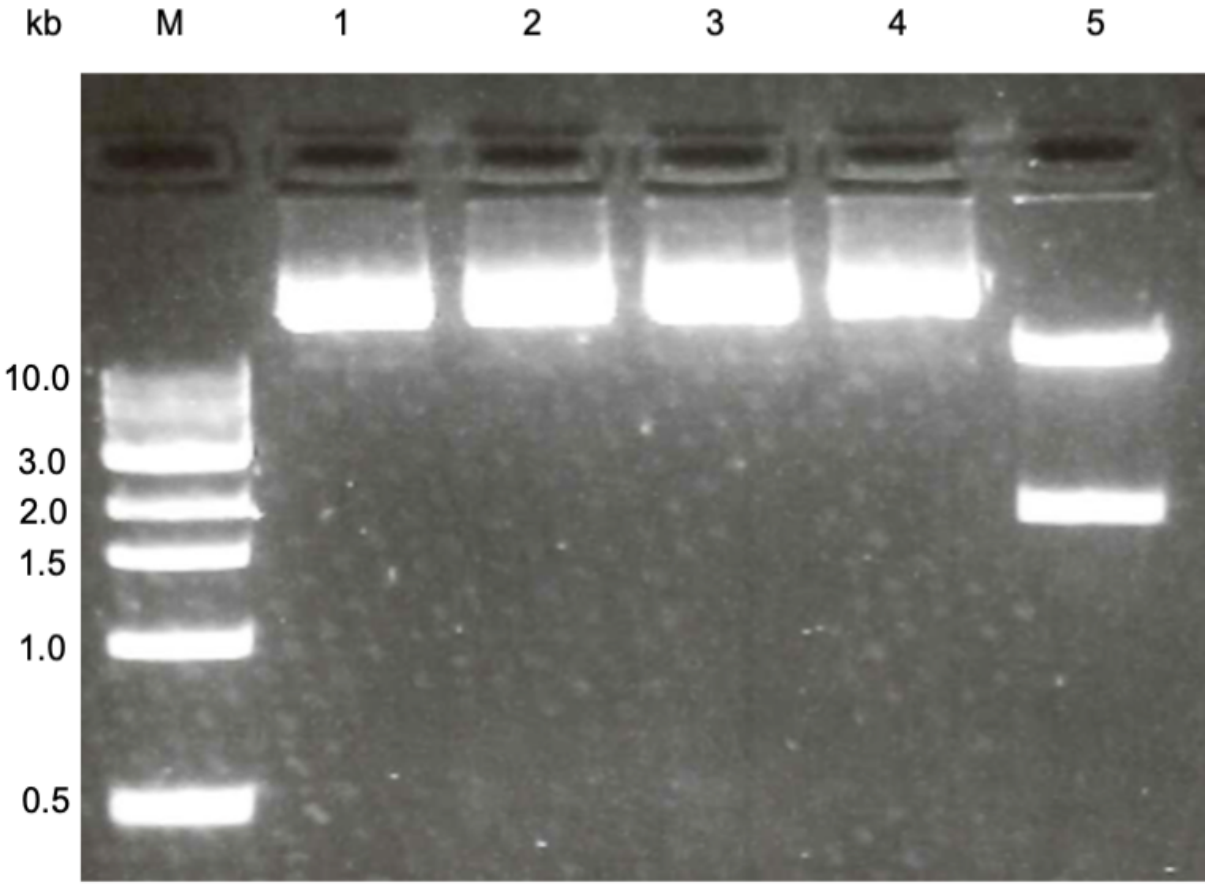

Figure 3.5: sgRNAs which target CD81 were successfully cloned into pLentiCRISPRv2.

To determine if the annealed sgRNAs which target CD81 were ligated into pLentiCRISPRv2, plasmid DNA was extracted from transformant clones and digested with Bsm*BI*. Lane M, 1kb DNA ladder, lanes 1-4, recombinant plasmid from transformant clones no. 1-4 respectively, lane 5, LCv2-WT plasmid.

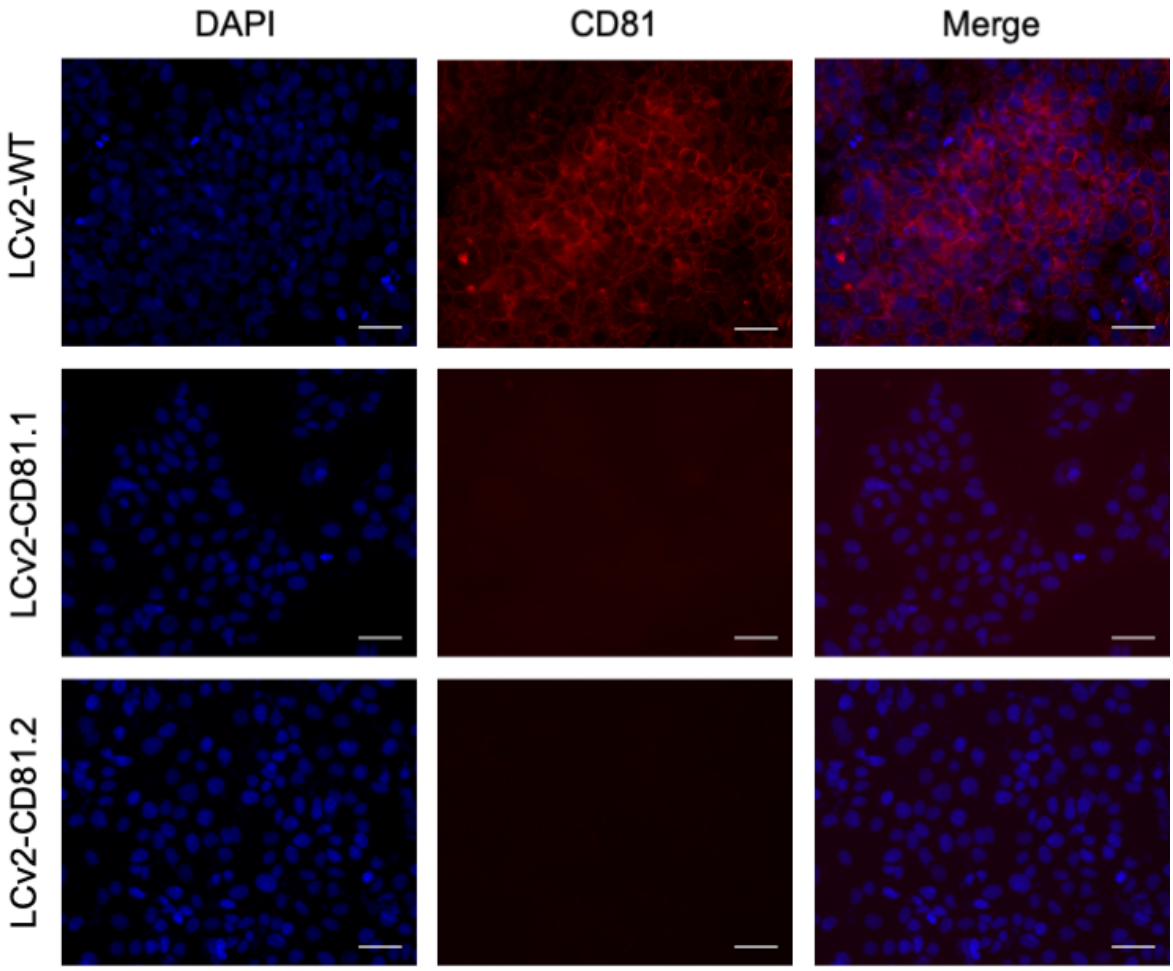

Figure 3.6: Transduction of LCv2-CD81 results in elimination of CD81 fluorescence in Huh7.5 cell line via immunofluorescence microscopy.

To evaluate LentiCRISPRv2 efficiency to knockout host factors important for the HCV lifecycle, LentiCRISPRv2 wildtype control (LCv2-WT), LCv2-CD81.1 and LCv2-CD81.2 were stained with mouse anti-CD81 and Alexa Fluor 555-conjugated goat anti-mouse IgG secondary Ab. Post DAPI staining, cells were visualised using a Nikon TiE inverted fluorescence microscope. Scale bars are 50μm.

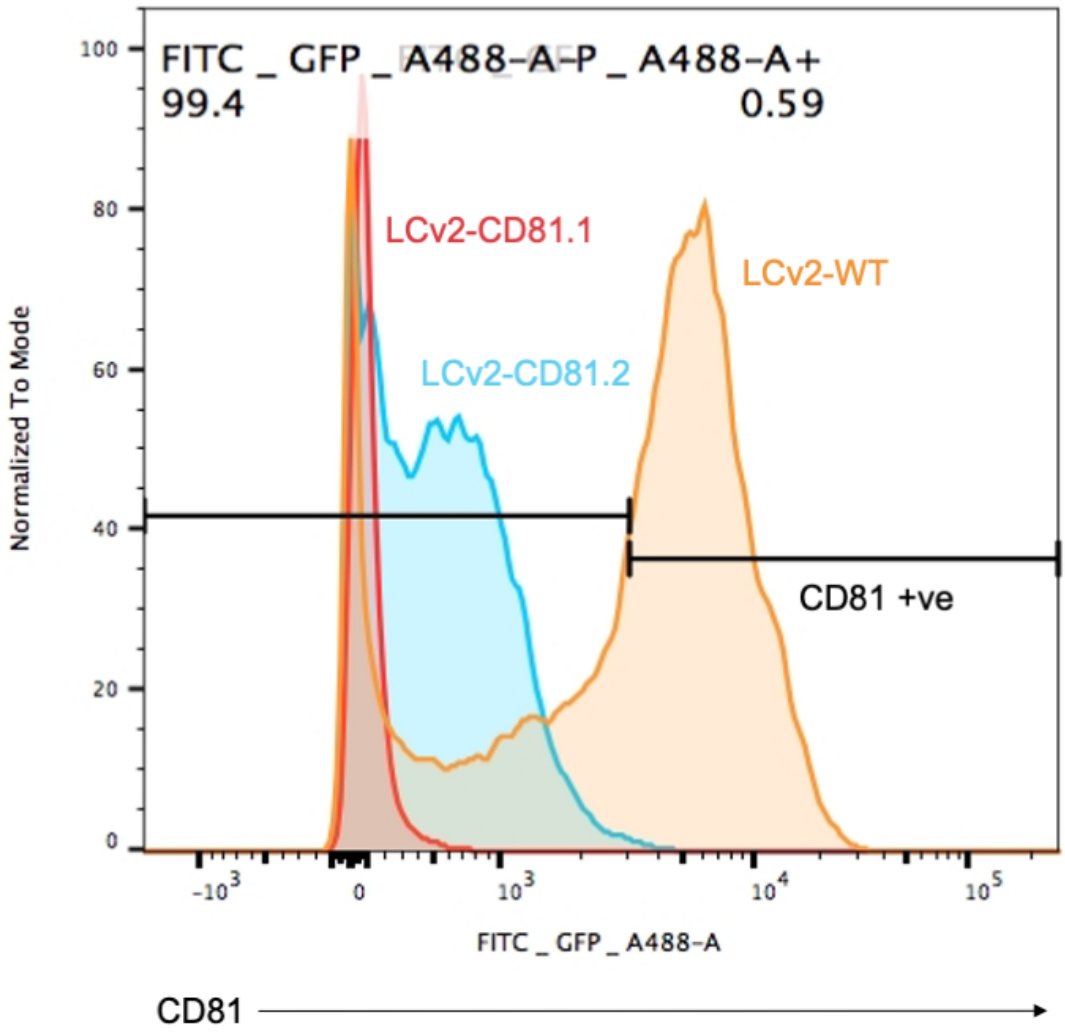

Figure 3.7: Transduction of LCv2-CD81 results in elimination of CD81 fluorescence in Huh7.5 cell line via flow cytometry.

To evaluate LentiCRISPRv2 efficiency to knockout host factors important for the HCV lifecycle, LentiCRISPRv2 wildtype control (LCv2-WT), LCv2-CD81.1 and LCv2-CD81.2 transduced cell lines were harvested and stained with mouse anti-CD81 and Alexa Fluor 488-conjugated goat anti-mouse IgG secondary Ab. Single cells were analysed by flow cytometry. LCv2-WT is indicated as yellow, LCv2-CD81.1 is shown as red and LCv2-CD81.2 is represented in blue.

confirmatory assay to assess HCV RNA abundance (see section 2.1.15). As expected, both LCv2-CD81 monoclonal populations, indicating reduced HCV replication as a result of ablated CD81 expression (Fig. 3.8). qRT-PCR was also employed as a confirmatory assay to assess HCV RNA abundance (see section 2.1.15). As expected, LCv2-WT are readily infected with HCV as determined by high levels of HCV RNA within the cell (Fig. 3.9). In contrast, both LCv2-CD81 monoclonal populations have significant reduction in HCV RNA levels (Fig. 3.9). Collectively, these results demonstrate that knockout of an endogenous host factor critical for entry of HCV, results in the inhibition of HCV replication within the cell, as expected. Additionally, despite incomplete knockout of CD81, it is still possible for HCV entry to be halted demonstrating the sensitivity of the genome-wide screen is not compromised should potential novel host factors have incomplete knockout.

Although we have validated LentiCRISPRv2's ability to knockout a host factor that resulted in inhibition of HCV entry, the HCV-SGR replicon system which will be used in the CRISPR genome-wide screen bypasses the HCV entry phase and focuses solely on the replication stage of the virus lifecycle (Zhou et al. 2011). Therefore, we deemed it important to determine if LentiCRISPRv2 could knockout a host factor important in the genome replication stage of the HCV lifecycle. Phosphatidylinositol 4-kinase Alpha (PI4KA), which is a highly characterised host factor critical for HCV replication was selected as it was one of fifteen novel host factors which had overlap between two siRNA genome-wide knockdown screen with HCV, where one screen used the HCV-SGR JFH-1 strain which we intend to use (Tai et al. 2009; Li et al. 2009). Thus, it was useful to determine whether there could be any overlap in results between genome-wide screens with either siRNA or CRISPR technology.

As described previously, two single guide RNA (sgRNA), each 20 nucleotides long targeting PI4KA were designed using Benchling and generated with *Bsm*BI overhangs as complementary primers (see Appendix 1). Following ligation and transformation of the anneal oligonucleotides into the *Bsm*BI digested LentiCRISPRv2 plasmid, colonies were diagnostically digested with *Bsm*BI to detect colonies which contain successful integration of the sgRNA targeting PI4KA (LCv2-PI4KA). Lentivirus was generated with LCv2-PI4KA and Huh7.5 were transduced with lentivirus, monoclonal populations isolated using cloning rings and selected colonies expanded. Unfortunately, using this

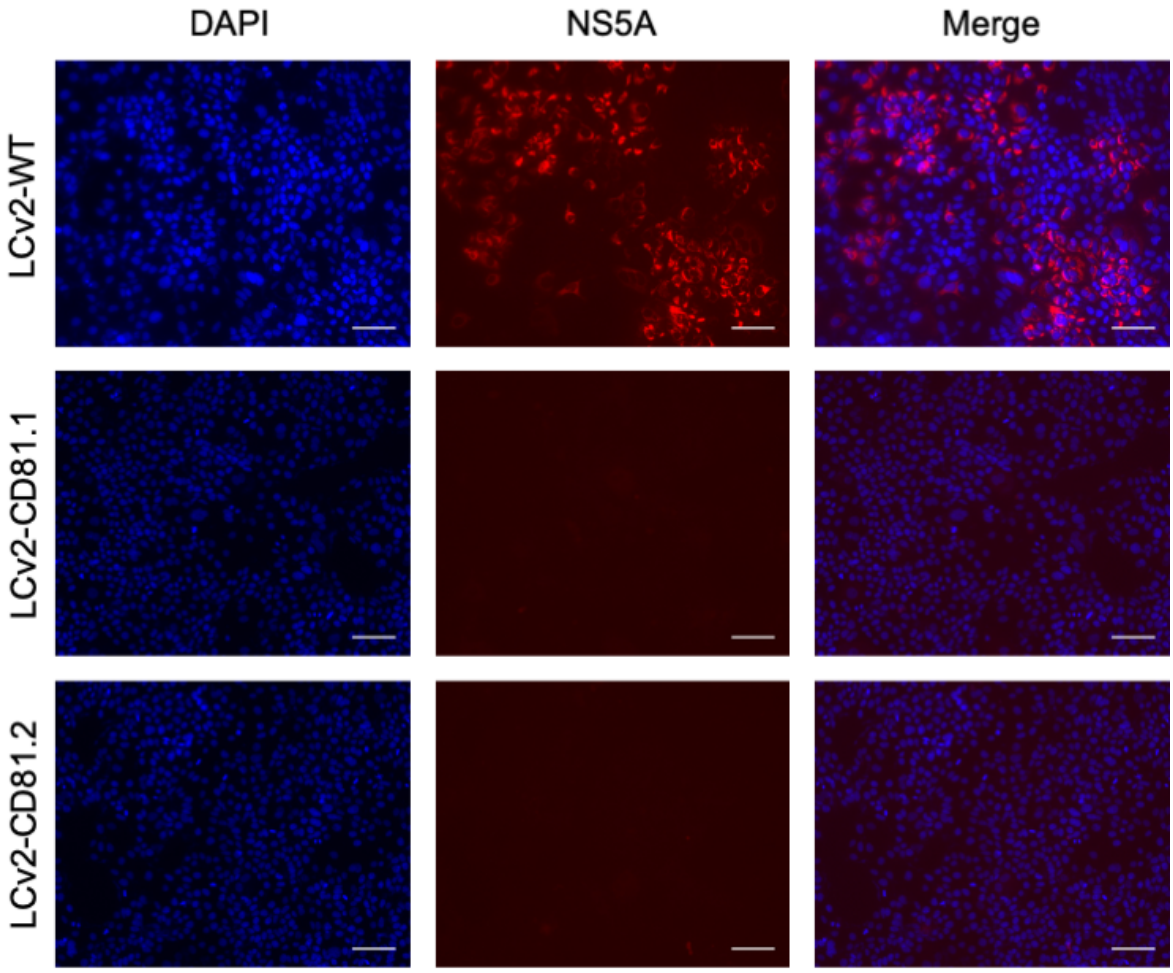

Figure 3.8: Knockout of CD81 results in complete perturbation of HCV entry into Huh7.5 cells via immunofluorescence microscopy.

To determine whether loss of CD81 via LentiCRISPRv2 activity would result in a loss of HCV entry and therefore replication, LentiCRISPRv2 wildtype control (LCv2-WT), LCv2-CD81.1 and LCv2-CD81.2 were infected with HCV-JC1-GFP infectious virus (MOI=2). Cells were stained with mouse anti-NS5A and Alexa Fluor 555-conjugated goat anti-mouse IgG secondary Ab. Post DAPI staining, cells were visualised using a Nikon TiE inverted fluorescence microscope. Scale bars are 100μm.

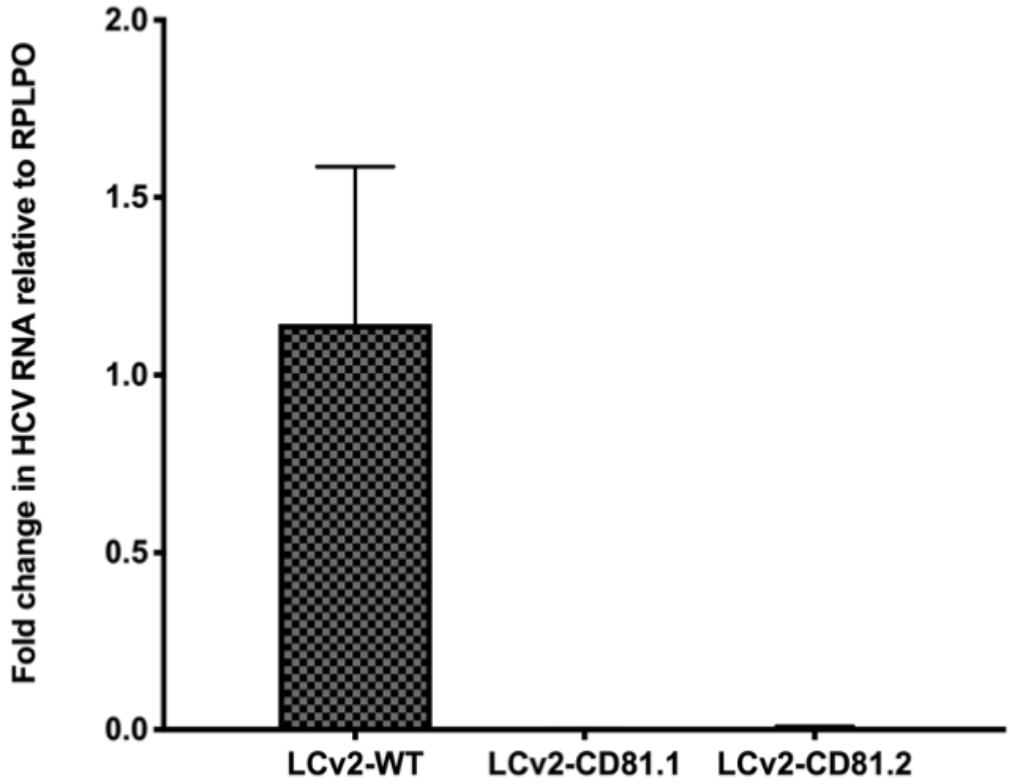

Figure 3.9: Knockout of CD81 results in complete perturbation of HCV replication into Huh7.5 cells via qRT-PCR.

To determine whether loss of CD81 by LentiCRISPRv2 would result in a loss of HCV entry and therefore replication, LentiCRISPRv2 wildtype control (LCv2-WT), LCv2-CD81.1 and LCv2-CD81.2 were infected with HCV-JC1-GFP infectious virus (MOI=2). RNA was extracted from infected cells and cDNA synthesised. qRT-PCR was performed with primers targeting the house-keeping gene RPLPO (36B4) and HCV IRES (see Appendix 1) (error bars = SD).

experimental approach, a high number of monoclonal cell lines that survived puromycin selection, perished during the expansion process, suggesting that PI4KA is critical for cell survival. Western blotting to ascertain PI4KA expression levels in the surviving puromycin resistant cell lines were unsuccessful.

However, one colony survived the expansion process and was tested for HCV-JC1 GFP permissibility with a MOI of approximately two. 24 hours post infection, immunofluorescence was performed and unfortunately, this line was found to be positive for NS5A staining, indicating that this colony remained permissive to HCV replication (Fig. 3.10). Since PI4KA expression is critical for active HCV replication, positive staining for NS5A implies that this one colony retained expression of the former and thus not pursued further.

The inability of CRISPR/Cas9 to knockout PI4KA illustrates a limitation of our CRISPR genome-wide screen approach, as essential genes for cell function will not be represented. On the contrary, these host factors where reduced expression can still support HCV replication would be missed in a siRNA-based screen but will be detected in our CRISPR knockout screen. PI4KA is important in the IP3/DAG pathway and is responsible for the production of phosphatidylinositol 4-phosphate (PtdIns(4)P), an intermediate to phosphatidylinositol 4,5-bisphophate (PtdIns(4,5)P2), and one of the most critical regulatory lipids in the plasma membrane (D'Angelo et al. 2008). Furthermore, addition of inhibitors of PI4KA in mice results in sudden death, likely due to cardiovascular insufficiency (Bojjireddy et al. 2014). In addition, Cre-KO mice for PI4KA exhibited moribund properties where histopathology after 7 days showed severe epithelial cell degeneration and/or necrosis, indicating that PI4KA is an essential gene and that siRNA knockdown of PI4KA results in sufficient protein expression levels to fulfil its housekeeping functions (Bojjireddy et al. 2014).

3.3 Generation of HCV replicon reporter cell lines

In any genome-wide CRISPR screen, it is critical that the factors that determine selection are robust and reproducible. Replication of HCV in culture can result in a moderate cytopathic effect, however, HCV in general is considered to be non-cytopathic relative to other members of the *flaviviridae* family, and as such, the use of a survival screen following knockout of an essential host factor is not applicable to

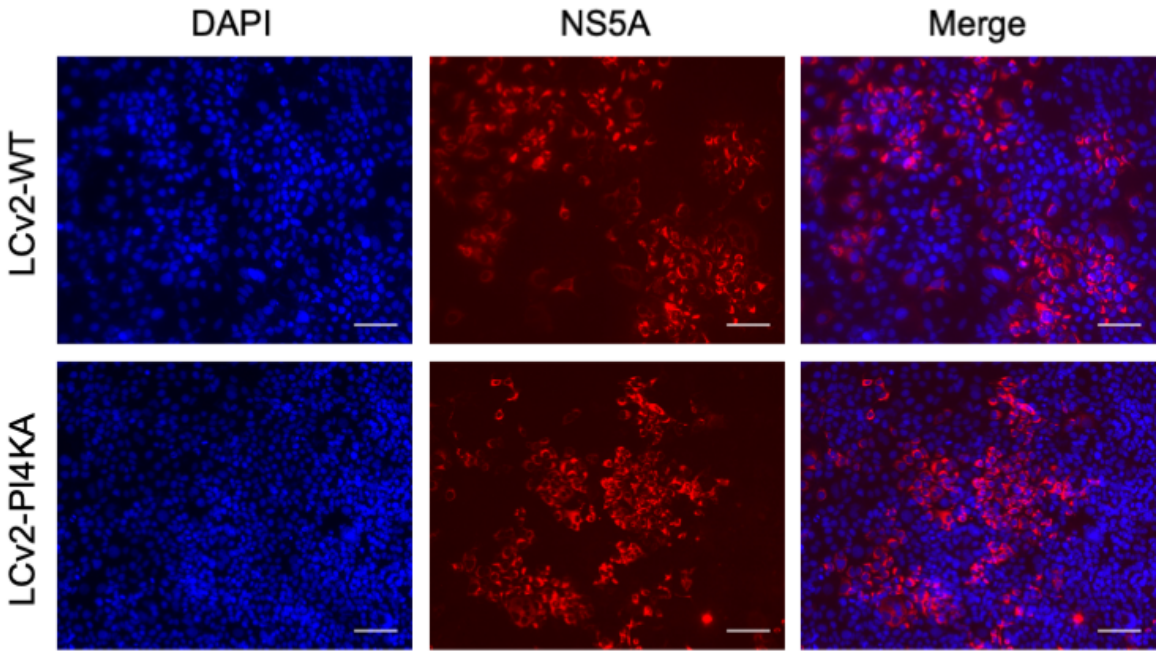

Figure 3.10: Incomplete knockout of PI4KA results in HCV replication in Huh7.5 cells via immunofluorescence microscopy.

To determine whether incomplete knockout of PI4KA via LentiCRISPRv2 activity would result in establishment of HCV replication, LentiCRISPRv2 wildtype control (LCv2-WT), and LCv2-PI4KA were infected with HCV-JC1-GFP infectious virus (MOI=2). Cells were stained with mouse anti-NS5A and Alexa Fluor 555-conjugated goat anti-mouse IgG secondary Ab. Post DAPI staining, cells were visualised using a Nikon TiE inverted fluorescence microscope. Scale bars are 100μm.

HCV. Therefore, it was necessary to develop a suitable screening system in which knockout of host genes that affect HCV replication could be identified and characterised. To achieve this aim, we decided to use the HCV sub-genomic replicon (HCV-SGR) (see section 1.8). This sub-genomic replicon consists of a modified HCV genome that includes essential parts of the viral replication machinery, including the HCV 5' and 3' UTRs and the non-structural proteins NS3-NS5B (Fig. 3.11) (Zhou et al. 2011). A Blasticidin resistance gene (BSD) is encoded immediately downstream of the HCV IRES to allow for selection of cells with high levels of HCV replication (Fig. 3.11). A 2A-cleavage site from VP-1 foot and mouth disease virus is located between the BSD-HCV polyprotein to retain coding integrity of the HCV polyprotein. Due to the loss of the structural HCV proteins required for virus progeny production, this tool allows for the identification of host factors critical for virus replication stage of the lifecycle. High levels of HCV replication due to BSD allows for selection of a homogeneous pool across the entire cell population, which should result in improved consistency during screening compared to the infectious based system.

While this HCV-SGR setup is useful for replication studies, the lack of a suitable marker of viral clearance following knockout of an essential host factor makes the system inefficient for genome-wide screening studies. Thus, to identify cells which have lost HCV replication and facilitate subsequent extraction of enrichment of sgRNAs, reporter cell lines were generated. To achieve this, we inserted a reporter protein located immediately downstream of BSD, resulting in a BSD-reporter fusion protein (Fig. 3.11). Current HCV-SGR plasmid constructs within the laboratory consisted of a BSD-renilla luciferase fusion protein, however, this is not practical for CRISPR genome-wide screening since expression of renilla luciferase will not allow for selection of cells which are negative for HCV replication. To overcome this obstacle, renilla luciferase was removed and a more appropriate reporter protein inserted in its place. Reporter proteins chosen included the fluorescent proteins, GFP or mCherry and the negative selection marker thymidine kinase. Utilising fluorescence proteins will allow for direct visualisation of HCV replication during the entire screening process and will enable separation of cells with loss of HCV replication using flow cytometry. Our second approach involved the utilisation of the thymidine kinase negative selection marker, which will enable selection of cells which have lost HCV replication through their ability to survive ganciclovir (GCV) treatment, as thymidine kinase

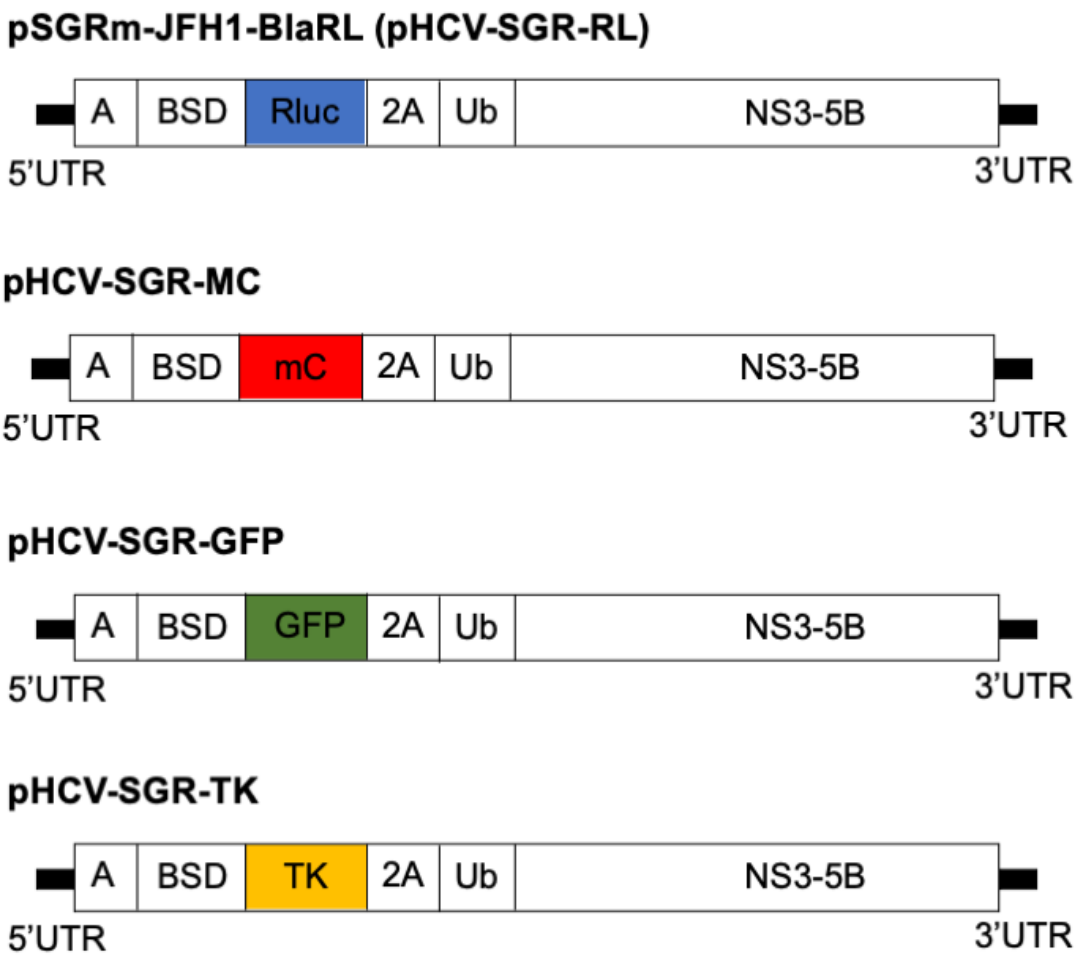

Figure 3.11: Schematic of the parental pSGRm-JFH1-Bla and generated reporter systems.

To develop the required reporter systems in order to commence the genome-wide CRISPR screen with HCV, (A) renilla luciferase was removed from parental pSGRm-JFH1-Bla and (B) mCherry, (C) GFP or (D) thymidine kinase inserted in its place. A is the HCV IRES, BSD is the Blasticidin resistance gene fused to the renilla luciferase (Rluc), mCherry (mC), GFP or thymidine kinase (TK). Downstream of the fusion protein is a 2A auto-cleavage site (2A) and ubiquitin (Ub) to allow for separation from the HCV non-structural proteins 3 to 5B (NS3-5B). Schematic is not to scale.

phosphorylates GCV into a potent DNA synthesis inhibitor, killing expressing cells (Tomicic et al. 2002). Utilising both approaches will enable comparison between enriched novel host factors and allow for the elimination of false positives.

To generate the three desired constructs for potential use in our CRISPR genome-wide screen, the renilla luciferase gene from parental pHCV-SGR-RL (pSGRm-JFH1-BlaRL) was removed via *Mlu*I and *Bgl*II restriction enzyme digestion (Zhou et al. 2011). Amplification of mCherry, GFP or thymidine kinase was achieved via PCR with primers containing the *Mlu*I/*Bgl*II restriction enzymes sites (see Appendix I) and subsequently digested with the former restriction enzymes. PCR fragments were ligated into *Mlu*I/*Bgl*II digested parental pHCV-SGR-RL plasmid and transformation yielded HCV-SGR recombinant plasmids containing either mCherry (pHCV-SGR-MC), GFP (pHCV-SGR-GFP) or thymidine kinase (pHCV-SGR-TK). Recombinant plasmids were digested with *Mlu*I and *Bgl*II to release the corresponding bands sizes (mCherry= ~700bp, GFP=~700bp, Thymidine kinase=~1.2kb), confirming generation of HCV-SGR with the three reporter plasmids (Fig. 3.12). All three reporter plasmids were sequenced (see section 2.1.10) and confirmed no mutations were present and in frame insertion of the reporter proteins.

To generate HCV RNA which can be transfected into Huh7.5 cells to allow for initiation of HCV replication, all three reporter constructs were digested with *Pme*I overnight to linearise the plasmid template for *in vitro* T7 polymerase HCV RNA transcription. Following RNA transcription and assessment of RNA integrity by gel electrophoresis, HCV RNA was transfected into Huh7.5 cells with DMRIE-C. Cells were serial diluted onto 100mm dishes and individual colonies formed following selection with BSD. Individual colonies were isolated using cloning rings and expanded to produce monoclonal HCV replicon cell lines containing either mCherry, GFP or thymidine kinase expression. Only monoclonal Huh7.5 cells that contained high levels of mCherry or GFP expression and were also positive for NS5A staining were perpetuated for use in the screen (Fig. 3.13). In contrast, monoclonal Huh7.5 cells harbouring HCV genomes containing thymidine kinase were selected only if cells showed high levels of NS5A staining based on fluorescence intensity and cell death was observed within approximately five days post addition of GCV. Illustration of HCV

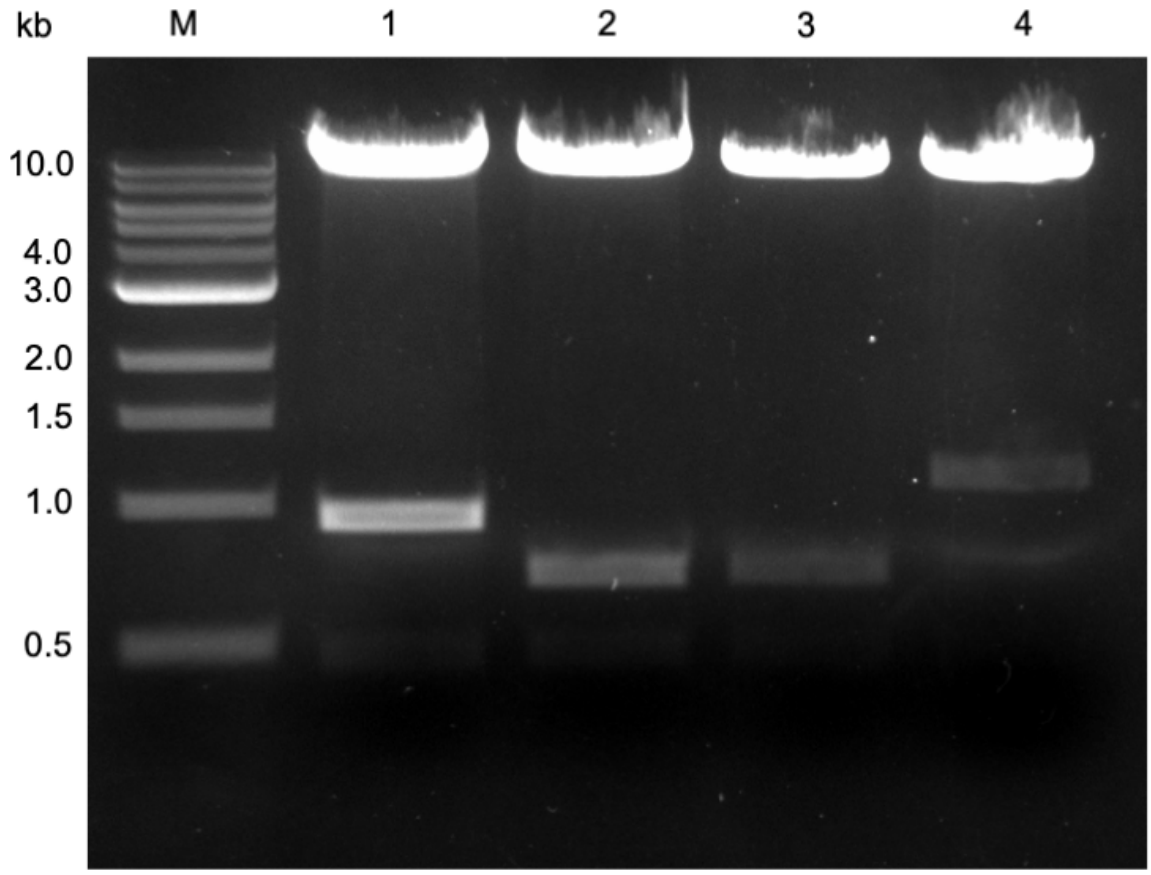

Figure 3.12: mCherry, GFP or thymidine kinase was successfully cloned into pSGRm-JFH1-Bla.

To confirm that mCherry, GFP or thymidine kinase was inserted into pSGRm-JFH1-Bla, plasmid DNA was extracted from transformant clones and digested with *Mlu*I and *Bgl*II. Lane M, 1kb DNA ladder, lane 1, parental pSGRm-JFH1-BlaRL, lane 2, pSGRm-JFH1-Bla with mCherry, lane 3, pSGRm-JFH1-Bla with GFP and lane 4, pSGRm-JFH1-Bla with thymidine kinase.

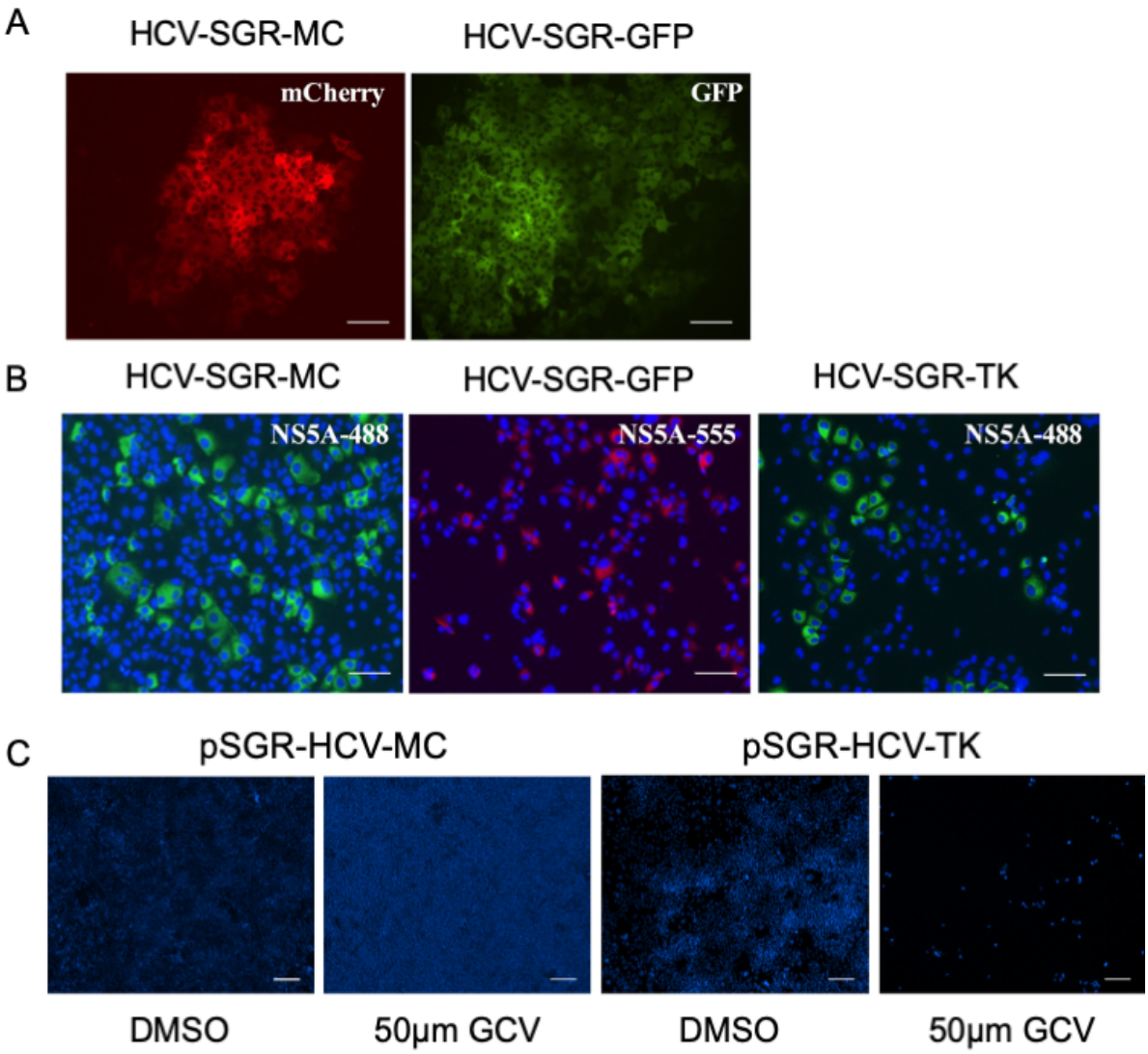

Figure 3.13: All pSGRm-JFH1-BSD reporter lines express their reporter genes and are competent for HCV replication.

(A) To determine if monoclonal pSGR-HCV reporter cell lines were functional, endogenous mCherry or GFP was observed using a Nikon TiE inverted fluorescence microscope. Scale bars are 200μm. (B) Cells were also stained with mouse anti-NS5A and Alexa Fluor 488-conjugated goat anti-mouse IgG secondary Ab (pSGR-HCV-MC) or Alexa Fluor 555-conjugated goat anti-mouse IgG secondary Ab (pSGR-HCV-GFP and pSGR-HCV-TK). Scale bars are 100μm. (C) 50μm of GCV was added to the pSGR-HCV-TK and pSGR-HCV-MC reporter cell line as well as DMSO vehicle control was added to determine if the thymidine kinase was functional. Five days post infection, cells were stained with DAPI and imaged using a Nikon TiE inverted fluorescence microscope. Note the significant cell death in pSGR-HCV-TK cells in the presence of 50μm GCV. Scale bars are 200μm.

replicon harbouring cells with fully functional inserts in all three constructs demonstrates that these constructs harbour HCV replication. These cell lines now provide a tool for use in our genome-wide CRISPR screen.

3.4 Validation of LentiCRISPRv2 GeCKO plasmid library

The Zhang Lab located within the Broad Institute at the Massachusetts Institute of Technology (MIT) provided the LentiCRISPRv2 plasmid library via Addgene (cat. #1000000048 and cat. #1000000049) to enable CRISPR based genome-wide screening. This library consists of two libraries that when combined have a total number of 122,411 sgRNAs which target 19,050 genes representing the complete human genome (Sanjana et al. 2014). 65,383 sgRNAs are present in library A and 58,028 sgRNAs are present in library B, all of which have the same LentiCRISPRv2 plasmid backbone used in the proof-of-concept experiments above (see Appendix 1). The ratio between sgRNA and targeted gene is 6:1, split evenly between the two libraries. The library also contains sgRNAs which target 1864 miRNAs and 1000 non-targeting sgRNAs, the latter of which functions as controls.

To generate a sufficient quantity of lentiviruses to enable full representation of the library during transduction, an appropriate stock of plasmid must be generated before screening can proceed. It is critical that during the expansion process that none of the ~120,000 sgRNAs are lost potentially jeopardising the integrity of the library. To generate additional stock of the LentiCRISPRv2 plasmid library, each library was electroporated into Endura competent cells. These have the highest efficiency among commercially available cells for lentiviral based constructs and were recommended by the Zhang Lab for transformation of the libraries. A total of 4 electroporations were completed per library, which were then pooled and spread onto pre-warmed agar containing ampicillin petri dishes. All petri dishes were grown at 32^{o}C for 14 hours to decrease plasmid recombination and a confluent lawn of bacteria developed, indicating successful transformation of the LentiCRISPRv2 library. To ascertain whether transformation efficiency was sufficient to enable complete representation of the libraries, a 40,000 dilution of the transformation was plated on a separate petri dish and counted to determine if the total number of colonies exceeded $3x10^6$. Approximately 415 colonies were present on the 40,000-dilution plate for library A and 241 colonies in library B, giving an estimated total colony count of $1.6x10^7$ and $9.6x10^6$

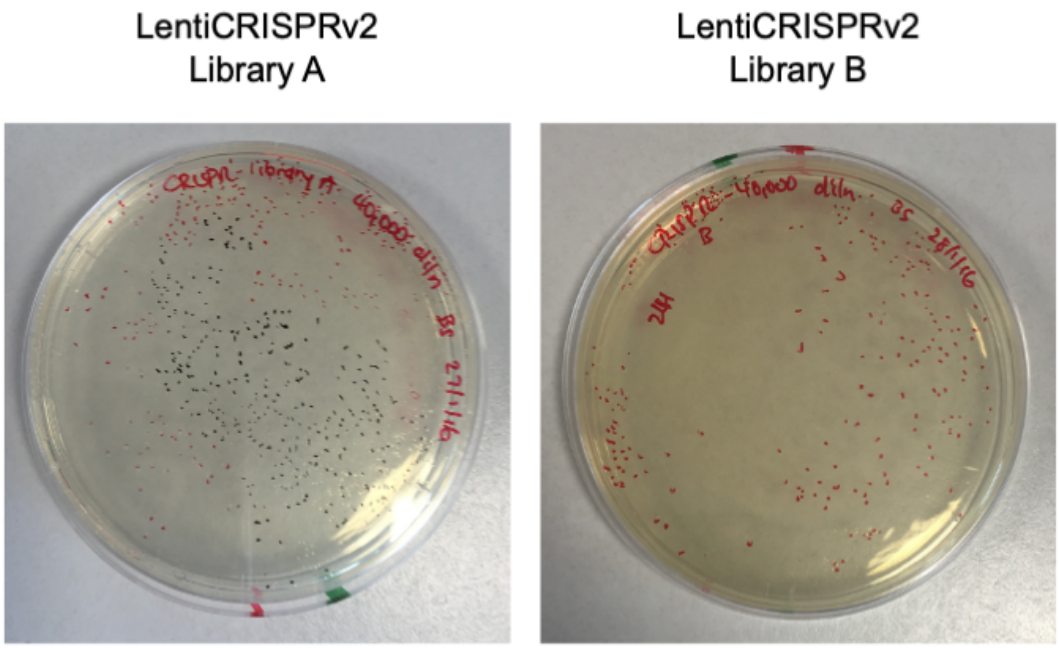

Figure 3.14: Efficient transformation allows for complete representation of the LentiCRISPRv2 libraries.

To gauge the transformation efficiency during the amplification process of the LentiCRISPRv2 library, a 40,000 dilution of the bacterial transformation of each half library was spread onto ampicillin agar plates and colonies counted the following day. Each dot (either red or black) indicates one bacterial colony.

for library A and B respectively and therefore sufficient transformation of the LentiCRISPRv2 library to retain representation of all the sgRNAs (Fig. 3.14). A sufficient number of colonies present indicated that no sgRNAs were lost in the transformation process, where it is assumed that one bacterial colony observed on an agar plate contains a sgRNA targeting a single gene. The colonies were subsequently harvested directly to isolate the LentiCRISPRv2 library plasmid through maxi-preparation (see section 2.1.4).

Lentivirus harbouring representation of the LentiCRISPRv2 library was generated via transfection of 293T cells with plasmid and lipofectamine 2000 as per section 2.3.9. A critical aspect of the CRISPR-mediated screening process is to use a low MOI during transduction to ensure only one gene knockout per cell and therefore, it is critical to determine the titre of the lentivirus produced. The Zhang Lab recommended an indirect method to determine the lentiviral supernatant titre by calculation of transduction efficiency via exploitation of the puromycin resistance gene (Joung et al. 2017). Huh7.5 cells in a 12 well plate was transduced with increasing volumes of virus (in the ranges of 5-500μl) and supplemented with cell media. 5 hours post transduction, media was replaced, and cells left to incubate overnight. Cells were trypsinised, split across 2 wells of a 6 well plate and seeded into separate wells. Five days post transduction, cells were treated with puromycin, to not only remove un-transduced cells but also to simulate conditions during the genome-wide CRISPR screening process. After three days or after the mock-transduced control with puromycin were all dead, cells were trypsinised and counted to determine the transduction percentage as follows:

$$\frac{cell\ count\ of\ transduction\ with\ puromycin}{cell\ count\ of\ transduction\ without\ puromycin} \times 100\%$$

The volume of lentiviruses added which yielded a transduction percentage closest to 30% was selected and scaled accordingly during the genome-wide CRISPR screening process, with the assumption that a 30% transduction percentage correlates with one lentivirus transduction and subsequently one targeted gene knockout per cell.

It is essential that all sgRNAs are present within the LentiCRISPRv2 library to ensure broad coverage knockout across the genome. Loss of any sgRNAs may result in

overlooking a subset of genes that could be important, compromising the integrity of the genome-wide screening process. Thus, to ensure that the LentiCRISPRv2 plasmid library has complete representation, the sgRNA sequences were PCR amplified and analysed by next generation sequencing.

The GeCKO LentiCRISPRv2 plasmid library was first PCR amplified using Q5 polymerase and custom primers generated by the Zhang Lab (see Appendix 1) as per section 2.1.12. The first PCR is required for the amplification of the area of interest (sgRNA) and to generate the necessary binding sites for subsequent primers to bind to in the second PCR stage. A band size of ~300bp which includes the sgRNA region was observed during the first step PCR stage, as expected (Fig. 3.15 and 3.16). Following gel extraction, the second PCR stage was performed utilising a mixture of custom forward and reverse primers generated by the Zhang Lab (see Appendix 1), which contain the necessary Illumina adaptors and barcode sequences to be compatible with the Illumina Miseq system. A band size of ~350bp was visible and gel extracted (Fig. 3.15 and 3.16). Following the second round of PCR amplification, the samples were sequences at the David Gunn Genomics Facility (SAHMRI) using the MiSeq system. The MiSeq paired end 150 cycles reagent kit was used to allow for the sequencing of 80bp from the 5' end of the PCR product where the sgRNA sequence is located (Fig. 3.15). Cycling conditions include 80 cycles of read one (forward) and eight cycles of index one. 5% of PhiX was also spiked with the sgRNA-PCR products to improve library diversity, as the 5' end of each PCR fragment to be sequenced are almost identical. The adaptors were trimmed post sequencing *in silico* and barcodes used to group sequences based on their origin (library A or B).

Analysis by our collaborator, Dr. Auda Eltahla at the Kirby Institute, UNSW revealed 10 million of the total 20 million reads aligned to the reference library provided by the Zhang Lab. One million of the 20 million reads aligned to the PhiX control library with the remainder (nine million) consisting of poor reads. Approximately half of the 10 million reads aligned to each half library (library A or B). 62,558 out of 65,383 or 96% of sgRNAs were present in library A and 51,620 out of 53,627 or 96% of sgRNAs were present in library B. Although the loss of 4859 sgRNAs was initially concerning, design of the GeCKO LentiCRISPRv2 library consists of six sgRNAs per gene, where on average approximately 4000 out of 18,080 genes would have five sgRNAs instead of

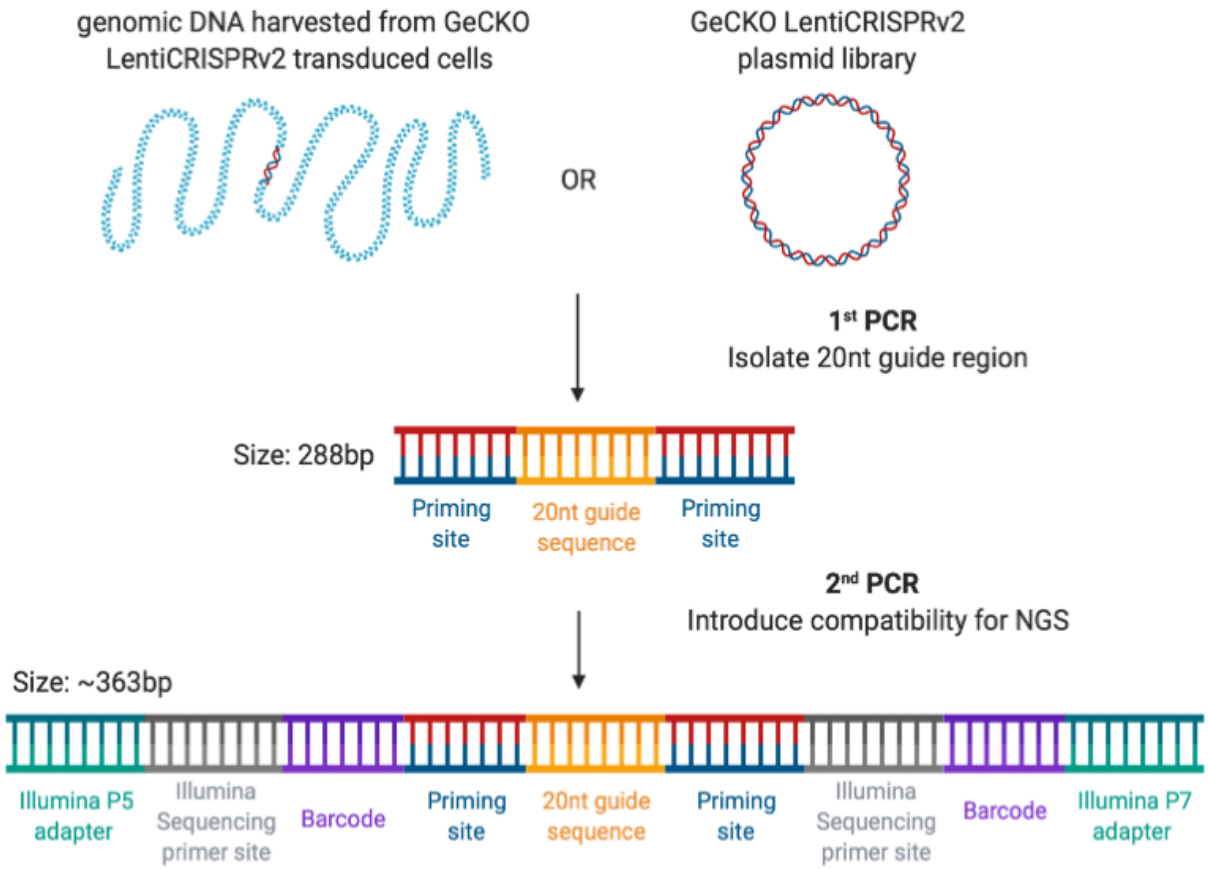

Figure 3.15 Schematic of two-step PCR performed to enable guide sequences to be sequenced by NGS

GeCKO LentiCRISPRv2 plasmid library or genomic DNA harvested from cells after genome-wide CRISPR screening will be amplified twice by PCR to enable sequencing by NGS. The primers for the 1st PCR bind to the priming site either side of the 20nt guide sequence to allow for enrichment of this region to perform the 2nd PCR. The primers for the 2nd PCR bind to the priming site of the PCR product from the 1st PCR and introduces the required components to enable compatibility of the PCR product for NGS (Illumina P5 and P7 adapters and sequencing sites) as well as barcodes to allow tagging of samples. Schematic not to scale.

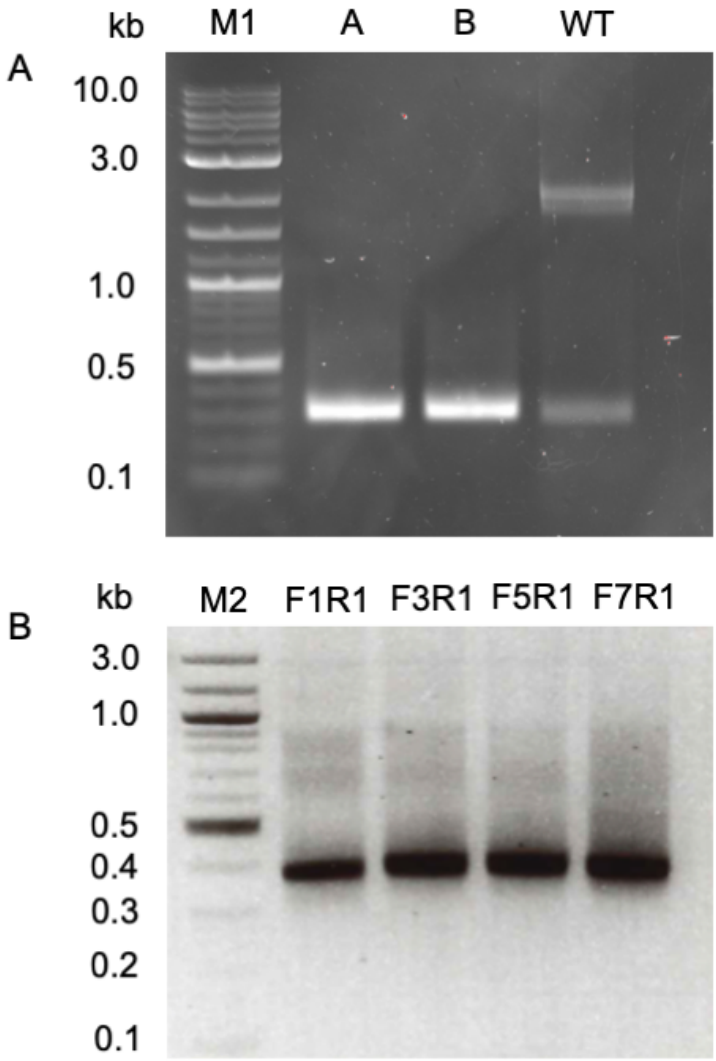

Figure 3.16: Successful PCR amplification of the sgRNA region of interest to enable compatibility with next-generation sequencing.

To determine if all the sgRNAs are present in the GeCKO LentiCRISPRv2 library, a two-step PCR amplification process was followed, where the first amplifies the region of interest and the second includes the addition of Illumina adaptors to enable compatibility for MiSeq next-generation sequencing. Both reactions were performed with NEB Q5 polymerase, where a sample was run on an agarose gel to verify that both the first (A) and second (B) PCR amplification steps were successful. (A) Lane M1, 2-log DNA ladder. Lane A, B and WT, first amplification step with LentiCRISPRv2 library A, B or WT plasmid respectively. (B) Lane M2, 100bp ladder, all lanes present after lane M2 are combinations of primer utilised in the second amplification step i.e. F1R1 is PCR amplification with forward primer 1 and reverse primer 1 (see Appendix 1).

six, and thus it is highly unlikely that all six sgRNAs for one gene were lost out of the 4859 sgRNAs not present. This coupled with the knockout efficiency of CRISPR/Cas9, led us to conclude that 96% of the intact GeCKO lentiCRISPRv2 library was sufficient to commence genome-wide screening.

3.5 Optimisation of LentiCRISPRv2 library screening conditions with HCV replicon systems

Monoclonal populations of the HCV-SGR reporter cell lines containing either mCherry, GFP or thymidine kinase were successfully generated and ready to be used for genome-wide screening as per section 3.2. In addition, each LentiCRISPRv2 half library was successfully verified to contain 96% of sgRNAs and lentivirus generated to necessary concentrations to allow for transduction of the required cell quantity to enable complete representation of the library as per section 3.6. Thus, it was now possible to begin the CRISPR genome-wide knockout screen with the HCV SGR reporter cell lines.

3.5.1 Genome-wide screening using HCV-SGR-MC/GFP cell lines

Our strategy to perform the genome-wide CRISPR screen using the Huh7.5 cells harbouring HCV-SGR-MC or -GFP involves transduction with the LentiCRISPRv2 library, where half of the cells will be transduced with library A or library B respectively at a MOI of approximately 0.3 to allow for one transduction event per cell and therefore one knockout per cell. Five days post transduction, puromycin will be added to select for cells which had successfully undergone lentivirus integration of the sgRNA cassette and Cas9 complex and the puromycin resistance gene. Cells surviving puromycin treatment represent cells which, (A) retain fluorescence (i.e. either MC or GFP) is indicative of active HCV replication, where knockout of a gene within these cells is not required for virus replication or (B), cells which have lost fluorescence activity represent cells in which knockout of a potential proviral host factor has occurred resulting in a loss of HCV replication. Genomic DNA will be harvested from both cellular populations displaying either mCherry and GFP positive and negative fluorescence and the two stage PCR and next generation sequencing performed as per section 3.6. This screening method is summarised in figure 3.17.

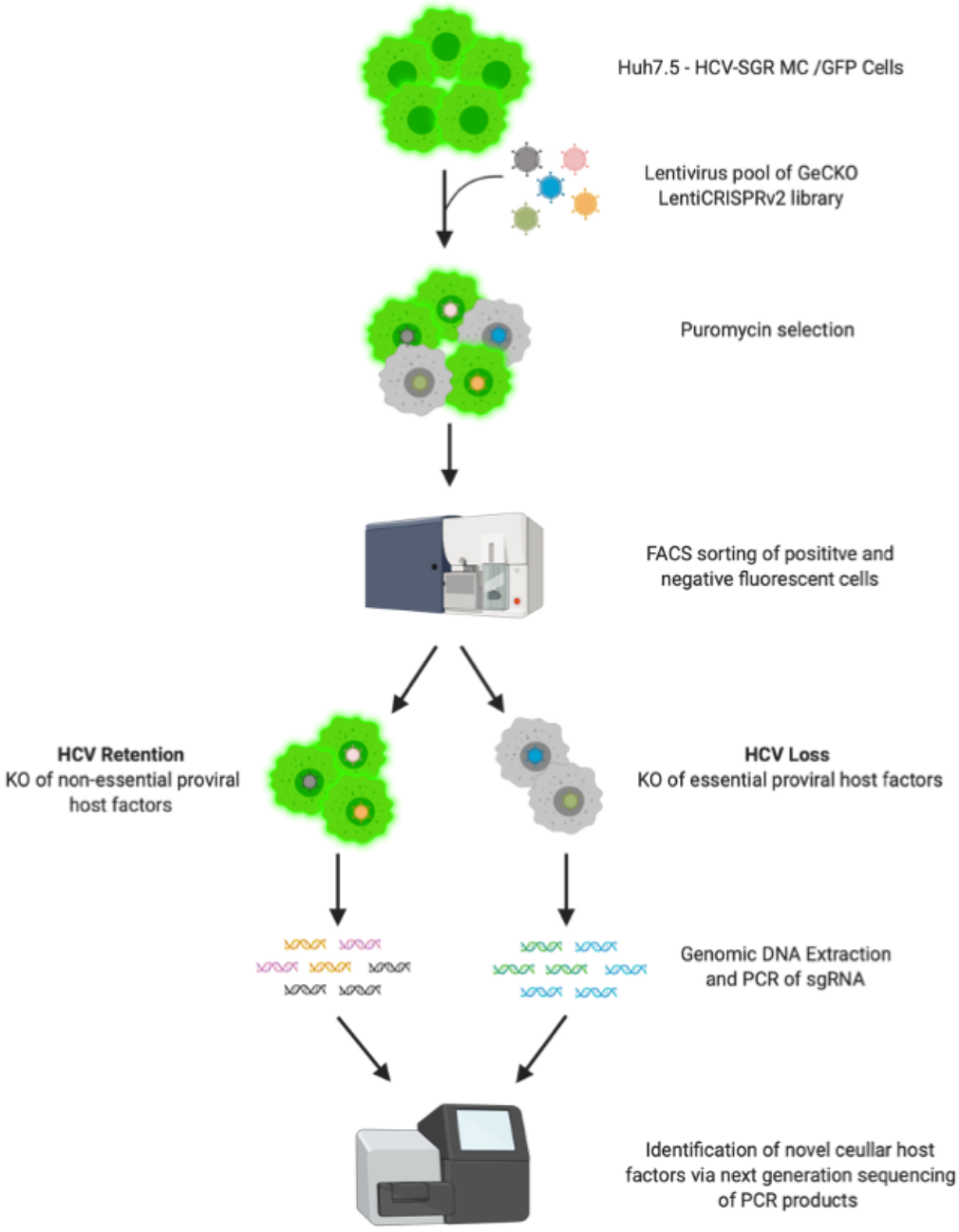

Figure 3.17: Screening process for the identification of novel host factors for HCV replication with HCV-SGR-MC/GFP.

The GeCKO LentiCRISPR library in a lentivirus pool infects HCV replicon positive cells expressing either GFP (or mCherry - not illustrated). If a host factor single knockout is important for HCV replication (illustrated as a blue or green virus), fluorescence expression will be lost as a result (illustrated as a grey cell). Cells can be sorted based on flow cytometry to sort fluorescence positive and negative cells and next generation sequencing utilised to ascertain which host factors regulate HCV replication.

Although the HCV-SGR-MC and HCV-SGR-GFP reporter cell lines were resistant to BSD, a high proportion of cells were negative for either MC or GFP fluorescence activity, which would ultimately impact the genome-wide screening process. This mixed cell population is intriguing as BSD resistance suggests active HCV replication in all cells. The reason for this mixed population is not immediately apparent. One plausible explanation is the reliance of active virus replication on the HCV IRES, which controls the expression of both the HCV non-structural proteins and the BSD-reporter protein (either MC, GFP or thymidine kinase). The HCV IRES has been shown to be enhanced during the mitotic phase (G_2/M) and relatively inactive during the early S phase of the cell cycle (Honda et al. 2000). This could explain our observation of fluctuating expression levels of our reporter protein of interest. Alternatively, selected cells may have inherent differences in HCV replication efficiency and therefore differences in reporter gene expression. Therefore to address the latter, we proceeded to enrich the cells with maximal fluorescence activity using flow cytometry. Following FACS, HCV-SGR-MC cells with the highest expression of mCherry were pooled into a separate flask and grown to reach suitable cell density levels for genome-wide screening. Initially, all pooled HCV-SGR-MC cells contained a high level of mCherry expression, however, after three passages the expression of mCherry reverted to levels prior to flow cytometry (Fig. 3.18). Reversion of fluctuating mCherry levels within the cell population post-sort may suggest that upon multiple passages, the SGR system may have removed the mCherry reporter protein whilst retaining BSD resistance, likely due to decreased fitness of virus replication as the mCherry reporter contributes no significant advantage to HCV replication. Although this observation was of concern, we proceeded to modify the screening process where multiple rounds of flow cytometry were performed to ensure only cells with a complete loss of mCherry were selected for the next step of extraction of gDNA and next-generation sequencing. Although feasible, this approach was deemed not viable due to time constraints and the exposure of the flow sorting facility to high numbers of HCV positive (albeit non-infectious SGR) cells.

3.5.2 Genome-wide screening using HCV-SGR-TK cell line

Given the issues faced above, we next moved to using the genome-wide CRISPR screen utilising the TK cell survival model. $3x10^8$ of Huh7.5 cells containing HCV-SGR-

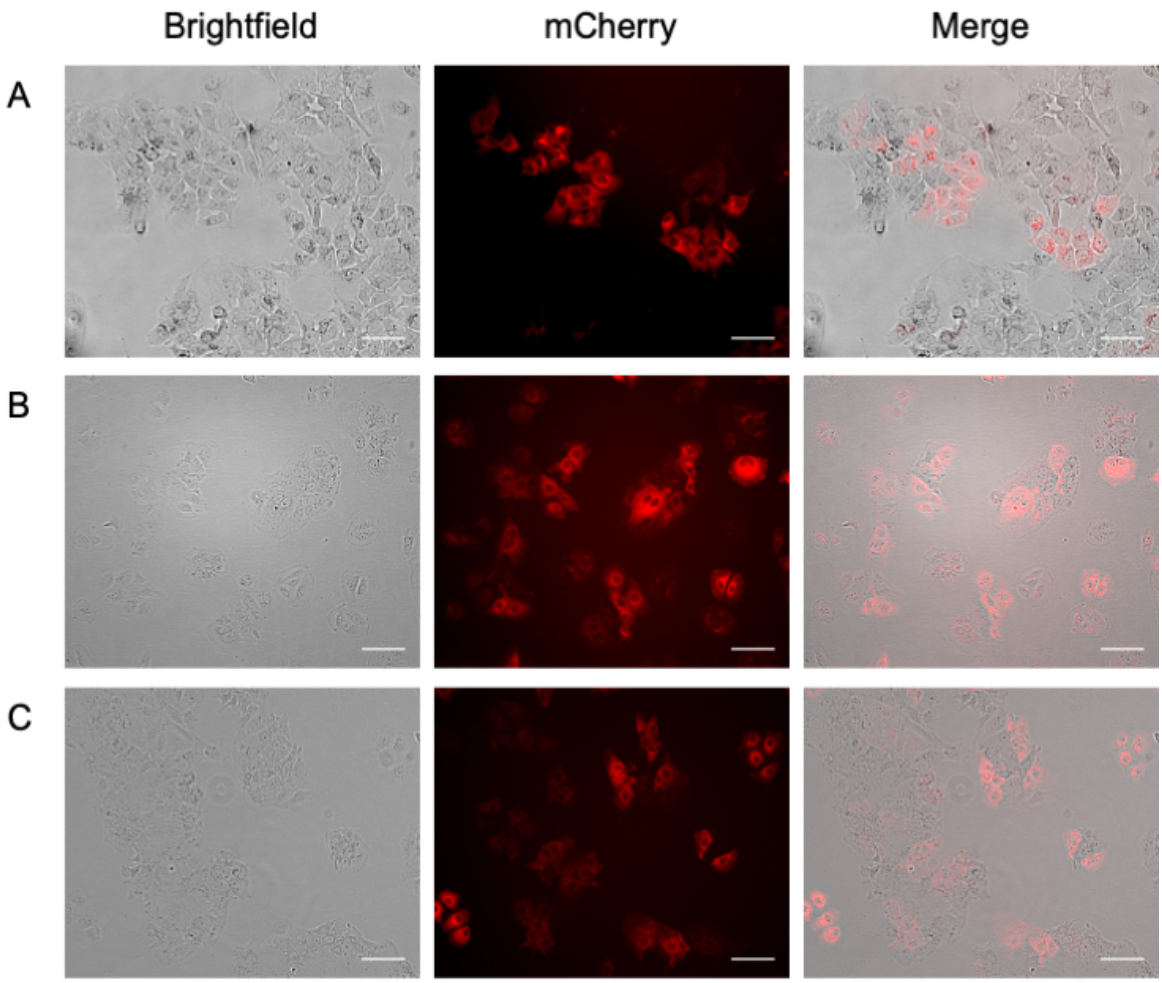

Figure 3.18: Attempted enrichment of mCherry positive HCV-SGR-MC cells through flow cytometry.

Huh7.5 cells with HCV-SGR-MC with high levels of HCV replication were selected utilising flow cytometry, gating for cells with the highest levels of mCherry fluorescence. To determine if enrichment of mCherry cells were successful, cells were imaged either one day prior (A), the day post sorting (B) and three days post sorting (C) via flow cytometry utilising a a Nikon TiE inverted fluorescence microscope. Scale bars are 100μm.

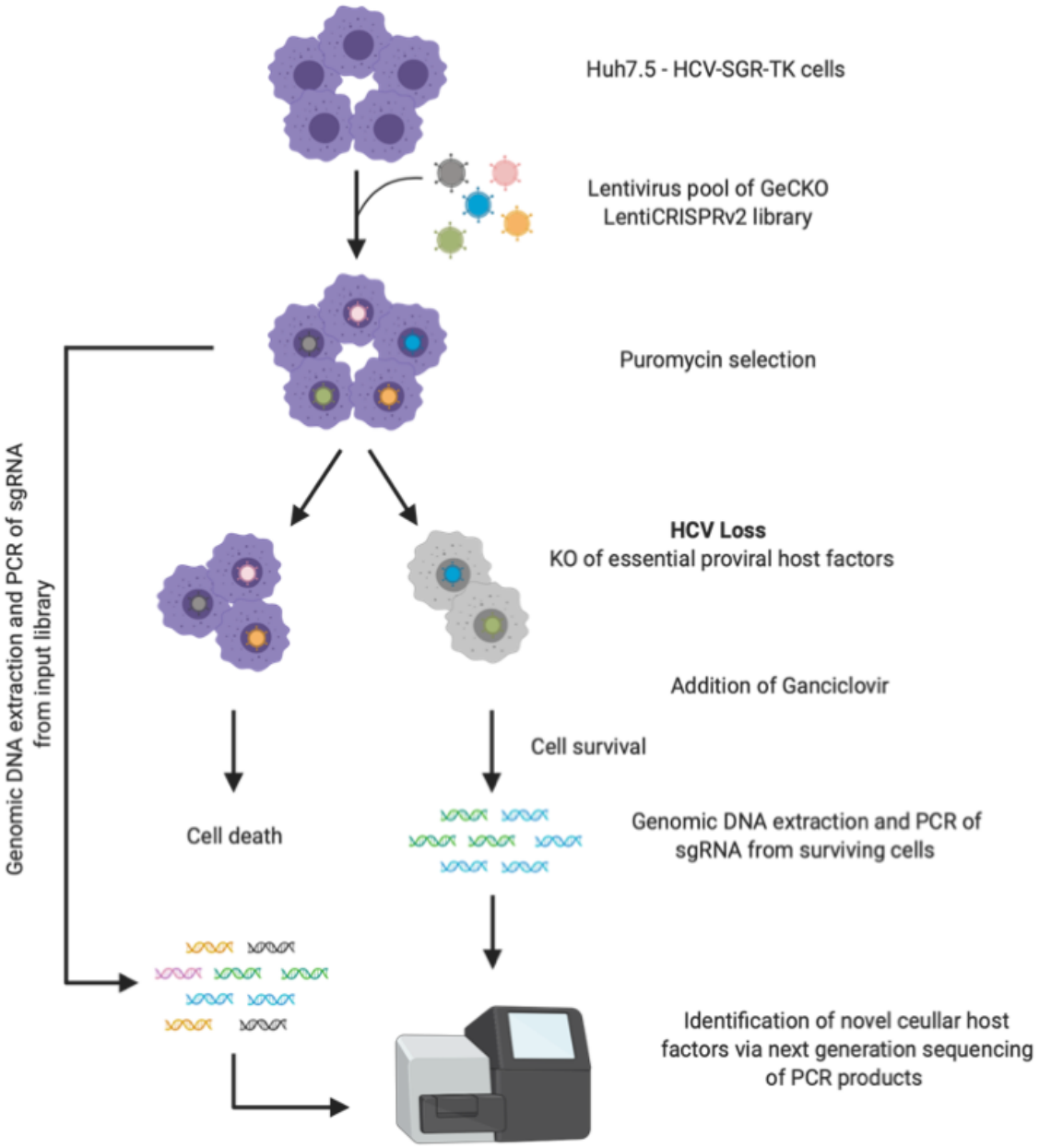

Figure 3.19: Screening process for the identification of novel host factors for HCV replication with HCV-SGR-TK.

The GeCKO LentiCRISPR library in a lentivirus pool infects HCV replicon positive cells expressing thymidine kinase. If a host factor single knockout is important for HCV replication (illustrated as a blue or green virus), thymidine kinase expression and HCV replication will be lost as a result (illustrated as a grey cell). Addition of Ganciclovir in the presence of thymidine kinase will ultimately result in a toxic analogue that integrates into DNA, where cells which have lost HCV replication will survive. Next generation sequencing will be utilised to ascertain which host factors regulate HCV replication.

TK were transduced with the LentiCRISPRv2 library, where each half of the cells were transduced with library A or library B respectively at a MOI of approximately 0.3 to allow for one transduction event per cell and therefore one knockout per cell. Five days post transduction, 3μg/ml of puromycin was added to select for cells that had successfully undergone lentivirus integration and were expressing both the sgRNA/Cas9 complex and the puromycin resistance gene. Following complete cell death of the mock transduced control cells, 50μm of ganciclovir (GCV) was added so cells that retained HCV replication and thus thymidine kinase expression, would phosphorylate the GCV to a toxic metabolite, resulting in cell death. Therefore, cells that have lost HCV replication due to knockout of a host factor will be resistant to GCV induced cell death. A small percentage of cells were expected to survive due to the assumption that a vast majority of genes would not be important for HCV replication. Following complete cell death by GCV in the mock lentivirus transduced control cells, genomic DNA would then be harvested from the surviving GCV resistant cells and the two stage PCR and next generation sequencing performed as per section 3.6. Genomic DNA would also be harvested from cells that had been successfully transduced with the LentiCRISPRv2 library prior to treatment with GCV, as a reference to ensure that there was good representation of all sgRNAs prior to cell selection. This screening process is illustrated in figure 3.19.

Following the addition of puromycin to $3x10^8$ HCV-SGR-TK cells that had been transduced with the LentiCRISPRv2 library, one third of the cells died as expected, due to unsuccessful integration of the lentivirus. 50μm of GCV was added to the puromycin resistant cells for one week to enrich for cells which have lost thymidine kinase expression and subsequently HCV replication as a result of the knockout of a key proviral host factor. Unfortunately, after one week of incubation of cells with GCV, cell death was not of the magnitude expected, based on the assumption that most genes within the genome are not important for HCV replication. Further incubation with an increased concentration of GCV (100μm) also yielded minimal cell death, indicating the entire cell population was resistant to GCV induced cell death and suggests the majority of cells had lost HCV replication. GCV was biologically active as the un-transduced HCV-SGR-TK cells remained susceptible to GCV induced cell death (100%), indicating production of thymidine kinase catalysed production of toxic metabolites.

Given that the HCV-SGR-TK GeCKO LentiCRISPRv2 library transduced cells were resistant to GCV treatment, it was imperative to determine the status of cellular population with regards to both active HCV replication and expression of the thymidine kinase gene. Cells transduced with GeCKO LentiCRISPRv2 library (A+B) resistant to GCV displayed significantly reduced levels of NS5A staining via immunofluorescence microscopy, indicating that the majority of cells contained no active HCV replication compared to the parental HCV-SGR-TK cell line (Fig. 3.20A). For the surviving population to be resistant to GCV induced cell death, thymidine kinase must be absent to enable the cells to survive. Since we had no access to an antibody to detect the HSV thymidine kinase, total RNA was harvested as an indirect measure to determine thymidine RNA levels. RNA was extracted from the GCV resistant cell population as per section 2.1.10. RNA extraction was also performed on HCV-SGR-TK cells prior to lentivirus transduction as positive controls. cDNA was synthesised with the HCV 5970 reverse primer used for cloning the HCV JFH strain to enable conversion of the HCV SGR RNA into cDNA (see Appendix 1 and as per section 2.1.13) (Wakita 2009). PCR amplification with primers that bind to thymidine kinase was performed to determine if surviving cells still retained the capability to express thymidine kinase (see Appendix 1). A band with an approximate size of 1kb was observed for the plasmid positive control, indicating that PCR amplification of thymidine kinase was successful (Fig. 3.20B). A similar band was also evident for the HCV-SGR-TK positive control sample, demonstrating that HCV SGR specific cDNA was produced from RNA within the cells and the cells were capable of expressing thymidine kinase. However, no band was present for both GCV resistant HCV-SGR-TK transduced with either library, indicating that the entire cell population had lost the ability to express thymidine kinase and was thus resistant to GCV induced cell death.

A potential source of the loss of thymidine kinase and the entire HCV-SGR RNA could be caused by lentiviral transduction of the LentiCRISPRv2 library during the screening process. All genome-wide CRISPR screens with viruses from the *flaviviridae* family performed to date have used infectious virus, where infection occurs after transduction of the genome-wide CRISPR library. Our system also relies on the removal of BSD prior to the transduction of the GeCKO lentiCRISPRv2 library as knockout of a proviral host factor (and consequently HCV replication) will also render the cell susceptible to BSD. Therefore, there may be a possibility where introduction of the LentiCRISPRv2

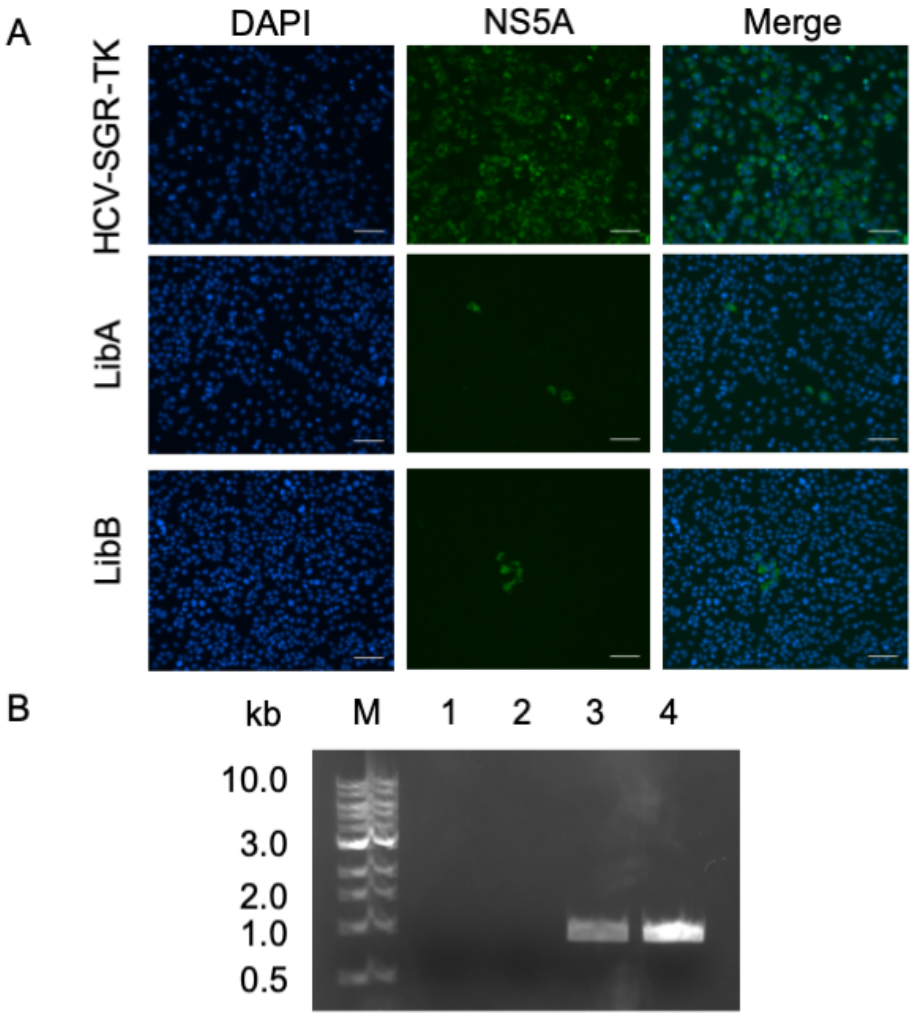

Figure 3.20: HCV-SGR-TK cells transduced with LentiCRISPRv2 library which have survived GCV treatment are both HCV replication and thymidine kinase deficient.

To ascertain whether HCV-SGR-TK cells which survive GCV treatment post LentiCRISPRv2 transduction contain active HCV replication, immunofluorescence microscopy was employed to determine presence of NS5A protein within the cell population. (A) Cells were stained with mouse anti-NS5A and Alexa Fluor 555-conjugated goat anti-mouse IgG secondary Ab. Post DAPI staining, cells were visualised using a Nikon TiE inverted fluorescence microscope. Scale bars are 100μm. (B) To determine if thymidine kinase was present and therefore resistant to GCV induced cell death, RNA was extracted and cDNA synthesised from HCV-SGR-TK cells transduced with either library A (lane 1) or B (lane 2). RNA from parental HCV-SGR-TK cells (lane 3) were also extracted in addition to HCV-SGR-TK plasmid (lane 4) as controls. Thymidine kinase was amplified with Q5 polymerase and run on a 1% agarose gel. Lane M, 1kb ladder.

library after the establishment of HCV replication may directly or indirectly interfere with the former due to the loss of selection pressure by the removal of BSD within the culture media. To test this theory, where the addition of lentivirus may interfere with HCV replication, lentiviruses encoding mCherry were transduced into cells expressing either HCV-SGR-TK or parental HCV-SGR and NS5A visualised (Immunofluorescence) to determine the levels of both HCV replication and lentivirus transduction expression via flow cytometry. To mimic our genome-wide screening process, cells were fixed five (prior to addition of puromycin) and 20 days post transduction (expected end point of screen). Five days post transduction, approximately 70% of cells were positive for NS5A for the parental HCV-SGR and slightly lower for the HCV-SGR-TK (top left and right quadrants). 50% of cells were also positive for mCherry expression, indicating successful lentivirus transduction (bottom right quadrant) (Fig. 3.21A). However, 20 days post transduction, which is the expected end point of the screening process, 95% of the population for both HCV-SGR and HCV-SGR-TK were negative for NS5A staining (bottom left and right quadrants), while the remaining were positive for mCherry expression (top left and right quadrants). Since mCherry expression was expected to not have an effect on HCV replication, it is likely that lentivirus transduction indirectly resulted in the ejection of the HCV-SGR RNA and subsequent loss NS5A expression, due to the loss of BSD selection pressure prior to commencement of genome-wide screening (illustrated in Fig. 3.22). Unfortunately, these results indicate the HCV-SGR-TK system is not suitable for genome-wide screening and was thus not pursued further.

3.6 Discussion

Although direct acting antivirals are the main treatment for chronic hepatitis C, HCV infection still remains a major health issue worldwide, primarily through the lack of an effective vaccine. Secondary factors include the high cost and availability of HCV antivirals within developing countries. Thus, further understanding of the HCV lifecycle is critical to enable development of cost-effective antivirals and efficacious vaccines. Viruses including HCV have a limited coding capacity and thus exploit host proteins to fully support the entire lifecycle from entry to egress. Through the use of both RNAi and CRISPR technology, host factors have been identified and characterised for HCV replication. For example, PI4KA, which is a critical host factor for the construction of

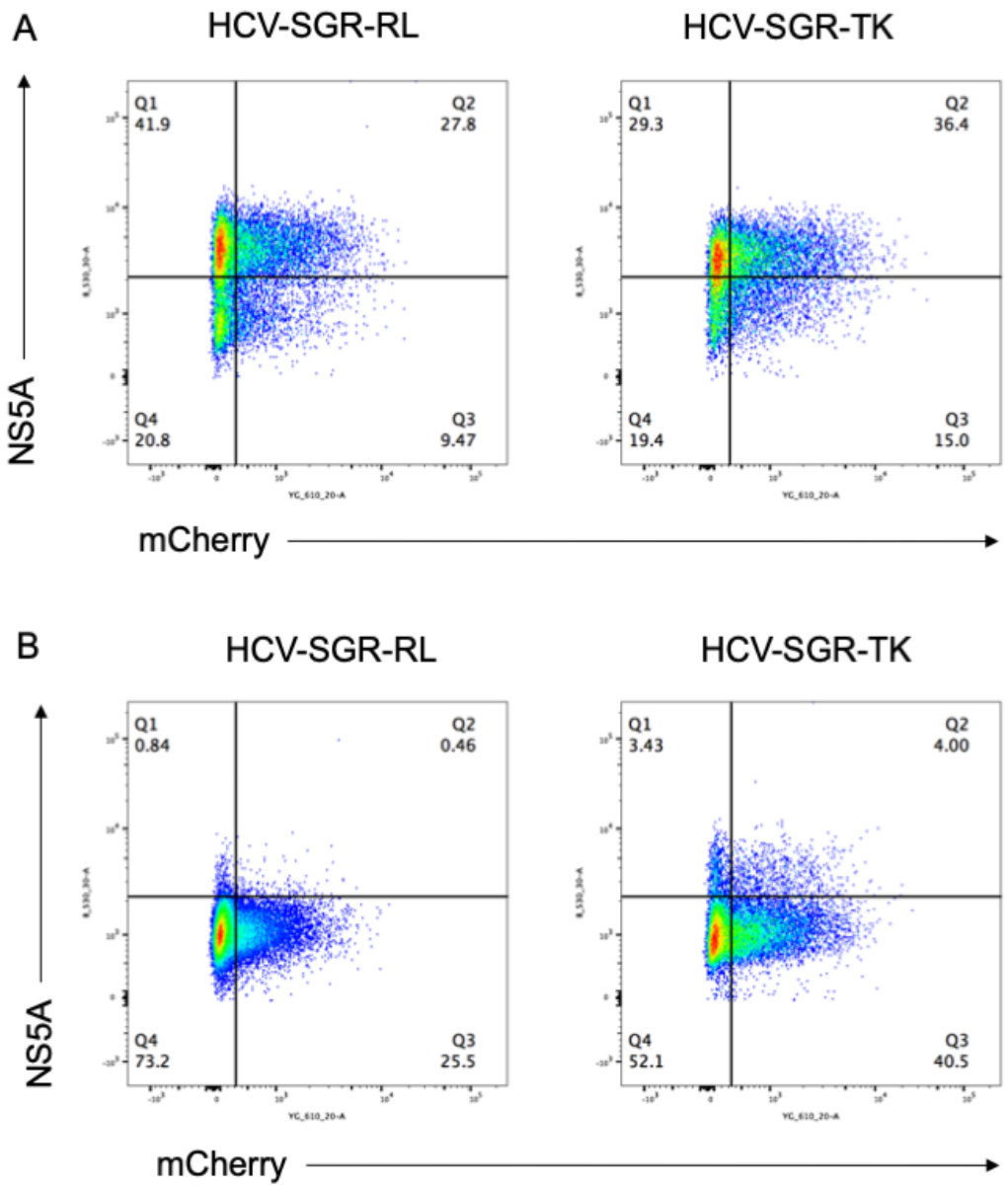

Figure 3.21: Transduction of lentiviruses with a loss of Blasticidin selection results in the reduction of HCV replication.

To visualise the effect of transduction of the LentiCRISPRv2 library on HCV replication in HCV-SGR-TK cells, lentiviruses encoding mCherry were transduced into HCV-SGR-TK and grown without BSD 5 (A) or 20 (B) days prior to flow cytometry. Cells were stained with mouse anti-NS5A and Alexa Fluor 488-conjugated goat anti-mouse IgG secondary Ab and gated for both NS5A and mCherry expression levels.

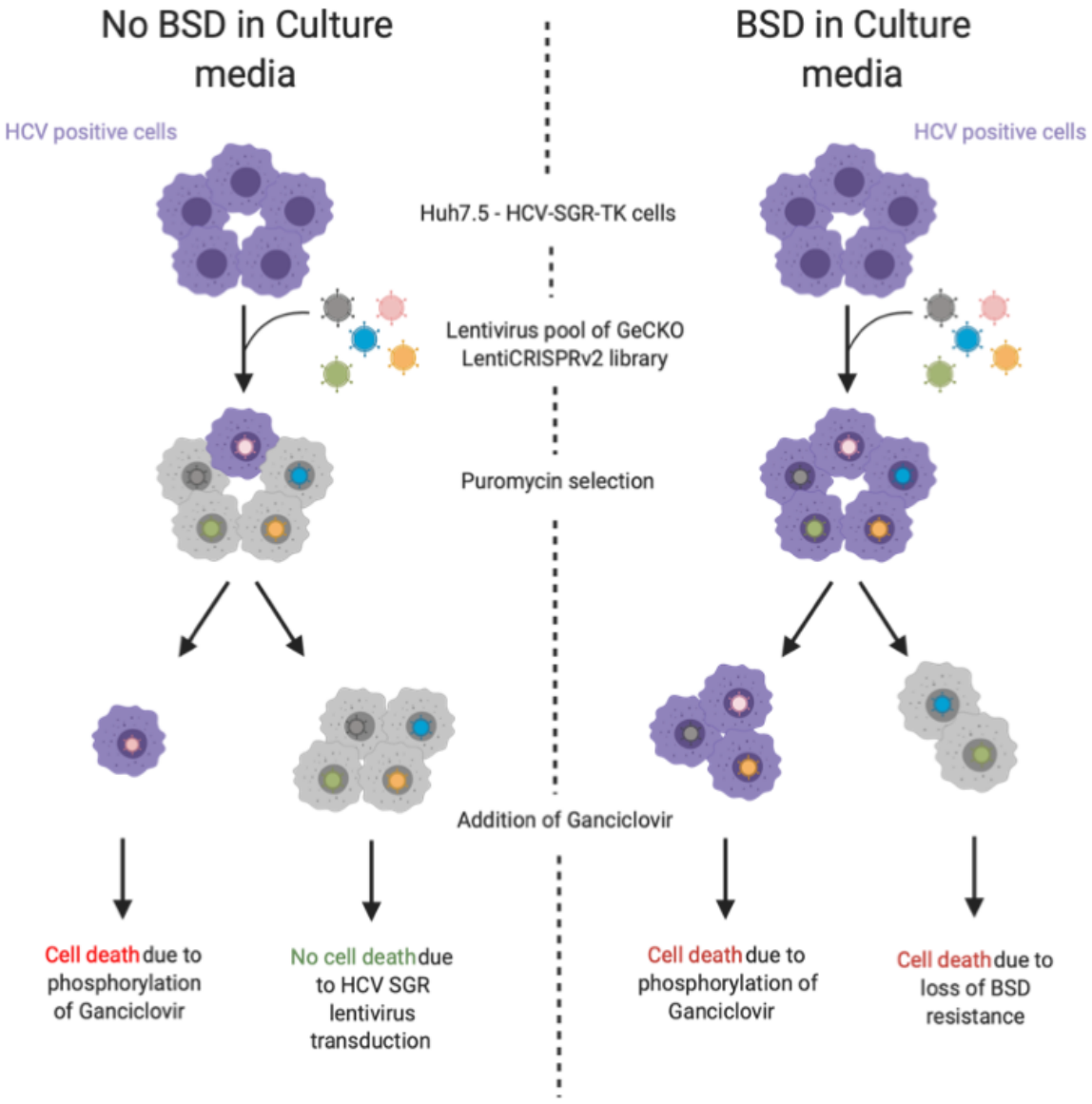

Figure 3.22: Projected outcomes when utilising the HCV-SGR-TK system for genome-wide CRISPR screening.

When Huh7.5-HCV-SGR-TK cells are cultured with no BSD throughout the genome-wide screening process, cells which retain HCV replication undergo Ganciclovir (GCV) induced cell death due to thymidine kinase expression. However, the majority of the cellular population which survive GCV treatment have lost HCV replication due to the combination of lentivirus transduction of the library with the loss of selection pressure from BSD. In contrast, when Huh7.5-HCV-SGR-TK cells are cultured with BSD throughout the genome-wide screening process, cell death is observed in both HCV positive and negative populations as loss of the HCV SGR results in loss of BSD resistance for the latter.

the replication complex through the recruitment of both host (OSBP, hVAP-A and CypA) and viral proteins (NS5A) towards the ER membrane (see section 1.9) (Chukkapalli and Randall 2014). Exploitation of host-viral interactions has resulted in the identification of inhibitors which target host factors such as OSBP and CypA, leading to a reduction of HCV replication (see section 1.9). However, additional host factors for the HCV lifecycle remain to be characterised and utilisation of CRISPR technology to screen at the genome level will allow for the identification of novel HCV proviral host factors.

There are two main aspects to consider when designing a genome-wide CRISPR screen to identify novel proviral host factors, (i) the selection of a genome-wide CRISPR library with the appropriate Cas9/dCas9 and (ii) the phenotypic output of the screen (Albulescu et al. 2017). A number of lentiviral based CRISPR knockout libraries were available to screen for novel host factors using the SGR system at the commencement of this project. These were readily available for purchase via Addgene and include, (i) the GeCKO LentiCRISPRv2 library (Shalem et al. 2014), (ii) the human activity-optimised CRISPR knockout library (Wang et al. 2015) and (iii) the human genome-wide library v1 (Ma et al. 2015). The most popular library at the time was the GeCKO LentiCRISPRv2 library, with a number of publications from broad research fields successfully utilising this system (Virreira Winter et al. 2016; Sun et al. 2018; Han et al. 2019; Wheeler et al. 2019; Du et al. 2020). In addition, protocols for screening and troubleshooting with lentiviral CRISPR libraries were not established, unlike today, and thus it was important to choose a library that had dedicated support. The Zhang lab who constructed the GeCKO LentiCRISPRv2 library provides a Google support forum webpage and was the system of choice. The one-plasmid system (LentiCRISPRv2) was selected over the two-plasmid system (LentiGuide) due to the need of stably integrated expression of Cas9 within the Huh7.5 cells harbouring HCV SGR prior to transduction of the sgRNA for the latter and may impact HCV replication. In addition, selection of Cas9 stable cells relies on BSD, which is also present within the HCV SGR system. Thus, the one-plasmid GeCKO LentiCRISPRv2 library was chosen to be used in conjunction with the SGR system for genome-wide CRISPR screening of HCV novel host factors.

After selection of the GeCKO LentiCRISPRv2 library and commencement of our genome-wide screening, lentiviral based CRISPR libraries developed by other laboratories were released onto the Addgene market. Refinement of sgRNA computational design rules also resulted in maximised activity of Cas9 at target sites with minimisation of off-target cleavage, further improving on library performance during screening (Doench et al. 2016; Ong et al. 2018). Thus, CRISPR knockout libraries developed after GeCKO LentiCRISPRv2 incorporate the improved sgRNA design rules like the Brunello LentiCRISPRv2 library that has fewer sgRNAs (77,441 total sgRNAs compared to 122,471 total sgRNAs in GeCKO) targeting each gene but outperforms the GeCKO LentiCRISPRv2 library in both on-target activity and generation of frame shift mutations (Doench et al. 2016; Sanson et al. 2018). Repeat of a genome-wide CRISPR screen with HCV would likely use one of the newer libraries described above due to improved performance over our current library in combination with fewer resources required to retain full complexity of the library due to the reduction in total sgRNAs present.

In addition to the traditional CRISPR knockout libraries described above, the mutation of the catalytically active RuvC and HNH nuclease domains of Cas9 (dCas9) creates a RNA-guided DNA binding protein that when coupled with the addition of numerous activation or repression domains has ushered in a new group of CRISPR libraries for molecular research, namely CRISPR activation (CRISPRa) and CRISPR interference (CRISPRi) (Fig. 3.23). As an example, introduction of a dCas9-KRAB fusion protein with sgRNAs to target transcription start sites (TSS) of a target gene results in reduced expression of a target gene. In contrast, the addition of gene transcription activator domains to dCas9 such as VP64 have isolated numerous interferon stimulated genes critical in controlling virus infection (IFI6, TRIM25) and the glycotransferase B4GALNT2, which is an inhibitory factor for Influenza A Virus (IAV) entry (Heaton et al. 2017; Richardson et al. 2018; Orchard et al. 2019). To date, a CRISPRi screen that investigates host factor involvement in viral infection has not been published and thus represents an opportunity where CRISPRi and a traditional CRISPR knockout screen can be performed simultaneously and the novel host factors identified and compared.

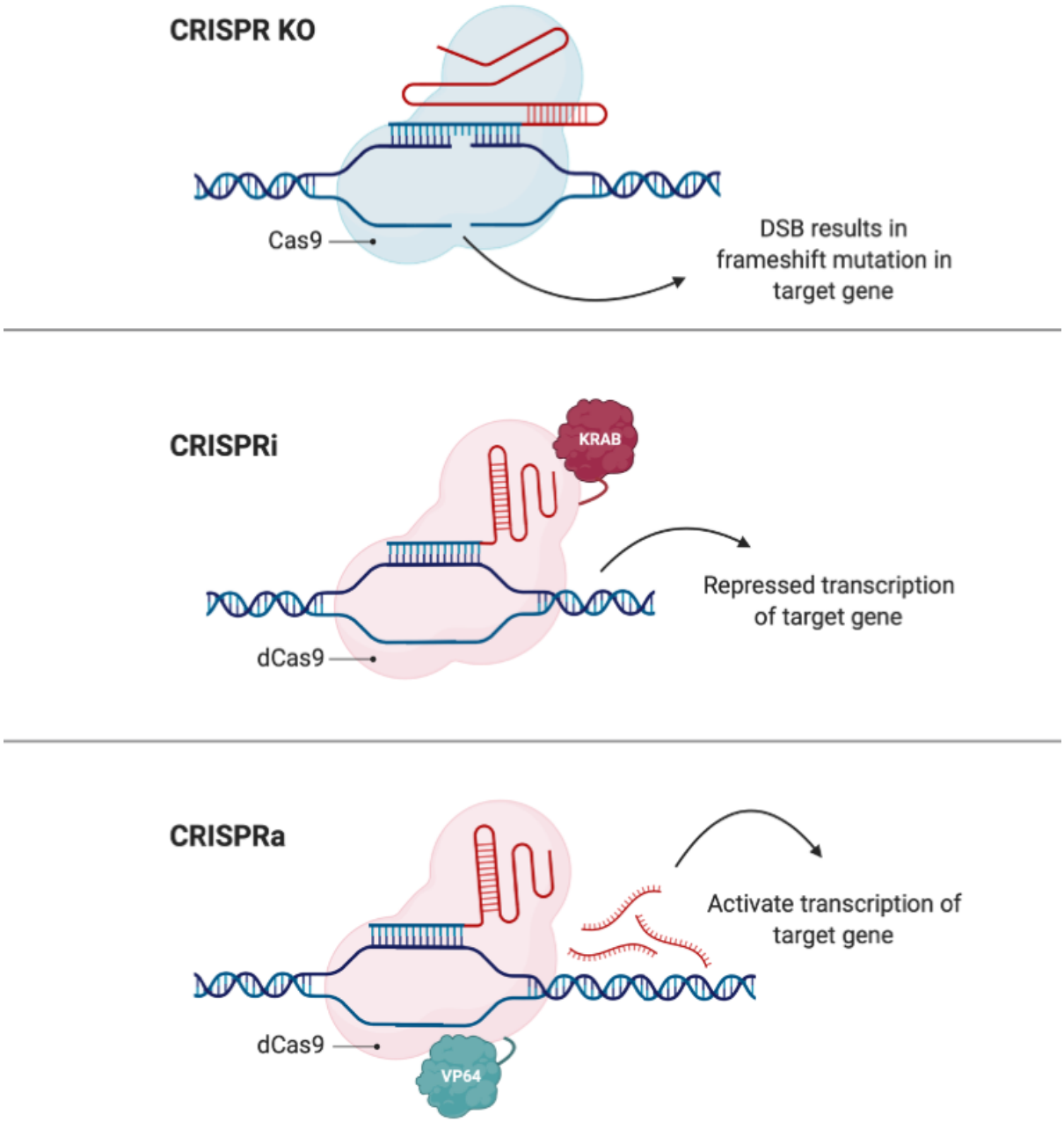

Figure 3.23: Comparison between traditional CRISPR KO and CRISPRi and CRISPRa.

Traditional CRISPR KO involves the binding of Cas9 to the target gene of interest resulting in the formation of a double stranded break (DSB). Frameshift mutations are introduced upon DNA repair, resulting in knockout of the target gene. In contrast, both CRISPRa and CRISPRi utilise a dead Cas9 (dCas9) where attached effector domains either induce (VP64) or repress (KRAB) transcription of a target gene respectively.

In addition, CRISPRi can target long non-coding RNAs (lncRNA), which are critical for numerous host cellular processes, where traditional Cas9 induced NHEJ are often incapable of blocking (Ponting et al. 2009; Sun and Kraus 2015). Genome-wide CRISPRi screens have not been performed with virus infection, compared to the numerous traditional Cas9 knockout screens, likely due to the lack of robustness of the sgRNA computational design rules.

The other main aspect to consider when designing a genome-wide CRISPR screen to identify novel proviral host factors is the output of the screen and the associated enrichment of a selected pool of cells (i.e., cells which have lost HCV replication). With regards to genome-wide CRISPR screens as they apply to virus infection to identify essential host factors, it is critical to have a clear phenotypical outcome following viral infection. In identifying novel proviral host factors, other investigations using CRISPR technology have taken advantage of the cytopathic effect (CPE) viruses induce during infection, rendering the infected cell unviable. These include the flaviviruses (DENV, WNV, ZIKV) as well as influenza A virus and norovirus (see table 1.1). This strategy is useful for loss of function screens using CRISPR technology as cells that are resistant to virus infection survive due to a knockout of a novel proviral host factor. However, HCV is generally non-cytopathic relative to other *flaviviridae* family members (Larrubia et al. 2014). However, one group has used HCV infectious virus and its ability to cause CPE as a readout for a genome-wide CRISPR screen post commencement of this project. Marceau *et al.* used Huh7.5.1-Cas9 stable cells which were transduced with the GeCKO LentiGuide library (the two-plasmid system described earlier) (Marceau et al. 2016). CPE was visible 5 days post infection with HCV JFH-1 virus, where clusters of virus resistant surviving cells were expanded. Although our HCV viral stocks are the same strain as the one Marceau *et al.* used for their genome-wide CRISPR screen, we rarely see HCV induced CPE to the levels required to enable virus resistant cells to be separated. One reason for this contradiction could be due to the Huh7.5 cells, where Huh7 cells from multiple laboratories can differ significantly in their ability to support not only HCV infection and replication but also viral induced CPE (Sainz et al. 2009). Given that our Huh7.5 cells are not susceptible to HCV induced CPE, other viral systems must be considered to enable separation of cells which have lost HCV replication due to knockout of a proviral host factor for further analysis.

Reporter constructs with HCV infectious virus are also a suitable alternative as a readout of a genome-wide CRISPR screen. The isolation of the genotype type 2A JFH1 strain, which can support high levels of HCV replication was improved via the generation of chimeric HCV genomes stitched together from multiple isolates, which yielded infectious titres 100 fold higher than parental JFH1 (T. Kato et al. 2003; Pietschmann et al. 2006; Wakita 2009). Introduction of cell culture adapted replication enhancing mutations through serial passage, primarily in NS5A, has resulted in reporter constructs that produce acceptable levels of infectious virus titres to enabling study the HCV lifecycle (Hughes et al. 2009; Liu et al. 2012b). In addition, multiple reporter constructs such as EGFP and nano-luciferase have been inserted into domain III of NS5A within the HCV infectious virus system to study the intricate details of HCV replication (Gottwein et al. 2011; Eyre et al. 2014; Eyre et al. 2017a). However, use of the infectious virus-based reporter systems can be limited by the insertion size of the reporter construct, where the virus is unable to tolerate large insertions such as thymidine kinase, and the gradual loss of reporter construct expression after virus passaging. To overcome these limitations, reporter systems have been developed where the reporter system is located within the infected cell and exploitation of unique functions within the HCV non-structural proteins drive the activation of the reporter system. One such reporter system, NIrD, consists of 2 modules, the sensor which during HCV infection, NS3 is able to cleave rtTA-MAVS(C) attached to the mitochondria. The free rtTA is able to enter the nucleus and activate the tight-TRE promoter located within the amplifier module, resulting in the production of thymidine kinase and mCherry, which can be utilised in genome-wide CRISPR screening scenarios to sort populations which contains HCV positive and negative cells (Fig. 3.24) (Ren et al. 2015). Although the NIrD reporter system was able to satisfy our requirements, we ultimately decided to utilise the HCV SGR system for our genome-wide CRISPR screen as our laboratory had many years of experience with the HCV replicon system. In addition, we wanted to eliminate the need to produce infectious HCV to high titre, which in itself is time consuming and problematic. In addition, our access to flow cytometry in a PC2 laboratory was limited in Adelaide and for the above reasons, we utilised the HCV SGR system described herein.

The HCV sub-genomic replicon (SGR) was developed for our screen due to the need for a reporter system that had high homogeneity of HCV replication within a cell

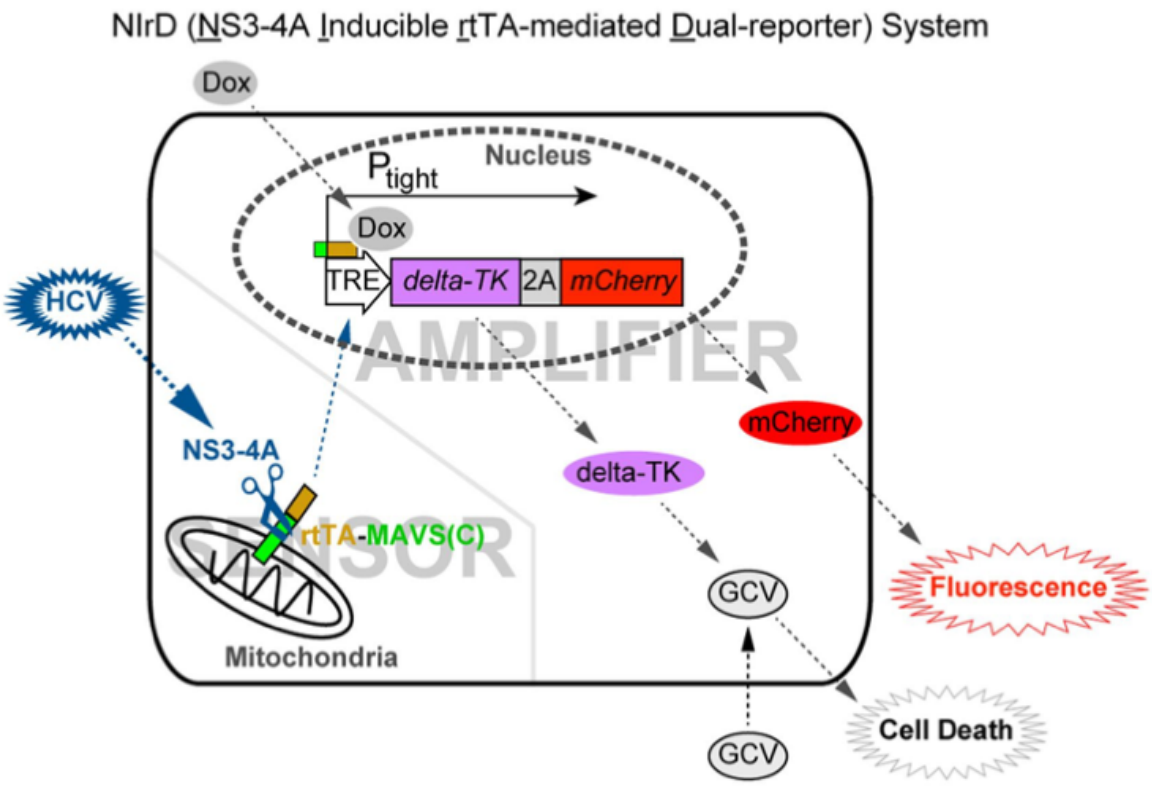

Figure 3.24: The NIrD reporter system enables genome-wide CRISPR screening with HCV infectious virus.

The NIrD reporter system consists of 2 modules, the sensor which during HCV infection, NS3 is able to cleave rtTA-MAVS(C) attached to the mitochondria. The free rtTA is able to enter the nucleus and activate the tight-TRE promoter located within the amplifier module, resulting in the production of mCherry, resulting in fluorescence within HCV infected cells. Addition of GCV results in phosphorylation by thymidine kinase (TK) and subsequent cell death. Modified from Ren *et al.* 2015.

population coupled with a simple readout to easily determine levels of HCV replication, both of which are required for a genome-wide CRISPR screen. The HCV SGR system was originally constructed by the removal of the structural proteins and replacement with a selection resistance cassette (neomycin or BSD) and a reporter gene (renilla luciferase) [reviewed extensively in (Lohmann 2019)]. The advantage of the SGR system is the ability to select for cells with high levels of HCV replication through the selection resistance cassette (BSD) and therefore the elimination of the dynamics of HCV replication and spread compared to the heterogenous nature of infectious virus-based systems. The other main benefit of the SGR system is the ability to add a reporter protein to allow for accurate measurement of HCV replication levels with the desired treatment conditions in a fast, simplistic and safe manner, as no infectious virus is produced. However, a disadvantage of removal of the structural proteins needed to construct HCV progeny is that only the genome replication stage of the HCV lifecycle can be studied. In addition, the lack of structural proteins in the SGR system can result in both altered HCV replication dynamics and structures as all three structural proteins play minor roles in the replication stage through interactions with the non-structural proteins due to the high association of the assembly stage with the replication phase (see section 1.7.3). If the required time and facilities were available, performing the genome-wide CRISPR screen with both the SGR and NIrD systems simultaneously would allow for comparison between novel host factors identified. As the NIrD system uses HCV infectious virus, novel host factors present in the NIrD which are absent in the SGR system would allow easy separation of novel host factors critical for HCV entry and assembly of virions.

Given that we had chosen the HCV SGR system for our genome-wide CRISPR screen, we noticed that both our monoclonal populations of Huh7.5 cells harbouring either HCV-SGR-MC or -GFP had variable fluorescence intensity (Fig. 3.18). Our genome-wide CRISPR screen strategy relied on homogenous expression of our reporter protein, where cells which have lost fluorescence after GeCKO LentiCRISPRv2 library transduction were assumed to have deletion of a novel proviral host factor (Fig. 3.17). An explanation for the heterogenous expression of mCherry and GFP within cells harbouring HCV-SGR could be explained by the influence of cell cycle on the activity of the HCV IRES, which controls the expression of the BSD-reporter protein (either MC, GFP or thymidine kinase). The activity of the HCV IRES has been shown to be

enhanced during the mitotic phase (G_2/M) and relatively inactive in both the early S phase of the cell cycle and in poorly proliferating confluent cells (Honda et al. 2000; Pietschmann et al. 2001; Scholle et al. 2004). The reliance of HCV genome replication to occur in dividing cells, in combination with inherent differences in virus replication levels and therefore reporter protein expression in select cells may also explain the heterogeneity of HCV replication noted in our population of Huh7.5 cells. To investigate if we could select for cells that inherently have increased HCV replication (independent of cell cycle), we performed flow cytometry to enrich for cells with higher levels of active HCV replication and therefore reporter protein expression. Unfortunately, five days post FACS sorting, mCherry fluorescence within the population reverted to levels prior to enrichment (Fig. 3.18). This was unexpected and we speculate that although all cells had high levels of mCherry expression post FACS sorting, the cellular population were still at varying stages of the cell cycle and thus synchronisation with serum starvation or small molecule inhibitors such as Nocodazole may need to be used (Bindels et al. 2017). Additional rounds of flow cytometry were proposed to ensure all cells within the mCherry negative population remained negative due to fluctuating levels observed within the cellular population. Although feasible, this approach was deemed not viable due to time constraints.

The simple phenotypic screen used in a majority of genome-wide CRISPR screens with other viruses involves the ability to cause cell death that allows for selection of resistant cells where a proviral host factor has been knocked out. To adapt this concept to HCV, we developed a HCV-SGR-TK genome-wide CRISPR screen that relies on the capability of thymidine kinase to phosphorylate GCV into a toxic metabolite, resulting in cell death and thus separation of the population with no HCV replication (Tomicic et al. 2002). The HCV-SGR-TK genome-wide CRISPR screen was performed as per figure 3.18, where the GeCKO lentiCRISPRv2 library was transduced into HCV-SGR-TK expressing cells. Following the addition of puromycin, significant cell death was observed which was expected due to the addition of the lentiviral library at a low MOI. Upon the addition of GCV, it was expected that a majority of cells would initiate TK-mediated cell death due to the retention of active HCV replication. However, minimal cell death was observed, indicating that all the GeCKO lentiCRISPRv2 library transduced HCV-SGR-TK cells were resistant to GCV-induced cell death. This could suggest a number of scenarios where either a large number of

proviral host factors had been knocked out or replication had been lost which was independent of CRISPR knockout. The latter was indeed the case as the majority of living cells did not retain HCV replication (as determined by immunofluorescence of NS5A and PCR amplification of the thymidine kinase RNA – Fig. 3.20). The reasons for the lack of HCV replication across the entire GCV resistant cellular population is not entirely clear, but further experiments suggest that lentiviral transduction in the absence of BSD selection results in removal of the HCV-SGR which is discussed below.

For both genome-wide LentiCRISPRv2 screens utilising either the fluorescence or thymidine kinase cell survival methods, a dilemma emerged within the protocol of when to remove the BSD. This nucleoside antibiotic promotes positive retention of the replicon and therefore selects for HCV replicating cells. However, upon knockout of a potential host factor, HCV replication will be lost along with BSD resistance and cells will be susceptible to BSD induced cell death (Fig. 3.22). Therefore, to preserve cells which have lost HCV replication due to knockout of a proviral host factor, BSD must be removed prior to LentiCRISPRv2 library transduction. However, the loss of BSD selection may impact the HCV replicon's ability to remain within the cell, especially during lentivirus transduction. Using mCherry lentivirus to mimic transduction of the GeCKO LentiCRISPRv2 library, we revealed that Huh7.5 cells harbouring HCV-SGR-TK transduced with mCherry lentivirus and cultured in the absence of BSD resulted in a loss of HCV replication (Fig. 3.21 and 3.22). Other genome-wide CRISPR screens regarding virus infection do not face this issue due to the transduction of the CRISPR library prior to virus infection. As active HCV replication is required for the entire duration of the genome-wide screening process, our toolkit would need to be modified and utilisation of the NIrD system may be required to allow for HCV entry post transduction of the GeCKO LentiCRISPRv2 library to ensure active HCV replication is present throughout the screening process.

In summary, we have validated the use of LentiCRISPRv2 to knockout genes from both endogenous (CD81) and exogenous (EGFP) origins, where high knockout efficiency was observed within five days post lentiviral transduction. In addition, we have developed the HCV sub-genomic replicon to express multiple reporter proteins with the intention to be used in genome-wide CRISPR screens. The GecKO

LentiCRISPRv2 plasmid library was successfully amplified and library complexity verified via next-generation sequencing. However, the proposed genome-wide CRISPR screens to be performed with either the fluorescence cell sort based or cell survival with thymidine kinase were ultimately incompatible with the HCV-SGR system as lentiviral transduction of mCherry and therefore LentiCRISPRv2 without BSD selection resulted in loss of active HCV replication regardless if the protein which was knocked out in question was important for HCV replication or not (Fig. 3.22). However, given that the complexity of the expanded GecKO LentiCRISPRv2 plasmid library had been successfully verified and lentiviral pools constructed, we decided to repurpose our genome-wide screen with infectious ZIKV, which would circumvent the limitations with utilising a sub-genomic replicon based system and is illustrated in the manuscript outlined in chapter 4.

Chapter 4 - Genomic CRISPR KO screen identifies RACK1 as a critical host factor for flavivirus replication – MANUSCRIPT

Genome-wide CRISPR KO screen identifies RACK1 as a critical host factor for flavivirus replication

Byron Shue[1], Abhilash I. Chiramel[2], Berati Cerikan[3], Thu-Hien To[4], Stephen M. Pederson[4], Nicholas S. Eyre[1*], Ralf F.W. Bartenschlager[3], Sonja M. Best[2] and Michael R. Beard[1#]

[1] Research Centre for Infectious Diseases, Department of Molecular and Biomedical Science, The University of Adelaide, Adelaide, SA 5005, Australia
[2] Rocky Mountain Laboratories, National Institutes of Health (NIH), Hamilton, Montana, United States of America
[3] Department of Infectious Diseases, Molecular Virology, Heidelberg University, Heidelberg, 69120 Germany
[4] Bioinformatics Hub, The University of Adelaide, Adelaide, SA 5005, Australia

[#]Correspondence to be addressed to:
Professor Michael Beard PhD
Research Centre for Infectious Diseases, Molecular Life Sciences Building,
Gate 8 Victoria Drive, The University of Adelaide, Adelaide SA 5005
Email: michael.beard@adelaide.edu.au

* Current address: College of Medicine and Public Health, Flinders University, Bedford Park, SA 5042 Australia

Running title: Genome-wide CRISPR KO screen and ZIKV

Manuscript wordcount (including materials and methods): 7489

Abstract

Cellular factors have important roles in all facets of the flavivirus replication cycle. Deciphering viral-host protein interactions is essential for understanding the flavivirus lifecycle as well as development of effective antiviral strategies. To uncover novel host factors that are co-opted by multiple flaviviruses, a CRISPR/Cas9 genome wide knockout (KO) screen was employed to identify genes required for replication of Zika virus (ZIKV). Receptor for Activated Protein C Kinase 1 (RACK1) was identified as a novel host factor required for ZIKV replication, which was confirmed via complementary experiments. Depletion of RACK1 via siRNA demonstrated that RACK1 is important for replication of a wide range of mosquito- and tick-borne flaviviruses, including West Nile Virus Kunjin (WNV_{KUN}), Dengue Virus (DENV), Powassan Virus (POWV) and Langat Virus (LGTV) as well as the coronavirus SARS-CoV-2, but not for YFV, EBOV, VSV or HSV. Notably, flavivirus replication was only abrogated when RACK1 expression was dampened prior to infection. Utilising a non-replicative flavivirus model, we show altered morphology of viral replication factories and reduced formation of vesicle packets (VPs) in cells lacking RACK1 expression. In addition, RACK1 interacted with NS1 protein from multiple flaviviruses; a key protein for replication complex formation. Overall, these findings reveal RACK1's crucial role to the biogenesis of pan-flavivirus replication organelles.

Introduction

The *Flavivirus* genus includes dozens of virus species transmitted by arthropods and with high potential to inflict significant morbidity and mortality worldwide (Daep et al. 2014). Antiviral therapeutics are not available for the vast majority of these flaviviruses and vaccines remain limited in efficacy and not suitable for extremes of ages (Dawes et al. 2016; Deen 2016). Thus, further investigation of host-viral interactions in the flavivirus lifecycle may potentially expedite development of novel treatments and vaccines. Flaviviruses have single stranded positive sense RNA genomes, similar virion structure, and replicate exclusively in the cytoplasm. Binding and entry is mediated by numerous host receptors followed by endocytosis of the viral particle and release of viral RNA into the cytosol via endosomal acidification. The positive sense RNA genome is then translated to yield a large single polyprotein that is then cleaved by host and viral proteases to produce the structural proteins (capsid [C], pre-

membrane [prM] and envelope [Env] and non-structural (NS) proteins (NS1, NS2A, NS2B, NS3, NS4A, NS4B and NS5). Expression of the NS proteins induces invagination of the ER membrane, allowing formation of the replication complex; a viral specific membrane structure that harbours active viral replication (Chatel-Chaix and Bartenschlager 2014). At all stages of the viral life-cycle, interactions between host factors and viral proteins are crucial in the replication process and biogenesis of ER membrane rearrangement to allow formation and maintenance of the replication complex (Aktepe and Mackenzie 2018). Following budding into the ER, immature virions are transported via the Golgi pathway to enable release of viral particles via exocytosis. Thus, identification and characterisation of virus-host interactions impacting replication will inform our understanding not only of flavivirus biology but possible targets for therapeutic intervention.

Recent advances in genome-wide screening technology provides a platform to further identify novel viral host factors [reviewed in (Puschnik et al. 2017a)]. One such technology is clustered regularly interspaced short palindromic repeats (CRISPR) genome-wide silencing in which the GeCKO (genome-wide CRISPR knockout) screening library has been used to investigate virus-host interactions across multiple viral families and mammalian cell types (Ma et al. 2015; Savidis et al. 2016a; Marceau et al. 2016; Zhang et al. 2016; Li et al. 2019). Although identification of a number of host factors are reproducible from one CRISPR screen to the next, variations in experimental design and the screening process can influence the potential hits and thus host factors which may surface.

In this study, we sought to identify cellular proteins involved in ZIKV replication through the use of a genome-wide GeCKO screen. This screen identified Receptor for Activated C Kinase 1 (RACK1) as a critical host factor for not only ZIKV infection, but other mosquito and tick-borne flaviviruses. RACK1 is a highly conserved multifunctional protein and a member of the tryptophan-aspartate repeat (WD-repeat) family of proteins that shares significant homology to the ß-subunit of G-proteins. Through its interaction directly or in a complex with other cellular proteins, it functions in shuttling proteins throughout the cell, anchoring proteins at particular locations, stabilising protein activity and has specific roles in modulation of signalling pathways [reviewed in (Adams et al. 2011)]. Here, we show that RACK1 interacts with flavivirus

NS1 protein and localises to replication complexes to specifically alter the latter's cellular morphology. Depletion of RACK1 resulted in both altered morphology and a decrease in the number of VPs generated by DENV and ZIKV non-structural protein expression. These results indicate that RACK1 through the interaction with NS1 is crucial for the construction of flaviviral replication complexes.

Results

CRISPR/Cas9 genome-wide KO screen reveals RACK1 as a critical host factor for ZIKV replication

To identify host genes required for the ZIKV lifecycle, we performed a lentiviral-mediated whole genome CRISPR screen to uncover sgRNAs that rendered cells resistant to ZIKV-induced cytopathic effect (CPE) (Fig. 1A). The LentiCRISPRv2-GecKO library was stably transduced into Huh7.5 cells, selected with puromycin, and infected with ZIKV (MR766, MOI=5). In contrast to other screening approaches that expanded surviving cells following viral infection (Marceau et al. 2016; Zhang et al. 2016), we harvested genomic DNA from unamplified surviving cells to identify host factors that may be lost through expansion as a consequence of altered cell proliferation. sgRNAs sequences from surviving cells were PCR amplified and sequenced (Illumina NextSeq) and analysed using the CaRpools package (Fig. 1B) (Winter et al. 2016). We identified several genes which were statistically enriched using DESeq2 and/or MAGeCK, some of which were previously identified as playing a role in viral replication. These include the ER membrane protein complex proteins (EMC) (EMC1, MMGT1 (EMC5) and EMC6) as well as BAX. (Fig. 1B). However, our most significant hit identified was sgRNAs targeting GNB2L1, otherwise known as RACK1. Interestingly, RACK1 has previously been shown to be an important host factor in virus infections including HCV (Majzoub et al. 2014; Lee et al. 2019). In addition, a proteomics screen involving DENV NS1 also identified RACK1 as an interacting partner and thus was pursued further (Hafirassou et al. 2018). To confirm our screen results, we generated independent EMC1, EMC6 and RACK1 CRISPR polyclonal knockouts in Huh7.5 cells and infected with ZIKV (MR766) and assessed viral replication by qRT-PCR and plaque assay (Fig. 1C & D). As expected, both ZIKV RNA accumulation and the production of infectious viral particles were significantly reduced in cells depleted for EMC1 and EMC6 expression, and similar replication

defects were observed in the absence of RACK1. The identification of EMC1 and EMC6 validate our screening approach and thereby identify RACK1 as a potential host factor involved in ZIKV replication.

Confirmation of RACK1 as a critical host factor for ZIKV infection

To confirm if RACK1 is an important host factor for ZIKV replication, siRNA targeting RACK1 was utilised as a complementary method of abrogating RACK1 expression. Time-course knockdown experiments with siRNA targeting RACK1 showed that mRNA (Fig. 2A) and subsequently protein levels (Fig. 2B) are reduced significantly after 24 hours siRNA transfection and remain low for at least 72 hours post transfection. Since the genome-wide CRISPR KO screen was performed with the liver derived Huh7.5 cell-line, we also thought it imperative to determine whether perturbation of ZIKV replication was evident in cells of non-hepatic origin. siRNA knockdown in both HeLa and the placental cell line HTR8 followed by infection with ZIKV (MR766) revealed a reduction in RACK1 mRNA expression that was associated with a significant decrease in ZIKV RNA (Fig. 2C). Our original genome-wide CRISPR KO screen utilised the MR766 ZIKV strain of African lineage, which through continued passage in mouse brains may have resulted in adaptations and changes in host factor reliance (Shao et al. 2017). Thus, HeLa cells with RACK1 siRNA knockdown were infected with ZIKV MR766 or PRVABC59, the latter of Asian lineage that revealed a similar impact on ZIKV replication, indicating that RACK1 is important for replication of both African and Asian ZIKV lineages (Fig. 2D). Rescue experiments were performed where transfection of plasmid encoding siRNA resistant RACK1 into cells which have depleted RACK1 expression and infected with ZIKV (PRVABC59) showed restoration of ZIKV RNA levels (Fig. 2E). To ensure the loss of ZIKV RNA by RACK1 knockdown resulted in perturbation in active viral replication and NS protein formation, immunoblot detection revealed a significant decrease in ZIKV NS5 protein levels in the absence of RACK1 expression (Fig. 2F). In a complementary approach, immunofluorescence microscopy was employed that revealed a reduction in ZIKV envelope protein staining post siRNA knockdown of RACK1 (Fig. 2G). Together, these findings indicate RACK1 is an important proviral host factor for different ZIKV strains and in multiple cell types.

RACK1 is required for flavivirus replication

To determine whether RACK1 is also a proviral host factor for other flaviviruses, we explored whether other mosquito or tick-borne flavivirus species require RACK1 for virus replication. Compared to siRNA non-targeting control (NTC) cells, knockdown of RACK1 had a significant impact of at least a 1 $\log_{10}$ decrease in infectious virus release of the mosquito-borne flaviviruses including ZIKV (strain 2013 French Polynesia), WNV (strain NY99) and DENV (strain NGC, serotype 2). Interestingly, there was no effect on YFV (strain 17D) replication in the absence of RACK1 expression (Fig. 3A). Demonstrating that this effect is not specific to mosquito-borne flaviviruses, we also noted that the tick-borne flaviviruses, Langat virus (LGTV; an attenuated member of the TBEV serocomplex) and Powassan virus (POWV; strain LB) also had a dependency for expression of RACK1. In fact, of all the flaviviruses investigated, POWV revealed the greatest dependency on RACK1 with a consistent 2 $\log_{10}$ decrease in viral RNA following RACK1 depletion (Fig. 3A). We next investigated if other RNA viruses required a dependency for RACK1. Using an EBOV luciferase reporter virus, we noted no significant impact of RACK1 on viral replication in comparison to the NTC siRNA (Fig 3B). Interestingly, RACK1 was required for SARS-CoV-2 replication, as shown by reduced infectious virus release (approx 1 $\log_{10}$) and intracellular spike protein expression (Fig. 3B and 3C). No requirement for RACK1 was observed for either VSV (negative strand RNA virus) or HSV (DNA virus) replication. Collectively, this suggests that positive strand RNA viruses of the flavivirus genus exhibit dependency for RACK1 expression.

RACK1 is important prior to establishment of replication

To gain insight into the mechanism of action of RACK1, we next determined at which stage of the viral lifecycle RACK1 was functioning. To achieve this, we used a sub-genomic reporter DENV expressing *Renilla Luciferase* (*Rluc*). Following transfection of *in vitro* transcribed DENV sub-genomic (SGR) replicon RNA, replication is established that recapitulates the complete RNA replication cycle, although infectious virions are not produced due to the lack of structural proteins required for virion morphogenesis. Using this approach, *Rluc* is expressed at low levels as a function to translation of the input RNA and increases thereafter during genome amplification. Huh7 cells were pre-treated with NTC or RACK1 siRNA prior to transfection with RNA representing DENV SGR or DENV SGR containing a GND mutation in the NS5 protein

encoding the viral RNA-dependent RNA polymerase to control for input RNA mediated luciferase expression (Fig. 4A). In addition, we also infected siRNA treated cells with DENV (16681). In the absence of RACK1, DENV SGR replication was supressed at late but not early time points following transfection of RNA suggesting that primary viral translation was not impacted (Fig. 4B). Furthermore, the pattern of *Rluc* expression in the absence of RACK1 from DENV SGR GND was similar to DENV SGR confirming no impact on viral translation. As expected, DENV RNA levels were significantly reduced when RACK1 expression is decreased prior to infection with DENV (16681) infectious virus (Fig. 4C). We also investigated the impact of RACK1 depletion post establishment of viral replication (Fig. 4D). siRNA treatment of cells with NTC or RACK1 post infection with DENV or transfection of the DENV SGR revealed no impact on viral replication as determined by qRT-PCR or luciferase assay respectively (Fig 4E and 4F). Collectively, these results suggest that entry and translation of viral RNA are not impacted, whereas RACK1 is important for viral RNA genome replication.

RACK1 is instrumental to the formation of the flavivirus replication complex

Following translation and processing of the viral polyprotein, a hallmark of flavivirus replication is rearrangement of ER membranes to form single membrane vesicle packets (VPs) that house sites of viral RNA replication in a replication complex (RC) (Paul and Bartenschlager 2015). However, the requirement of RACK1 for viral replication will inevitably impact RC formation and thus uncoupling polyprotein synthesis from viral replication is necessary to determine the role of RACK1 on flavivirus RNA replication. To achieve this, we used a replication independent expression system, termed pIRO (plasmid induced replication organelle formation) that induces DENV and ZIKV vesicle packets that are morphologically indistinguishable from infected cells (Cerikan et al. 2020). Huh7/Lunet-T7 cells were reverse transfected with either NTC or RACK1 siRNA, following which cells were transfected with either ZIKV or DENV pIRO constructs and 20 hrs later cells were fixed and processed for immunofluorescence and TEM (Fig. 5A). Transfection efficiencies determined for both ZIKV NS4B and DENV NS3 were comparable between siRNA treatments (Fig 5E and 5F). Cells transfected with siRNA targeting RACK1 revealed a significant decrease in RACK1 expression at 48 and 68 hrs post treatment that

correlated with significant impairment of VP formation for both DENV and ZIKV pIRO systems (Fig. 5B and 5C). In cells treated with NTC siRNA and expressing pIRO-DENV or -ZIKV constructs, distinct ER membrane alterations were visible representing VPs, however this was not the case for cells lacking RACK1 expression (Fig. 5C). Furthermore, VP quantification by TEM were classified into three categories; cells with no VPs, cells with 2-5 VPs and cells > 5 VPs. For cells transfected with either pIRO-DENV or -ZIKV, there was a significant increase in the numbers of cells lacking VPs when RACK1 expression is depleted (Fig. 5D). Conversely, under the same conditions, we also noted a decrease in the number of cells harbouring VPs. Collectively, our results show that RACK1 is an essential host factor for mediating the biogenesis of convoluted ER membrane structures and VPs essential for RNA viral replication.

RACK1 is required for the positioning of flavivirus molecular components during virus replication

The NS1 protein across the flaviviruses has a major role in the virus lifecycle, particularly in VP formation [reviewed in (Rastogi et al. 2016)]. Given our results above and based on a previous study identifying NS1 interaction with RACK1 (Hafirassou et al. 2018), we next investigated the impact of RACK1 deletion on the subcellular localisation of NS1 and dsRNA as a marker of replication complex formation following either DENV or ZIKV infection. Under normal infection conditions, confocal microscopy assumed NS1 localisation to a punctate and reticular subcellular localisation with significant colocalization to dsRNA, representing replication complexes and the ER respectively as previously demonstrated (Fig. 6). However, following RACK1 depletion, there was a significant decrease in NS1 expression as expected and altered NS1 localisation to a predominantly peri-nuclear localisation juxtaposed to dsRNA punctate VPs. This altered NS1 and dsRNA localisation is consistent with our EM studies in which we showed a decrease in VPs with altered morphology (Fig. 5D).

RACK1 interacts with multiple flavivirus NS1 within the ER lumen

Re-modelling of ER membranes is required for flavivirus replication complex formation, driven by interactions between viral and ER-associated host factors (Rothan and Kumar 2019). One of the viral proteins critical for VP biogenesis is NS1, which localizes to the ER lumen (Ci et al. 2020). In addition, a recent DENV NS1 interactome

map has identified RACK1 as an interaction partner (Hafirassou et al. 2018). Therefore, to investigate whether RACK1 was associated with the ER and in a position to potentially interact with NS1, HeLa cells were infected with DENV, WNV_{Kun} or ZIKV following RACK1 knockdown. Immunoblotting was utilised to determine levels of both flavivirus NS1 and RACK1 within fractional whole cell lysates (WCL) containing cytosolic (digitonin-sensitive) and membranous organelles (NP-40-sensitive) which include the ER (Holden and Horton 2009). Flavivirus NS1 was only present within the NP-40 fraction, indicating its predominant localisation within the membranous organelles, such as the ER lumen as expected (Fig. 7A). However, RACK1 was present in both the digitonin and NP-40 fraction, indicating RACK1 localisation within the cytosol and membranous organelles and thus potentially capable of interacting spatially with RACK1 within the replication complex.

Given that both NS1 and RACK1 are integral to flavivirus VP formation and reside in the same cellular compartment, we next assessed if they interact. This was achieved by transfection of Huh7 cells with flavivirus NS1 expression constructs bearing an N-terminal FLAG-tag and RACK1 bearing an N-terminal HA-tag. Indeed, the co-expression of NS1 (DENV, WNV_{Kun}, YFV_{17D} and ZIKV) and RACK1 revealed a reticular cytoplasmic staining pattern consistent with co-localisation and robust interaction between NS1 and RACK1 also observed using proximity ligation assays (Fig. 7B and 7C). As overexpression can result in mis-localised proteins, we next sought to investigate the interaction of NS1 with endogenous RACK1 in HeLa cells infected with DENV, WNV_{KUN}, YFV_{17D} or ZIKV. Co-immunoprecipitation experiments were conducted to pull down NS1 (humanized NS1 4G4 antibody) from virus-infected HeLa cells, followed by immunoblotting to detect endogenous RACK1. Comparative analysis of NS1 expression revealed a strong interaction for DENV and ZIKV NS1 with endogenous RACK1 which was not as pronounced for WNV_{Kun} and YFD_{17D} (Fig. 7D).

Discussion

Host factors play critical roles in all facets of the flavivirus lifecycle and identification of such factors is essential to not only our understanding of viral replication but also to exploit these host-virus interactions in the development of novel antiviral therapeutics. Although numerous host factors important for ZIKV and other flaviviruses have been

identified, it is likely that additional host factors remain to be discovered. Therefore, to expand our understanding of virus-host interactions, we used a genome-scale CRISPR KO approach to screen for single guide RNAs (sgRNAs) that upon gene knockout conferred cell survival following infection with ZIKV. Similar approaches using genome-wide CRISPR KO screens have identified novel host factors essential for a range of viruses including the flaviviruses and include the OST, EMC and TRAP complexes [reviewed in (McDougall et al. 2018)]. Although CRISPR technology has significant advantages to siRNA mediated screens in the form of improved consistency as a result of a reduction in false positives, differences in experimental parameters can result in bias during the recovery of sgRNAs and therefore influence novel host factors identified. In contrast to previous CRISPR screens in which cells are expanded (allowing for sgRNA enrichment) following viral induced CPE, we harvested cells immediately following viral induced cell death in the control cells to allow for identification of sgRNAs that may target genes that confer inherent defects in cell proliferation and that would otherwise be missed during the expansion process. Interestingly, using this approach we identified a limited number of sgRNAs compared to previous screens, indicating the expansion stage is critical for the augmentation of the number of gRNAs required to surpass the threshold of significance utilising the DESeq2 or MAGeCK algorithims. Nevertheless, among our top hits, in addition to RACK1 (GNBL21), our screen identified sgRNAs targeting the EMC complex (EMC1, MMGT1 (EMC5) and EMC6) that have been previously identified in supporting biogenesis of flaviviral NS4A and NS4B and thus confirms the validity and reproducibility of our approach (Fig. 1) (Savidis et al. 2016a; Li et al. 2019; Lin et al. 2019a). In addition, we identified sgRNAs targeting BAX, a member of the BCL2 family regulating apoptosis. This is not surprising, given that DENV and ZIKV both rely on BCL_x to suppress activation of BAX to prolong cell survival (Suzuki et al. 2018). However, sgRNAs targeting RACK1 were the most significantly enriched in the current screen and thus we focused on the role of RACK1 in flavivirus biology.

Previous studies have identified a role for RACK1 in the lifecycle of a number of unrelated viruses, the mechanism of which falls into two main categories; (i) RACK1 support of IRES mediated translation by virtue of RACK1 being localised to the 40s ribosomal subunit for viruses such as HCV, polio virus, cricket paralysis virus (CrPV) and picorna-like *Drosophila* C Virus (DCV), and (ii) RACK1 mediated intracellular

signalling or as a scaffolding protein which assists the virus lifecycle of viruses such as porcine reproductive and respiratory syndrome virus (PRRSV), IAV and HIV (Gallina et al. 2001; Demirov et al. 2012; Majzoub et al. 2014; Bi et al. 2018; LaFontaine et al. 2020). Our results indicate that the flaviviruses can now be added to the list of viruses for which RACK1 is a host dependency factor. Using an siRNA depletion approach, we report that RACK1 is an essential host factor for multiple strains of ZIKV in different cell types and as expected given the similarities in their viral lifecycles, RACK1 was important for other mosquito (DENV, WNV) and tick-borne flaviviruses (LGTV and POWV). Interestingly, the vaccine strain YFV_{17D} used in this study is evolutionally distinct from other flaviviruses such as DENV and ZIKV was not affected by RACK1 knockdown. While DENV and ZIKV have likely streamlined their lifecycles to require minimal host factors to improve efficiency, YFV exhibits slower evolutionary dynamics and therefore may utilise multiple redundant proteins to fulfil the same role as RACK1 (Sall et al. 2010). Another factor to consider is that although the vaccine strain of YFV results in active viral replication, this strain is both evolutionarily and replication divergent from circulating YFV, which may behave differently when RACK1 expression is lost (Beck et al. 2014; Fernandez-Garcia et al. 2016). It will be interesting to determine in future studies if WT strains of YFV are dependent on RACK1. We extended our RACK1 studies to determine if viruses outside the flavivirus genus also had a dependency for RACK1. Depletion of RACK1 had no impact on VSV or Ebola (negative strand RNA genome), MERS-CoV (positive stand RNA) or the DNA virus HSV. While the list of viruses we included was not exhaustive, our results suggest selective dependency of the flavivirus lifecycle for RACK1.

From our initial studies it was not apparent at what stage of the flavivirus lifecycle RACK1 was playing a role. To investigate this further, we utilised a DENV SGR expressing *Rluc* to separate viral entry from viral RNA replication. Following transfection of *in vitro* transcribed DENV SGR RNA in cells devoid of RACK1, we noted a significant reduction of DENV replication suggesting viral genome replication was inhibited. Given that RACK1 is a constituent protein of the eukaryotic ribosome and has been reported to play a role in HCV and CrPV IRES-dependent translation, it is possible that RACK1 may effect DENV 5'UTR cap dependent translation (Majzoub et al. 2014). This was improbable as input *in vitro* transcribed DENV SGR RNA (including

the GND replication mutant) was translated with equal efficiency at early time points following transfection, ruling out RACK1 as playing a role at the level of translation. Moreover, the depletion of RACK1 post initiation of viral replication has no apparent impact on flavivirus replication. This indicates that RACK1 is a proviral host factor that must be present prior to the establishment of replication and supports the finding that it may target virus-induced ER membrane alteration and generation of vesicle packets and the virus replication complex.

Following flavivirus infection expression of the viral NS proteins results in the reorganisation of host ER membranes to generate viral replication organelles (ROs). These ROs are comprised of arrays of vesicle-like invaginations into rough ER membranes that have been designated as vesicle packets (VPs) (Chatel-Chaix and Bartenschlager 2014). Evidence that the VPs is the site of viral RNA replication stems from the detection of dsRNA (a flavivirus RNA genome replication intermediate) and viral replication components including viral NS proteins and essential host factors (Gillespie et al. 2010). However, while we have a good understanding of the architecture of flavivirus VPs, the host factors and mechanisms of biogenesis are not well understood. Evidence to suggest that RACK1 may play a role in flavivirus VP formation comes from the recent observation that it plays a role in the biogenesis of HCV ROs through an interaction with the HCV NS5A protein and ATG14L to induce autophagasome formation (Lee et al. 2019). However, the mechanism of RO formation and the double-membrane vesicle morphology following HCV infection are fundamentally different to that of ROs generated following either DENV or ZIKV infection suggesting specific mechanisms are a play (Chatel-Chaix and Bartenschlager 2014; Lee et al. 2019). For example, the HCV protein NS5A recruits and interacts with phosphatidylinositol 4-kinase-α (PI4Kα) resulting in increased local levels of PI4P that induces high amounts of localised phosphatidylinositol-4-phosphate that is required to modulate membrane lipid composition and drive the formation of double membrane vesicles and generation of HCV replication ROs. However, PI4P is dispensable for DENV RO formation (Reiss et al. 2011). Moreover, the significant perturbation of NS1 and dsRNA localisation following depletion of RACK1, and the requirement of RACK1 prior to infection combined with its interaction with NS1 (a key NS protein involved in VP formation) suggests that RACK1 may significantly influence VP formation.

A number of viral proteins and host factors have been implicated in flavivirus VP biogenesis, however evaluation of their role in this process has been problematic as deletion of these factors can impact replication in the context of virus infection or using autonomous SGR based cell lines (Aktepe et al. 2017; Richardson et al. 2018; Neufeldt et al. 2019). To overcome this limitation, we adopted the recently described pIRO transcription-translation system that relies on T7 RNA polymerase and a heterologous IRES to achieve robust production and cleavage of DENV and ZIKV polyproteins with subsequent VP formation that is indistinguishable to VPs in infected cells (Cerikan et al. 2020). Thus, the production of VPs in this system is independent of replication and allows the study of host cells factors involved in RO production. Using this system coupled with siRNA knockdown of RACK1, we determined that RACK1 is important in the formation of VPs for both DENV and ZIKV. TEM revealed that in the absence of RACK1, the morphology of VPs for both DENV and ZIKV was significantly altered while quantification of VPs revealed that the percentage of cells with 2-5 or >5 VPs was also decreased with reduced RACK1 expression. These results are consistent with our immunofluorescence data in which we revealed significant alteration of NS1 and dsRNA positive DENV and ZIKV ROs in the absence of RACK1 expression. Collectively these results indicate that RACK1 is crucial for the biogenesis of both DENV and ZIKV (and most likely other flavivirus VPs) VPs to support robust viral replication. This raises the question as to how RACK1 drives VP formation. In the case of HCV, even though the VPs are morphologically distinct to DENV and ZIKV, the HCV NS5A protein induces autophagy and DMV formation through its interaction with RACK1 and ATG14L. Like HCV, we revealed that RACK1 resides interacts with a flavivirus NS protein namely NS1 using a number of experimental approaches. Interestingly, as for HCV NS5A protein, the flavivirus NS1 protein has recently been shown to be required for the biogenesis of DENV ROs independent of RNA genome replication. It is not inconceivable to envisage that RACK1 helps stabilise NS1 at the ER membrane to facilitate VP formation or alternatively it provides a scaffold for the autophagy nucleation complex and formation of altered membrane vesicles as with HCV. Autophagy, the mechanism proposed for RACK1 assisted HCV DMV construction is also proposed to be induced during DENV and ZIKV infection [reviewed in (Chiramel and Best 2018)] and it is possible that even

though the ROs are morphologically different, similar mechanisms may be at play for flavivirus RO biogenesis and warrants further investigation.

The dependency for RACK1 with regards to the flavivirus replication cycle most likely relates to its role in the biogenesis of ROs. Interestingly, the coronaviruses also initiate an extensive remodelling of intracellular ER membranes forming a three-dimensional structure referred to as the replication membranous web containing multiple interconnected vesicles with single or double membrane vesicles (DMVs) [reviewed in (Hopfer et al. 2020)]. DMV formation is not completely understood, however, non-structural viral proteins are critical for this process and hence it is not inconceivable to assume that RACK1 may also play a role in coronavirus DMV formation. While not a complete surprise, RACK1 depletion had a significant impact on SARS-CoV-2 genome replication, suggesting coronavirus cellular membrane rearrangements are RACK1 dependent and highlights the possibility of a shared mechanism by which positive stranded viruses remodel ROs. Given that both HCV and coronaviruses induce DMVs which are principle sites of virus replication (reviewed in (Wolff et al. 2020)), future experiments should investigate the role of RACK1 and autophagy as a common mechanism in the biogenesis of viral replication complex formation.

In conclusion, we have successfully used a genome-wide CRISPR KO screening approach to identify RACK1 as a host factor important for flavivirus infection. We have demonstrated that RACK1 interacts with the flavivirus NS1 protein and colocalised to replication organelles containing dsRNA. Furthermore, depletion of RACK1 significantly impacts flavivirus replication and the formation of replication organelles highlighting the role of RACK1 as a key host factor essential for RO biogenesis. This study not only enhances our knowledge in the intricacies of the flavivirus lifecycle and RO biogenesis, but also may guide novel approaches toward the design of pan-flavivirus antiviral strategies that are currently lacking.

Materials and Methods

Cell and culture conditions

All mammalian cell lines were maintained at 37°C in a 5% CO_2 air atmosphere. Huh7 and Huh7.5 human hepatoma cells, HeLa human epithelial cells, HTR8/SVneo human

trophoblast cells, HEK293T human embryonic kidney cells and Vero monkey kidney epithelial cells were maintained in DMEM (Gibco) containing 10% (v/v) FCS and 1% (v/v) penicillin and streptomycin. Huh7/Lunet-T7 cells stably expressing the bacteriophage T7 RNA polymerase have been described previously (Appel et al. 2005). C6/36 *Aedes albopictus* cells were maintained in Basal Medium Eagle (BME) supplemented with L-glutamine, MEM non-essential amino acids, sodium pyruvate, 10% FBS and P/S and cultured at 28 °C with 5% CO_2.

Antibodies and Chemicals

Mouse anti-envelope glycoprotein 4G2 (D1-4G2-4-15) was prepared from hybridoma cells purchased from ATCC. Mouse anti-dsRNA 3G1, mouse anti-flavivirus NS1 4G4 and human anti-flavivirus NS1 4G4 was a generous gift from Roy Hall (University of Queensland). Mouse anti-RACK1 was purchased from Santa Cruz Biotechnology (SC-17754) and mouse anti-FLAG and anti-HA was purchased from Sigma Aldrich. Mouse anti-myc and Rabbit anti-FLAG was purchased from Cell Signalling Technologies. Mouse anti-SARS-CoV-2 spike antibody (1A9-GTX632604) was purchased from GeneTex. All secondary antibodies were purchased from Thermo Fisher Scientific.

Viruses and Plasmids

The ZIKV strains MR766 (Uganda, 1947) and PRVABC59 (Puerto Rico, 2015) were propagated in C6/36 cells by infection at a multiplicity of infection (MOI) of 0.01 and supernatants harvested at 5-6 dpi. PRVABC59 is a contemporary strain that was isolated by CDC from the serum of a ZIKV infected patient who travelled to Puerto Rico in 2015. The complete genome sequence is published (Ref. Gene bank accession # KU501215). DENV infections utilised Mon601, a derivative of the New Guinea C strain that was produced from *in vitro* transcribed RNA, transfected into BHK-21 baby hamster kidney cells, amplified in C6/36 insect cells and titered in Vero cells. DENV 16681 infectious virus was generated as previously described (Eyre et al. 2017b). Other flaviviruses (Chiramel et al. 2019) and EBOV (Kondoh et al. 2018) have been described previously. SARS-CoV2 nCoV-WA1-2020 (MN985325.1) was provided by the Centers of Disease Control and Prevention (CDC) and propagated in

Vero E6 cells in DMEM, supplemented with 2% (v/v) FCS, 1mM L-glutamine and 1% (v/v) penicillin and streptomycin.

Plasmids were transfected with Lipofectamine 3000 (Thermo Fisher Scientific) following manufacturer's recommendations. RACK1 tagged plasmids were cloned via PCR of cDNA from Huh7 cells and Gibson Assembly performed with restriction enzyme digested pcDNA6.2. N-EmGFP-DEST. pEGFP-N1-RACK1 was a gift from Anna Huttenlocher (Addgene plasmid # 41088). ZIKV NS tagged proteins were individually cloned via PCR of pZIKV-ICD (strain Paraiba_01/2015) and Gibson Assembly performed with restriction enzyme digested pcDNA6.2. N-EmGFP-DEST. LentiCRISPRv2 was a gift from Feng Zhang (Addgene plasmid# 52961). Plasmid encoding for RACK1 which was resistant to RACK1 siRNA (described below) was constructed by Gibson Assembly of restriction enzyme digested pcDNA6.2. N-EmGFP-DEST and a gBlock with silent mutations within RACK1 where the siRNA bound.

In vitro transcription of viral RNA

Plasmid pFK-DVs containing the full-length DENV-2 genome (strain 16681), pFK-sgDVs-R2A and pFK-sgDVs-R2A-GND which are the sub-genomic DENV replicon and GND mutant based on the DENV-2 genome (strain 16681) respectively was provided by Ralf Bartenschlager (Fischl and Bartenschlager 2013). To initiate virus replication, all DENV plasmid constructs were linearized with *Xba*I prior to *in vitro* RNA transcription with the mMessage Machine SP6 transcription kit (Thermo Fisher Scientific) and transfection of viral RNA into Huh7.5 cells by transfection with Lipofectamine 3000 (Thermo Fisher Scientific) following manufacturer's recommendations.

CRISPR/Cas9 Genome-wide KO Screen

The Human GeCKOv2 CRISPR knockout pooled library was a gift from Feng Zhang (Addgene #1000000048). Generation of the lentiviral CRISPR knockout pooled library and subsequent screening has been described previously (Shalem et al. 2014; Joung et al. 2017). Briefly, the library was amplified with the supplied protocol and lentivirus generated via transfection of 293T cells with Lipofectamine 2000 (Thermo Fisher

Scientific) and psPAX2 and PMD2.G lentiviral packaging plasmids. Following determination of the lentiviral titre, 300 million Huh7 cells were transduced with the lentiviral pooled library at a MOI of 0.3. One week post transduction, puromycin (3μg/ml) was added for a week to select for cells with successful transduction. ZIKV (MR766) was added to the 300 million puromycin resistant transduced cells at a MOI=5 and the screen terminated when the control un-transduced cells had died following ZIKV induced CPE. Surviving lentiCRISPRv2 transduced cells were harvested and genomic DNA isolated using a Blood and Cell Culture DNA Midi Kit (Qiagen). Genomic DNA from LentiCRISPRv2 transduced cells in the absence of ZIKV infection was also harvested to determine the representation of the library prior to ZIKV infection. Two rounds of PCR (Q5 - NEB) was performed on the genomic DNA to first amplify the guide region of both control and ZIKV-infected samples and secondly, introduce the Illumina primers to enable the samples to be run on next-generation sequencing. The NextSeq 2x75 bp kit (Illumina) was utilised and the data run through caRpools with the assistance of the Adelaide Bioinformatics Hub to identify enriched genes and therefore novel host factors required for ZIKV infection.

Generation of EMC1/EMC6/RACK1 CRISPR KO polyclonal cell lines

Benchling was utilised to generate 20nt guide sequences targeting EMC1, EMC6 and RACK1. 20nt oligos were synthesized and annealed prior to insertion into *Bsm*BI digested LentiCRISPRv2. Sanger sequencing was employed to confirm insertion of the appropriate guide into LentiCRISPRv2. Following the generation of lentiviruses encoding LentiCRISPRv2 with EMC1, EMC6 or RACK1, Huh7.5 were transduced and puromycin selected 5 days post transduction for 1 week. Surviving cells were infected with ZIKV (PRVABC59) and qRT-PCR performed to quantify mRNA levels of EMC1, EMC6 or RACK1 and ZIKV RNA levels. sgRNA sequences are listed below: EMC1= TCCTGGGAGACTAACATCGG, EMC6=CCGGCAATAATCCAGGACGG and RACK1=CGCCATTTTGCATGGTCGAG.

RACK1 knockdown and pIRO plasmid transfection

RACK1 knockdown for use in infection, immunofluorescence and pIRO assays was achieved using a RACK1 siRNA pool (Dharmacon: L-006876-00-0005, 5 nmol). Concentrations of reagents were modified dependent on vessel size. For a well of a

6-well plate, 3 µl of either RACK1 or non-targeting control (NTC) (Dharmacon: D-001810-10) siRNA pool from a stock solution of 20µM was added to 100µl of Opti-MEM (ThermoFisher: 31985070) and 5 µl of Lipofectamine RNAi-MAX was added to another tube containing 100 µl of OPTI-MEM. After 5 mins incubation at RT, Opti-MEM solutions containing the siRNA and transfection reagent were mixed and incubated for 15 mins at RT. siRNA transfection mix was added to Huh-7 cells (seeded 24hrs prior) and 24hrs post transfection cells were either infected with virus or transfected with plasmids/RNA. Studies using the pIRO system are described eleswhere (Cerikan et al. 2020). In brief, Huh7/Lunet T7 cells (3×10^5) were seeded per well of a 6-well plate well, together with either RACK1 or NTC siRNA transfection mixture (reverse transfection). After 24 hrs cells, were trypsinized and 5×10^4 cells were seeded per well of a 24-well plate containing a glass coverslip. For expression of viral proteins (ZIKV or DENV) in these cells, either plasmid DNA (500 ng) pIRO-Z:∆ 5'SLAB or pIRO-D:∆ 5'SLAB was added to 100 µl of Opti-MEM media, mixed briefly and 1.5 µl of Trans-IT-LT1 transfection reagent (Mirus: MIR2304) was added to the DNA - Opti-MEM mixture and mixed briefly. After 20 mins incubation at RT, the transfection mixture was added onto the cells. Following a 4hr incubation period, medium was changed, and cells were fixed 16 to 20 hrs after transfection for transmission electron microscopy (EM) or immunofluorescence (IF) analysis. TEM was performed as has been recently described (Cerikan et al. 2020).

Immunofluorescence microscopy, Immunoprecipitation and Immunoblot

Immunofluorescent labelling was performed as described previously (Van der Hoek et al. 2017). Cells were examined using either a Nikon Eclipse Ti microscope or an Olympus FV3000 confocal microscope. To perform immunoprecipitation, cell lysates were harvested from cells using a lysis buffer containing 1% Triton X-100, 50mM Tris pH 8, 150mM NaCl and 1x Protease Inhibitor cocktail (Sigma) and centrifuged at 21,000xg to remove cell debris. Following overnight incubation of the antibody of interest (0,5ug/sample at 4°C), Protein A MagBeads (Genscript) was added to each sample and the manufacturers recommended protocol followed. To isolate bound protein from the beads during elution, 2x sample buffer (Bio-Rad) was added to each sample and boiled at 100°C for 10 minutes. After separation from the MagBeads, the boiled lysate was utilised for western blotting. Western blotting was performed as

described elsewhere (Van der Hoek et al. 2017). Chicken anti-NS5 and mouse and human anti-flavivirus NS1 4G4 ab were used to detect expression of infection-based NS5 and NS1 respectively. Mouse anti-SARS-CoV-2 spike ab was used to detect SARS-CoV-2 spike protein expression following infection. Mouse anti-RACK1, mouse anti-Vinculin and mouse anti-β-actin were used to detect endogenous expression of RACK1, Vinculin and β-action respectively. Membrane-bound protein was detected by chemiluminescence using SuperSignal West Femto (Thermo Fisher Scientific) and imaged using a ChemiDoc MP imaging system (Bio-Rad).

Nano Luciferase Assays

Luciferase assays to quantify nano-luciferase (NLuc) were performed as described previously (Eyre et al. 2017a). Briefly, Huh7.5 cells were seeded into 48 well plates prior to transfection with NTC/RACK1 siRNA or infection with DENV2-NS1-Nluc at the indicated MOI. Samples were harvested with 1x passive lysis buffer before measurement of NLuc activity using the Nano-Glo luciferase assay system (Promega) with the GloMax 20/20 luminometer (Promega).

Proximity Ligation Assay

Proximity ligation assay kits (Duolink PLA) were purchased from Sigma Aldrich and the manufacturer's protocol was followed. Briefly, cells were fixed with acetone/methanol, blocked with 5% BSA and incubated with primary antibodies of interest raised in divergent species. Cells were then incubated with mouse PLA probe PLUS and rabbit PLA probe MINUS for 1 hour in a humidity chamber at 37^{o}C. The ligation mix containing the ligase enzyme was incubated with the cells for 30 minutes in the humidity chamber at 37^{o}C, followed by the amplification mix (90 minutes in the humidity chamber at 37^{o}C) containing the polymerase which facilitates rolling circle amplification if the PLA probes are sufficient proximity in the cells. Cells were then incubated with DAPI for 5 minutes at room temperature and visualised under the immunofluorescence microscope as outlined above.

Plaque Assay

Virus infectivity was determined by plaque assay as described previously (Van der Hoek et al. 2017). Briefly, Vero cells in 24-well plates were infected with 200 µl of

serially-diluted virus-containing supernatants (ZIKV, DENV, WNV, YFV, LGTV, POWV, SARS-CoV-2, VSV and HSV) for 1 hr at 37 °C before the addition of 1ml overlay of complete media containing 1.5% (w/v) carboxymethylcellulose (CMC) (Sigma) and cells returned to culture for various days dependent on the virus. Following fixation with 10% formation for 1 hour, the CMC overlay was removed and plaques visualised via crystal violet stain. Plaques were counted and virus infectivity expressed as plaque-forming units (PFU) per ml.

Quantitative Real-Time PCR

Cells were seeded in 24 well plates for 24 hours prior to transfection or infection. Total RNA was extracted from cells using NucleoZOL (Macherey Nagel) per manufacturers recommendation. Both cDNA synthesis and qRT-PCR were performed simultaneously with the Luna Universal One-Step RT-qPCR Kit (NEB) with the Quantstudio 7 Flex (Life Technologies) to quantitate relative levels of ZIKV RNA, RACK1 mRNA and house-keeping gene ribosomal protein lateral stalk subunit PO (RPLPO) (36B4). All primer sequences used are outlined below: EMC1 FP: 5'CGGCCTGAGCGGCTGTATATC3', EMC1 RP: 5'CTCCACAGCACCACCTTCCC3', EMC6 FP: 5'TTCTACCTGCTCGCCTCCGT3', EMC6 RP: 5' CCCGATGAGGCCTCCTGTAA3', RACK1 FP: 5' TAACCGCTACTGGCTGTGTG3' and RACK1 RP: 5' GCCTTGCTGCTGGTACTGAT3'.

Statistics

Data was graphed and analysed with Prism 9 (GraphPad Software) using student T-tests.

Author Contributions

B.S, A.I.C, B.C. and M.R.B conducted experiments and analysed the results, T-H.T and S.M.P provided bioinformatics analysis while N.S.E, S.M.P, R.F.W.B and S.M.B provided experimental design input and reagents. B.S. and M.R.B conceived the study and wrote the manuscript.

Acknowledgements

This work was supported by the NHMRC of Australia (APP1145613).

Figure legends

Figure 1: Identification of RACK1 as a critical host factor for the ZIKV lifecycle. **(A**) Schematics of the genome-wide CRISPR/Cas9 screen with ZIKV strategy. **(B)** Enriched genes after CaRpools analysis isolated several genes of interest including proteins from the EMC complex (EMC1, MMGT1, EMC6), BAX2 and GNB2L1 (RACK1). **(C)** Independent polyclonal CRISPR knockouts were performed for EMC1, EMC6 and RACK1, infected with ZIKV (MOI=2) and qRT-PCR utilised to determine levels of both the respective knockout gene transcripts as well as ZIKV RNA. NTC = non-targeting control (n=3, *p<0.05, error bars=SD). **(D)** Plaque assays were also performed concurrently with EMC1, EMC6 and RACK1 knockout cell lines to determine levels of ZIKV virions within the supernatant. NTC = non-targeting control (n=3, *p<0.05, error bars=SD).

Figure 2: RACK1 is a critical host factor for ZIKV infection.
Huh7 cells were transfected with either NTC or RACK1 siRNA and cells harvested for RNA extraction and qRT-PCR **(A)** or western blot **(B)** at indicated time points (n=3 *p<0.05). HeLa **(C)** and HTR8 **(D)** cells were transfected with either NTC or RACK1 siRNA prior to infection with ZIKV (PRVABC59, MOI=2). 48hpi, RNA was harvested and qRT-PCR performed (n=3 *p<0.05). **(E)** HeLa cells were infected with either ZIKV MR766 or PRVABC59 (MOI=2) 24 hrs post NTC/RACK1 siRNA transfection and RNA harvested for qRT-PCR 48 hours post infection (n=3 *p<0.05). **(F)** Immunofluorescence was performed on endogenous RACK1 and ZIKV envelope by transfecting NTC/RACK1 siRNA into HeLa cells and infection with ZIKV (PRVABC59, MOI=1) 24 hrs post transfection. Cells were fixed 48hpi and stained as indicated. (n=3, *p<0.05, scale bar: 250μm)

Figure 3: RACK1 is required for flavivirus replication.
Huh7 cells were transfected with either NTC/RACK1 siRNA and infected with the following viruses 24 hrs post transfection: (A) ZIKV (MOI=0.5), DENV (MOI=0.5), WNV (MOI=0.5), YFV (MOI=0.5), LGTV (MOI=0.5), POWV (MOI=0.5), (B) VSV (MOI=0.5), MERS-CoV/EMC12, EBOV/MAY (10^3 TCID50) and HSV (MOI=0.05). Plaque assays were performed to determine viral titers within the supernatant (n=3, *p<0.05). (C) A549 cells stably expressing the ACE2 receptor was transfected with NTC/RACK1

siRNA prior to infection with SARS-CoV-2 (MOI=0.1). WCL was harvested and immunoblot analysis performed with primary (anti-vinculin, anti-SARS-CoV-2 spike and anti-RACK1) and secondary (anti-mouse conjugated HRP) antibodies. Vinculin served as sample loading control (n=3).

Figure 4: RACK1 is important prior to flavivirus replication complex formation. **(A)** Huh7.5 cells were transfected with NTC/RACK1 siRNA for 24 hrs prior to **(B)** transfection of DENV2 SGR/SGR GND RNA or **(C)** infection with DENV2. (**B)** Cells transfected with DENV-SGR RNA were lysed at the appropriate time points and luciferase assay performed to determine *Renilla Luciferase* levels. **(C)** RNA was harvested and extracted from DENV-infected cells 24hpi and qRT-PCR performed. **(D)** In contrast, Huh7.5 cells were transfected with DENV2 SGR/SGR GND RNA **(E)** or infected with DENV2 **(F)** for 24 hrs prior to transfection of NTC/RACK1 siRNA for 24 hrs. **(E)** Cells transfected with the DENV SGR RNA were lysed at the appropriate time points and luciferase assay performed immediately to determine *Renilla Luciferase* levels . **(F)** RNA from DENV infected cells was extracted and qRT-PCR performed (n=3, *p<0.05).

Figure 5: RACK1 is critical for the formation of the flavivirus replication complex. **(A)** Huh7/Lunet-T7 cells were reverse transfected with NTC/RACK1 siRNA for 24 hrs prior to re-seeding onto glass coverslips. Cells were transfected with pIRO-DENV or -ZIKV constructs for 20 hrs before fixation and electron microscopy. **(B)** Immunoblot analysis performed to evaluate RACK1 levels 48 and 72 hrs post transfection of siRNA. ß-actin served as sample loading control. **(C)** Thin-section TEM images of altered morphology of VPs upon transfection of pIRO-DENV or -ZIKV constructs when RACK1 expression is reduced. Upper panel scale bar: 500nm. Lower panels are magnifications of yellow squared areas in the upper panel images. Lower panel scale bar: 100nm. **(C)** For each condition, VPs present within whole-cell sections from 100 cells were counted (n=3, *p<0.05). **(E&F)** Transfection efficiency of pIRO-DENV and -ZIKV constructs were analysed via immunofluorescence with anti-NS3 and NS4B primary antibodies and appropriate secondary antibodies and multiple fields of view quantified by counting positive staining cells and normalization to total number of cells (n=3, *p<0.05).

Figure 6: RACK1 is required for the positioning of flavivirus molecular components during virus replication.

Huh7 cells were transfected with NTC/RACK1 siRNA for 24 hours prior to infection of DENV2 or ZIKV PRVABC59 (MOI=1). Cells were subjected to indirect immunofluorescence labelling with primary (anti-NS1 and anti-dsRNA) and secondary (mouse anti-IgG 488 and anti-IgM-555) antibodies. DAPI was used to stain nuclear DNA in the merged images (scale bar: 5μm, inset scale bar: 2μm, images representative of 3 biological triplicates where 5 cells were imaged for each replicate)

Figure 7: RACK1 interacts with multiple flavivirus NS1 proteins within the ER lumen.

(A) HeLa cells were infected with DENV, WNV_{KUN}, YFV_{17D} or ZIKV (MOI=2) and 48hpi, WCL were harvested and incubated with human flavivirus NS1 4G4 antibody overnight. Immunoblot analysis was performed with mouse flavivirus NS1 4G4 and RACK1 antibodies. Vinculin served as sample loading control (n=3). (**B)** Huh7.5 cells were transfected with DENV, WNV_{KUN}, YFV_{17D} or ZIKV NS1-FLAG and RACK1-HA tagged constructs. 24 hours post transfection, cells were fixed and stained with primary antibodies - anti-mouse FLAG/anti-rabbit HA, secondary antibodies – anti-mouse 488/anti rabbit 555. DAPI was used to stain for nuclear DNA (scale bar: 70μm, images representative of n=3). **(C)** HeLa cells were transfected with DENV, WNV_{KUN}, YFV_{17D} or ZIKV NS1-FLAG and RACK1-HA tagged constructs. 24 hrs post transfection, cells were fixed and proximity ligation assay performed. DAPI was used to stain for nuclear DNA (scale bar: 15μm, images representative of n=3). **(D)** HeLa cells were infected with DENV2, WNV_{KUN} or ZIKV (MOI=1) for 24 hours and WCL extracted for immunoblot analysis with primary (anti-vinculin, anti-NS1 and anti-RACK1) and secondary (anti-mouse conjugated HRP) antibodies. Vinculin served as sample loading control. Lysates were also used for immunoprecipitation using human anti-NS1 4G4 antibody and subjected to immunoblot analysis with primary (mouse anti-NS1 4G4 and -RACK1) and secondary (anti-mouse conjugated HRP) antibodies.

Figure 1

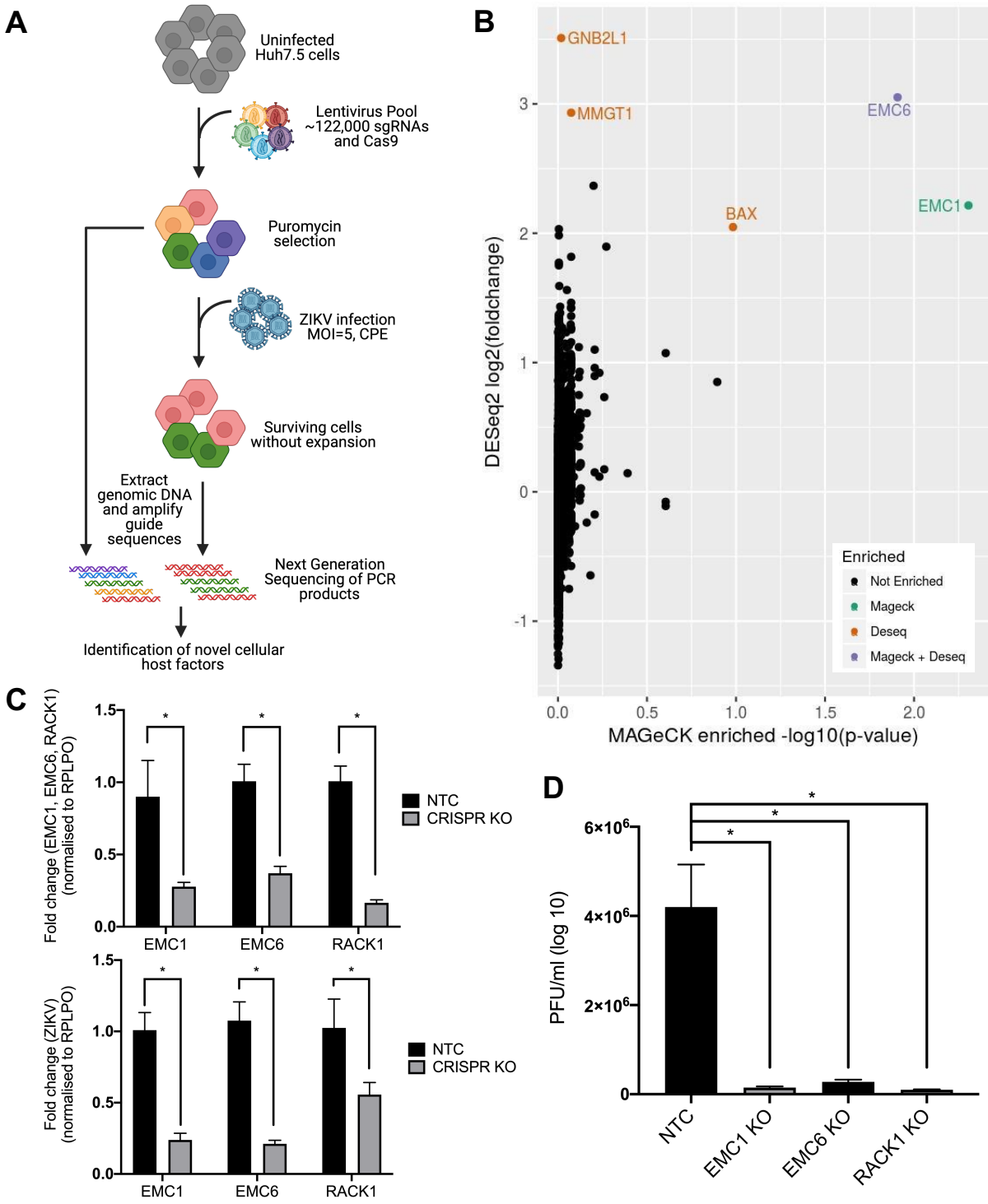
A
Uninfected Huh7.5 cells
Lentivirus Pool ~122,000 sgRNAs and Cas9
Puromycin selection
ZIKV infection MOI=5, CPE
Surviving cells without expansion
Extract genomic DNA and amplify guide sequences
Next Generation Sequencing of PCR products
Identification of novel cellular host factors
B
GNB2L1
MMGT1
BAX
EMC6
EMC1
DESeq2 log2(foldchange)
MAGeCK enriched -log10(p-value)
Enriched
Not Enriched
Mageck
Deseq
Mageck + Deseq
C
Fold change (EMC1, EMC6, RACK1) (normalised to RPLPO)
Fold change (ZIKV) (normalised to RPLPO)
NTC
CRISPR KO
EMC1
EMC6
RACK1
D
PFU/ml (log 10)
NTC
EMC1 KO
EMC6 KO
RACK1 KO

Figure 2

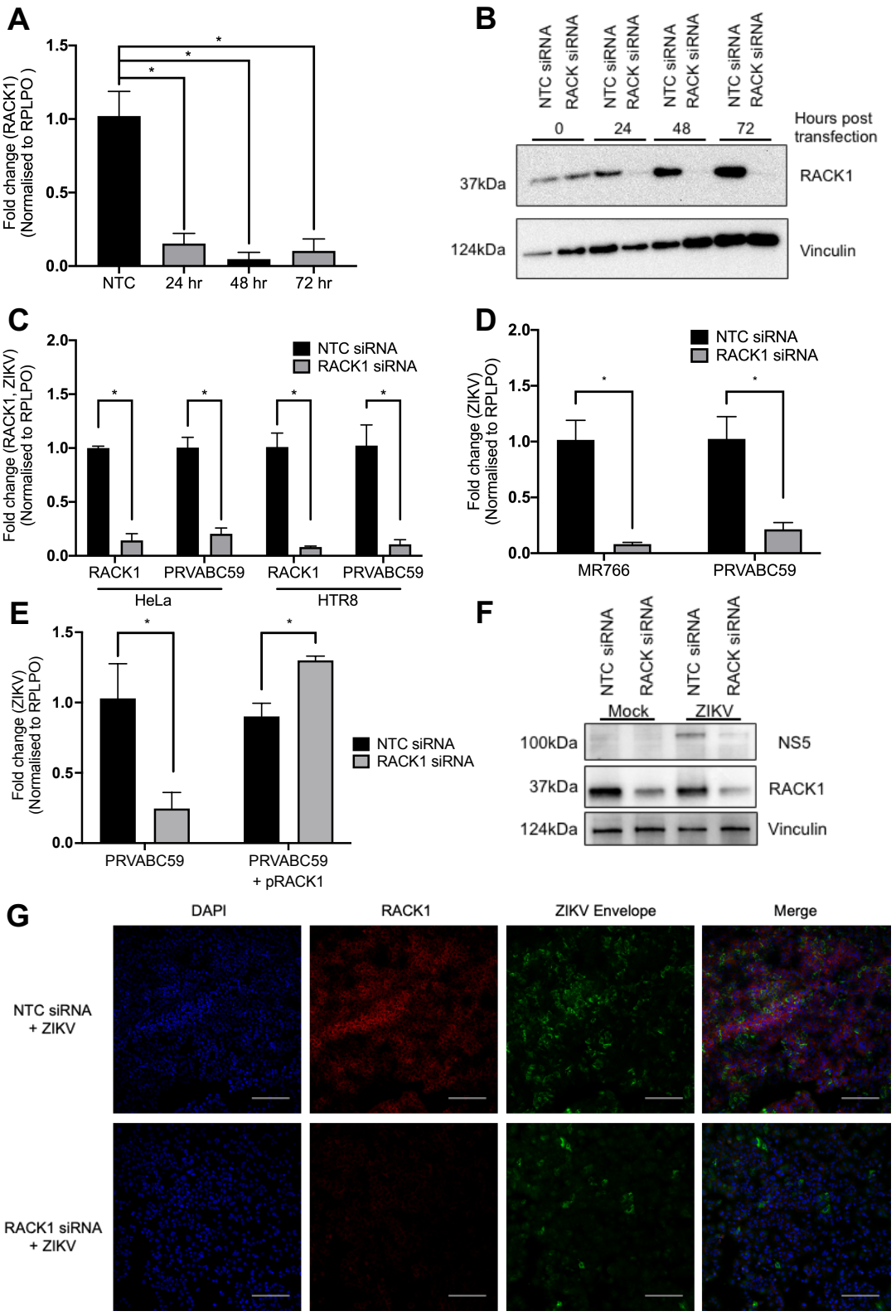
A
Fold change (RACK1)
(Normalised to RPLPO)
1.5
1.0
0.5
0.0
NTC
24 hr
48 hr
72 hr
B
NTC siRNA
RACK siRNA
0
24
48
72
Hours post transfection
37kDa
RACK1
124kDa
Vinculin
C
Fold change (RACK1, ZIKV)
(Normalised to RPLPO)
NTC siRNA
RACK1 siRNA
2.0
1.5
1.0
0.5
0.0
RACK1
PRVABC59
RACK1
PRVABC59
HeLa
HTR8
D
Fold change (ZIKV)
(Normalised to RPLPO)
NTC siRNA
RACK1 siRNA
2.0
1.5
1.0
0.5
0.0
MR766
PRVABC59
E
Fold change (ZIKV)
(Normalised to RPLPO)
1.5
1.0
0.5
0.0
NTC siRNA
RACK1 siRNA
PRVABC59
PRVABC59
+ pRACK1
F
NTC siRNA
RACK siRNA
NTC siRNA
RACK siRNA
Mock
ZIKV
100kDa
NS5
37kDa
RACK1
124kDa
Vinculin
G
DAPI
RACK1
ZIKV Envelope
Merge
NTC siRNA
+ ZIKV
RACK1 siRNA
+ ZIKV

Figure 3

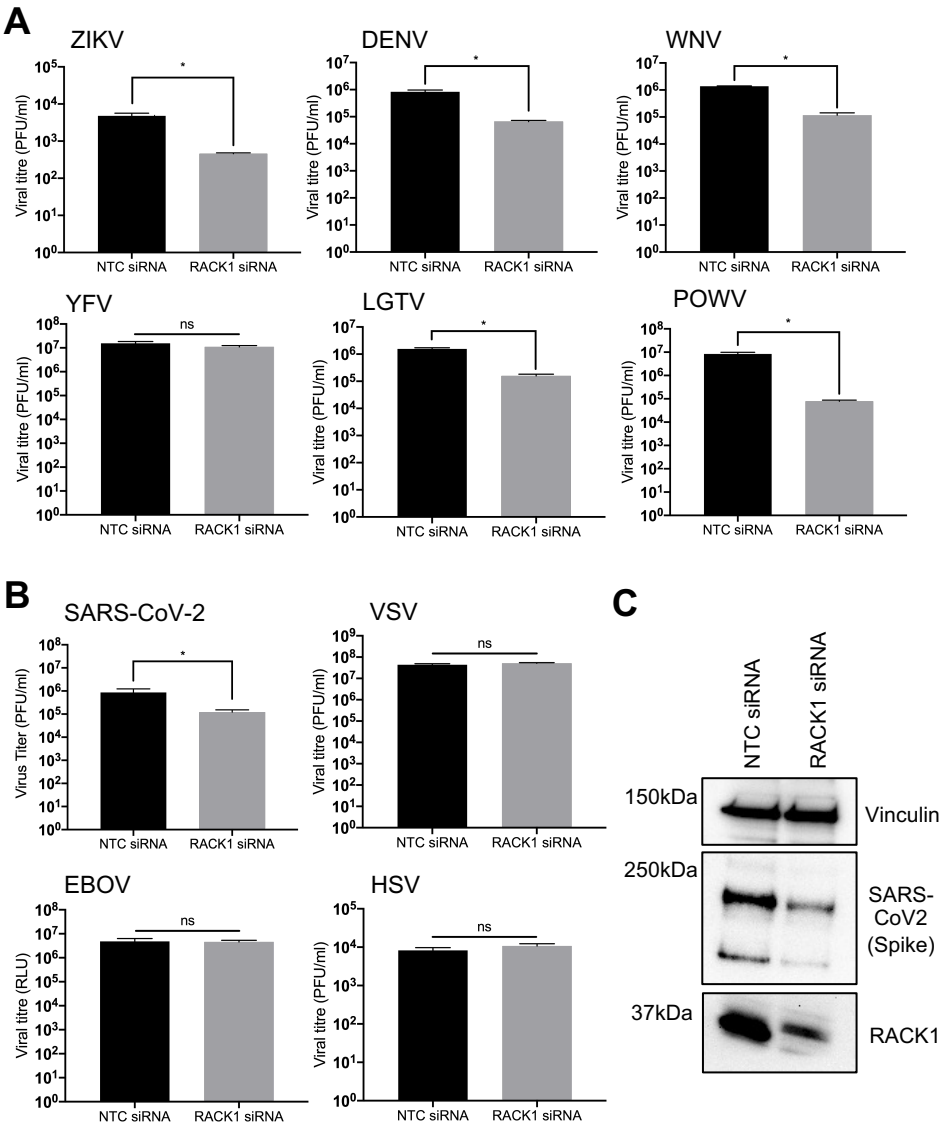
A
ZIKV
DENV
WNV
YFV
LGTV
POWV
Viral titre (PFU/ml)
NTC siRNA
RACK1 siRNA
*
ns
B
SARS-CoV-2
VSV
EBOV
HSV
Virus Titer (PFU/ml)
Viral titre (RLU)
C
NTC siRNA
RACK1 siRNA
150kDa
Vinculin
250kDa
SARS-CoV2 (Spike)
37kDa
RACK1

Figure 4

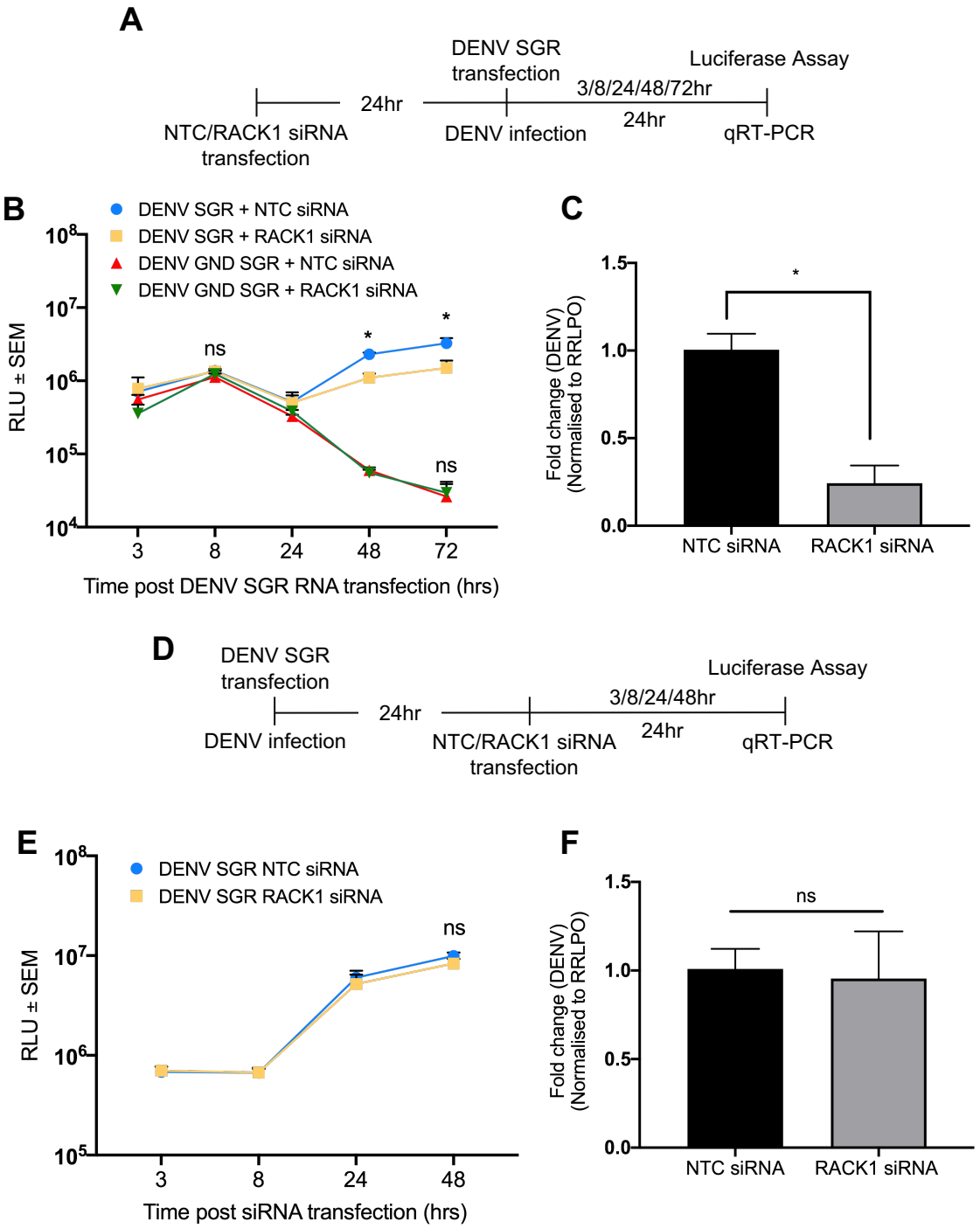
A
DENV SGR transfection
Luciferase Assay
3/8/24/48/72hr
24hr
24hr
NTC/RACK1 siRNA transfection
DENV infection
qRT-PCR
B
DENV SGR + NTC siRNA
DENV SGR + RACK1 siRNA
DENV GND SGR + NTC siRNA
DENV GND SGR + RACK1 siRNA
RLU ± SEM
ns
*
*
ns
Time post DENV SGR RNA transfection (hrs)
C
Fold change (DENV) (Normalised to RRLPO)
*
NTC siRNA
RACK1 siRNA
D
DENV SGR transfection
Luciferase Assay
3/8/24/48hr
24hr
24hr
DENV infection
NTC/RACK1 siRNA transfection
qRT-PCR
E
DENV SGR NTC siRNA
DENV SGR RACK1 siRNA
RLU ± SEM
ns
Time post siRNA transfection (hrs)
F
Fold change (DENV) (Normalised to RRLPO)
ns
NTC siRNA
RACK1 siRNA

Figure 5

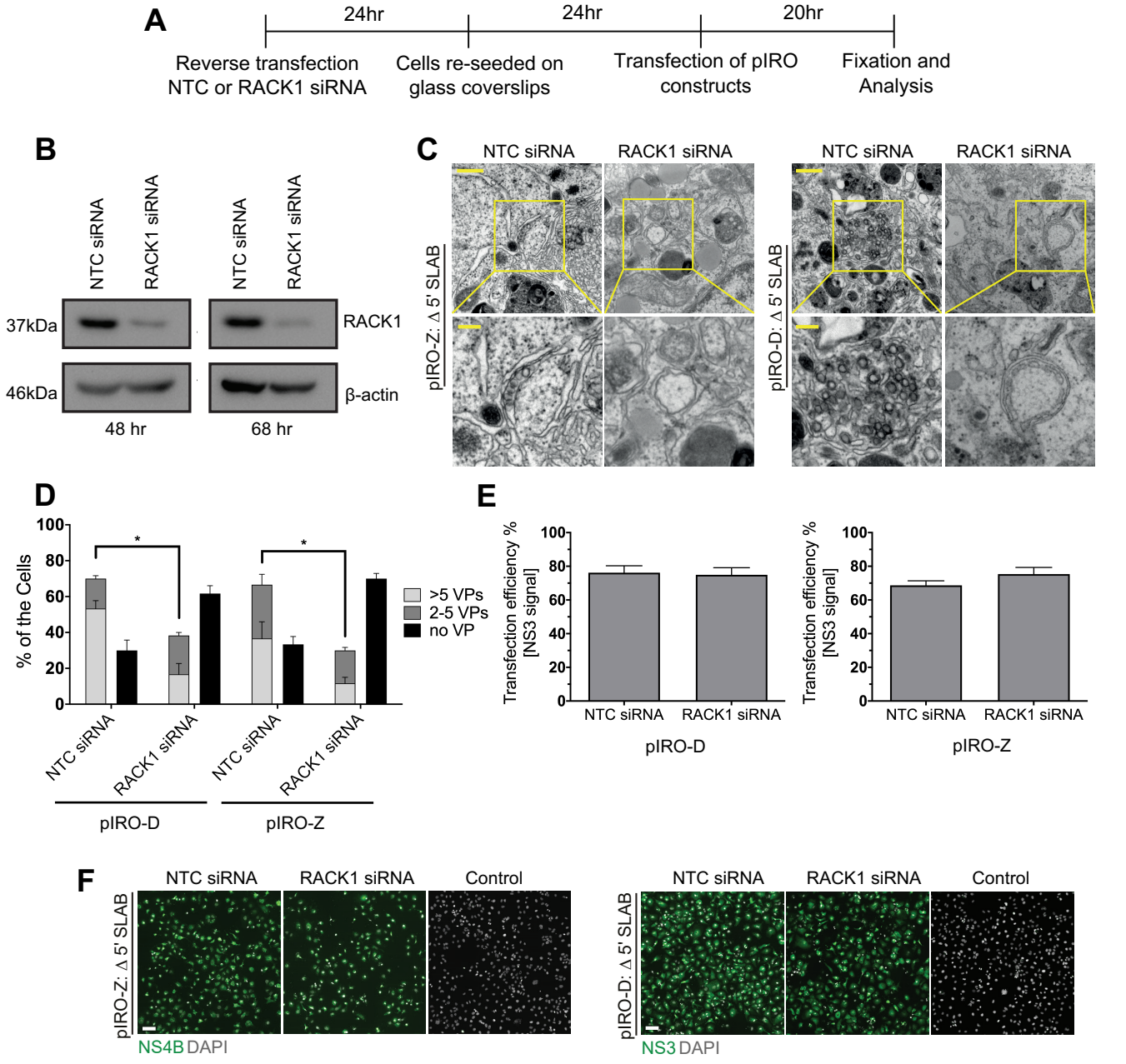
A
24hr
24hr
20hr
Reverse transfection NTC or RACK1 siRNA
Cells re-seeded on glass coverslips
Transfection of pIRO constructs
Fixation and Analysis
B
NTC siRNA
RACK1 siRNA
NTC siRNA
RACK1 siRNA
37kDa
RACK1
46kDa
β-actin
48 hr
68 hr
C
NTC siRNA
RACK1 siRNA
NTC siRNA
RACK1 siRNA
pIRO-Z: Δ 5' SLAB
pIRO-D: Δ 5' SLAB
D
% of the Cells
>5 VPs
2-5 VPs
no VP
NTC siRNA
RACK1 siRNA
NTC siRNA
RACK1 siRNA
pIRO-D
pIRO-Z
E
Transfection efficiency % [NS3 signal]
NTC siRNA
RACK1 siRNA
pIRO-D
Transfection efficiency % [NS3 signal]
NTC siRNA
RACK1 siRNA
pIRO-Z
F
NTC siRNA
RACK1 siRNA
Control
pIRO-Z: Δ 5' SLAB
NS4B DAPI
NTC siRNA
RACK1 siRNA
Control
pIRO-D: Δ 5' SLAB
NS3 DAPI

Figure 6

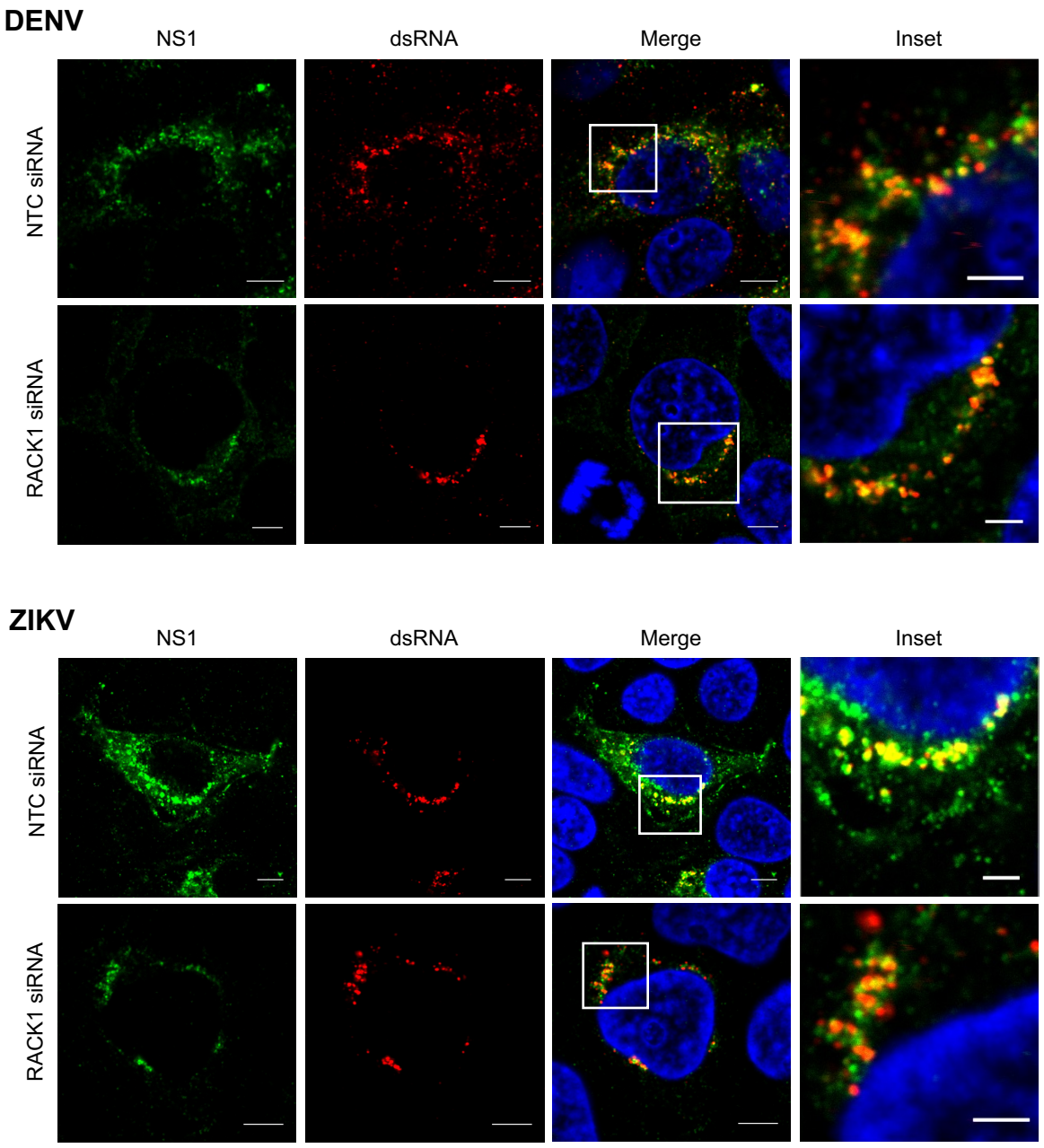
DENV
NS1
dsRNA
Merge
Inset
NTC siRNA
RACK1 siRNA
ZIKV
NS1
dsRNA
Merge
Inset
NTC siRNA
RACK1 siRNA

Figure 7

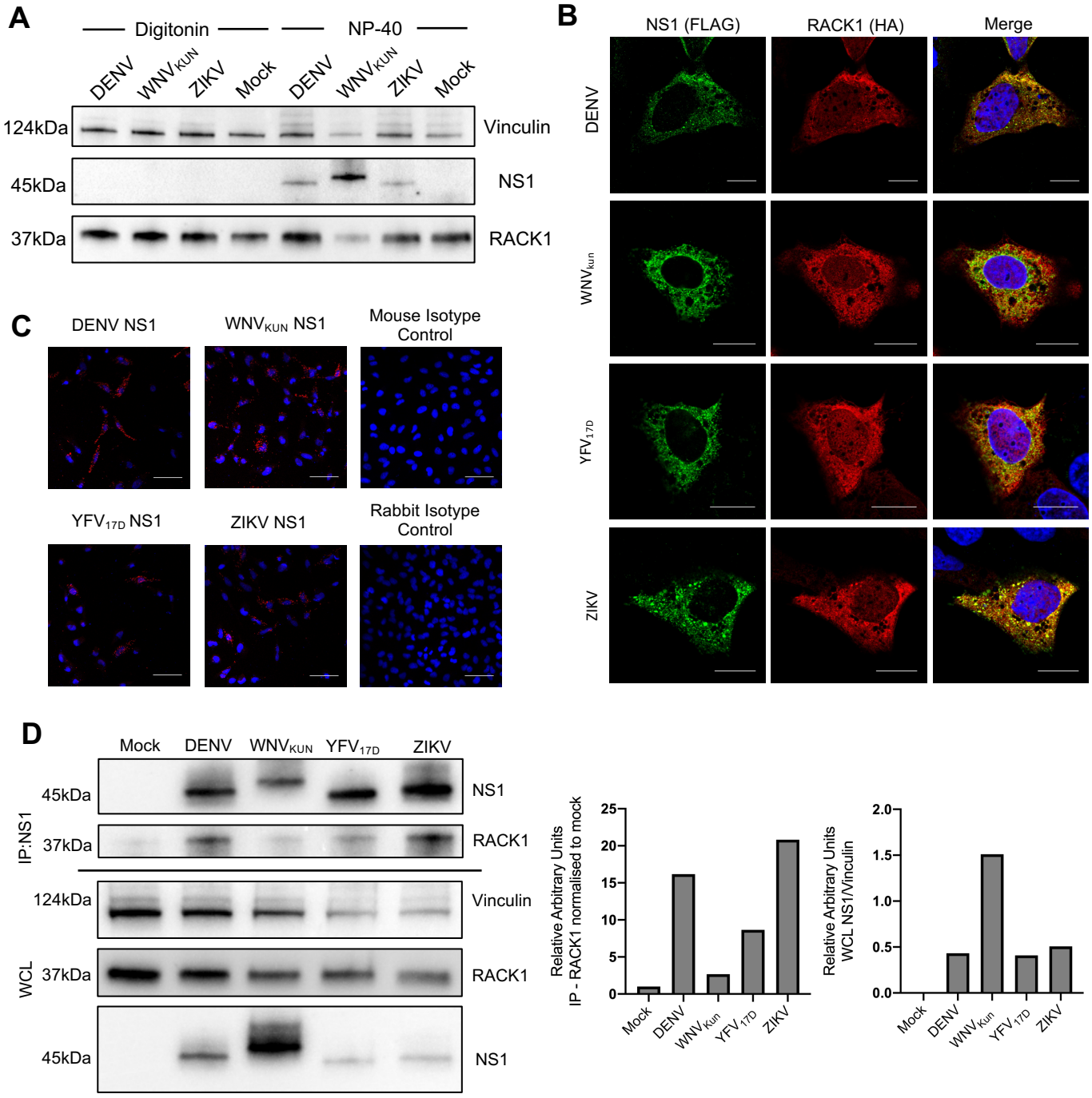
A
Digitonin
NP-40
DENV
WNVKUN
ZIKV
Mock
DENV
WNVKUN
ZIKV
Mock
124kDa
Vinculin
45kDa
NS1
37kDa
RACK1
B
NS1 (FLAG)
RACK1 (HA)
Merge
DENV
WNVKun
YFV17D
ZIKV
C
DENV NS1
WNVKUN NS1
Mouse Isotype Control
YFV17D NS1
ZIKV NS1
Rabbit Isotype Control
D
Mock
DENV
WNVKUN
YFV17D
ZIKV
IP:NS1
45kDa
NS1
37kDa
RACK1
124kDa
Vinculin
WCL
37kDa
RACK1
45kDa
NS1
Relative Arbitrary Units
IP - RACK1 normalised to mock
25
20
15
10
5
0
Mock
DENV
WNVKun
YFV17D
ZIKV
Relative Arbitrary Units
WCL NS1/Vinculin
2.0
1.5
1.0
0.5
0.0
Mock
DENV
WNVKun
YFV17D
ZIKV

Statement of Authorship

Title of Paper	Genome-wide CRISPR KO screen identifies RACK1 as a critical host factor for flavivirus replication
Publication Status	☐ Published ☐ Accepted for Publication ☐ Submitted for Publication ☑ Unpublished and Unsubmitted work written in manuscript style
Publication Details	The flavivirus family are a group of pathogens that cause substantial burden on society, particularly in the developing world. Cellular factors play important roles in all facets of the flavivirus life cycle and deciphering viral-host protein interactions is essential for understanding the flavivirus lifecycle and development of effective antiviral strategies. To uncover novel host factors for multiple flaviviruses, a CRISPR/Cas9 genome wide KO screen was employed to identify cells resistant to ZIKV-induced cytopathic effect (CPE). RACK1 was identified as a novel host factor for ZIKV infection and confirmed via complementary experiments. Knockdown of RACK1 via siRNA indicated that RACK1 is important for replication of a wide range of mosquito and tick borne flaviviruses, including WNV_{kun}, DENV, Powassan Virus (POWV) and (Langat Virus) LGTV. Flavivirus replication is only abrogated when RACK1 is knockdown prior to infection and is critical for vesicle packet formation. RACK1 is able to interact with NS1 from multiple flaviviruses, a key protein critical for replication complex formation. Overall, these findings illustrate the importance of host factors such as RACK1 which are instrumental to the generation for pan-flavivirus replication organelles.

Principal Author

Name of Principal Author (Candidate)	Byron Shue		
Contribution to the Paper	Developed study Intellectual input Experimental design Sample processing and analysis of experiments (All figures excluding Fig. 3&5) Writing the original draft and data presentation		
Overall percentage (%)	80%		
Certification:	This paper reports on original research I conducted during the period of my Higher Degree by Research candidature and is not subject to any obligations or contractual agreements with a third party that would constrain its inclusion in this thesis. I am the primary author of this paper.		
Signature		Date	04/12/20

Co-Author Contributions

By signing the Statement of Authorship, each author certifies that:

i. the candidate's stated contribution to the publication is accurate (as detailed above);

ii. permission is granted for the candidate in include the publication in the thesis; and

iii. the sum of all co-author contributions is equal to 100% less the candidate's stated contribution.

Name of Co-Author	Abhilash I. Chiramel
Contribution to the Paper	Viral assays (Fig. 3)
Signature	Date 12/18/20

Name of Co-Author	Berati Cerikan
Contribution to the Paper	Experiments using pIRO DENV/ZIKV system including EM and quantification of VPs (Fig. 5)
Signature	Date 30/12/2020

Name of Co-Author	Thu-Hien To
Contribution to the Paper	Bioinformatics NGS analysis of genome-wide CRISPR screen
Signature	Date 11/12/2020
Name of Co-Author	Stephen M. Pederson
Contribution to the Paper	Bioinformatics NGS analysis of genome-wide CRISPR screen
Signature	Date 14/12/2020
Name of Co-Author	Nicholas S. Eyre
Contribution to the Paper	Intellectual input and supply of viral stocks including DENV WT and NS1-Nluc (Fig 4,6&7)
Signature	Date 9/12/2020
Name of Co-Author	Ralf F.W. Bartenschlager
Contribution to the Paper	Intellectual input for pIRO DENV/ZIKV experiments (Fig. 5)
Signature	Date 30/12/2020
Name of Co-Author	Sonja M. Best
Contribution to the Paper	Intellectual input for viral assay experiments (Fig. 3)

Signature		Date	17-12-20.
Name of Co-Author	Michael R. Beard		
Contribution to the Paper	Developed study Intellectual input Experimental design Sample processing and analysis of experiments (Fig. 3) Writing the original draft and data presentation		
Signature		Date	4/12/20

Data in addition to the manuscript

4.1 RACK1 interacts with multiple ZIKV NS proteins

The exploitation of host factors to support the viral lifecycle is often mediated by direct interactions with one or more viral proteins. Proteins within the EMC complex (EMC1 and EMC6) are required for the biogenesis of both flavivirus NS4A and NS4B (Lin et al. 2019a). This is also true for viral induced antagonism of the innate immune response, where NS1 and NS4B both interact with TBK1 to inhibit RLR signalling and the production of the type I IFNs (Wu et al. 2017). Given that each flavivirus NS protein has specific main roles within the virus lifecycle, association of RACK1 with a particular flaviviral NS protein may assist in the characterisation of RACK1's role within flavivirus replication. Cells transfected with RACK1 in combination with each ZIKV NS protein were subjected to Proximity Ligation Assay (PLA), an antibody-based interaction assay. RACK1 was able to interact with all ZIKV NS proteins with the exception of ZIKV NS5, as observed by punctate red fluorescence (Fig. 4.1). Previous reports have shown that most but not all flavivirus NS5 accumulates within the nuclei of both transfected and infected cells [396-398]. In addition, although RACK1 is a cytoplasmic adapter protein, it can also enter the nucleus after stimuli from the cAMP signalling pathway (Neasta et al. 2012). Thus, lack of interaction of RACK1 with ZIKV NS5 suggests that the former's role in the flavivirus lifecycle is not confined to the nucleus. It is probable that RACK1 has a specific role with each ZIKV NS protein (except NS5) given its role as a cytoplasmic chaperone protein, possibly in complex with other host factors. However, it is more likely that RACK1 plays a key role within the virus lifecycle where all ZIKV NS proteins share common roles within close proximity, one of which is the construction and maintenance of the replication complex.

4.2 The WD2 domain of RACK1 is important for flavivirus NS1 binding

RACK1 is an evolutionary conserved chaperone protein and a key mediator of various signalling pathways [reviewed in (Adams et al. 2011)]. Interactions between RACK1 and host proteins is facilitated by the 7 WD40 repeat domains present within the β-propeller structure, where miniscule structural differences between each WD40 repeat domain dictates binding specificity. Multiple interacting proteins are often bound to the

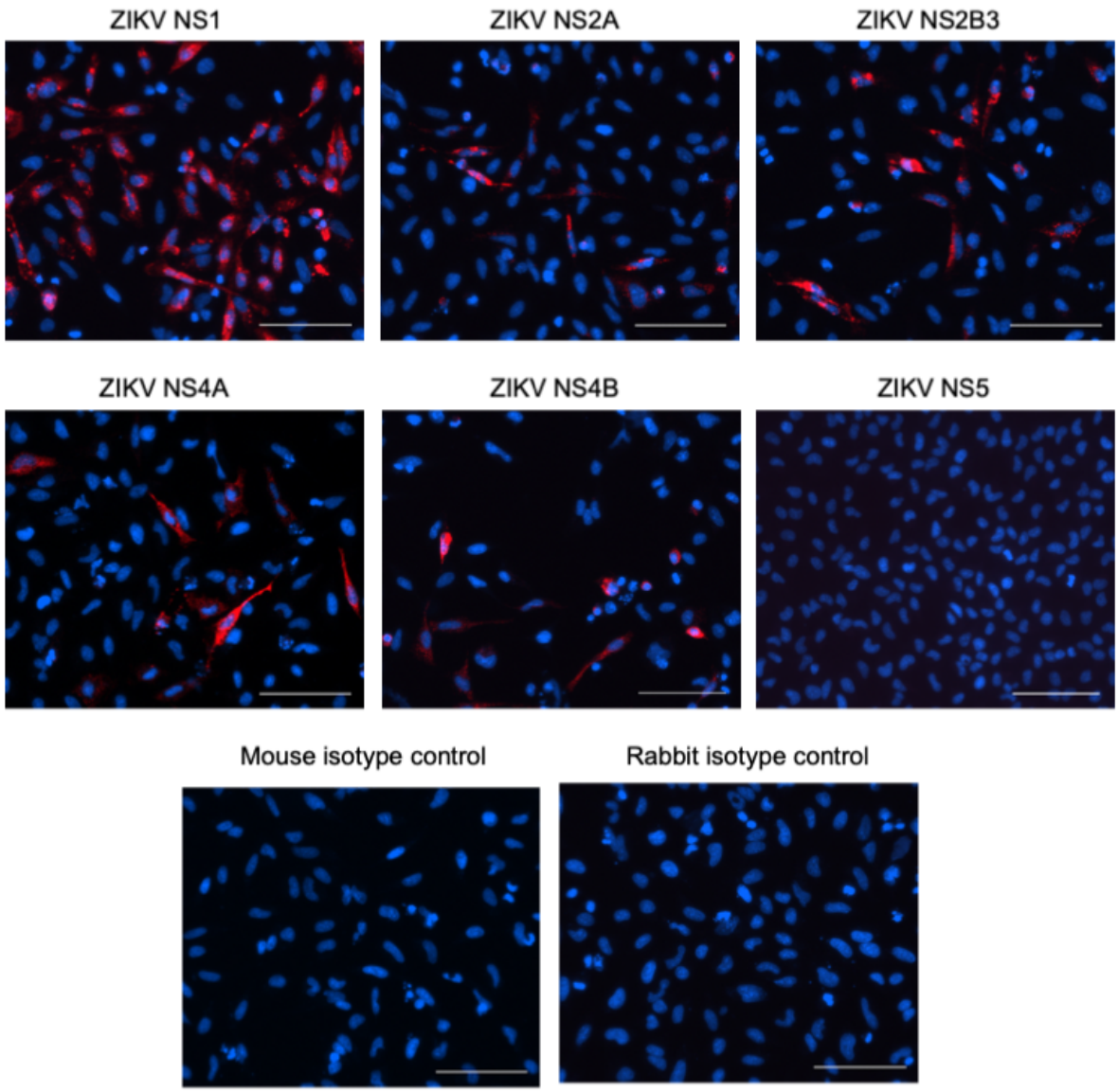

Figure 4.1: Interaction of ZIKV NS proteins with RACK1.

ZIKV NS FLAG tagged constructs were transfected in combination with the RACK-HA plasmid construct and subjected to proximity ligation assay (PLA) to determine interaction. Mouse-FLAG and Rabbit-HA antibodies were utilised and after DAPI staining, visualised using a Nikon TiE inverted microscope. Scale bars are 100μm.

same WD domain of RACK1 to facilitate signal transduction. Isolation of the binding site of NS1 to RACK1 relative to other binding partners may identify the potential signalling pathways mediated by RACK1 with regards to replication complex formation. Expression of highly truncated RACK1 resulted in poor protein stability in contrast to other studies (Chang et al. 2002). Thus, RACK1 mutants, where each lack one WD40 repeat domain were constructed to determine the binding location of NS1 as outlined in Figure 4.2. Co-immunoprecipitation was performed on both DENV NS1 and ZIKV NS1 with each RACK1 ΔWD mutant was performed and interaction was lost with both flaviviral NS1 when the WD2 domain of RACK1 was absent (Fig. 4.3A, 4.3B). Interestingly, interaction between NS1 and RACK1 was increased when the WD7 domain of RACK1 was absent for both flaviviruses.

4.3 ZIKV NS1 interacts with ATG14 in a complex with RACK1

It has been reported during the development of this manuscript that HCV NS5A interacts with RACK1 in a complex with ATG14L-Beclin1-Vps34-Vps15, all of which are major components of autophagy regulation (Lee et al. 2019). In addition, Lee *et al.* show that RACK1 is critical for the induction of autophagy by HCV NS5A, and that both RACK1 and ATG14L are required for NS5A mediated DMV formation. ATG5 has also been shown to be an interacting partner with RACK1 to induce autophagy (Erbil et al. 2016). Since flaviviruses also induce autophagy during virus replication [reviewed in (Ke 2018)], we assessed whether flavivirus NS1 can also interact with either ATG5 and/or ATG14L to determine a potential mechanism by which RACK1 supports the biogenesis of VPs. Co-immunoprecipitation experiments were performed on cells transfected with ZIKV NS1-FLAG in combination with ATG5-myc or ATG14-myc constructs. Pull down of ZIKV NS1 showed that both endogenous RACK1 and ectopically expressed ATG14L were interacting partners (Fig. 4.4). Since ZIKV NS1, like HCV NS5A are critical for the formation of VPs and DMVs respectively, the interaction of flavivirus NS1 with RACK1 may recruit members of autophagy regulation including ATG14 to promote the biogenesis of replication organelles.

Figure 4.2: Schematic of RACK1 ΔWD mutants.

To construct all seven RACK1 ΔWD mutants, primers containing *Kpn*I restriction sites were designed flanking each domain in the opposite direction. PCR amplification was performed, digested with *Kpn*I and self-ligated. Sanger sequencing confirmed the loss of one WD domain in each of the 7 RACK1 ΔWD mutants.

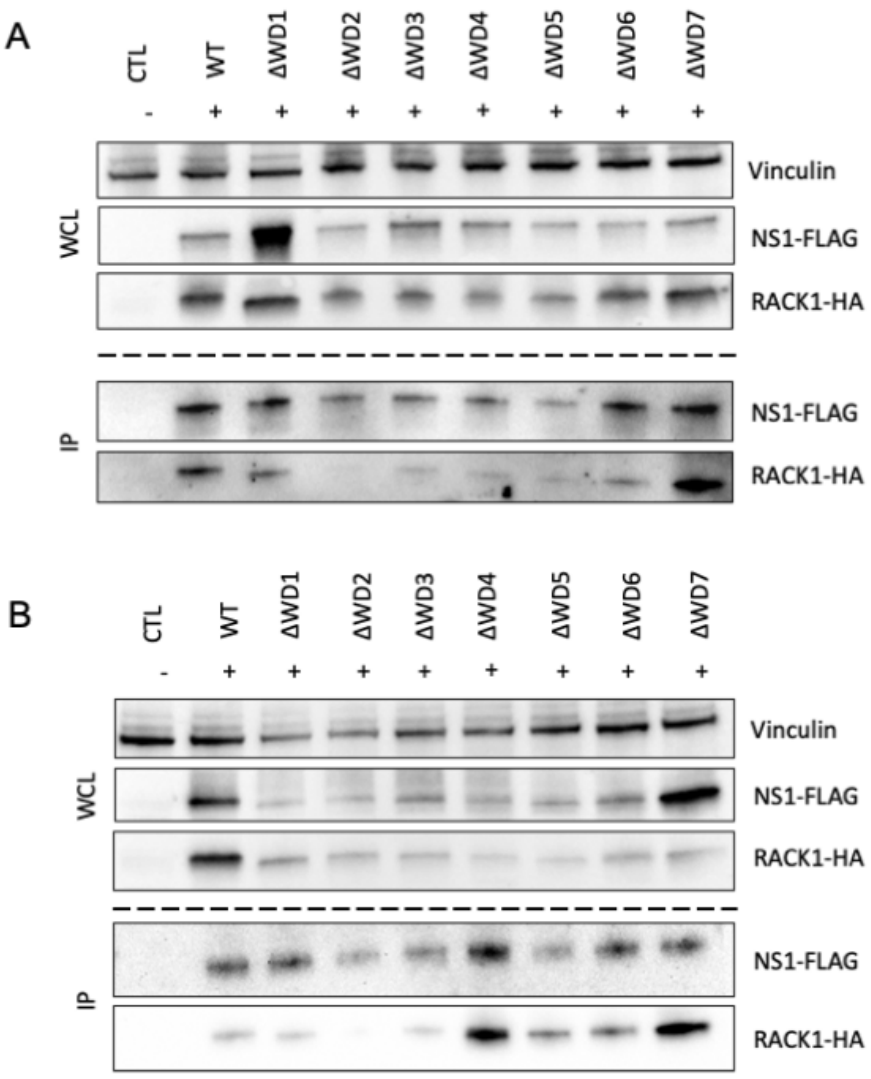

Figure 4.3: The WD2 domain of RACK1 is important for interaction with DENV and ZIKV NS1.

293T cells were transfected with wildtype (WT) or RACK1ΔWD mutants alongside **(A)** DENV NS1-FLAG or **(B)** ZIKV NS1-FLAG plasmid constructs for 24 hours prior to whole cell lysate extraction. Rabbit anti-FLAG antibody was incubated with lysates overnight prior to immunoprecipitation. Western blotting was performed with mouse anti-FLAG or anti-HA primary and anti-mouse HRP secondary antibodies. CTL=Control (mock transfection), WT=wildtype, WCL=whole cell lysate, IP=immunoprecipitation. Vinculin was included as a protein loading control. Image representative of 3 experiments.

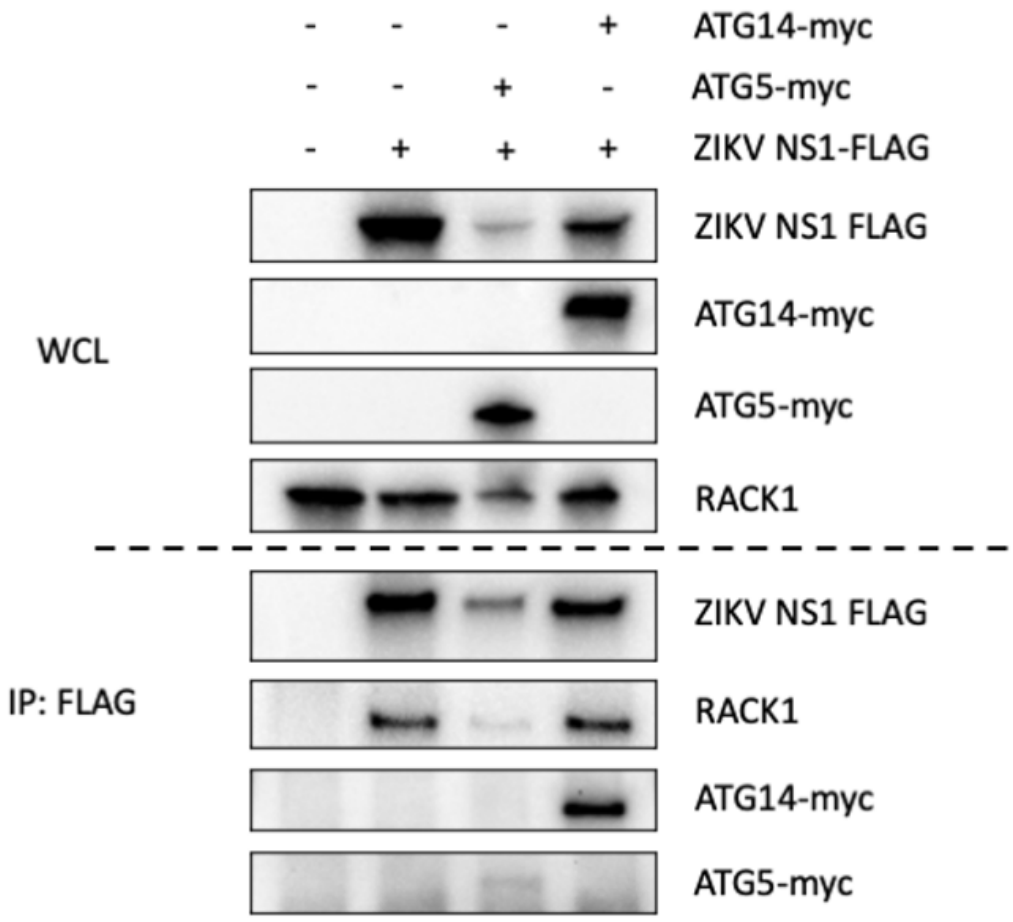

Figure 4.4: ZIKV NS1 interacts with both RACK1 in complex with ATG14 but not ATG5.

293T cells were transfected with the only ZIKV NS1-FLAG or in combination with ATG5-myc or ATG14-myc plasmid constructs for 24 hours prior to whole cell lysate extraction. Rabbit anti-FLAG antibody was incubated with lysates overnight prior to immunoprecipitation. Western blotting was performed with mouse anti-FLAG or anti-myc primary and anti-mouse HRP secondary antibodies. Image representative of 3 experiments.

Chapter 5: Viperin is an important restriction factor in control of Zika virus infection - MANUSCRIPT

Manuscript published in Scientific Reports

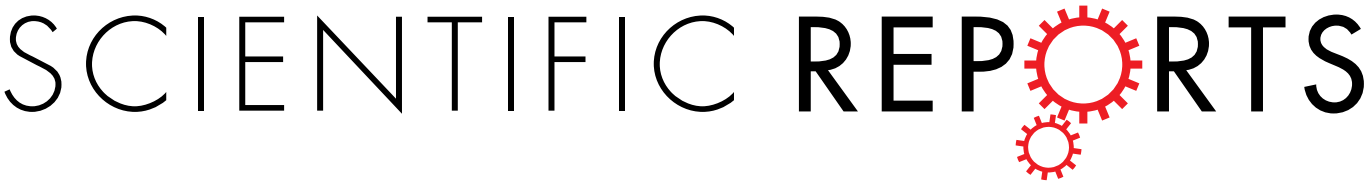

OPEN

Viperin is an important host restriction factor in control of Zika virus infection

Received: 7 February 2017
Accepted: 24 May 2017
Published online: 30 June 2017

Kylie H. Van der Hoek[1,3], Nicholas S. Eyre[1,3], Byron Shue[1,3], Onruedee Khantisitthiporn[1,3], Kittirat Glab-Ampi[1,3], Jillian M. Carr[4], Matthew J. Gartner[1,3], Lachlan A. Jolly[2], Paul Q. Thomas[1], Fatwa Adikusuma[1], Tanja Jankovic-Karasoulos[2], Claire T. Roberts[2], Karla J. Helbig[5] & Michael R. Beard[1,3]

Zika virus (ZIKV) infection has emerged as a global health threat and infection of pregnant women causes intrauterine growth restriction, spontaneous abortion and microcephaly in newborns. Here we show using biologically relevant cells of neural and placental origin that following ZIKV infection, there is attenuation of the cellular innate response characterised by reduced expression of IFN-β and associated interferon stimulated genes (ISGs). One such ISG is viperin that has well documented antiviral activity against a wide range of viruses. Expression of viperin in cultured cells resulted in significant impairment of ZIKV replication, while MEFs derived from CRISPR/Cas9 derived viperin$^{-/-}$ mice replicated ZIKV to higher titers compared to their WT counterparts. These results suggest that ZIKV can attenuate ISG expression to avoid the cellular antiviral innate response, thus allowing the virus to replicate unchecked. Moreover, we have identified that the ISG viperin has significant anti-ZIKV activity. Further understanding of how ZIKV perturbs the ISG response and the molecular mechanisms utilised by viperin to suppress ZIKV replication will aid in our understanding of ZIKV biology, pathogenesis and possible design of novel antiviral strategies.

Zika virus (ZIKV) is an arbovirus and a member of the *Flaviviridae* family that is a significant health threat on a global scale[1]. ZIKV gained global attention in 2007 when the first major outbreak was reported in Micronesia followed by smaller outbreaks in other pacific islands thereafter[2]. However, the largest outbreak to date was reported in 2015 in Brazil and was followed by widespread dissemination in Central and South America. While the majority of infections in humans are either asymptomatic or associated with fever, rash and conjunctivitis, the 2015 outbreak was associated with an alarming number of neurological and birth defects including microcephaly[3]. Evidence linking ZIKV to the above mentioned pathologies include ZIKV RNA present in the amniotic fluid and fetal and newborn brain tissue[4]. It is now well accepted that ZIKV can cross the placenta and subsequently infect neural progenitor cells of the fetus leading to significantly impaired brain development. ZIKV antigen has been identified in the placental chorionic villi from an infected mother who gave birth to a microcephalic infant and can also infect human placental trophoblasts and macrophages *in vitro*[5,6]. Moreover, recent mouse models have revealed that ZIKV infection can result in placental insufficiency, alterations in neural progenitor proliferation and fetal demise[7–10]. In addition to the classical mosquito transmission, ZIKV can be sexually transmitted via infected seminal fluid[11–13]. The growing association of ZIKV infection during pregnancy with serious neurological defects in newborns has resulted in ZIKV being declared as a public health emergency by the WHO.

The innate immune response to virus infection plays a crucial role in controlling viral infection in addition to shaping the adaptive immune response. This innate response is initiated by the recognition of genetic components expressed during viral replication, collectively termed pattern associated molecular patterns (PAMPs), by cellular sensors termed Pattern Recognition Receptors (PRRs)[14]. In the case of RNA viral infection, the best-characterized

[1]Molecular and Cellular Biology, Research Centre for Infectious Diseases, The University of Adelaide, Adelaide, SA, 5005, Australia. [2]Adelaide Medical School and Robinson Research Institute, The University of Adelaide, Adelaide, SA, 5005, Australia. [3]Centre for Cancer Biology, University of South Australia, Adelaide, SA, 5000, Australia. [4]Microbiology and Infectious Diseases, School of Medicine, Flinders University, Bedford Park, SA, 5042, Australia. [5]Department of Physiology, Anatomy and Microbiology, La Trobe University, Melbourne, Vic, 3086, Australia. Kylie H. Van der Hoek, Nicholas S. Eyre and Byron Shue contributed equally to this work. Correspondence and requests for materials should be addressed to M.R.B. (email: michael.beard@adelaide.edu.au)

PRRs are the membrane bound toll-like receptors (TLRs) and the cytoplasmic RNA sensors RIG-I and MDA5[15]. Engagement of PRRs by viral PAMPs results in the activation of NF-κB, IRF-3 and IRF-7 and production of the type I interferons. Further amplification of the interferon (IFN) system occurs when IFN binds to the interferon receptor (IFNAR) and activates the Jak/Stat signaling cascade to ultimately drive expression of hundreds of interferon stimulated genes (ISGs). These ISGs inhibit viral replication and drive the inflammatory process in an attempt to limit viral replication. The importance of this system is exemplified by the fact that most viruses have evolved mechanisms to evade or inactivate the innate response[16]. As an example the *Flaviridae* members West Nile Virus (WNV) and dengue virus (DENV) target multiple sites following PRR activation and IFN signaling and most recently ZIKV has been shown to degrade STAT2 to inhibit ISG expression[17–19]. Furthermore the observation that mice deficient in the type I IFN receptor are more susceptible to ZIKV infection in comparison to WT mice highlights the importance of the innate response and ISG expression in controlling ZIKV infection[20–22].

Although it is firmly established that the interferon response is an important determinant of host resistance, the antiviral mechanisms responsible for direct suppression of virus replication are less well understood. This, together with the observations that placental cells can resist ZIKV infection due to the actions of the type III IFN-λ and susceptibility of *Ifnar*$^{-/-}$ mice to ZIKV infection suggests a role for specific ISGs in control of ZIKV infection[21]. With this in mind we investigated the innate response to ZIKV infection and revealed that ZIKV infected cells of neural and placental origin fail to induce a robust ISG response. In particular we noted significant abrogation of expression of the ISG viperin that prompted us to investigate the antiviral role of viperin against ZIKV. We and others have demonstrated that the evolutionary conserved ISG viperin can inhibit the replication of a wide range of viruses that are responsible for significant disease in humans[23]. These include the *Flaviviridae* family members, DENV, TBEV, WNV and HCV[24–28]. Interestingly viperin exerts its antiviral effect by diverse mechanisms; for example viperin interacts with the HCV NS5A protein and the proviral host factor VAP-A, both of which are important in HCV replication, while in TBEV infection viperin restricts viral RNA replication dependent on the radical S-adenosyl-l-methionine (SAM) domain[25,28,29]. As for other *flaviviruses* we observed that expression of viperin in Huh-7 cells limited ZIKV replication, whereas viperin$^{-/-}$ MEFs displayed heightened permissiveness to ZIKV infection. Taken together, this work suggests that the ability of ZIKV to impair innate immune recognition and specific ISG expression may be fundamental in enabling virus replication to proceed unchecked in specific cell types. Thus, viperin is a key ISG in controlling ZIKV infection. Understanding the ISGs that control ZIKV and other emerging viral infections is essential for defining mechanisms of viral pathogenesis and possible novel therapeutic strategies.

Results

The antiviral response is attenuated in placental and neural progenitor derived cell lines following ZIKV infection. The cellular innate immune response to viral infection results in expression of the interferons and ISG expression that is critical to the establishment of an antiviral state. However, viruses can block this innate response and ZIKV is no exception with recent work showing that the ZIKV NS5 protein can degrade STAT2, a key transcription factor in the IFN signaling pathway[18,19]. Host innate responses are often cell type specific and with this in mind, we investigated ISG expression in a range of cell types following ZIKV infection. Initially, we infected the liver derived cell line Huh-7 with ZIKV (MOI of 0.1 and 1.0) and assessed ISG mRNA expression by qRT-PCR and ZIKV infectivity using an antibody (4G2) that detects pan-flavivirus envelope including ZIKV. As previously described, Huh-7 cells were readily infected by ZIKV resulting in spreading infection that ultimately resulted in significant cytopathic effect (CPE) at 72 hr post-infection (h.p.i)[30]. We previously reported that infection of Huh-7 cells with the closely related flavivirus DENV results in significant ISG expression; however, this was not the case with ZIKV infection[24]. We quantitated the induction of IFIT1, viperin, IFN-β, IFITM1, ISG15, OAS1 and Mx1 mRNA by qRT-PCR at 24 and 48 h.p.i. Early in infection (24 h.p.i) cells were particularly unresponsive to ZIKV infection even though a significant proportion of the culture was infected (Fig. 1A,B). Even after establishment of infection (48 h.p.i) there was minimal expression of ISGs. In contrast, stimulation of these cells with the double-stranded RNA (dsRNA) mimic poly(I:C) resulted in robust induction of ISG expression (Supplementary Fig. S1), indicating that the weak response observed in ZIKV-infected cells cannot be attributed to defects in dsRNA sensing or signaling pathways in these cells.

Next we investigated ISG expression in a number of more physiologically relevant cell lines, namely the first trimester immortalised extravillious trophoblast line HTR8/SVNeo and JEG3 a trophoblast derived choriocarcinoma line[31]. Following ZIKV infection at MOI of 0.1 and 1.0, HTR8/SVNeo cells harbored productive viral replication as determined by immunolabeling of both E protein and dsRNA (Fig. 1D). Even in the face of significant viral replication at 24 and 48 h.p.i there was minimal or no induction of mRNA expression of our ISG panel and only a moderate increase in IFN-β mRNA at 48 h.p.i. (Fig. 1C). A similar pattern of ISG expression was seen following infection of cultures with ZIKV strain PRVABC59 confirming that this observation is not strain dependent (Supplementary Fig. S2). In contrast, JEG3 choriocarcinoma cells were more responsive to infection with increases, albeit moderate, in mRNA expression for IFIT1 and IFN-β at 24 and 48 h.p.i, however viperin expression was attenuated at both time points post ZIKV infection (Fig. 1E). As above, this attenuation of ISG mRNA expression was not a result of a defect in innate immune sensing or signaling as significant increases in ISG induction could be seen following stimulation with poly (I:C) in all cell-lines tested (Supplementary Fig. S1).

Our results suggest that while ZIKV may induce a cellular innate response, the early response may be actively attenuated. To investigate this further we quantified viperin, IFIT1 and IFN-β mRNA following polyI:C stimulation of Huh-7 cells in the presence or absence of ZIKV infection. As expected, mRNA for viperin, IFIT1 and IFN-β significantly increased following polyI:C stimulation, however this was significantly attenuated in the presence of ZIKV infection (Fig. 2A). Consistent with the notion that ZIKV can actively suppress early ISG expression we also demonstrate that ZIKV can attenuate the IFN-β promoter in response to both polyI:C and expression of constitutively active RIG-I (RIG-N) (Fig. 2B,C). RIG-I PAMP recognition ultimately induces IRF3

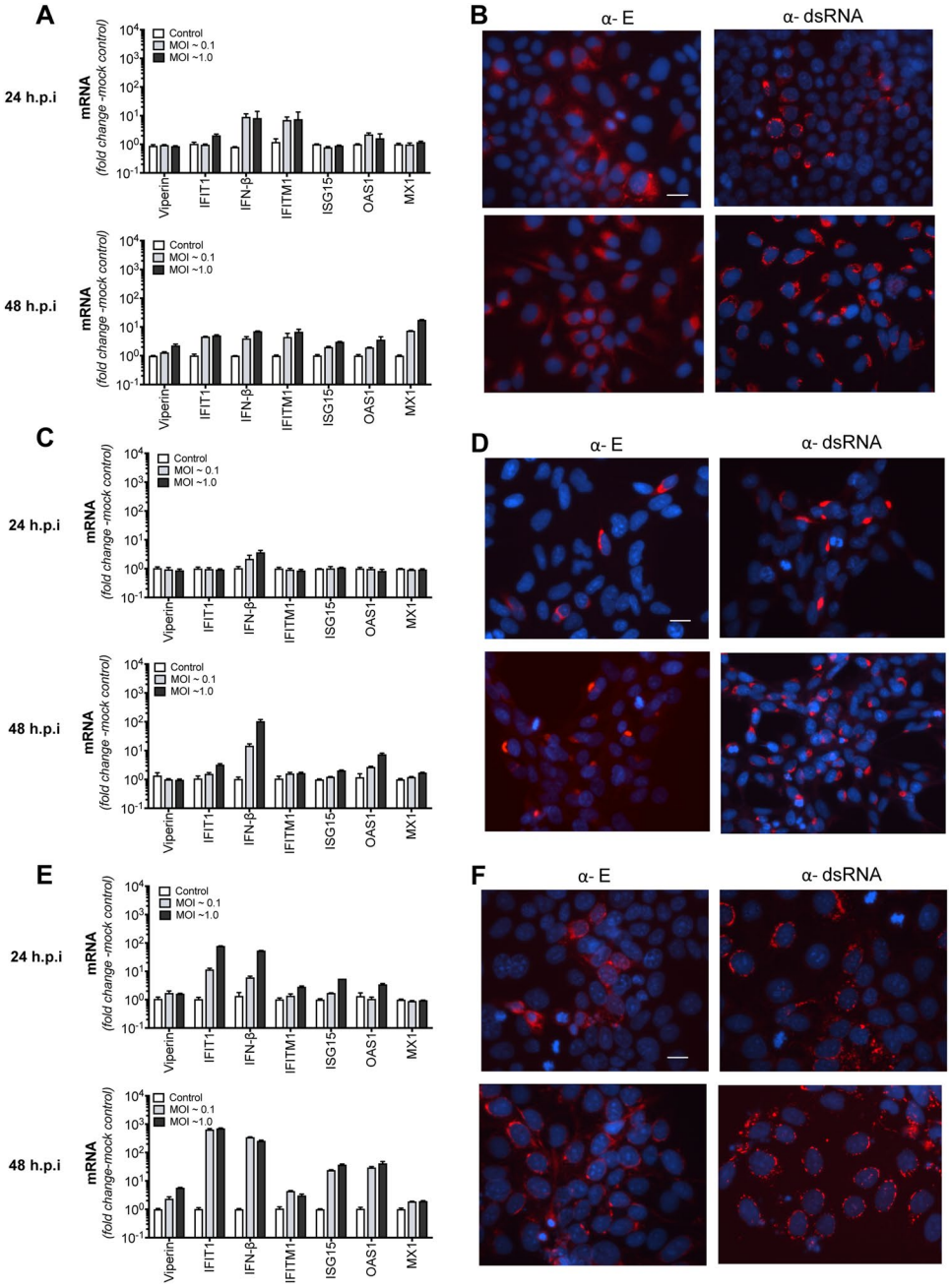

Figure 1. ZIKV infection results in an attenuated interferon-stimulated gene (ISG) response. (**A**,**C** and **E**) Huh-7, HTR8/SVNeo and Jeg3 cells, respectively were infected with ZIKV (MR766) at indicated multiplicity of infection (MOI). At 24 and 48 h.p.i total RNA was extracted and qRT-PCR was used to detect mRNA for IFN-β and the ISGs IFIT1, viperin, IFITM1, ISG15, OAS1 and Mx1. Data are normalised to the RPLPO housekeeping gene and expressed as a fold-change relative to mock-infected control (data are means + SD, n = 3). (**B**,**D** and **F**) Indirect immunofluorescence of corresponding ZIKV infection in Huh-7, HTR8/SVNeo and Jeg3 cells respectively. Cells were stained with the 4G2 antibody to detect ZIKV E antigen or 3G1 antibody to detect dsRNA (red) and DAPI DNA stain (blue). Scale bars represent 20 μm.

phosphorylation and nuclear translocation and collectively these results suggest that ZIKV can actively reduce RIG-I sensing of ZIKV RNA and downstream ISG expression.

ZIKV has been shown to infect both human and mouse neural progenitor cells (mNPCs) resulting in cell-cycle arrest and apoptosis thus providing a direct potential link between ZIKV infection and microcephaly[8,9,30,32]. We therefore investigated innate responses to ZIKV (MR766 strain) infection, in NPCs derived from mouse E14-18 cortices. To investigate which cells were infected by ZIKV, cultures were immunostained using Sox2 and Pax6 as markers of apical progenitor cells and radial glial cells respectively, GFAP to identify astrocytes, βIII-Tubulin to identify neurons and histone H3 to identify mitotic cells. ZIKV infection was noted as early as 12 h.p.i with a significant number of cells in the culture positive for ZIKV E antigen at 48 h.p.i (Fig. 3A). Consistent with previous

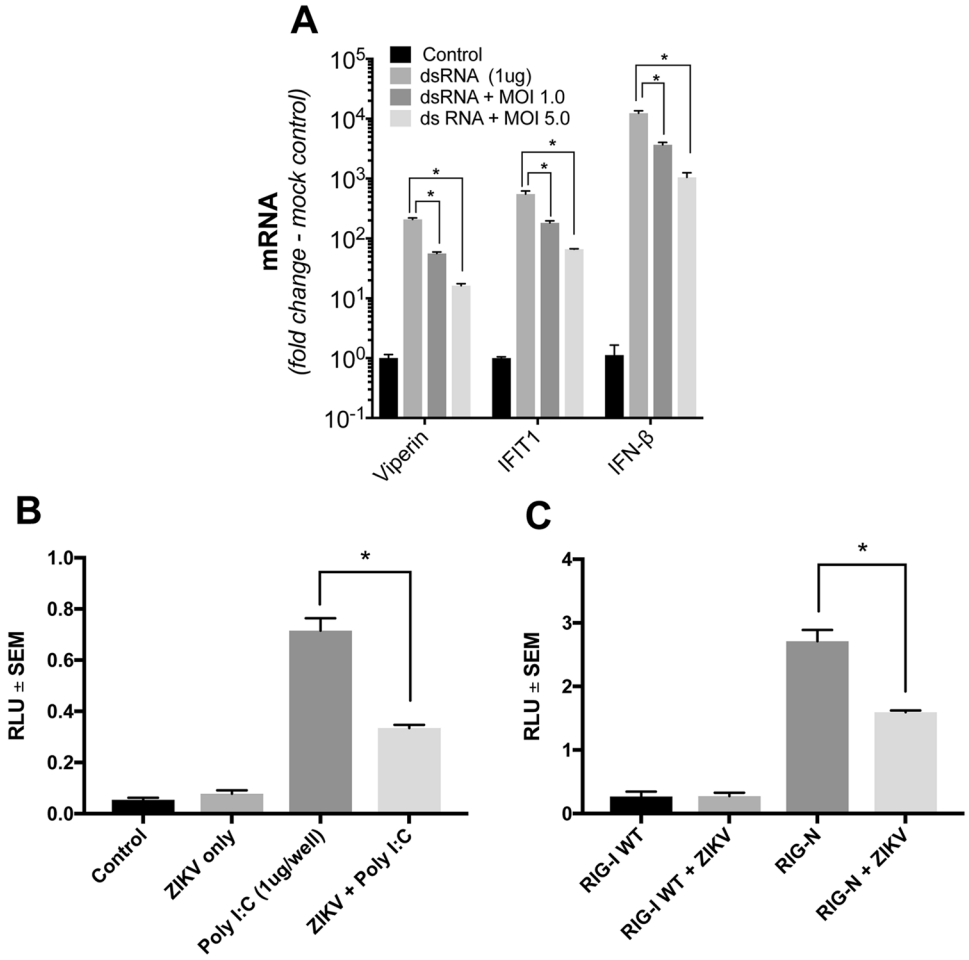

Figure 2. Poly I:C stimulated ISG expression and IFN-β promoter activity is attenuated in the presence of ZIKV infection. (**A**) Huh-7 cells were infected with ZIKV (MR766) at indicated MOIs and 16 h.p.i cells were transfected with polyI:C (1 μg). 24 hr later total RNA was extracted and qRT-PCR was used to detect mRNA for IFN-β and the ISGs IFIT1 and viperin. Data are normalised to the RPLPO housekeeping gene and expressed as a fold-change relative to mock-infected control (data are means + SD, n = 3, *P = 0.0003, Students t-test). (**B**) Huh-7 cells were transfected with a luciferase reporter plasmid driven by the IFN-β promoter followed by infection with ZIKV (MR766, MOI 5). 16 h.p.i cells were transfected with polyI:C and 24 hr post transfection cell lysates were harvested for luciferase assay. Data are normalised to transfection with TK-Renilla plasmid and expressed as a relative light units compared to mock-infected control (data are means + SEM, n = 3, *P = 0.003, Students t-test). (**C**) Huh-7 cells were transfected with either a plasmid expressing WT RIG-I or a constitutively active RIG-I (RIG-N), together with a luciferase reporter plasmid driven by the IFN-β promoter followed by infection with ZIKV (MR766, MOI 5). 24 h.p.i cell lysates were harvested for luciferase assay. Data are normalised to transfection with TK-Renilla plasmid and expressed as a relative light units compared to uninfected cells (data are means + SEM, n = 3, *P = 0.002, Students t-test).

reports *in vitro* and *in vivo*, ZIKV-infected cells were positive for Sox2, Pax6 and GFAP suggesting the potential for ZIKV to infect NPCs and, to a lesser extent, astrocytes in the developing brain (Fig. 3A)[9,30,33,34]. Next we investigated IFN-β and ISG expression at various time points post ZIKV infection. Consistent with our observations above there was a delayed and attenuated response to ZIKV infection with IFN-β and ISG responses not seen until 48 h.p.i (Fig. 3B). Given that this culture is a mixed population of cells, it is unclear at this stage if the ISG response is derived from ZIKV infected cells or from uninfected bystander cells that may be responding to low levels of IFN-β produced from infected cells. We also infected mNPC cultures with ZIKV strain PRVABC59 and observed similar innate immune responses to infection with MR766, suggesting that the innate response noted above is not strain dependent (Supplementary Fig. S3). Further experiments are required to determine the cell types responsible for ISG expression in NPC cultures. Nevertheless, these results suggest that primary neural progenitor cells also have a delayed innate response to ZIKV infection.

ZIKV infects and induces an antiviral response in monocyte-derived macrophages. ZIKV has been shown to infect human placental macrophages (Hofbauer cells [HCs])[5] and given that the closely related flavivirus, DENV targets primary monocyte-derived macrophages (MDM) *in vivo*, we also investigated if MDMs

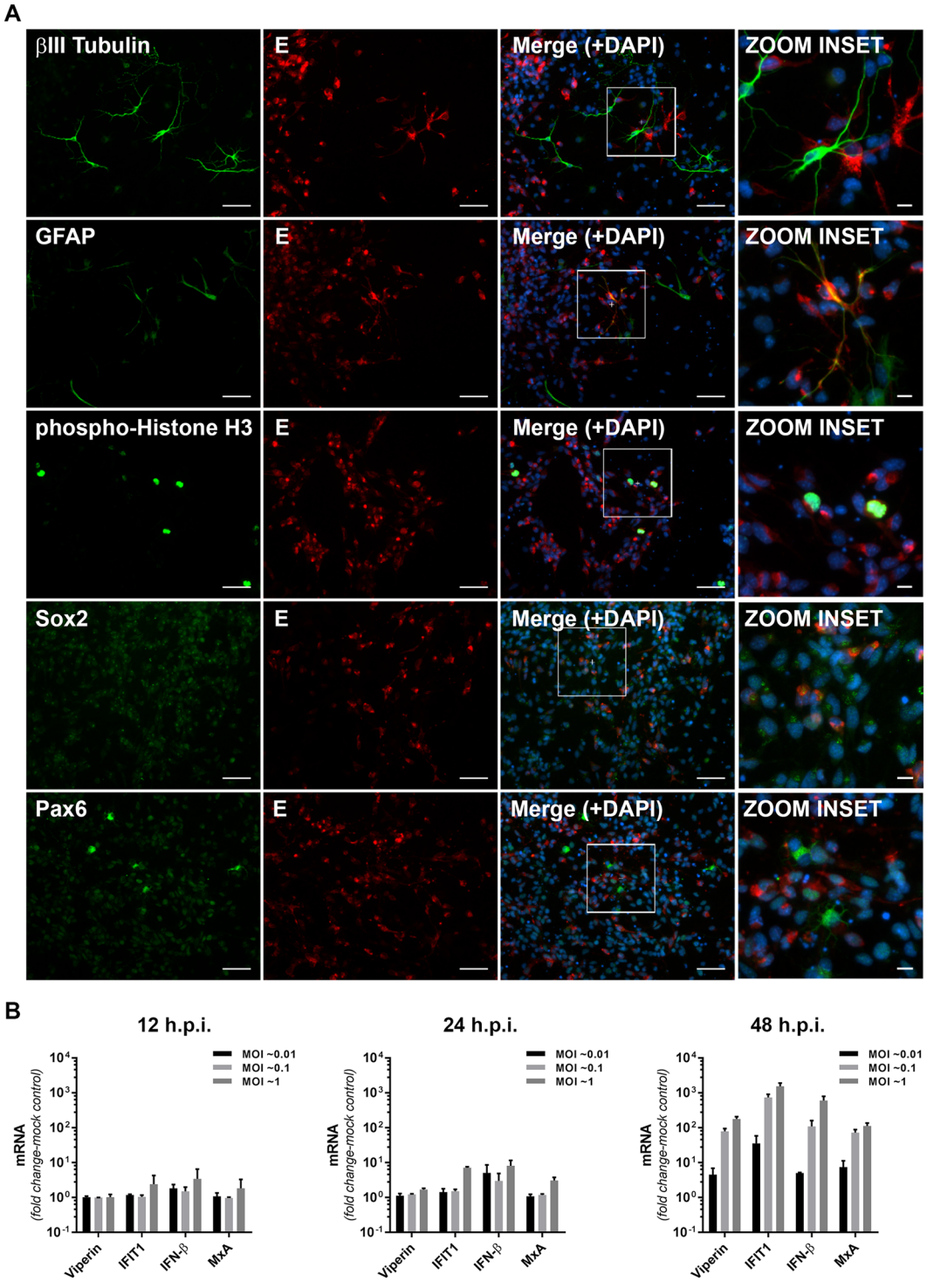

Figure 3. Mouse neural progenitor cells (NPCs) are susceptible to ZIKV infection and display delayed interferon-stimulated gene (ISG) expression responses. (**A**) Immunofluorescence analysis of ZIKV infection in neural cell subpopulations within NPC cultures. NPCs were infected with ZIKV (MR766, MOI: 0.1) for 48 h prior to fixation and staining of the ZIKV E protein (red) in combination with βIII tubulin (neurons), GFAP (astrocytes), phospho-Histone H3 (mitotic cells), Sox2 (apical progenitor cells) or Pax6 (radial glia) markers of neural cell sub-populations (green). Nuclei were counterstained with DAPI (blue). Scale bars are 100 μm for main images and 10 μm for 'zoom insets'. (**B**) Mouse neural progenitor cells were infected with ZIKV (MR766) at the indicated MOI before extraction of total cell RNA at 12–48 h.p.i and analysis of ISG expression by qRT-PCR. Data are normalised to the RPLPO housekeeping gene and expressed as a fold-change relative to mock-infected control (data are means + SD, n = 3).

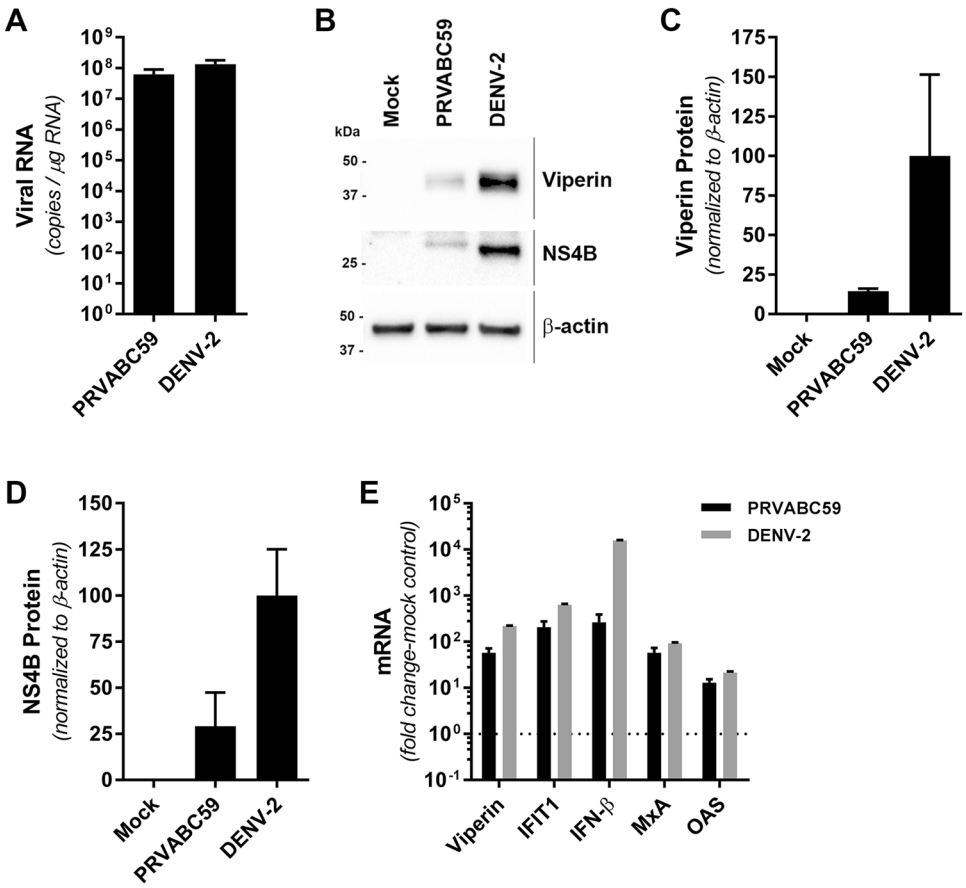

Figure 4. Human monocyte-derived macrophages are moderately susceptible and responsive to ZIKV infection. Human monocyte-derived macrophages were infected with ZIKV (PRVABC59) or DENV-2 (Mon601) for 48 h (MOI = 1) prior to analysis of viral replication and ISG expression by qRT-PCR and Western blotting in parallel. (**A**) ZIKV and DENV-2 RNA levels were determined by qRT-PCR using plasmid DNA standard curves. Data are expressed as viral RNA copy numbers per μg of total cell RNA (means + SD, n = 3). (**B**) Parallel cultures were subjected to immunoblotting analysis of viperin and NS4B expression, with β-actin serving as a loading control. (**C**,**D**) Quantitation of Viperin and NS4B protein levels, normalized to β-actin (means + SD, n = 3). (**E**) ISG mRNA levels were determined by qRT-PCR. Data are normalised to the RPLPO housekeeping gene and expressed as a fold-change relative to mock-infected controls (means + SD, n = 3).

were also permissive to ZIKV infection and the associated antiviral response. In this instance we used a low cell culture passaged ZIKV strain PRVABC59, isolated from the sera of an infected patient in Puerto Rico in 2015 that is closely related to the epidemic strains circulating in the Americas that have been linked to *in utero* ZIKV infection. We demonstrate that MDMs are permissive to productive ZIKV infection as determined by both qRT-PCR and immunoblot for detection of NS4B (Fig. 4A,B,C,D). We also evaluated the antiviral potential of MDMs infected with ZIKV. MDMs were infected with ZIKV (MOI 1.0) and 48 h.p.i mRNA for viperin, IFIT1, IFN-β, MxA and OAS were quantified (Fig. 4E). For comparison we also infected MDMs with DENV (MOI 1.0), given that these cells are a well-validated target cell *in vivo*. We observed increased expression of transcripts for viperin, IFIT1, IFN-β, MxA and OAS at 48 h.p.i for both ZIKV and DENV. However, transcript levels were significantly more elevated in DENV infection (Fig. 4E), although this may be a result of more efficient DENV replication as evident by qRT-PCR and immunoblot analysis (complete unprocessed immunoblots can be seen in Supplementary Fig. S4) of DENV RNA and NS4B expression respectively (Fig. 4A,B). Most notable was the significantly elevated expression of IFN-β in DENV, compared to ZIKV infected MDMs that may in turn drive higher viperin and IFIT1 mRNA and viperin protein expression. Collectively these results show that MDMs are susceptible to ZIKV infection and respond through activation of antiviral signaling pathways.

The antiviral ISG viperin modulates ZIKV replication. Our results above revealing attenuated viperin mRNA induction following ZIKV infection prompted us to investigate the antiviral nature of viperin against ZIKV. We and others have shown that viperin restricts replication of the related *flaviviridae* family members, HCV, DENV TBEV and WNV[24,25,27–29]. To investigate the antiviral potential of viperin against ZIKV we transfected a plasmid that drives viperin expression into Huh-7 cells and 16 hr post transfection cells were infected with ZIKV strain MR766 at an MOI of 0.1 and 1.0 and analysis of viral replication was assessed at 24 and 48 h.p.i. Consistent with previous observations with other flaviviruses, viperin restricted replication of ZIKV MR766. In Huh-7 cells expressing viperin, compared to control cells there was a significant decrease in the proportion of

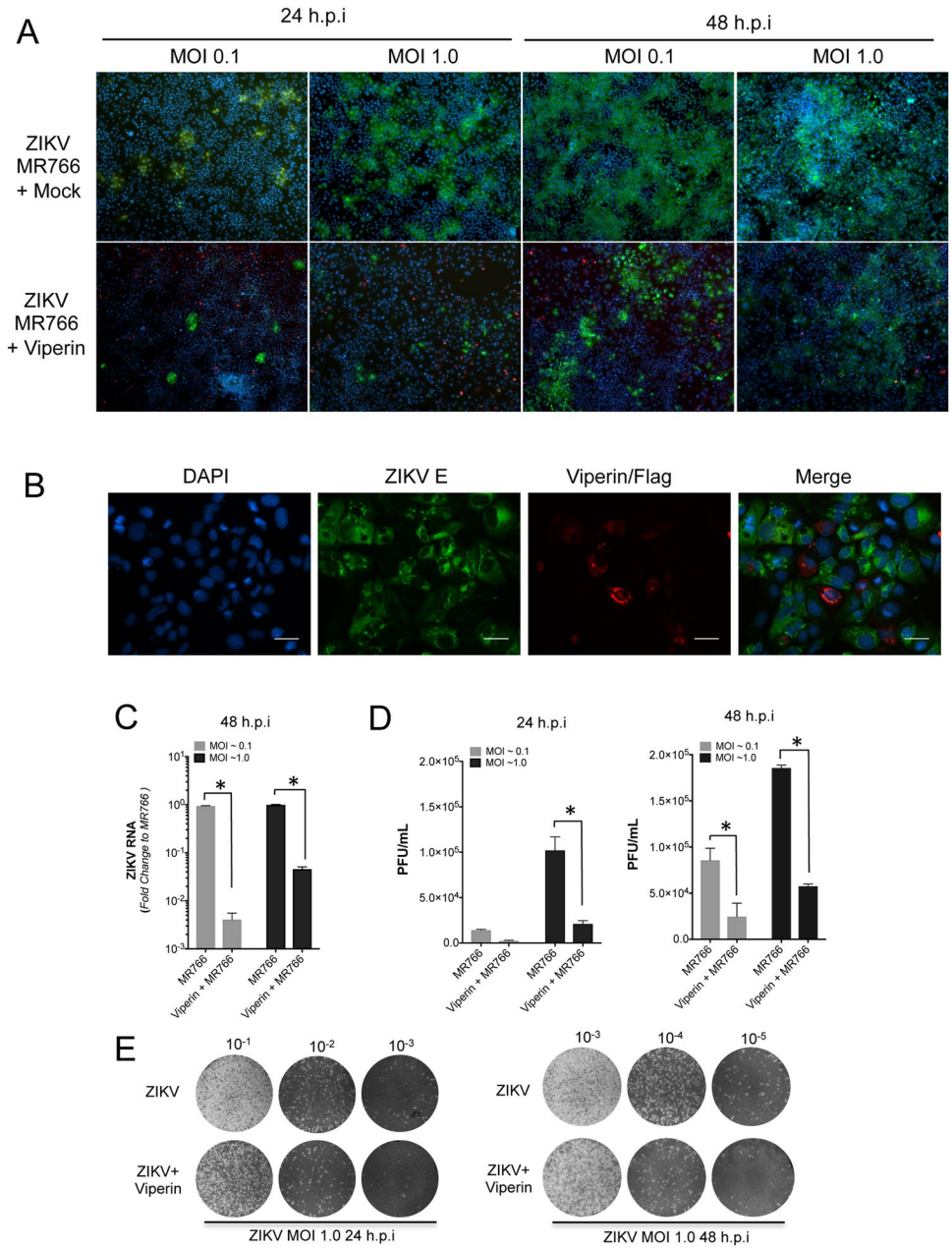

Figure 5. Viperin expression inhibits ZIKV infection in Huh7 cells. (**A**,**B**) Huh7 cells were mock transfected or transfected with a plasmid expressing viperin-FLAG. 16 hr post transfection, cells were infected with ZIKV (MR766) at the indicated MOI. Cells were fixed at the indicated time points and stained for ZIKV E antigen (green) in combination with viperin-FLAG (red). Nuclei were counterstained with DAPI (blue). Panel A 4x magnification. Scale bar on high-power images in (**B**) represents 50 μm. (**C**) RNA was extracted from ZIKV (MR766) infected Huh7 cells and ZIKV RNA levels analysed by qRT-PCR. Data is normalised to the RPLPO housekeeping gene and expressed as a fold-change relative to mock-infected controls (data are means + SD, n = 3, *p ≤ 0.0001, Two-Way Anova). (**D**,**E**) Supernatants from ZIKV (MR766) infected Huh7 cells were collected and plaque assay performed using Vero cells. Plaques were counted and averaged to deduce plaque forming units and subsequently ZIKV infectivity load. A representative plaque assay at 24 and 48 h.p.i is presented. (*p ≤ 0.03, Two-Way Anova).

ZIKV positive cells at both 24 and 48 h.p.i as determined by immunofluorescence microscopy to detect the ZIKV E protein (Fig. 5A). Even though approximately 30–40% of cells expressed viperin we could rarely detect cells positive for both viperin and ZIKV (Fig. 5B). Quantitative analysis of ZIKV RNA and release of infectious virus by qRT-PCR and plaque assay concurred with the microscopy analysis showing that compared to mock transfection, Huh-7 cells expressing viperin displayed a significant decrease in ZIKV RNA and production of infectious ZIKV 24 and 48 h.p.i. (Fig. 5C,D,E). Collectively these results indicate that the ISG viperin has significant antiviral activity against ZIKV.

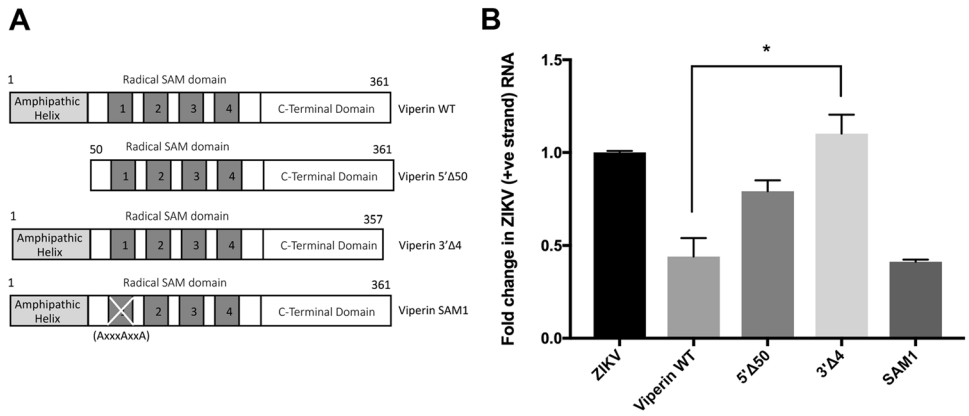

Figure 6. The C-terminal region of viperin is responsible for anti-ZIKV activity. (**A**) Schematic of Viperin WT and associated mutants used to transfect Huh-7 cells to assess the domains responsible for viperin's anti-ZIKV activity. (**B**) Huh-7 cells were transfected to express WT or viperin mutants and at 24 hr infected with ZIKV (MR766, MOI = 1). RNA was extracted and ZIKV RNA quantitated by qRT-PCR. Results were normalised against control RPLPO mRNA levels and expressed as fold change (data are means + SD, n = 3, *p ≤ 0.025, Students t-test).

Next we investigated the anti-viral potential of viperin against ZIKV using a panel of viperin mutants that have previously been used to investigate viperin's antiviral activity against the closely related flavivirus, DENV[24]. Huh-7 cells were transfected with the WT and mutant viperin constructs after which cells were infected with ZIKV and ZIKV RNA quantified by qRT-PCR (Fig. 6). Consistent with our previous results with DENV, the radical SAM domain mutant (SAM1) and the amino-terminal deletion mutant (5′Δ50) retain antiviral activity while the carboxy-terminal deletion mutant (3′Δ4) abolished viperin's anti-ZIKV activity (Fig. 6). These results highlight the importance of the carboxy-terminal domain of viperin for anti-viral activity against ZIKV.

CRISPR/Cas9-derived Viperin null MEFs result in increased ZIKV infection. Murine viperin has been shown to limit replication of a number of viruses *in vivo*[27,35]. To assess the impact of viperin deletion on ZIKV infection, we generated viperin null mice using CRISPR/Cas9 genome editing. Our approach used a gRNA to create indels in the ORF of exon I, thus generating frameshift null alleles. All 16-founder mice generated from CRISPR/Cas9 injection contained indels (mostly deletions) around the expected position within the *viperin* coding sequence as shown by Sanger sequencing, suggesting highly efficient editing of CRISPR/Cas9 system in our experiment. A 32 bp deletion derived from founder #67 and a 113 bp deletion derived from founder #72 were selected for further analysis (referred to hereafter as $Vip^{-/-}del32$ and $Vip^{-/-}del113$ *respectively*). In both lines of mutant mice, these deletions are predicted to generate a premature stop codon within the first viperin exon. Viperin immunoblot analysis of the isolated MEFs from both lines of mice following IFN-α stimulation revealed an absence of viperin expression (results not shown), indicating successful disruption of the *viperin* locus in the viperin KO lines.

Next we investigated the role of viperin in controlling ZIKV replication in $Vip^{-/-}del32$ mouse embryonic fibroblasts (MEFs) following ZIKV infection. Infection of WT and $Vip^{-/-}del32$ MEFs with either ZIKV strains MR766 or PRVABC59 revealed that at 48 h.p.i viperin expression was induced in the WT MEFs but not the $Vip^{-/-}del32$ MEFs indicating that the innate cellular response to ZIKV infection is activated and results in viperin expression (Fig. 7A). Moreover, in the $Vip^{-/-}del32$ MEFs there was a significant increase in ZIKV NS4B protein compared to WT MEFs suggesting that endogenous viperin can restrict ZIKV replication (complete unprocessed immunoblots can be seen in Supplementary Fig. S5). This was further confirmed by immunofluorescence analysis of infected cultures that revealed an increased proportion of ZIKV positive cells in $Vip^{-/-}del32$ MEFs compared to WT MEFs (Fig. 7B,D). Furthermore quantification of ZIKV RNA by qRT-PCR analysis from infected cultures of WT and $Vip^{-/-}del32$ MEFs revealed a significant increase in ZIKV RNA in the $Vip^{-/-}del32$ MEFs at 48 h.p.i. (Fig. 7C). It should be noted that this represents experiments using MEFs derived from $Vip^{-/-}del32$, however similar results were also obtained with the independent $Vip^{-/-}$ *del113* line. These results reveal that endogenously expressed viperin can limit ZIKV infection of MEFs and together with our transfection studies above indicate that viperin is a host innate restriction factor for ZIKV infection.

Discussion

The host innate response to viral infection is critical in controlling viral replication through the induction of a type I interferon response and ISG expression which serves to limit viral replication and accelerate the inflammatory process[36]. Recent studies using mice with a defect in the type I interferon signaling axis such as *Ifnar* or *Irf3/5/7* knockout mice develop neurological disease and increased viral replication in the brain, spinal cord and testes following ZIKV infection[7]. Moreover, *in utero* infection of *Ifnar* knock out mice early in pregnancy resulted in ZIKV infection of the placenta, and brain causing intrauterine growth restriction and spontaneous abortion[37]. Further evidence for the importance of the type-I response comes from recent work showing that like DENV, the NS5 protein of ZIKV abrogates IFN signaling through NS5 protein binding to STAT2 inducing its proteosomal

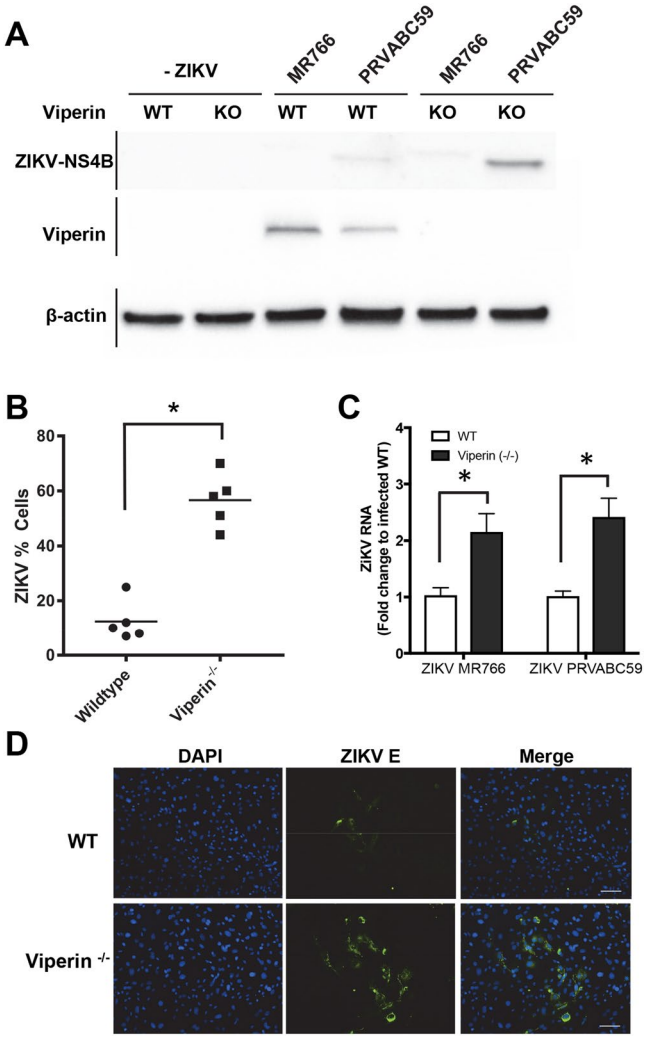

Figure 7. Viperin knockout mouse embryonic fibroblasts (MEF) are more susceptible to ZIKV infection. (**A**) MEFs derived from either WT or CRISPR/Cas9 viperin Ko (*Vip*$^{-/-}$*del32*) mice were infected with ZIKV (MR766 or PRVABC59 at MOI ~1) for 48 hours prior to immunoblot analysis of Viperin and ZIKV-NS4B expression, with β-actin serving as a loading control. (**B**) MEFs from WT and viperin KO (*Vip*$^{-/-}$*del32*) were infected with ZIKV (MR766) at an MOI of 1.0 and at 48 h.p.i the number of ZIKV positive cells (E antigen) was counted using Nikon ImageQuant software. (*$p \leq 0.0001$, Students t-test). (**C**) RNA was extracted from ZIKV (MR766) infected WT and *Vip*$^{-/-}$*del32* MEFs 48 h.p.i and ZIKV RNA levels analysed by qRT-PCR. Data is normalised to the RPLPO housekeeping gene and expressed as a fold-change relative to mock-infected control (data are means + SD, n = 3). (*$p \leq 0.02$, Two-Way Anova). (**D**) Indirect immunofluorescence of corresponding ZIKV infection of WT and *Vip*$^{-/-}$*del32* MEFs. Cells were stained with the 4G2 antibody to detect ZIKV E antigen (green) and DAPI DNA stain (blue). Scale bar represents 100 μm.

degradation[18,19]. These results highlight the importance of the type I interferon response in controlling ZIKV replication and pathogenesis, but the molecular mechanisms that underpin this restriction are not well understood. However, as for other viral infections, host control is most likely a combination of antiviral ISG expression, initiation and exacerbation of an inflammatory response and maturation of the adaptive antiviral response.

With this in mind we investigated the role that ZIKV infection has in induction of antiviral gene expression by measuring the induction of IFN-β and a panel of ISGs (viperin, IFIT1, IFITM1, ISG15, OAS and Mx1) at various time points following infection using physiologically relevant cell lines of placental and neurological origin. Consistent with other *flavivirus* infections we expected to see an early response to infection that is mediated independently of the synthesis of IFN-β. However, even at 24 h.p.i significant induction of IFN-β or ISGs in Huh-7 cells, HTR8/SVNeo (first trimester trophoblastic line) or murine neural progenitor cell cultures was not detected even though there was significant ZIKV replication. This attenuation of ISG expression seems to be an active process as polyI:C stimulation of ZIKV infected Huh-7 cells resulted in a significant reduction in ISG expression (Fig. 2A). Interestingly the JEG3 choriocarcinoma cell line, displayed a robust ISG response to infection suggesting that the ISG response may be determined by a combination of viral suppression of the innate response and cell intrinsic factors. While it has been reported that ZIKV can inhibit innate signaling post engagement of the

type I IFN receptor, as discussed above, the lack of an early response is likely indicative of interferon independent suppression[18,19]. IFN-β transcription is coordinately regulated by IRF3/7 and NF-κB and numerous ISGs such as IFIT1 and viperin can also be regulated independently of IFN by IRF3[38,39]. Accordingly, the lack of expression of IFN-β and ISGs suggests that ZIKV may impact innate immune signaling upstream of IFN signaling. This is not inconceivable as DENV NS2B/3 can block the kinase activity of IKKε and cleave human STING while NS2A and NS4B can inhibit the autophosphorylation of TBK1 thereby inhibiting IRF3 phosphorylation[40–42]. Moreover, it was recently reported that ZIKV can suppress reporter expression from the IFN-β, IRF3 and NF-κB promoters[19]. With this in mind we confirmed that ZIKV can suppress IFN-β promoter activity in response to polyI:C and expression of constitutively active RIG-I (RIG-N) indicating that the blockade occurs post engagement of RIG-I (Fig. 2B,C). Clearly more work is required to determine the molecular mechanisms that underpin ZIKV mediated suppression of the early innate immune response upstream of IFN signaling.

We also investigated ZIKV infection and its ability to induce IFN-β and ISGs in primary MDMs a defined target cell type for the related DENV. ZIKV has been previously shown to infect and replicate in primary human placental macrophages (HC: Hofbauer cells) resulting in production of IFN-α and associated cytokines and ISGs[5]. Similarily, in MDMs we demonstrate significant expression of IFN-β, IFIT1, viperin, MxA and OAS mRNA and viperin protein expression at 48 hpi. Interestingly, even though both DENV and ZIKV infection of MDMs resulted in a similar number of infected cells, as determined by qRT-PCR, DENV infection resulted in greater levels of DENV NS4B protein and significantly higher viperin expression, suggesting that DENV RNA may be a more potent inducer of the innate response or that ZIKV can suppress innate immune activation. However, this is complicated by the possibility that DENV infection of MDMs may be more efficient than that of ZIKV and further experiments are required to dissect this difference. Interestingly, it should be noted that the observed innate response is the result of a relatively small proportion of MDMs directly infected with ZIKV (and for DENV), an observation that was also reported in the infection of HC cells (0.6–6.3% infection rate) suggesting that ISG expression may be largely derived and amplified from uninfected bystander cells in response to type I IFN production that would contribute to making bystander cells refractory to infection.

Activation of the innate immune response following RNA viral infection results in the production of type I interferons and the production of hundreds of IGS. While antiviral properties have been assigned to a number of these ISGs, the role of many of these ISGs remain undefined[36]. Given the growing list of ISGs with antiviral action against RNA viruses, it is likely that multiple ISGs act in a coordinated response in an attempt to limit viral infection. As an example it has recently been reported that the IFITM family of ISGs can limit ZIKV as it also does for a number of other RNA viruses including HCV[43,44]. Interestingly, we noted during our investigations that the antiviral ISG viperin was only weakly induced following ZIKV infection of cells of placental and neural origin, and prompted us to investigate the antiviral potential of viperin against ZIKV. Viperin is strongly induced following a number of viral infections and has been shown by many laboratories including ours to be antiviral against HCV, DENV, WNV, TBEV, HIV, CHIV and HCMV (reviewed in ref. 23). We now show in this study that ZIKV can also be added to the list of viruses that can be restricted by viperin. Using a similar based approach to our previous studies in which we transiently expressed viperin and coupled with MEFs isolated from CRISPR/Cas9 derived viperin null mice we clearly demonstrate that viperin can limit ZIKV infection. Together these data clearly demonstrate that viperin is a potent host restriction factor of ZIKV replication.

The molecular mechanism(s) that underpins viperin-mediated viral restriction varies between viruses and even between viruses of the same family. Viperin restriction of HIV and influenza A seems to be mediated at the stage of viral egress in which viperin can disrupt lipid raft formation and membrane fluidity via dysregulation of cholesterol biosynthesis by inhibition of farnesyl diphosphate synthase a key enzyme in cholesterol and sterol biosynthesis[45,46]. In contrast restriction of HCV and DENV (both *Flaviviridae* family members) is at the level of viral RNA replication. Here, viperin demonstrates antiviral restriction against a HCV replicon and interacts with both HCV NS5A and with the cellular pro-viral host factor VAP-A that are both viral replication complex components essential to HCV replication[25,29]. Furthermore viperin co-localized and co-precipitated with dsRNA in DENV-2-infected cells and interacted with the DENV-2 NS3 (protease/helicase) protein, suggesting a possible interaction of viperin at sites of DENV-2 replication[24]. In addition, viperin can also restrict TBEV RNA replication and it would be logical to assume that common molecular mechanisms are at play. However this is not the case as restriction of TBEV is dependent on a radical S-adenosyl-L-methionine (SAM) domain within viperin while this domain is dispensable for DENV and HCV restriction[28]. Interestingly, the carboxy-terminus of viperin is important for restriction of DENV while for HCV restriction the carboxy-terminus and the amino-terminal amphipathic helix are important with the latter crucial for viperin's interaction with NS5A and VAP-A[24,25]. To this end we show using a panel of viperin mutants that the antiviral activity of viperin is similar to that of DENV in that the carboxy-terminus of viperin is essential while the amino–terminus and the SAM domain are dispensable. This is not surprising given the similarity between DENV and ZIKV and suggests that like DENV viperin interferes with ZIKV RNA replication and future studies are required to determine if viperin interacts with ZIKV replication complex proteins and/or essential pro-viral host factors. Understanding how viperin restricts ZIKV is not only important to our understanding of the innate host response to infection but also in our understanding of the ZIKV life cycle. Ultimately this knowledge may be used to develop therapeutic options to combat emerging viral infections.

Materials and Methods

Cells and Culture Conditions. All mammalian cell lines were maintained at 37 °C in a 5% CO_2 air atmosphere. The human hepatoma cell line Huh-7 was maintained as previously described[25]. The placental lines, HTR8/SVneo cells (from Professor Charles Graham, Queen's University, Kingston, Ontario) and JEG3 cells (purchased from ATCC) were maintained in RPMI-1640 media supplemented with 10% FBS, penicillin and streptomycin (P/S). Vero cells were cultured in DMEM supplemented with 10% FBS and P/S. Murine Embryonic Fibroblasts

(MEFs) were prepared from day 13.5–14.5 embryos. Isolated MEFs were maintained in DMEM supplemented with 10% FBS and P/S. Neural progenitor cells (NPCs) were isolated from E14-18 embryonic cortices and grown as neurospheres as previously described[47]. Cells were grown in the presence of growth factors Epidermal Growth Factor (rhEGF, 20 ng/ml; STEMCELL Technologies) and Fibroblast Growth Factor (bFGF2, 10 ng/ml; GIBCO). NPCs from dissociated neurospheres (at first or second passage) were plated onto poly-l-lysine coated coverslips and culture surfaces at a density of 50,000 cells/cm^2, and cultured overnight prior to infection with ZIKV, as indicated. C6/36 *Aedes albopictus* cells were maintained in Basal Medium Eagle (BME) supplemented with L-glutamine, MEM non-essential amino acids, sodium pyruvate, 10% FBS and P/S and cultured at 28 °C with 5% CO_2. Human monocyte-derived macrophages (MDM) were prepared by adherence of PBMC isolated from blood from healthy donors provided by the Australian Red Cross Blood Service and were cultured for 5 days in the presence of 7.5% (v/v) human serum, as described previously[48].

Viruses. The ZIKV strains MR766 (Uganda, 1947) and PRVABC59 (Puerto Rico, 2015) were propagated in C6/36 cells by infection at a multiplicity of infection (MOI) of 0.01 and supernatants harvested at 5–6 days post-infection. PRVABC59 is a contemporary strain that was isolated by CDC from the serum of a ZIKV infected patient who travelled to Puerto Rico in 2015. The complete genome sequence is published (Ref. Gene bank accession # KU501215). DENV infections utilised, Mon601, a derivative of the New Guinea C strain that was produced from *in vitro* transcribed RNA, transfected into BHK-21 baby hamster kidney cells, amplified in C6/36 insect cells and titered in Vero cells.

Plaque Assay. Virus infectivity was determined by plaque assay. Briefly, Vero cells in 6-well trays at approximately 90% confluency were infected with 800 µl of serially-diluted virus-containing supernatants for 1 hour at 37 °C. Supernatants were then replaced with a 2ml overlay of complete media containing 1.5% (w/v) carboxymethylcellulose (CMC) (Sigma) and cells returned to culture for 5–6 days. Cell monolayers were then fixed by addition of 2 ml of 10% formalin and incubation for 1 h. The CMC overlay was then removed and plaques were visualised via crystal violet stain. Plaques were counted and virus infectivity expressed as plaque-forming units (PFU) per ml.

Plasmids and transfections. The human viperin cDNA expression plasmid with an N-terminal FLAG tag in the pLenti6/V5-D-TOPO plasmid was previously described[24]. Transfection of plasmids and PolyI:C (Sigma) was performed using Lipofectamine 3000 (Thermo Fisher Scientific) according to the manufacturer's recommendations. Plasmids expressing a constitutively active RIG-I (RIG-N), the IFN-β promoter driving luciferase and viperin WT and mutant plasmids have been described elsewhere[24,49].

Real-time PCR. Extraction of total cellular RNA, first-strand cDNA synthesis and real-time qRT-PCR was performed as described previously[26]. All primer sequences used are outlined in Supplementary Table 1. Primer sequences for ZIKV RNA have been described previously[50]. Generation of a ZIKV RT-PCR standard curve used plasmids pFK-DVs (DENV-2, strain 16681)[51] and pZIKV-ICD (strain Paraiba_01/2015)[52].

Antibodies. Mouse anti-envelope glycoprotein 4G2 (D1-4G2-4-15) was prepared from hybridoma cells purchased from ATCC. Mouse anti-dsRNA 3G1 was a generous gift from Roy Hall (University of Queensland)[53]. Mouse anti-viperin (ab107359), rabbit anti-PAX6 (ab2237) and rabbit anti-phospho(S10) Histone H3 (ab5176) were obtained from Abcam. Rabbit anti-SOX2 (ab5603) was obtained from Merck Millipore. Rabbit anti-GFAP (G9269), rabbit anti-β-tubulin isotype III (T2200) and mouse anti-β-actin (AC15) was purchased from Sigma-Aldrich. Mouse anti-NS4B mAb 44-4-7 was generously provided by Qing Yin Wang (Novartis Institute for Tropical Diseases, Singapore). All secondary antibodies were purchased from Thermo Fisher Scientific.

Immunofluorescence Microscopy. Immunofluorescent labelling and wide-field fluorescence microscopy was performed essentially as described[54]. Briefly, cells growing in cell culture plates or on glass coverslips coated with poly-L-lysine (0.1% [w/v]) were washed with PBS, fixed with 4% paraformaldehyde in PBS for 15 min at room temperature and permeabilised with 0.1% Triton X-100 in PBS for 15 min at 4 °C. Alternatively, cells were fixed with ice-cold acetone:methanol (1:1) for 5 minutes at 4 °C. Samples were then blocked with 5% BSA in PBS for 30 min at room temperature and incubated with primary antibody diluted in PBS/1% BSA for 1 h at room temperature. After washing twice with PBS, cells were incubated with Alexa Fluor-conjugated secondary antibody diluted 1:200 in PBS/1%BSA for 1 h at 4 °C in the dark. Samples were then washed with PBS and incubated with DAPI (Sigma-Aldrich, 1 µg/ml) for 15 min at room temperature. Samples were then washed with PBS and, for cells grown on coverslips, mounted with Vectashield Antifade Mounting Medium (Vector Laboratories). Images were then acquired using a Nikon TiE inverted fluorescent microscope equipped with Plan Apochromat 60× NA 1.4 oil immersion, Super Plan Fluor 40× NA 0.4, Super Plan Fluor 20× NA 0.4 and Plan Fluor 10× NA 0.3 objectives (Nikon). Illumination was provide by an Intensilight C-HGFIE Precentered Fiber Illuminator mercury light source (Nikon), while BrightLine single-band filter sets (DAPI-5060C-NTE-ZERO, FITC-3540C-NTE-ZERO and TxRed-4040C-NTE-ZERO) were from Semrock and emitted light was collected with a monochrome 12-bit cooled charge-coupled device (CCD) camera with a maximum resolution of 1,280 × 1,024 (DS-Qi1; Nikon). Unless otherwise indicated images were processed using NIS Elements AR v.3.22. (Nikon) and Photoshop 6.0 (Adobe) software. In most instances contrast stretching was applied using the 'Autoscale' function of NIS Elements v.3.22.

Immunoblotting. Western blotting was performed essentially as described elsewhere[55]. Membrane bound protein was detected by chemiluminescence using SuperSignal West Femto (Pierce) and imaged using a ChemiDoc MP imaging system (Bio-Rad).

Generation of Viperin null mice. A CRISPR gRNA was designed to target exon 1 of murine Viperin (5′-agggtggctagatcccggga-3′) using CRISPR Design tool (crispr.mit.edu) and then generated according to the protocol as previously described[56]. gRNA IVT was performed using HiScribe™ T7 Quick High Yield RNA Synthesis Kit. Cas9 mRNA was generated by IVT using mMESSAGE mMACHINE® T7 ULTRA Transcription Kit (Ambion) from pCMV/T7-hCas9 (Toolgen) digested with *Xho*I. gRNAs and Cas9 mRNA were purified using MEGAclear™ Transcription Clean-Up Kit (Ambion). CRISPR gRNA (50ng/mL) and gRNA pairs (100 ng/mL each) were injected into C57BL/6N zygotes, transferred to psuedopregnant recipients and allowed to develop to term as previously described[57]. Founder pups were screened for exon deletion by PCR amplification across the targeted region (F-5′gtgtttgcctggaatataccagtcttgagtcct -3′, R-5′ - gacaatctgcaaggattgaatgcta -3′). PCR products from founders with deletions were Sanger sequenced to identify specific mutations. Routine genotyping was performed by PCR with the above primers spanning the target region and separated on 1% agarose gels. The University of Adelaide animal ethics committee approved generation and experiments involving viperin null mice.

Statistics. Data were graphed and analysed within the Prism 7 software (Graphpad Software Inc CA) using either T tests or Ordinary One or Two way Anova, all tests were corrected for multiple comparison using the Holm-Sidak method.

References

1. Lazear, H. M. & Diamond, M. S. Zika virus: new clinical syndromes and its emergence in the Western Hemisphere. *Journal of virology* **90**, 4864–4875 (2016).
2. Duffy, M. R. *et al*. Zika virus outbreak on Yap Island, Federated States of Micronesia. *N Engl J Med* **360**, 2536–2543, doi:10.1056/NEJMoa0805715 (2009).
3. Rasmussen, S. A., Jamieson, D. J., Honein, M. A. & Petersen, L. R. Zika Virus and Birth Defects–Reviewing the Evidence for Causality. *N Engl J Med* **374**, 1981–1987, doi:10.1056/NEJMsr1604338 (2016).
4. Driggers, R. W. *et al*. Zika virus infection with prolonged maternal viremia and fetal brain abnormalities. *New England Journal of Medicine* **374**, 2142–2151 (2016).
5. Quicke, K. M. *et al*. Zika Virus Infects Human Placental Macrophages. *Cell Host Microbe* **20**, 83–90, doi:10.1016/j.chom.2016.05.015 (2016).
6. Tabata, T. *et al*. Zika Virus Targets Different Primary Human Placental Cells, Suggesting Two Routes for Vertical Transmission. *Cell Host Microbe* **20**, 155–166, doi:10.1016/j.chom.2016.07.002 (2016).
7. Lazear, H. M. *et al*. A Mouse Model of Zika Virus Pathogenesis. *Cell Host Microbe* **19**, 720–730, doi:10.1016/j.chom.2016.03.010 (2016).
8. Li, C. *et al*. Zika Virus Disrupts Neural Progenitor Development and Leads to Microcephaly in Mice. *Cell Stem Cell* **19**, 672, doi:10.1016/j.stem.2016.10.017 (2016).
9. Li, H. *et al*. Zika Virus Infects Neural Progenitors in the Adult Mouse Brain and Alters Proliferation. *Cell Stem Cell* **19**, 593–598, doi:10.1016/j.stem.2016.08.005 (2016).
10. Miner, J. J. *et al*. Zika Virus Infection during Pregnancy in Mice Causes Placental Damage and Fetal Demise. *Cell* **165**, 1081–1091, doi:10.1016/j.cell.2016.05.008 (2016).
11. D'Ortenzio, E. *et al*. Evidence of Sexual Transmission of Zika Virus. *N Engl J Med* **374**, 2195–2198, doi:10.1056/NEJMc1604449 (2016).
12. Musso, D. *et al*. Potential sexual transmission of Zika virus. *Emerg Infect Dis* **21**, 359–361, doi:10.3201/eid2102.141363 (2015).
13. Tang, W. W. *et al*. A Mouse Model of Zika Virus Sexual Transmission and Vaginal Viral Replication. *Cell Reports* **17**, 3091–3098 (2016).
14. Wilkins, C. & Gale, M. Jr. Recognition of viruses by cytoplasmic sensors. *Curr Opin Immunol* **22**, 41–47, doi:10.1016/j.coi.2009.12.003 (2010).
15. Jensen, S. & Thomsen, A. R. Sensing of RNA viruses: a review of innate immune receptors involved in recognizing RNA virus invasion. *J Virol* **86**, 2900–2910, doi:10.1128/JVI.05738-11 (2012).
16. Beachboard, D. C. & Horner, S. M. Innate immune evasion strategies of DNA and RNA viruses. *Curr Opin Microbiol* **32**, 113–119, doi:10.1016/j.mib.2016.05.015 (2016).
17. Gack, M. U. & Diamond, M. S. Innate immune escape by Dengue and West Nile viruses. *Curr Opin Virol* **20**, 119–128, doi:10.1016/j.coviro.2016.09.013 (2016).
18. Grant, A. *et al*. Zika Virus Targets Human STAT2 to Inhibit Type I Interferon Signaling. *Cell Host Microbe* **19**, 882–890, doi:10.1016/j.chom.2016.05.009 (2016).
19. Kumar, A. *et al*. Zika virus inhibits type-I interferon production and downstream signaling. *EMBO Rep* **17**, 1766–1775, doi:10.15252/embr.201642627 (2016).
20. Aliota, M. T. *et al*. Characterization of Lethal Zika Virus Infection in AG129 Mice. *PLoS Negl Trop Dis* **10**, e0004682, doi:10.1371/journal.pntd.0004682 (2016).
21. Lazear, H. M. *et al*. A mouse model of Zika virus pathogenesis. *Cell host & microbe* **19**, 720–730 (2016).
22. Yockey, L. J. *et al*. Vaginal Exposure to Zika Virus during Pregnancy Leads to Fetal Brain Infection. *Cell* **166**, 1247–1256 e1244, doi:10.1016/j.cell.2016.08.004 (2016).
23. Helbig, K. J. & Beard, M. R. The role of viperin in the innate antiviral response. *J Mol Biol* **426**, 1210–1219, doi:10.1016/j.jmb.2013.10.019 (2014).
24. Helbig, K. J. *et al*. Viperin is induced following dengue virus type-2 (DENV-2) infection and has anti-viral actions requiring the C-terminal end of viperin. *PLoS Negl Trop Dis* **7**, e2178, doi:10.1371/journal.pntd.0002178 (2013).
25. Helbig, K. J. *et al*. The antiviral protein viperin inhibits hepatitis C virus replication via interaction with nonstructural protein 5A. *Hepatology* **54**, 1506–1517, doi:10.1002/hep.24542 (2011).
26. Helbig, K. J., Lau, D. T., Semendric, L., Harley, H. A. & Beard, M. R. Analysis of ISG expression in chronic hepatitis C identifies viperin as a potential antiviral effector. *Hepatology* **42**, 702–710, doi:10.1002/hep.20844 (2005).
27. Szretter, K. J. *et al*. The interferon-inducible gene viperin restricts West Nile virus pathogenesis. *J Virol* **85**, 11557–11566, doi:10.1128/JVI.05519-11 (2011).
28. Upadhyay, A. S. *et al*. Viperin is an iron-sulfur protein that inhibits genome synthesis of tick-borne encephalitis virus via radical SAM domain activity. *Cell Microbiol* **16**, 834–848, doi:10.1111/cmi.12241 (2014).
29. Wang, S. *et al*. Viperin inhibits hepatitis C virus replication by interfering with binding of NS5A to host protein hVAP-33. *J Gen Virol* **93**, 83–92, doi:10.1099/vir.0.033860-0 (2012).
30. Hanners, N. W. *et al*. Western Zika Virus in Human Fetal Neural Progenitors Persists Long Term with Partial Cytopathic and Limited Immunogenic Effects. *Cell Rep* **15**, 2315–2322, doi:10.1016/j.celrep.2016.05.075 (2016).

31. Graham, C. H. *et al*. Establishment and characterization of first trimester human trophoblast cells with extended lifespan. *Exp Cell Res* **206**, 204–211 (1993).
32. Garcez, P. P. *et al*. Zika virus impairs growth in human neurospheres and brain organoids. *Science* **352**, 816–818, doi:10.1126/science.aaf6116 (2016).
33. Li, C. *et al*. Zika virus disrupts neural progenitor development and leads to microcephaly in mice. *Cell stem cell* (2016).
34. Tang, H. *et al*. Zika Virus Infects Human Cortical Neural Progenitors and Attenuates Their Growth. *Cell Stem Cell* **18**, 587–590, doi:10.1016/j.stem.2016.02.016 (2016).
35. Teng, T. S. *et al*. Viperin restricts chikungunya virus replication and pathology. *J Clin Invest* **122**, 4447–4460, doi:10.1172/JCI63120 (2012).
36. Schneider, W. M., Chevillotte, M. D. & Rice, C. M. Interferon-stimulated genes: a complex web of host defenses. *Annu Rev Immunol* **32**, 513–545, doi:10.1146/annurev-immunol-032713-120231 (2014).
37. Miner, J. J. *et al*. Zika virus infection during pregnancy in mice causes placental damage and fetal demise. *Cell* **165**, 1081–1091 (2016).
38. Grandvaux, N. *et al*. Transcriptional profiling of interferon regulatory factor 3 target genes: direct involvement in the regulation of interferon-stimulated genes. *J Virol* **76**, 5532–5539 (2002).
39. Wathelet, M. G. *et al*. Virus infection induces the assembly of coordinately activated transcription factors on the IFN-beta enhancer *in vivo*. *Mol Cell* **1**, 507–518 (1998).
40. Aguirre, S. *et al*. DENV inhibits type I IFN production in infected cells by cleaving human STING. *PLoS Pathog* **8**, e1002934, doi:10.1371/journal.ppat.1002934 (2012).
41. Anglero-Rodriguez, Y. I., Pantoja, P. & Sariol, C. A. Dengue virus subverts the interferon induction pathway via NS2B/3 protease-IkappaB kinase epsilon interaction. *Clin Vaccine Immunol* **21**, 29–38, doi:10.1128/CVI.00500-13 (2014).
42. Dalrymple, N. A., Cimica, V. & Mackow, E. R. Dengue Virus NS Proteins Inhibit RIG-I/MAVS Signaling by Blocking TBK1/IRF3 Phosphorylation: Dengue Virus Serotype 1 NS4A Is a Unique Interferon-Regulating Virulence Determinant. *MBio* **6**, e00553–00515, doi:10.1128/mBio.00553-15 (2015).
43. Narayana, S. K. *et al*. The Interferon-induced Transmembrane Proteins, IFITM1, IFITM2, and IFITM3 Inhibit Hepatitis C Virus Entry. *J Biol Chem* **290**, 25946–25959, doi:10.1074/jbc.M115.657346 (2015).
44. Savidis, G. *et al*. The IFITMs Inhibit Zika Virus Replication. *Cell Rep* **15**, 2323–2330, doi:10.1016/j.celrep.2016.05.074 (2016).
45. Nasr, N. *et al*. HIV-1 infection of human macrophages directly induces viperin which inhibits viral production. *Blood* **120**, 778–788, doi:10.1182/blood-2012-01-407395 (2012).
46. Wang, X., Hinson, E. R. & Cresswell, P. The interferon-inducible protein viperin inhibits influenza virus release by perturbing lipid rafts. *Cell Host Microbe* **2**, 96–105, doi:10.1016/j.chom.2007.06.009 (2007).
47. Jolly, L. A., Homan, C. C., Jacob, R., Barry, S. & Gecz, J. The UPF3B gene, implicated in intellectual disability, autism, ADHD and childhood onset schizophrenia regulates neural progenitor cell behaviour and neuronal outgrowth. *Hum Mol Genet* **22**, 4673–4687, doi:10.1093/hmg/ddt315 (2013).
48. Wati, S., Li, P., Burrell, C. J. & Carr, J. M. Dengue virus (DV) replication in monocyte-derived macrophages is not affected by tumor necrosis factor alpha (TNF-alpha), and DV infection induces altered responsiveness to TNF-alpha stimulation. *J Virol* **81**, 10161–10171, doi:10.1128/JVI.00313-07 (2007).
49. Helbig, K. J. *et al*. Differential expression of the CXCR3 ligands in chronic hepatitis C virus (HCV) infection and their modulation by HCV *in vitro*. *J Virol* **83**, 836–846, doi:10.1128/JVI.01388-08 (2009).
50. Waggoner, J. J. *et al*. Single-Reaction Multiplex Reverse Transcription PCR for Detection of Zika, Chikungunya, and Dengue Viruses. *Emerging infectious diseases* **22**, 1295–1297, doi:10.3201/eid2207.160326 (2016).
51. Fischl, W. & Bartenschlager, R. High-throughput screening using dengue virus reporter genomes. *Methods Mol Biol* **1030**, 205–219, doi:10.1007/978-1-62703-484-5_17 (2013).
52. Tsetsarkin, K. A. *et al*. A Full-Length Infectious cDNA Clone of Zika Virus from the 2015 Epidemic in Brazil as a Genetic Platform for Studies of Virus-Host Interactions and Vaccine Development. *MBio* **7**, doi:10.1128/mBio.01114-16 (2016).
53. O'Brien, C. A. *et al*. Viral RNA intermediates as targets for detection and discovery of novel and emerging mosquito-borne viruses. *PLoS neglected tropical diseases* **9**, e0003629 (2015).
54. Eyre, N. S. *et al*. Phosphorylation of NS5A Serine-235 is essential to hepatitis C virus RNA replication and normal replication compartment formation. *Virology* **491**, 27–44, doi:10.1016/j.virol.2016.01.018 (2016)
55. Eyre, N. S., Drummer, H. E. & Beard, M. R. The SR-BI partner PDZK1 facilitates hepatitis C virus entry. *PLoS Pathog* **6**, e1001130, doi:10.1371/journal.ppat.1001130 (2010).
56. Cong, L. *et al*. Multiplex genome engineering using CRISPR/Cas systems. *Science* **339**, 819–823, doi:10.1126/science.1231143 (2013).
57. Yang, H. *et al*. One-step generation of mice carrying reporter and conditional alleles by CRISPR/Cas-mediated genome engineering. *Cell* **154**, 1370–1379, doi:10.1016/j.cell.2013.08.022 (2013).

Acknowledgements

We would like to thank Sandy Piltz, Catherine Scougall and Ying Sun for technical assistance with generation of CRISPR/Cas9 viperin null mice, MEFS and neural progenitor cells respectively. This work was supported by grants from the NHMRC (APP1053206) of Australia and the Robinson Research Institute Innovation Seed Funding Program at The University of Adelaide.

Author Contributions

K.H.V., N.S.E. and B.S. conducted the experiments and analysed the results. O.K., K.G. and M.J.G. conducted experiments. L.A.J., T.J.-K. and C.T.R. provided mouse neural progenitior and placental cell cultures. J.M.C conducted MDM experiments. P.T., F.A. and K.J.H. generated viperin null mice. M.R.B. conceived the study, performed experiments, analysed results and wrote the manuscript.

Additional Information

Supplementary information accompanies this paper at doi:10.1038/s41598-017-04138-1

Competing Interests: The authors declare that they have no competing interests.

Statement of Authorship

Title of Paper	Viperin is an important host restriction factor in control of Zika virus infection
Publication Status	☑ Published ☐ Accepted for Publication ☐ Submitted for Publication ☐ Unpublished and Unsubmitted work written in manuscript style
Publication Details	Zika virus (ZIKV) infection has emerged as a global health threat and infection of pregnant women causes intrauterine growth restriction, spontaneous abortion and microcephaly in newborns. Here we show using biologically relevant cells of neural and placental origin that following ZIKV infection, there is attenuation of the cellular innate response characterised by reduced expression of IFN-β and associated interferon stimulated genes (ISGs). One such ISG is viperin that has well documented antiviral activity against a wide range of viruses. Expression of viperin in cultured cells resulted in significant impairment of ZIKV replication, while MEFs derived from CRISPR/Cas9 derived viperin$^{-/-}$ mice replicated ZIKV to higher titers compared to their WT counterparts. These results suggest that ZIKV can attenuate ISG expression to avoid the cellular antiviral innate response, thus allowing the virus to replicate unchecked. Moreover, we have identified that the ISG viperin has significant anti-ZIKV activity. Further understanding of how ZIKV perturbs the ISG response and the molecular mechanisms utilised by viperin to suppress ZIKV replication will aid in our understanding of ZIKV biology, pathogenesis and possible design of novel antiviral strategies.

Principal Author

Name of Principal Author (Candidate)	Byron Shue		
Contribution to the Paper	Intellectual input Experimental design Sample processing and performed experiments (Fig. 2,5,6&7) Assist in writing manuscript and drafting		
Overall percentage (%)	50%		
Certification:	This paper reports on original research I conducted during the period of my Higher Degree by Research candidature and is not subject to any obligations or contractual agreements with a third party that would constrain its inclusion in this thesis. I contributed equally to this work as a primary author with KVDH and NSE on this paper.		
Signature		Date	04/12/20

Co-Author Contributions

By signing the Statement of Authorship, each author certifies that:

i. the candidate's stated contribution to the publication is accurate (as detailed above);

ii. permission is granted for the candidate in include the publication in the thesis; and

iii. the sum of all co-author contributions is equal to 100% less the candidate's stated contribution.

Name of Co-Author	Kylie H. Van der Hoek
Contribution to the Paper	Intellectual input Experimental design Sample processing and performed experiments Assist in writing manuscript and drafting

Signature		Date	9/12/2020

Name of Co-Author	Nicholas S. Eyre		
Contribution to the Paper	Intellectual input Experimental design Sample processing and performed experiments Assist in writing manuscript and drafting		
Signature		Date	9/12/2020

Name of Co-Author	Onruedee Khantisithiporn		
Contribution to the Paper	Provided viperin expression plasmids		
Signature		Date	11/12/2020
Name of Co-Author	Kitirat Glab-Ampi		
Contribution to the Paper	Provided experimental support		
Signature		Date	4/12/2020
Name of Co-Author	Jillian M. Carr		
Contribution to the Paper	Providing monocyte-derived macrophages and associated experiments		
Signature		Date	15/12/2020
Name of Co-Author	Matthew J. Gartner		
Contribution to the Paper	Sample processing and performed experiments		
Signature		Date	07.12.2020
Name of Co-Author	Lachlan A. Jolly		
Contribution to the Paper	Provided mouse neural progenitor cell lines		
Signature		Date	15/12/2020
Name of Co-Author	Paul Q. Thomas		

Contribution to the Paper	Generated Viperin CRISPR knockout mice		
Signature		Date	10/12/2020
Name of Co-Author	Fatwa Adikusuma		
Contribution to the Paper	Generated Viperin CRISPR knockout mice		
Signature		Date	10/12/2020
Name of Co-Author	Tanja Jankovic-Karasoulos		
Contribution to the Paper	Provided HTR8/JEG3 cell lines		
Signature		Date	14/12/2020
Name of Co-Author	Claire T. Roberts		
Contribution to the Paper	Provided HTR8/JEG3 cell lines		
Signature		Date	14/12/2020.
Name of Co-Author	Karla J. Helbig		
Contribution to the Paper	Intellectual input Helped generate Viperin CRISPR knockout mice and viperin reagents		
Signature		Date	9/12/2020
Name of Co-Author	Michael R. Beard		
Contribution to the Paper	Conceptualised study Intellectual input including data analysis Writing and drafting manuscript		
Signature		Date	4/12/20.

Chapter 6 - Final Discussion

Viruses within the *Flaviviridae* family are a major contributor of morbidity and mortality worldwide and inflict significant burden on healthcare systems. Effective vaccines are currently not available for the majority of viruses within this family including HCV, DENV and ZIKV. Furthermore, there are many facets of flavivirus biology that remain to be characterised. Therefore, in order to expedite vaccine development, further research is required to gain a better understanding of the virus lifecycle and the complex interplay between the host cell and infecting virus as a major regulator of the virus lifecycle. Proviral host factors are essential in supporting all facets of the virus lifecycle. Conversely, antiviral host factors induced upon viral recognition are able to potently subvert virus replication prior to the activation of adaptive immunity. The main objectives of this thesis were to not only uncover novel host factors required for both HCV and ZIKV replication but also to gain further understanding of the innate immune response in restricting ZIKV replication.

6.1 CRISPR Genome-wide KO Screens

At the commencement of this project, a number of proviral host factors had been identified utilising RNAi technology, however this technology is beset with multiple limitations stemming from poor and unpredictable knockdown efficiency ultimately resulting in false positives (see section 1.91). The discovery and adaption of the CRISPR/Cas9 system for molecular editing has revolutionised gene editing technology with its simplicity, enabling screening for host factors following virus infection at the whole genome level (Puschnik et al. 2017a). Despite the identification and characterisation of a number of host factors important for HCV replication prior to the introduction of CRISPR, we decided to utilise HCV in our studies, firstly as a proof of concept for use in CRISPR genome-wide screens, and secondly to further research into HCV replication cycle and molecular virology. In addition, the relative low priority of an HCV vaccine (from a pharmaceutical perspective) due to the high efficacy of DAAs, has transitioned research in HCV in the past five years from basic molecular studies to predominantly clinical investigations. Thus, many host factors required for HCV replication remain uncharacterised. We also chose to investigate ZIKV using genome-wide CRISPR screens given the explosive number of infections that emerged

in South America and the lack of understanding of the ZIKV lifecycle compared to other flaviviruses at the time (WHO).

CRISPR/Cas9 technology and especially genome-wide KO screens was in its infancy when this project was conceived in 2015, where it enabled targeted genetic manipulation in a simplistic manner, relative to other nucleases, including zinc finger proteins and TALENs [reviewed extensively in (Gaj et al. 2013)]. Its efficiency in knockout of host factors in the context of the viral lifecycle was relatively unknown. Therefore, we performed proof of concept experiments to evaluate the efficiency of CRISPR (and specifically the LentiCRISPRv2 system which forms the backbone of our chosen library) knockout of host factors against HCV infection. In short, we were able to efficiently knockout CD81 expression in Huh7.5 cells that resulted in cells which were no longer permissive to HCV infection (Fig. 3.6 - 3.10). These experiments gave us the confidence that efficient knockout could be achieved in Huh7.5 cells using the LentiCRISPRv2 system and provided scientific evidence for us to move onto genome-wide CRISPR screening.

When designing a genome-wide screen using either RNAi or CRISPR technology to identify novel host factors, a crucial aspect that needs to be carefully considered is the establishment of a clear phenotypic endpoint to allow separation of cells which are resistant to infection. Virus-based systems that generate high titres of virus, ultimately leading to CPE are the simplest to work with. Flaviviruses including DENV and ZIKV fit these criteria, where cells which remain permissive to infection after the introduction of genome-wide siRNA/CRISPR libraries undergo rapid viral induced CPE and allow separation of surviving cells that have knockdown/knockout of a proviral host factor. This enabled us to identify RACK1 in addition to other host factors critical for ZIKV infection within our genome-wide CRISPR screen and will be discussed further.

However, for viruses like HCV that don't propagate to high titres *in vitro,* producing the extreme quantity of virus and associated cytopathic effect is both problematic and untenable in the context of genome-wide CRISPR screens as outlined above. Despite these limitations, a genome-wide CRISPR screen has been reported with infectious HCV, resulting in the identification of multiple host factors required for virus entry (CD81, CLDN1 and OCLN) and replication (miR-122) phases of the viral lifecycle

(Marceau et al. 2016). In this genome-wide screen using the GeCKO LentiGuide library, Huh7.5.1 cells were infected with HCV JFH-1 at a MOI of 0.3 and CPE was visible after 5 days. This observation is intriguing in that we and others do not encounter mass HCV induced CPE. The differences in our experience compared to that of Marceau *et al.* is not immediately apparent, but may be due to differences in both the Huh7.5 cells used and experimental design. It is possible that Huh7 cells from one laboratory can support not only higher levels of HCV replication but also viral induced CPE (Sainz et al. 2009). We could have chosen to import the Huh7.5 cell line used by Marceau *et al.* to perform our genome-wide CRISPR screen, however we decided to utilise the SGR system to not only ensure homogenous HCV replication within our entire cell population but also specifically target the replication phase of the lifecycle which may help identify elusive novel host factors which may be obscured by more dominant host factors (such as entry receptors) in an infectious virus based system (Marceau et al. 2016).

The HCV SGR model does not induce CPE as a phenotypic endpoint for our genome-wide CRISPR screen and thus we needed to incorporate suitable reporter proteins to enable separation of HCV resistant cells due to knockout of a proviral host factor. Renilla luciferase has been used as a reporter protein for a HCV genome-wide siRNA screen (Tai et al. 2009). However, this experimental setup is not amendable for the genome-wide CRISPR screens used in this thesis. We therefore employed the reporter proteins mCherry, GFP or thymidine kinase, which their expression is directly coupled to active viral replication, to allow screening within a pooled setting. However, a key factor that we encountered during screening which ultimately made use of the HCV SGR for genome-wide CRISPR screens untenable, was that prior to commencement of our genome-wide CRISPR screen with either mCherry, GFP or thymidine kinase reporter proteins, required the removal of the eukaryotic selection reagent BSD from the culture medium. The BSD resistance gene expressed by the HCV SGR provides positive selection to establish and retain HCV replication, and while Huh7.5 cells can retain the HCV-SGR in the absence of selection within the culture media, the combination of lentivirus transduction of the GeCKO LentiCRISPRv2 library with the duration needed to complete the screen resulted in complete loss of HCV replication and thymidine kinase protein expression (Fig. 3.20 & 3.21). This was not an issue with the previous genome-wide siRNA HCV-SGR

screens since the screen was terminated 72 hours post transfection (Tai et al. 2009). Moreover, most genome-wide CRISPR screens to date have been performed where gene knockout is initiated prior to virus infection, collectively suggesting the possibility that introduction of CRISPR/Cas9 or lentiviral transduction may indirectly interfere with HCV replication (McDougall et al. 2018). Thus, in future experiments, a modified screening protocol would have to be adapted, where a reporter system such as NIrD would have to utilised to counteract the absence of HCV induced CPE within our Huh7.5 cells (Fig. 3.22).

The problems encountered with using the HCV SGR system and genome-wide CRISPR screening meant that we needed to refocus our efforts and we decided to investigate host factors important for the ZIKV lifecycle. During the course of this thesis, a number of similar screens have been undertaken. However, the ability of ZIKV to infect multiple cell types may indicate diverse exploitation of proviral host factors. Thus, multiple genome-wide CRISPR screens using different cell types may be useful to further our understanding of the viral-host interactome. Another factor to be considered in genome-wide CRISPR screens is the use of either immortalised or primary cells, as key genes involved in the viral lifecycle may differ between the two. To illustrate this point, a CRISPR screen for ZIKV host factors in human pluripotent derived neural progenitors (hNPC) identified top hits present in not only previously published CRISPR screens with flaviviruses but also ours (Li et al. 2019). These hits include proteins within the EMC complex (EMC1, EMC6, MMTG1), indicating that these host factors are commonly exploited during flavivirus replication, and thus could be targeted as a potential antiviral to combat infection within multiple cell types. Furthermore, the hNPC screen with ZIKV also identified additional pathways including heparan sulfation, active suppression of IFN activity, and the endosome lysosome pathway. The absence of these additional host factors in previous CRISPR screens performed in immortalised cells suggest that primary cells may respond and modulate virus infection somewhat differently to immortalised cells. Thus, in future experiments, it may be useful to perform genome-wide CRISPR screens on HCV infection with primary hepatocytes to identify elusive host factors which may not be expressed within immortalised Huh7.5 cells. However, the use of primary cells in a pooled genome-wide screening setting remains challenging due to a number of factors which include, (i) the high quantity of cells required coupled with limited life spans to enable completion of

a screen and, (ii) poor lentiviral transduction efficiency in primary cells to maintain library complexity and (iii) ensuring Cas9 expression is present to induce DSBs and subsequently knockout of target genes during screening. In addition, challenges of utilising primary cells for HCV include variable permissibility in stem cell-derived hepatocytes and further research is required to determine suitability of organoids containing liver-derived LGR5 positive stem cells for HCV infection (Dutta and Clevers 2017; Schöbel et al. 2018; Carpentier et al. 2020).

6.2 Identification and characterisation of host factors including RACK1 for flavivirus infection

Viruses are grouped according to similarities in their genome structure and replication strategies despite inflicting distinct pathologies during infection. Therefore, it is not inconceivable that viruses within the same family would exploit similar host factors to establish infection and replication. Host factors within the mosquito-borne flaviviruses are often shared for example the entry factors for both DENV and ZIKV include DC-SIGN and the TIM (T-cell Ig mucin) and TAM (TYRO3, AXL and MERTK) family members, resulting in infection of multiple cell types (Laureti et al. 2018). However, selectivity of cell types is influenced by the efficiency in binding to these receptors, where ZIKV, WNV and DENV can bind DC-SIGN with similar proficiency (Richard et al. 2017). However, ZIKV can bind the receptor AXL with a higher efficiency, which may lead to increased infection in cells with higher levels of AXL expression (Richard et al. 2017). During the replication phase of the virus lifecycle, multiple genome-wide CRISPR screens including ours have uncovered numerous novel host factors such as the OST and EMC complexes (Savidis et al. 2016a; Marceau et al. 2016; Zhang et al. 2016). The EMC proteins act as chaperones and promote the biogenesis of both DENV and ZIKV NS proteins, whereas the OST complex proteins likely play a structural role within the formation of the replication complex (Puschnik et al. 2017b; Lin et al. 2019a). Interestingly, the role of the OST complex, which is composed of 2 subunits STT3A and STT3B, differs between flaviviruses, where DENV is reliant on both subunits while ZIKV, WNV and YFV only utilise SST3A, highlighting similar but distinct requirements in host factor driven virus replication within the flavivirus family (Marceau et al. 2016). Our genome-wide CRISPR screen has identified RACK1 as a critical host factor for successful ZIKV infection and like the OST/EMC complex, it is

also important for replication of other flaviviruses (DENV and WNV), demonstrating that RACK1 is another host factor that is shared between flaviviruses. However, unlike the OST complex, RACK1 was not important for YFV infection. Since our study and that of Marceau *et al.* utilised the same YFV 17D vaccine strain, it is likely that YFV utilises an alternative host factor to fulfil the role RACK1 plays when it is absent from an evolutionary point of view, relative to other flaviviruses which have likely evolved streamlined replication strategies which rely heavily on RACK1. In addition, the YFV strain utilised is both replication and evolutionally divergent from circulating YFV strains and thus confirmation studies for RACK1 dependency will need to be performed with the latter strain (Beck et al. 2014; Fernandez-Garcia et al. 2016).

RACK1 is an evolutionary conserved intracellular member of the tryptophan-aspartate repeat (WD) family and is highly expressed in most tissues. RACK1 is also a dispensable subunit within the 40S ribosomal complex, allowing for efficient translation of capped mRNAs (Gallo et al. 2018). RACK1 consists of seven 40 amino acid repeats (WD40), which facilitate interactions with a large number of proteins to act as a signalling hub for the transduction of multiple signalling pathways including Protein Kinase C (PKC) and thus critical for cell homeostasis and proliferation [reviewed extensively in (Adams et al. 2011)]. The role RACK1 plays to maintain cellular homeostasis is likely a major factor of why we failed to generate a RACK1 monoclonal CRISPR knockout cell line and thus had to use siRNA as a complementary method to perform further experiments. It is also an explanation of why in comparison with other genome-wide CRISPR screens, our strategy identified RACK1 as a novel proviral host factor for ZIKV infection. We intentionally modified the recommended screening protocol to identify potential genes which when knocked out conferred a disadvantage to cell proliferation, a process where RACK1 expression is instrumental.

With regards to virus replication, RACK1 is critical for replication of multiple viral families using diverse mechanisms. RACK1 is proposed to be critical for the translation of IRES-mediated viral genomes which include HCV and Cricket Paralysis Virus (CrPV), likely due to its role with the 40S ribosome (Majzoub et al. 2014). However, its role in HCV translation is somewhat contentious as Lee *et al.* revealed no significant impact on IRES-dependent translation upon RACK1 knockdown (Lee et al. 2019). In addition, during the course of this project, RACK1 has been demonstrated to interact

with HCV NS5A, forming a complex with ATG14L-Beclin1-Vps34-Vps15 to enable induction of autophagy and construction of DMVs within the membranous web (Lee et al. 2019). It is not surprising that studies performed by us and Lee *et al.* have demonstrated RACK1's role in the biogenesis of replication organelles of flaviviruses and HCV respectively, given that both viruses belong to the *flaviviridae* family (Fig. 6.1). In addition, HCV NS5A and flavivirus NS1 play similar roles within their respective viral lifecycle, which include remodelling of ER membranes to form replication complexes (Romero-Brey et al. 2015; Ci et al. 2020). Since flaviviruses also induce autophagy during virus replication, we also investigated whether DENV and ZIKV NS1 could interact with autophagy proteins ATG5 and ATG14L, which have been shown to previously interact with RACK1 (Erbil et al. 2016; Lee et al. 2019). Preliminary co-immunoprecipitation experiments indicate that ATG14L interact with ZIKV NS1 (Fig. 4.4). Further experiments would need to be performed to determine if RACK1-NS1 interactions drive the biogenesis of VPs by an autophagy mediated mechanism (Fig. 6.1) (Echavarria-Consuegra et al. 2019).

Other viruses which also rely on RACK1 as a proviral host factor include Epstein Barr Virus (EBV), Hepatitis E Virus (HEV) and Mumps Virus (MuV). Yeast 2 hybrid assays were performed with RACK1 to identify viral interacting partners for EBV, HEV and MuV infection. For EBV infection, RACK1 was shown to interact with the EBV activator protein BZLF1, which is critical for reactivation of latently infected cells by the PKC signalling pathway, a pathway RACK1 is implicated in (Baumann et al. 2000). The MuV V and HEV X protein have also been identified by yeast 2 hybrid assays to interact with RACK1, where the former is responsible for antagonism of the IFN JAK-STAT pathway and the latter critical for virus replication (Kubota et al. 2002; Subramani et al. 2018). These studies illustrate the importance of RACK1 as a scaffolding protein, where protein-protein interactions with RACK1 are critical as its role as a proviral host factor. Thus, we decided to perform interaction studies with RACK1 with regards to flaviviruses and have demonstrated that RACK1 not only interacts with flavivirus NS1, but also all ZIKV NS proteins except NS5 (Fig. 7 in manuscript and 4.1). Further studies will need to be performed to not only confirm preliminary studies of RACK1-ZIKV NS protein interactions with co-

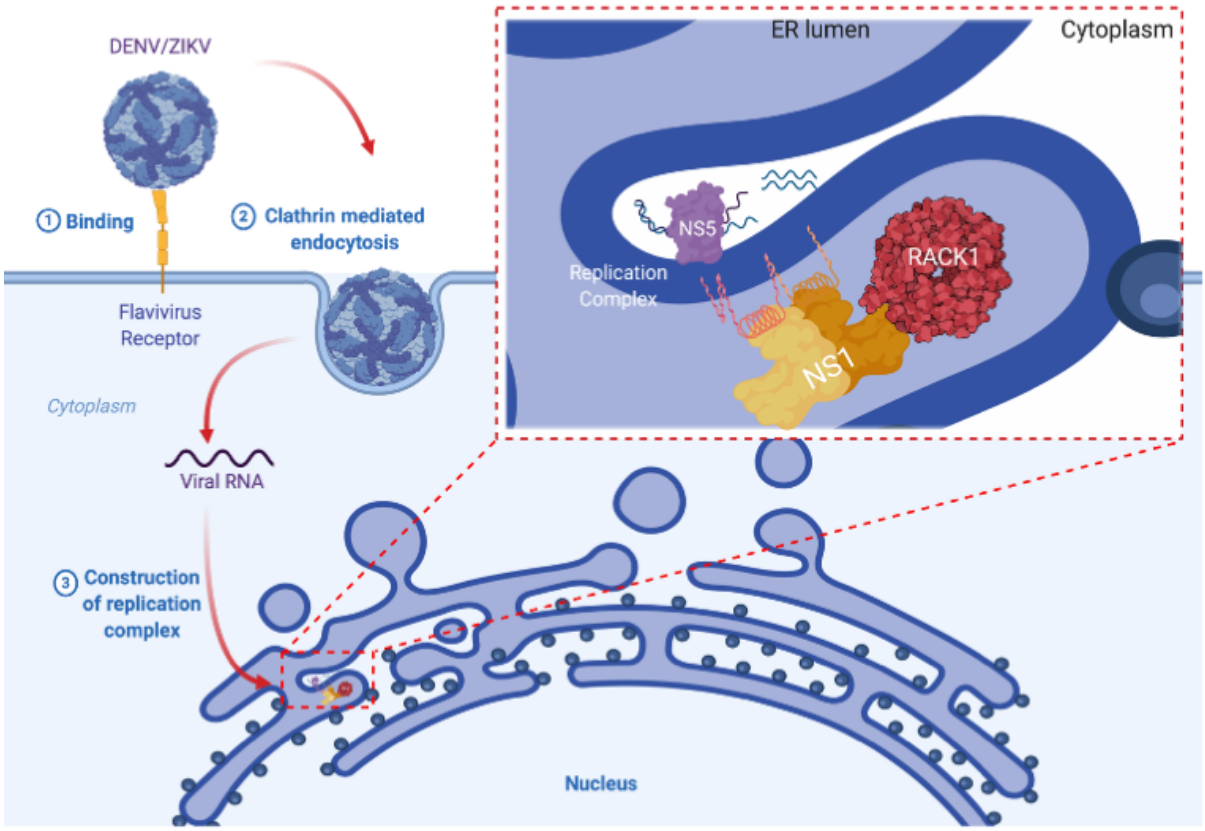

Figure 6.1 Proposed mechanism by which RACK1 supports the flavivirus lifecycle.

Upon entry of flaviviruses including DENV and ZIKV and translation and processing of the viral NS proteins, NS1 interacts with RACK1 within the ER lumen to drive construction of vesicle packets, the main site of virus replication.

immunoprecipitation and/or immunofluorescence co-localisation studies but also determine the consequences of these interactions. Although there may be distinct roles for each of these RACK1-ZIKV NS protein interactions within the virus lifecycle, it is likely that the RACK1 plays a common role shared by all ZIKV NS proteins in close proximity with the replication complex, which is the biogenesis of replication organelles (Fig 6.1).

Since RACK1 interacts with a large repertoire of proteins in multiple signalling cascades, we believed that pursuing mutant studies of RACK1 would help narrow down potential proteins and therefore signalling pathways which could interact with the RACK1-NS1 complex to drive the biogenesis of replication organelles. Loss of interaction between DENV and ZIKV NS1 and the RACK1 harbouring a ΔWD2 deletion suggests a putative binding site for NS1 within the RACK1 WD2 domain (Fig 4.2B, 4.2C). Interestingly, the WD1, WD2 and WD5 domains of ribosome associated RACK1 are obscured by rRNA, therefore the WD2 domain is likely more accessible for flavivirus NS1 to bind when RACK1 is acting as an adaptor molecule (Rabl et al. 2011). Proteins which may also bind the WD2 domain include the PKC mediated JNK2 signalling cascade, a key regulator in cell cycle proliferation and cell survival and induced during DENV infection (López-Bergami et al. 2005; Ceballos-Olvera et al. 2010; Wu et al. 2019a). Post-translational modifications are also present within RACK1, where phosphorylation of Tyr-52 at the boundary of WD1 and WD2 domains shown to be critical for interaction between c-Abl and FAK (Kiely et al. 2009). However, the RACK1 WD2 mutant retains Tyr-52 and thus this mechanism is unlikely responsible for flavivirus infection. The mediation of numerous cell responses by RACK1 is often dependent on its movement to distinct subcellular locations to facilitate signal transduction. In particular, RACK1 is sequestered into cytoplasmic stress granules to prevent induction of the MAPK signalling cascade to inhibit apoptosis, a process which all flaviviruses modulate during the virus lifecycle (Lee et al. 2005; Ceballos-Olvera et al. 2010). Although the majority of punctate dots containing RACK1 observed when expressed with ZIKV NS1 were localised to the ER, cytoplasmic punctate dots were also present and whether the interaction of NS1-RACK1 results in the movement and subsequent accumulation of RACK1 within cytoplasmic stress granules remain unclear and warrants further investigation (Fig. 7A in manuscript).

6.3 The innate immune response to ZIKV infection

The innate immune response is the first line of defence against invading pathogens of bacterial, fungal or viral origin, where the production of IFN and upregulation of ISGs is a key component to respond against virus infection (Schoggins 2019). Prior to the advent of unbiased identification of mRNA profiles, only a handful of ISGs were identified such as PKR, ISG15, OAS and MX-A (Kerr et al. 1977; Haller et al. 1979; Blomstrom et al. 1986; Meurs et al. 1990). However, with the development of microarray and RNA sequencing to profile mRNAs in multiple cell types stimulated with different IFNs, more than 300 ISGs are thought to exist (Schoggins et al. 2011). Although the antiviral function of a number of ISGs have been characterised mainly through ectopic expression, it is unclear which ISGs are necessary or contribute to virus mediated inhibition. Thus, both genome-wide siRNA and CRISPR KO libraries have been utilised to give an unbiased perspective on not only which ISGs directly inhibit virus infection, but also which non-ISGs host factors support the innate immune response. Richardson *et al.* performed a genome-wide CRISPR screen with flavivirus infection and identified IFI6 as the only classical ISG that has direct antiviral activity, along with STAT2 and IRF9 which are critical for the IFN JAK-STAT signalling cascade (Richardson et al. 2018). The absence of previously identified antiviral ISGs in this screen, such as viperin, suggest that CRISPR screens may only reveal genes that have an extremely potent phenotype and highlights a limitation of using CRISPR screens as a tool to uncover novel ISGs. Furthermore, it is likely that there is significant redundancy in antiviral ISGs and an antiviral state may be induced by multiple ISGs that can be expressed in specific cell types or a temporal manner.

The explosive number of ZIKV infections in 2016 that emerged in South America and associated increase of microcephaly in newborns led us to investigate the cellular ISG response upon ZIKV infection in different cell types and moreover the role the ISG viperin plays in restricting virus infection. Upon infection, flaviviruses including DENV and ZIKV trigger recognition of viral genomic RNA in both the cytoplasm (RIG-I/MDA5) and endosome (TLR3) resulting in the production of IFNs and upregulation of ISGs (Saito and Gale 2007). However, it is well recognised that the flaviviruses have evolved mechanisms to evade the innate immune response (Gack and Diamond 2016; Coldbeck-Shackley et al. 2020). This is demonstrated in this thesis by the lack of

upregulation of canonical ISGs, including viperin, IFIT1, IFN-β, IFITM1, ISG15, OAS1 and MX1, following ZIKV infection of Huh7 and the placental cell lines, HTR8 and JEG3 (Fig. 1 in manuscript). Furthermore, the addition of poly I:C to optimally stimulate the innate immune response in ZIKV infected cells resulted in reduced IFN-β promoter activity and ISG mRNA upregulation (Fig. 2 in manuscript). Interestingly, mouse neural progenitor cells (NPCs) infected with ZIKV displayed delayed ISG upregulation (Fig. 3 in manuscript). The delayed responses in ISG upregulation observed can be attributed to the numerous ZIKV immune evasion strategies orchestrated by the viral NS proteins (see section 1.16.2). However, monocyte-derived macrophages (MDMs) could upregulate innate signalling pathways in response to ZIKV infection (Fig. 4 in manuscript). Other publications also show that both patient and hPSC-derived macrophages are also susceptible to ZIKV infection which are consistent with our studies (Lang et al. 2018; Carlin et al. 2018). However, both reports demonstrate that low levels of pro-inflammatory cytokines and chemokines are expressed, resulting in dampened type I IFN responses and upregulation of ISGs. In addition, Lang *et al.* show that ZIKV but not DENV infection disrupts the NF-κB macrophage migration inhibitory factor (MIF) positive feedback loop, resulting in enhanced suppression of pro-inflammatory cytokine expression (Lang et al. 2018). This could explain the significant increase in IFN-β upregulation in DENV infected MDMs compared to ZIKV infected MDMs. Thus, it is highly probable that the high innate immune responses observed within MDMs in our study can be attributed to the low infection rate (0.6-6.3%), where the bulk of ISG regulation is derived from innate immune activation of uninfected bystander cells.

Viperin is a potent anti-viral ISG that has received much attention, due to its ability to not only directly restrict replication against multiple viruses with diverse mechanisms, but also its ability to augment the innate immune signalling pathways creating positive feedback loops (see section 1.15 and references therein). Encoded by the gene *RSAD2*, viperin is a part of the superfamily of radical *S*-adenosyl-L-methionine (SAM) domain-containing enzymes that cleaves SAM via utilisation of the 4Fe-4S cluster (Duschene and Broderick 2010). Through a SAM-dependent manner, viperin can catalyse cytidine triphosphate (CTP) to 3'-deoxy-3',4'-didehydro-CTP (ddhCTP), a novel antiviral ribonucleotide, where incorporation of ddhCTP into newly synthesised

viral RNA results in termination of translation via RNA dependent RNA polymerases (Gizzi et al. 2018). We show that ectopic expression of viperin inhibits ZIKV infection in Huh7 cells, where reduced ZIKV RNA and envelope expression is observed (Fig. 5 in manuscript). In addition, using MEFs generated from viperin$^{-/-}$ mice, we confirmed the importance of viperin in restricting ZIKV infection (Fig. 7 in manuscript). However, our viperin mutant studies show that although the SAM domain mutant impaired anti-ZIKV activity, the 3' domain mutant of viperin had lost complete antiviral activity relative to wildtype, indicating that there are multiple mechanisms by which viperin inhibits ZIKV replication (Fig. 6 in manuscript). This is not surprising given that the innate immune response is not selective and thus has evolved multiple mechanisms to combat virus infection. Vanwalscappel *et al.* showed that the lysine amino acid residue at position 358 in viperin is crucial for antiviral activity against ZIKV infection, which supports our findings as the 3' mutant of viperin we utilised has lost the amino acid present in positions 357-361 (Vanwalscappel et al. 2019).

Viperin has been shown previously to inhibit multiple members of the *flaviviridae* family including HCV, DENV, WNV, ZIKV and TBEV (Helbig et al. 2011; Helbig et al. 2013; Van der Hoek et al. 2017). Viperin interacts with viral proteins such as HCV NS5A, and ZIKV and TBEV NS3, to exert its antiviral activity (Helbig et al. 2005; Panayiotou et al. 2018). However, the mode of action in each case is strikingly different. Viperin binds to HCV NS5A on the surface of lipid droplets to disrupt interactions with host factors such as VAP-A, critical for formation and maintenance of the replication complex (Helbig et al. 2005). In contrast, despite viperin's ability to interact with the NS3 protein of JEV, TBEV, YFV and ZIKV, only TBEV and ZIKV NS3 is targeted for proteasomal degradation (Panayiotou et al. 2018). In addition, viperin promoted NS3-dependent degradation of other viral proteins prM, E, NS2A and NS2B, suggesting the capability of ISGs to co-opt viral protein enzymatic functions to respond against virus infection (Panayiotou et al. 2018). Given that our mutant studies and previous publications show that both the SAM domain and C-terminus of viperin is critical for ZIKV and TBEV antiviral activity respectively, it would be interesting to determine whether targeted interaction and subsequent proteasomal degradation of NS3 is linked to the SAM domain and the requirement of viperin's c-terminus interaction with CIAO1 to enable enzymatic activity of the SAM domain, or whether it is a SAM-

independent mechanism by which viperin restricts flavivirus replication (Upadhyay et al. 2014).

Although viperin is able to synthesise the novel ribonucleotide ddhCTP to facilitate premature termination of RNA synthesis by flavivirus NS5, it does not explain the diverse antiviral activities viperin displays against multiple pathogens. One unifying mechanism by which viperin could limit multiple pathogens is through positive regulation of the innate immune response. Viperin can enhance both TLR7 and TLR9 signalling pathways via interactions with IRAK1 and TRAF6, resulting in increased production of IFN (Saitoh et al. 2011). In addition, viperin can also interact with STING and induce TBK1 K63-linked polyubiquitination, resulting in enhancement of the innate immune response against dsDNA viral mimics and HBV infection (Crosse et al. 2020). Unpublished data in our laboratory also demonstrated that overexpression of viperin enhances the TLR3 signalling pathway via co-localisation with both TBK-1 and TRAF3 after stimulation with dsRNA mimics. Whether viperin enhances TLR3 and/or TLR7 signalling in the context of both HCV and ZIKV infection with a similar mechanistic nature remains unexplored and warrants further investigation.

Although viperin is primarily known for it's role to restrict virus replication from multiple viral families, Human Cytomegalovirus (HCMV) exploits viperin as a proviral host factor where interferon independent induced viperin is transported to the mitochondria, resulting in increased lipid synthesis required for progeny virion production (Seo et al. 2011). Conversely, it may therefore be possible for viruses to utilise pro-viral host factors such as RACK1 (as shown in this thesis) to regulate innate immune responses. It has been reported that RACK1 plays a role in multiple pathways of the innate immune response, where the literature suggests RACK1 acting in the capacity of both a positive and negative regulator of immune signalling. It has been postulated that the interaction of RACK1 with MAVS results in reduction of IFN-β promoter activity and disruption of signalling complexes (RACK1-TRAF6/TRAF3) (Xie et al. 2019a). In addition, RACK1 forms a complex with the phosphatase PP2A to dephosphorylate IRF3 and hence further strengthens the argument of RACK1 acting as a negative regulator within the RIG-I signalling pathway (Long et al. 2014). However, RACK1 mediates the interaction of the IFNAR and STAT1, resulting in STAT1 tyrosine

phosphorylation and activation of STAT2 within the IFN pathway (Usacheva et al. 2001). Given the prominent role of RACK1 in regulating the innate immune response, it is logical that viruses may exploit the former's ability to bind multiple proteins to subvert the innate immune response. Interestingly, the Mumps virus (MuV) V protein is able to competitively bind to RACK1 and disrupt binding of the IFNAR with STAT1, resulting in downregulation of specific ISGs (IFIT1) (unpublished preliminary data in this thesis) (Kubota et al. 2002). Therefore, ZIKV NS proteins may also utilise RACK1 as an adapter molecule to inhibit the innate immune response. ZIKV NS4A and NS2B3 have been reported to bind to MAVS and JAK1 respectively, the same proteins RACK1 interacts with (Fig. 6.2). Our preliminary data suggests that RACK1 also binds ZIKV NS4A and NS2B3 (Fig 4.1) and therefore it is possible that ZIKV may exploit RACK1 to subvert the innate immune response (Fig. 6.2). This could be achieved by recruitment of RACK1 by viral proteins to sites of innate signalling to exert a negative influence on target proteins such as MAVS and JAK1, ultimately resulting in decreased ISG upregulation. In addition, interaction of ZIKV NS1 with RACK1 during the biogenesis of the replication complex and subsequent relocation of RACK1 to the ER lumen may allow for sequestration of the latter to prevent induction of the IFN JAK-STAT signalling cascade (Fig. 6.2). Thus, investigations into RACK1 as a major contributor to immune evasion by flaviviruses in addition to its role as a proviral host factor should be considered in further studies.

6.4 Development of novel therapeutics to target flavivirus infection

Both proviral and antiviral host factors have a major impact on the virus lifecycle. Thus, knowledge of the function of these host factors could lead to further insight into the viral lifecycle and aid in the development of novel antiviral therapeutics. Host factors identified in genome-wide CRISPR screens are expected to have a particularly potent phenotype and could serve as antiviral drug targets. For example, a genome-wide CRISPR screen targeting flaviviruses, identified the OST complex as essential for virus replication (Marceau et al. 2016). A small cell-permeable compound NGI-1, originally developed to target the OST complex for the treatment in lung cancer, was then repurposed as a novel antiviral against multiple flaviviruses (Lopez Sambrooks et al. 2018). NGI-1 acted as a pan-flavivirus antiviral compound, where multiple serotypes of DENV infection were inhibited (Puschnik et al. 2017b). Antiviral activity associated with NGI-1 was separate from its main cellular N-glycosylation role

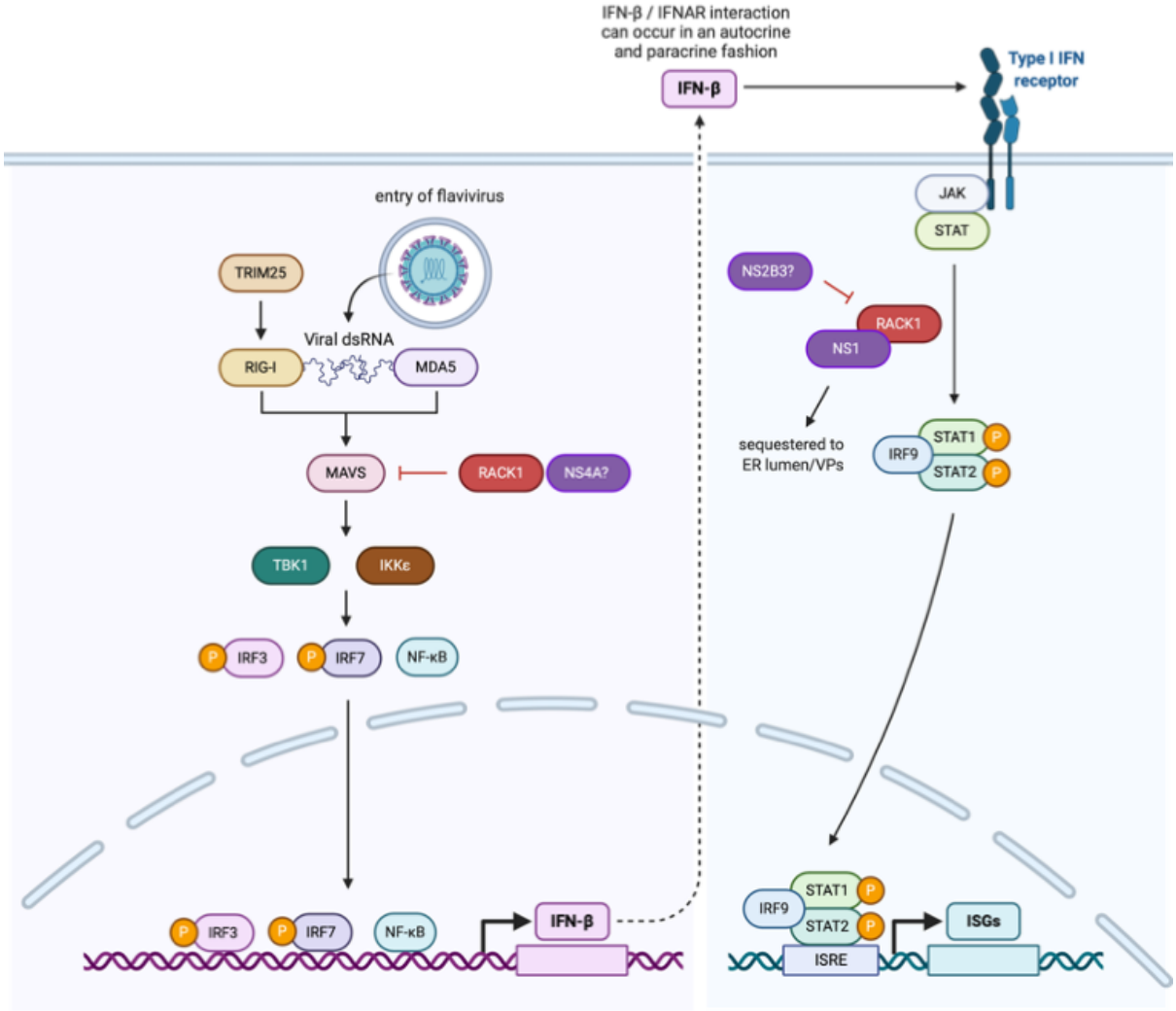

Figure 6.2 Potential mechanisms by which RACK1 regulates innate signalling pathways.

ZIKV NS4A may interact with MAVS to allow for virus induced disruption of signalling complexes to prevent induction of IFN-β. In addition, ZIKV NS2B3 may inhibit RACK1 mediated STAT1 tyrosine phosphorylation in the IFN JAK-STAT signalling pathway. In addition, ZIKV NS1 may bind to RACK1 to sequester the latter away from the IFN JAK-STAT signalling pathway to prevent induction of ISGs.

of the OST complex, making it a desirable therapeutic to treat flavivirus infection. Novel serotypes of DENV infection were inhibited (Puschnik et al. 2017b). Antiviral activity associated with NGI-1 was separate from its main cellular N-glycosylation role of the OST complex, making it a desirable therapeutic to treat flavivirus infection. Novel antiviral therapeutics could also be developed against RACK1, that we have identified in this thesis to be important for pan-flavivirus replication. Given that RACK1 possesses no enzymatic activity yet has multiple cellular roles critical for cell homeostasis, therapeutics would likely be targeted to exploit RACK1-protein interactions with either additional host factors or viral NS proteins rather than RACK1 expression itself. Likewise, exploitation of the mechanisms by which antiviral ISGs act against virus infection can lead to the development of novel antiviral drugs. For example, the discovery of the ddhCTP ribonucleotide that is produced by viperin to combat flavivirus infection, has led to the synthetic generation of the ddhCTP precursor ddhC, that is able to enter cells and inhibit ZIKV replication *in vitro* (Gizzi et al. 2018).

In summary, we have validated, optimised and performed a genome-wide CRISPR screen to identify novel host factors important for ZIKV infection. One enriched novel host factor, RACK1 was shown to be critical for replication complex formation via interactions with NS1 within the DENV and ZIKV lifecycles. In addition, we also show for the first time, the antiviral activity of the ISG viperin against ZIKV infection is mediated by the 3' terminus of the protein. Collectively, the studies conducted in this thesis demonstrate the importance of both proviral and antiviral host factors in understanding viral replication and highlights the complex interplay between host and virus proteins that ultimately determine the outcomes of virus infection. An improved understanding of the molecular mechanisms by which RACK1 and viperin influence virus infection may provide new therapeutic perspectives for the treatment of pan-flaviviral diseases.

Appendices

Appendix I: Primer sequences

Gene name	Forward primer (5’ to 3’)	Reverse primer (5’ to 3’)
Primers for cloning into mammalian expression plasmids		
HCV SGR mCherry	TATACGCGTATGGTGAGCAAGGGCGAG	ATCAGATCTCTTGTACAGCTCGTCCATGC
HCV SGR GFP	TATACGCGTATGGTGAGCAAGGGCG	TATAGATCTCTTGTACAGCTCGTCCATGCCG
HCV SGR TK	TATACGCGTATGGCTTCGTACCCCTGCCATCAACATGCGTC	TGTAGATCTGTTAGCCTCCCCCATCTCCCGGGCAAAC
RACK1-2xHA	GCCTCCGGACTCTAGAATGACTGAGCAGATGACC	TAGCCTCCCCCGTTTAAACTTAAGCGTAATCTGGAACATCGTATGGGTAAGCGTAATCTGGAACATCGTATGGGTAGTAGCGTGTGCCAATGGTC
ZIKV NS1-FLAG	ACCGATCCAGCCTCCGGACTCTAGAATGGATGTGGGGTGCTC	TCAGTTAGCCTCCCCCGTTTAAACTTACTTGTCGTCATCGTCTTTGTAGTCTGCAGTCACCACTG
ZIKV NS2A-FLAG	ACCGATCCAGCCTCCGGACTCTAGAATGGGATCAACTGATCACATGG	TCAGTTAGCCTCCCCCGTTTAAACTTACTTGTCGTCATCGTCTTTGTAGTCCCGCTTCCCACTC
ZIKV NS2B3-FLAG	ACCGATCCAGCCTCCGGACTCTAGAATGAGCTGGCCCCCTA	TCAGTTAGCCTCCCCCGTTTAAACTTACTTGTCGTCATCGTCTTTGTAGTCTCTTTTCCCAGCGG

ZIKV NS4A-FLAG	ACCGATCCAGCCTCCGGAC TCTAGAATGGGAGCGGCTT TTGG	TCAGTTAGCCTCCCCC GTTTAAACTTACTTGTC GTCATCGTCTTTGTAG TCTCTTTGCTTTTCTG GCTCA
ZIKV NS4B-FLAG	ACCGATCCAGCCTCCGGAC TCTAGAATGGGAGCGGCTT TTGG	TCAGTTAGCCTCCCCC GTTTAAACTTACTTGTC GTCATCGTCTTTGTAG TCTCTTTGCTTTTCTG GCTCA
ZIKV NS5-FLAG	GGGACCGATCCAGCCTCCG GACTCTAGAATGGGGGGTG GAACAG	GTTTCAGTTAGCCTCC CCCGTTTAAACTTACT TGTCGTCA
DENV NS1-2xFLAG	GCCTCCGGACTCTAGAATG GATAGTGGTTGCGTTGTGA GC	TAGCCTCCCCCGTTTA AACTTACTTGTCGTCA TCGTCTTTGTAGTCCT TGTCGTCATCGTCTTT GTAGTCGGCAGCTGT GACCAAGGAGTTG
WNV_{KUN} NS1-2xFLAG	ACCGATCCAGCCTCCGGAC TCTAGAATGGGTATCAACGC TC	TCAGTTAGCCTCCCCC GTTTAAACTTACTTGTC GTCATCGTCTTTGTAG TCCTTGTCGTCATCGT CTTTGTAGTCAGCATT CACTTGTGACTG
YFV NS1-2xFLAG	ACCGATCCAGCCTCCGGAC TCTAGAATGGTTGGCATCAA CACAAGAAACAT	TCAGTTAGCCTCCCCC GTTTAAACTTACTTGTC GTCATCGTCTTTGTAG TCCTTGTCGTCATCGT CTTTGTAGTCAGCCAC TGTGAGTTTCAGC
RACK1ΔWD1-2xHA	AGCGGTACCAGGGATGAGA CCAACTATG	GCAGGTACCGGTGCC ACGAAGGGTC

RACK1ΔWD2-2xHA	TTAGGTACCACGGGCACCACCAC	ATAGGTACCAGCACGCTGTGGAATTCC
RACK1ΔWD3-2xHA	CGAGGTACCGTCCAGGATGAGAGCCAC	CTAGGTACCGGTGGTGCCCGTTG
RACK1ΔWD4-2xHA	CTAGGTACCAACTGCAAGCTGAAGACCAAC	ATAGGTACCCTGGACAGTGTATTTGCACACA
RACK1ΔWD5-2xHA	ATCGGTACCGAAGGCAAACACCTTTATACATTAGACG	TTAGGTACCGGTCTTCAGCTTGCAGTTAGC
RACK1ΔWD6-2xHA	CGGGGTACCATCATTGTAGATGAACTGAAGCAAGAAG	CGAGGTACCTTCGTTGAGATCCCATAACATG
RACK1ΔWD7-2xHA	CGAGGTACCATTGGAACGAGGTATGCTAGCT	CGAGGTACCATTGGAACGAGGTATGCTAGCT
ATG5-myc	ACCGATCCAGCCTCCGGACTCTAGAATGGAACAAAAACTCATCTCAGAAGAGGATCTGGCTATGACAGATGACAAAGATG	TCAGTTAGCCTCCCCCGTTTAAACTCAATCTGTTGGCTGTG
ATG14-myc	ACCGATCCAGCCTCCGGACTCTAGAATGGAACAAAAACTCATCTCAGAAGAGGATCTGATGGCGTCTCCCAGTG	TCAGTTAGCCTCCCCCGTTTAAACTTAACGGTGTCCAGTGTAAGCTTTAAACC
Primers for cloning into LentiCRISPRv2 plasmid		
EGFP-1	CAACGGGGCGAGGAGCTGTTCACCG	AAACCGGTGAACAGCTCCTCGCCCC
EGFP-2	CACCGGTCGCCCTCGAACTTCACCT	AAACAGGTGAAGTTCGAGGGCGACC
CD81-1	CACCGTGGCTTCCTGGGCTGCTACG	AAACCGTAGCAGCCCAGGAAGCCAC
CD81-2	CACCGGGCTGCTACGGGGCCATCC	AAACGGATGGCCCCGTAGCAGCCC
PI4KA	CACCGCGGGGCTTCTATTTCAACA	AAACTGTTGAAATAGAAGCCCCGC

RACK1	CACCGATTCCACAGCGTGC TCTTGCG	AAACCGCAAGAGCAC GCTGTGGAATC
EMC1	CACCGTCCTGGGAGACTAA CATCGG	AAACCCGATGTTAGTC TCCCAGGAC
EMC6	CACCGCCGGCAATAATCCA GGACGG	AAACCCGTCCTGGATT ATTGCCGGC
Real-time primers		
Viperin	GTGAGCAATGGAAGCCTGA TC	GCTGTCACAGGAGATA GCGAGAA
RACK1	TAACCGCTACTGGCTGTGT G	GCCTTGCTGCTGGTAC TGAT
HCV	TCTTCACGCAGAAAGCGTCT AG	GGTTCCGCAGACCACT ATGG
RPLPO (36B4)	AGATGCAGCAGATCCGCAT	GGATGGCCTTGCGCA
ZIKV	CAGCTGGCATCATGAAGAA YC	CACYTGTCCCATCTTY TTCTCC
DENV	ATCCTCCTATGGTACGCACA AA	CTCCAGTATTATTGAA GCTGCTATCC
EMC1	CGGCCTGAGCGGCTGTATA TC	CTCCACAGCACCACCT TCCC
EMC6	TTCTACCTGCTCGCCTCCGT	CCCGATGAGGCCTCC TGTAA
Sequencing primers(5’ to 3’)		
T7	TAATACGACTCACTATAGGG C	-
CMV	CGCAAATGGGCGGTAGGCG TG	-
HSV TK		GAACAAACGACCCAAC ACCC
Genome-wide CRISPR screen primers		
LC-V2 adapters	AATGGACTATCATATGCTTA CCGTAACTTGAAAGTATTTC G	TCTACTATTCTTTCCCC TGCACTGTTGTGGGC GATGTGCGCTCTG
F1	AATGATACGGCGACCACCG AGATCTACACTCTTTCCCTA CACGACGCTCTTCCGATCTT	

	AAGTAGAGTCTTGTGGAAAG GACGAAACACCG	
F2	AATGATACGGCGACCACCG AGATCTACACTCTTTCCCTA CACGACGCTCTTCCGATCTA TACACGATCTCTTGTGGAAA GGACGAAACACCG	
F3	AATGATACGGCGACCACCG AGATCTACACTCTTTCCCTA CACGACGCTCTTCCGATCT GATCGCGCGGTTCTTGTGG AAAGGACGAAACACCG	
F4	AATGATACGGCGACCACCG AGATCTACACTCTTTCCCTA CACGACGCTCTTCCGATCTC GATCATGATCGTCTTGTGGA AAGGACGAAACACCG	
F5	AATGATACGGCGACCACCG AGATCTACACTCTTTCCCTA CACGACGCTCTTCCGATCTT CGATCGTTACCATCTTGTGG AAAGGACGAAACACCG	
F6	AATGATACGGCGACCACCG AGATCTACACTCTTTCCCTA CACGACGCTCTTCCGATCTA TCGATTCCTTGGTTCTTGTG GAAAGGACGAAACACCG	
F7	AATGATACGGCGACCACCG AGATCTACACTCTTTCCCTA CACGACGCTCTTCCGATCT GATCGATAACGCATTTCTTG TGGAAAGGACGAAACACCG	
F8	AATGATACGGCGACCACCG AGATCTACACTCTTTCCCTA CACGACGCTCTTCCGATCTC GATCGATACAGGTATTCTTG TGGAAAGGACGAAACACCG	
R1		CAAGCAGAAGACGGC ATACGAGATAAGTAGA G GTGACTGGAGTTCAGA CGTGTGCTCTTCCGAT CTTTCTACTATTCTTTC CCCTGCACTGT
R2		CAAGCAGAAGACGGC ATACGAGATACACGAT CGTGACTGGAGTTCAG ACGTGTGCTCTTCCGA TCTATTCTACTATTCTT TCCCCTGCACTGT

R3		CAAGCAGAAGACGGC ATACGAGATCGCGCG GTGTGACTGGAGTTCA GACGTGTGCTCTTCCG ATCTGATTCTACTATTC TTTCCCCTGCACTGT
R4		CAAGCAGAAGACGGC ATACGAGATCATGATC GGTGACTGGAGTTCA GACGTGTGCTCTTCCG ATCTCGATTCTACTATT CTTTCCCCTGCACTGT
R5		CAAGCAGAAGACGGC ATACGAGATCGTTACC AGTGACTGGAGTTCAG ACGTGTGCTCTTCCGA TCTTCGATTCTACTATT CTTTCCCCTGCACTGT
R6		CAAGCAGAAGACGGC ATACGAGATTCCTTGG TGTGACTGGAGTTCAG ACGTGTGCTCTTCCGA TCTATCGATTCTACTAT TCTTTCCCCTGCACTG T
R7		CAAGCAGAAGACGGC ATACGAGATAACGCAT TGTGACTGGAGTTCAG ACGTGTGCTCTTCCGA TCTGATCGATTCTACT ATTCTTTCCCCTGCAC TGT
R8		CAAGCAGAAGACGGC ATACGAGATACAGGTA TGTGACTGGAGTTCAG ACGTGTGCTCTTCCGA TCTCGATCGATTCTAC TATTCTTTCCCCTGCA CTGT
Miscellaneous		
Thymidine Kinase	TGGAGCAGAAAATGCCCAC G	GCAGATCGTCGGTATG GAGC
HCV 5970R		TTCTCGCCAGACATGA TCTT

Appendix II: Solutions

The following solutions were obtained from the Central Services Unit (CSU) and Tissue Culture Services Unit (TSU), School of Biological Sciences, The University of Adelaide.

- 0.85% saline solution
- 10x GTS buffer
- 10x TBS buffer
- 1x and 20x PBS (phosphate buffered saline) solutions
- 20% Glucose solution
- 4M NaCl solution
- Ampicillin 1 mg/ml
- EDTA (different concentration and pH)
- Kanamycin 1 mg/ml
- L-Agar + ampicillin plates
- Luria agar plates
- Luria Broth
- SDS
- SOC media
- Tris solutions (different concentration and pH)
- G418
- Penicillin/streptomycin
- Trypan blue
- Trypsin-EDTA
- FCS (Foetal Calf Serum)
- 0.2 % (w/v) gelatin

Solution Components

Cell lysis RIPA Buffer (40 ml)	150mM NaCl (1.5ml of 4M NaCl) 0.5% deoxych = 0.2g 0.1% SDS (0.4ml of 10% SDS) 1% NP-40 (0.4 ml of NP-40) 50mM Tris (2 ml of 1M Tris) dH_2O 35.7 ml
Cell lysis NP-40 Buffer (40 ml)	50 mM Tris-HCL (2 ml of 1M Tris-HCL,pH8) 150mm NaCl (1.5 ml of 4M NaCl) 1% NP-40 (0.4 ml of NP-40) dH_2O 36.1 ml
5X Laemmli Buffer	5% β-Mercaptoethanol 0.02% Bromophenol blue 30% Glycerol 10% SDS 0.25 mM Tris-Cl (pH 6.8)
SDS PAGE Running Buffer	2.9% Trisma Base 14.14% glycine 1% SDS
SDS PAGE Transfer Buffer	0.3% Trisma Base 1.44% glycine 20% (v/v) methanol
TBS-T washing solution ***(Western blot)***	1x TBS buffer in dH2O 0.1 % Tween® 20
Acetone:Methanol	50% acetone 50% methanol
4% Paraformaldehyde (100 ml)	4g of paraformaldehyde (PFA) 10ml of 10x PBS dH_2O up to a final volume of 100 ml
Redsafe solution	3 µl Redsafe 100 ml of melted-agarose gel
1% Agarose	1g Agarose

	100ml 1xTAE buffer
1% BSA	1 g of Bovine serum albumin (BSA) 100 ml of 1X PBS
5% BSA	5 g of BSA 100 ml of 1X PBS
2x Freezing medium (10 ml)	50% complete DMEM medium (5 ml) 30% FCS (3 ml) 20% DMSO (2 ml)

Competent Cells:

The *E.coli* α-Select Chemically Competent Cells used for bacterial transformation was: *deoR endA*1 *recA*1 *relA*1 *gyrA*96 *hsdR*17($r_k^-m_k^+$) *supE*44 *thi*-1 Δ*(lacZYA-argFV*169) *Φ80δlacZ*ΔM15 F^- *γ*$^-$.

The Endura™ Electrocompetent cells used for bacterial transformation of the GeCKO LentiCRISPRv2 library was: recA13 supE44 ara-14 galK2 lacY1 proA2 rpsL20(StrR) xyl-5 λ– leu mtl-1 F– mcrB mrr hsdS20(rB–, mB–).

Appendix III: Antibodies

Antibody dilution for Western blot analysis

Primary antibody	Dilution	Incubation	Supplier
Mouse anti-FLAG (M2)	1:1,000	O/N, 4°C	Sigma Aldrich
Rabbit anti-FLAG (D6W5B)	1:1,000	O/N, 4°C	Cell Signaling Technology
Mouse anti-β-actin (AC-74)	1:10,000	O/N, 4°C	Sigma Aldrich
Rabbit anti-viperin (AT131)	1:1,000	O/N, 4°C	Enzo life sciences
Mouse anti-HA (HA-7)	1:1,000	O/N, 4°C	Sigma Aldrich
Rabbit anti-HA (polyclonal)	1:1,000	O/N, 4°C	Sigma Aldrich
Mouse anti-myc (9B11)	1:1,000	O/N, 4°C	Cell Signaling Technology
Anti-EGFP	1:1,000	O/N, 4°C	N/A
Mouse anti-flavivirus NS1 4G2	1:1,000	O/N, 4°C	UQ
Chicken anti-flavivirus NS5	1:1000	O/N, 4°C	NIH
Mouse anti-vinculin (hVIN-1)	1:1000	O/N, 4°C	Sigma Aldrich
Mouse anti-RACK1 (B-3)	1:1,000	O/N, 4°C	Santa Cruz Biotechnology
Secondary Antibody			
Goat anti-mouse IgG (H+L), peroxidase conjugated	1:10,000	1 hr, RT	Thermo Fisher Scientific
Goat anti-rabbit IgG (H+L), peroxidase conjugated	1:1,000	1 hr, RT	Cell Signaling Technology

Rabbit anti-chicken IgY (H+L), peroxidase conjugated	1:10,000	1 hr, RT	Millipore

Antibody dilution for Immunofluorescence labelling

Primary antibody	Dilution	Incubation	Supplier
Mouse anti-FLAG (M2)	1:200	1 hr, RT	Sigma Aldrich
Rabbit anti-FLAG (D6W5B)	1:200	1 hr, RT	Cell Signaling Technology
Mouse anti-HA (HA-7)	1:200	1 hr, RT	Sigma Aldrich
Rabbit anti-HA (polyclonal)	1:200	1 hr, RT	Sigma Aldrich
Mouse anti-myc (9B11)	1:200	1 hr, RT	Cell Signaling Technology
Mouse anti-RACK1 (B-3)	1:200	1 hr, RT	Santa Cruz Biotechnology
Mouse anti-CD81 (JS-81)	1:100	1 hr, RT	BD Biosciences
Mouse anti-HCV NS5A	1:5	1 hr, RT	Hybridoma S/N
Mouse anti-flavivirus NS1 4G4	1:5	1 hr, RT	Hybridoma S/N
Mouse anti-flavivirus Envelope	1:5	1hr, RT	Hybridoma S/N
Mouse anti-dsRNA 3G2	1:5	1 hr, RT	Hybridoma S/N
Secondary Antibody			
Anti-mouse/Alexa 488 IgG	1:200	1 hr, RT	Invitrogen
Anti-mouse/Alexa 555 IgG	1:200	1 hr, RT	Invitrogen
Anti-mouse/Alexa 555 IgM	1:200	1 hr, RT	Invitrogen
Anti-rabbit/Alexa 488 IgG	1:200	1 hr, RT	Invitrogen
Anti-rabbit/Alexa 555 IgG	1:200	1 hr, RT	Invitrogen

Appendix IV: Target sequences of siRNA RACK1

A SMARTpool of ON-TARGETplus RACK1 siRNA (5 nmol) containing a mixture of four siRNA targets to human RACK1 (accessions NM_006098) was obtained as dry pellet from Dharmacon (part of GE Healthcare, USA, catalogue number L-006876-00-0005). The target gene sequences are listed below:

Individual siRNA	Target sequence
J-006876-05	GGCACACGCUAGAAGUUUA
J-006876-06	GAGAUAAGACCAUCAUCAU
J-006876-07	CAUCAAGAUCUGGGAUUUA
J-006876-08	GGCCACAACGGCUGGGUAA

ON-TARGETplus Non-targeting pool (5 nmol, catalogue number D-001810-10-05) was use as a control and the target sequences are provided below:

Non-targeting sequence
1) UGGUUUACAUGUCGACUAA
2) UGGUUUACAUGUUGUGUGA
3) UGGUUUACAUGUUUUCUGA
4) UGGUUUACAUGUUUUCCUA

Appendix V: Plasmid Maps

HCV SGR Rluc

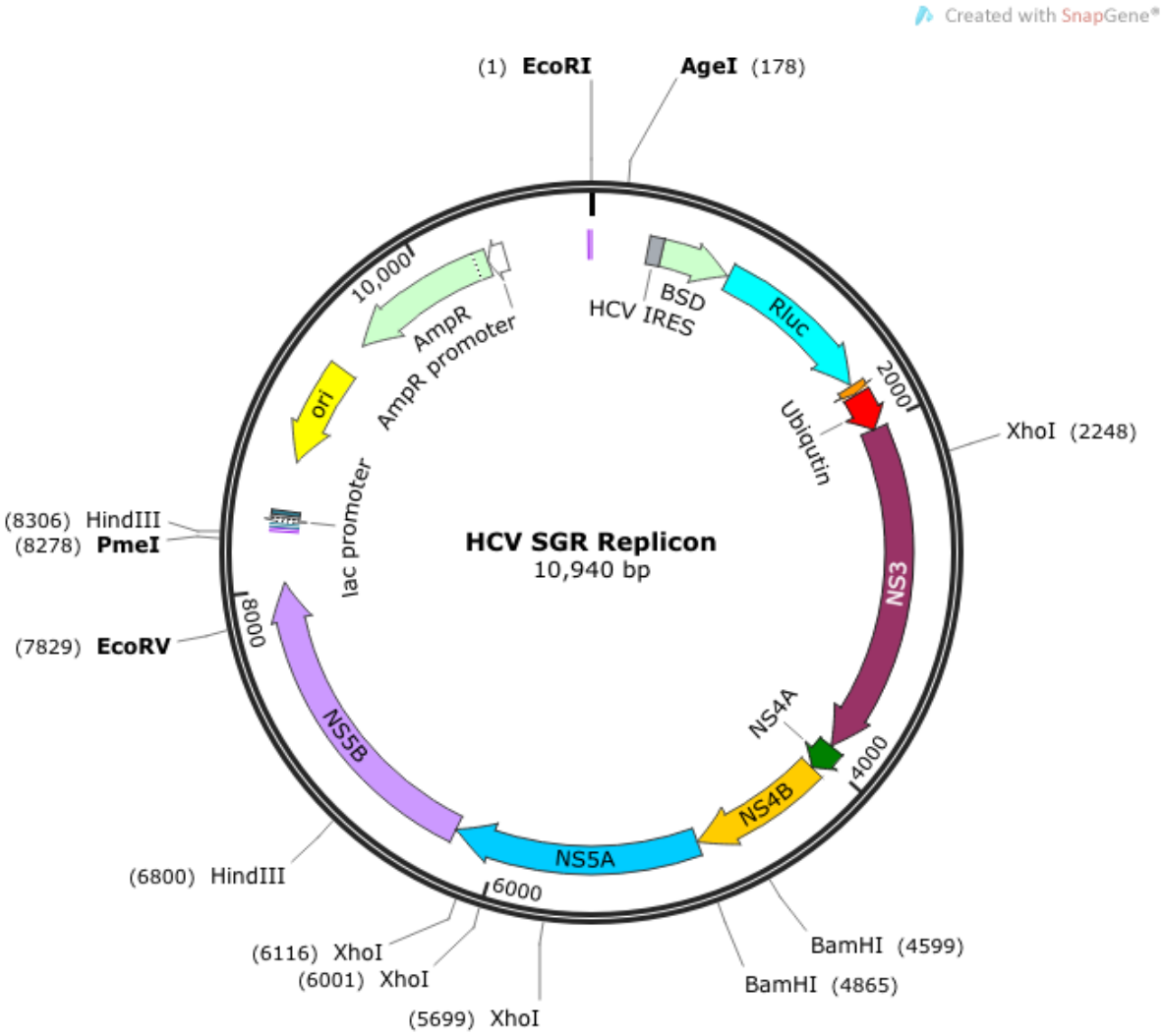

HCV SGR MC

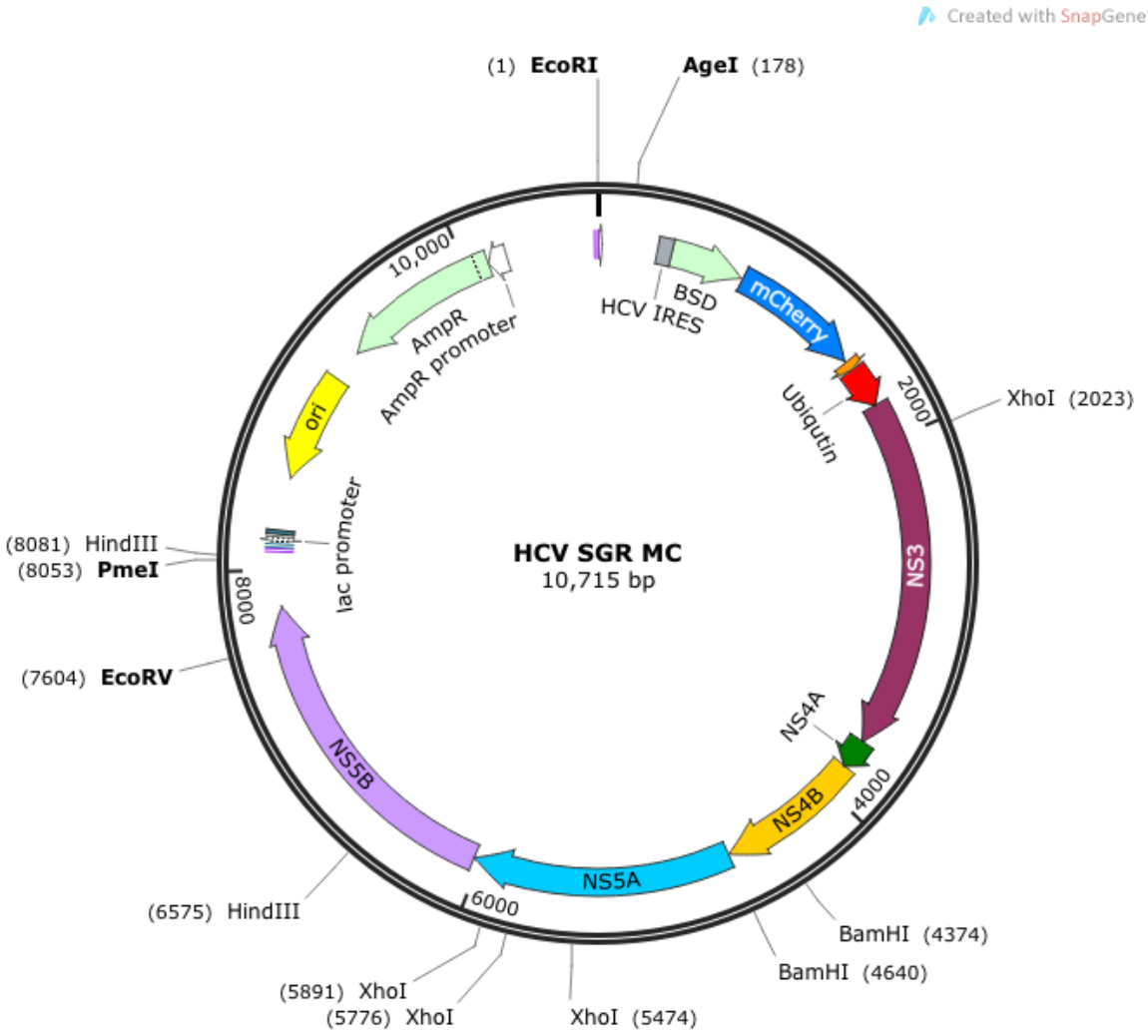
Created with SnapGene®
(1) EcoRI
AgeI (178)
10,000
AmpR
AmpR promoter
ori
HCV IRES
BSD
mCherry
Ubiqutin
2000
XhoI (2023)
NS3
NS4A
NS4B
4000
NS5A
6000
NS5B
8000
lac promoter
(8081) HindIII
(8053) PmeI
(7604) EcoRV
(6575) HindIII
(5891) XhoI
(5776) XhoI
XhoI (5474)
BamHI (4374)
BamHI (4640)
HCV SGR MC
10,715 bp

HCV SGR GFP

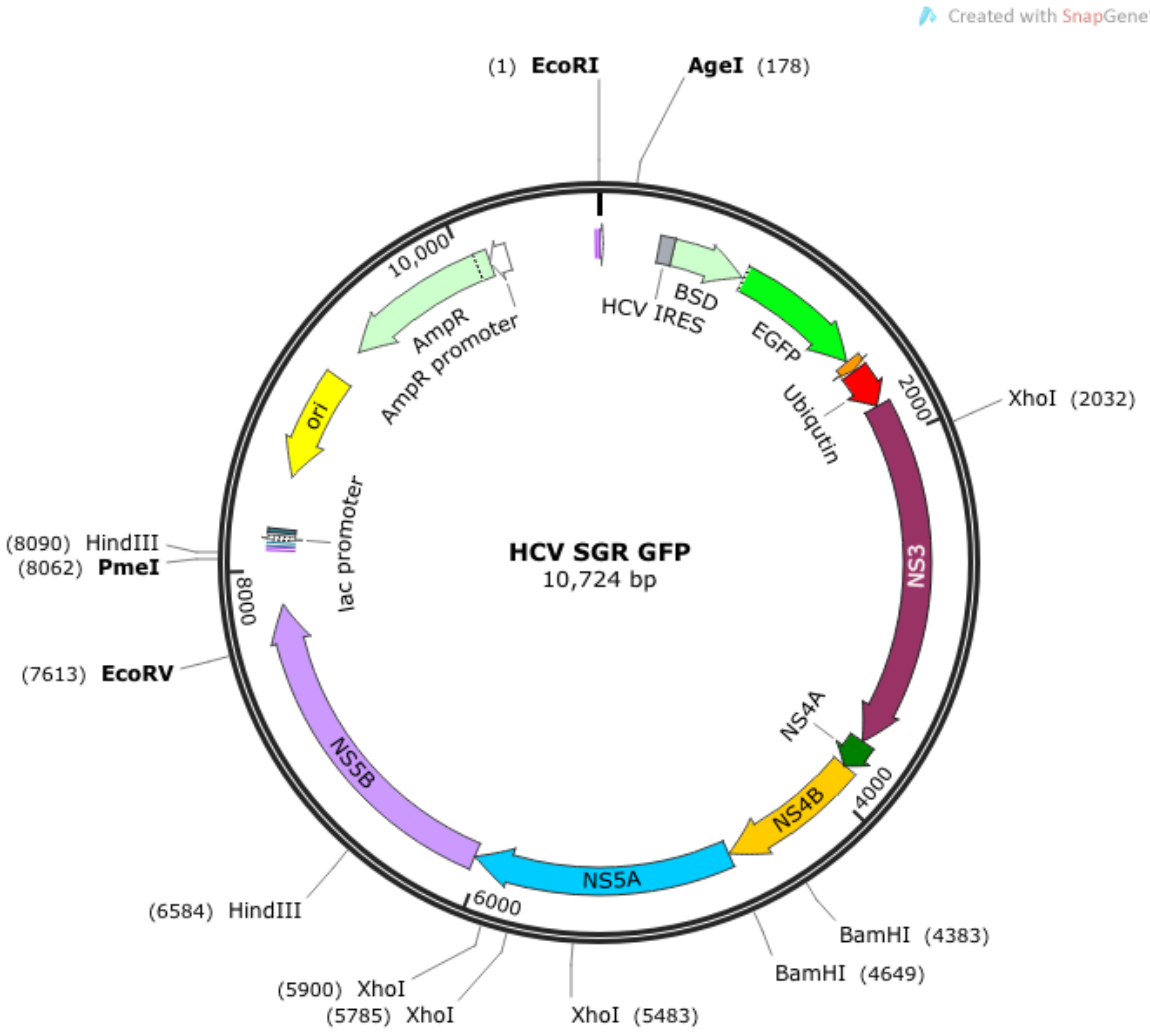
Created with SnapGene®
(1) EcoRI
AgeI (178)
10,000
AmpR
AmpR promoter
ori
HCV IRES
BSD
EGFP
Ubiqutin
2000
XhoI (2032)
NS3
NS4A
NS4B
NS5A
NS5B
4000
6000
8000
lac promoter
(8090) HindIII
(8062) PmeI
(7613) EcoRV
(6584) HindIII
(5900) XhoI
(5785) XhoI
XhoI (5483)
BamHI (4383)
BamHI (4649)
HCV SGR GFP
10,724 bp

HCV SGR TK

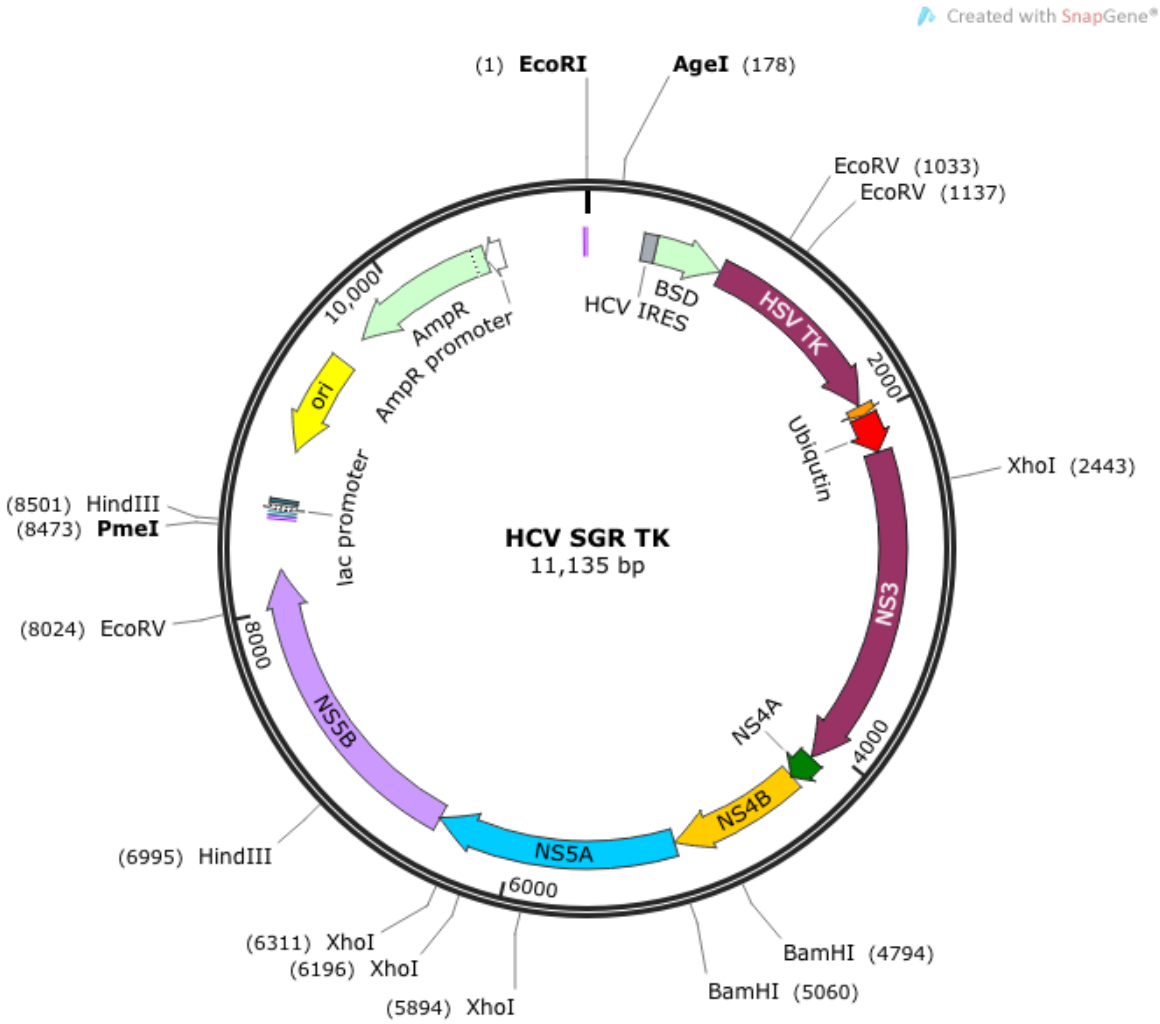
Created with SnapGene®
(1) EcoRI
AgeI (178)
EcoRV (1033)
EcoRV (1137)
XhoI (2443)
BamHI (4794)
BamHI (5060)
(5894) XhoI
(6196) XhoI
(6311) XhoI
(6995) HindIII
(8024) EcoRV
(8473) PmeI
(8501) HindIII
HCV SGR TK
11,135 bp
BSD
HCV IRES
HSV TK
Ubiquitin
NS3
NS4A
NS4B
NS5A
NS5B
lac promoter
ori
AmpR
AmpR promoter
2000
4000
6000
8000
10,000

The pcDNA6.2 N-EmGFP-DEST plasmid was digested with *Xba*I and *Pme*I and Gibson assembly performed for insertion to construct the following plasmids:

- RACK1-2xHA
- ZIKV NS1-FLAG
- ZIKV NS2A-FLAG
- ZIKV NS2B3-FLAG
- ZIKV NS4A-FLAG
- ZIKV 2K-NS4B-FLAG
- ZIKV NS5-FLAG
- DENV NS1-2xFLAG
- WNV_{KUN} NS1-2xFLAG
- YFV NS1-2xFLAG
- ATG5-myc
- ATG14-myc

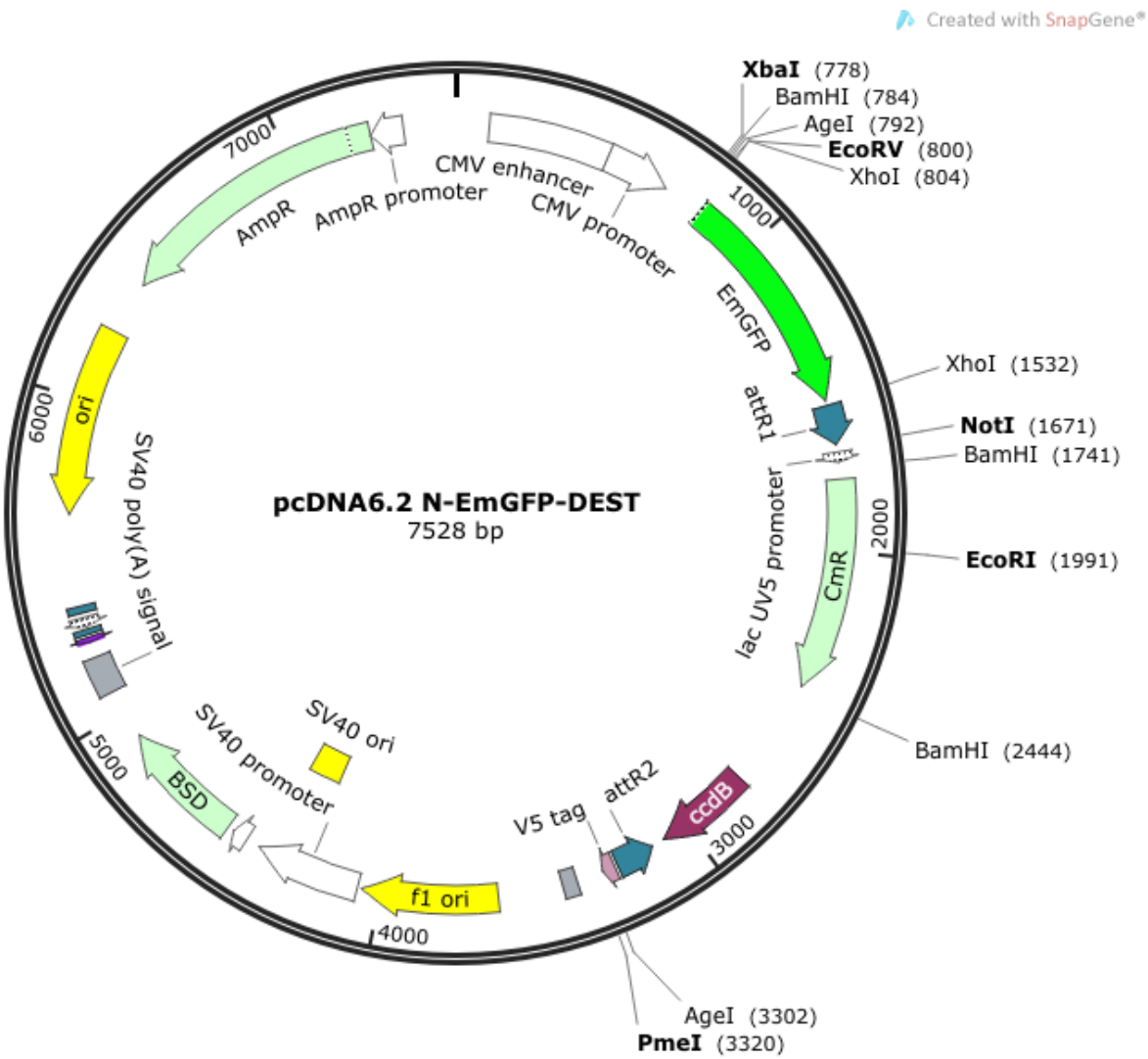

To construct the RACK1 mutant plasmids, each WD domain was removed via PCR amplification of pcDNA6.2 RACK1-2xHA with the appropriate primers (see Appendix I), digested with *Kpn*I and re-ligated.

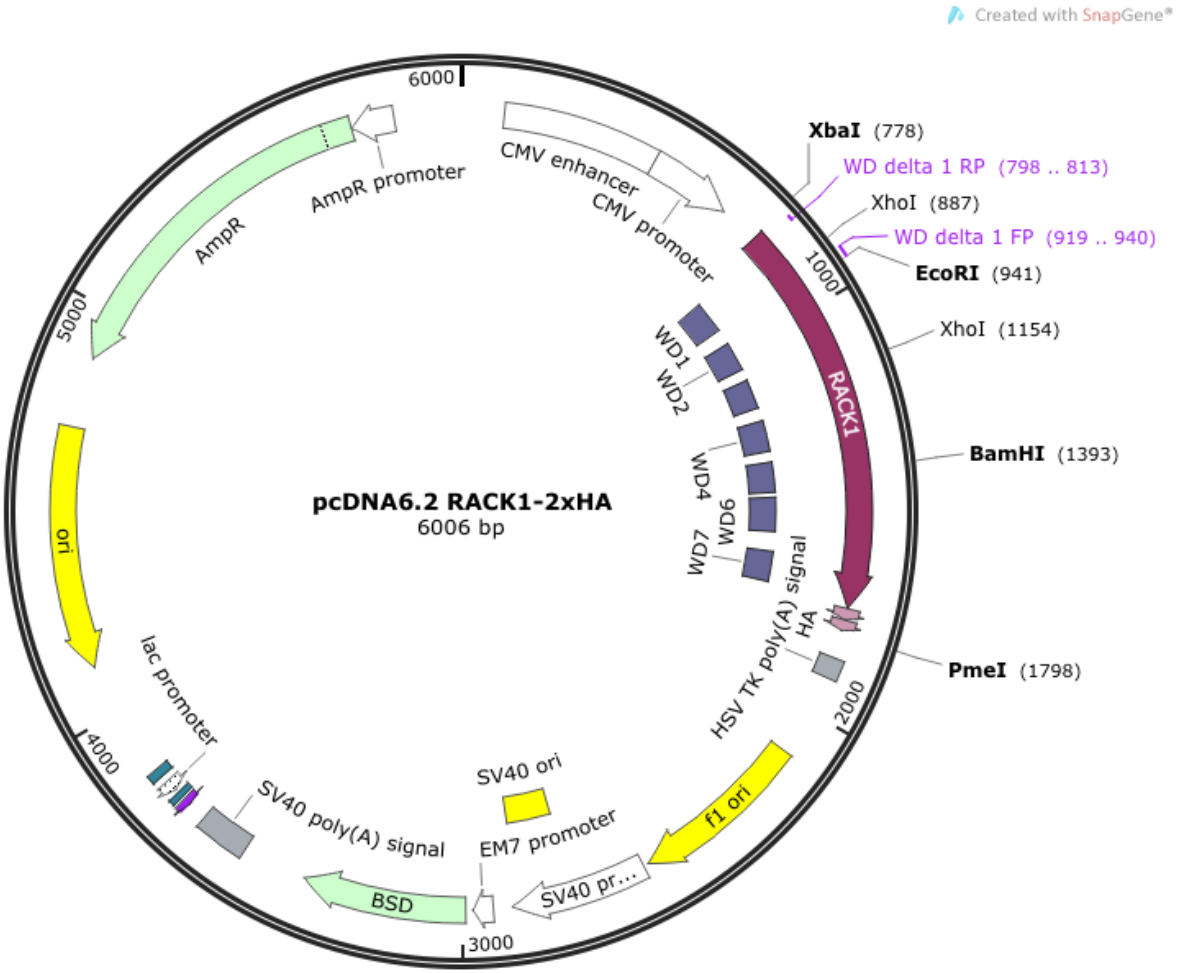

Following PCR amplification (for RACK1 WDΔ1 as an example)

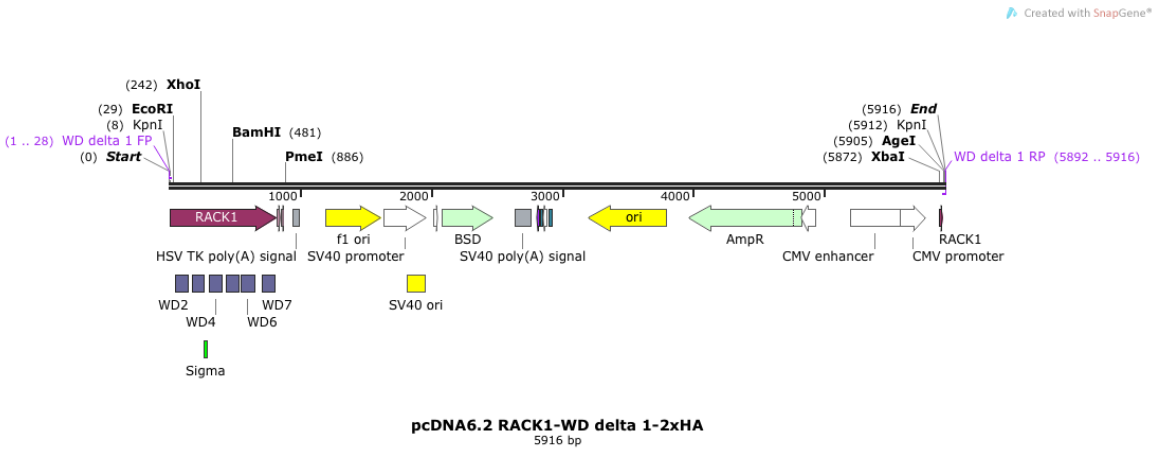

pLenti6-mCherry

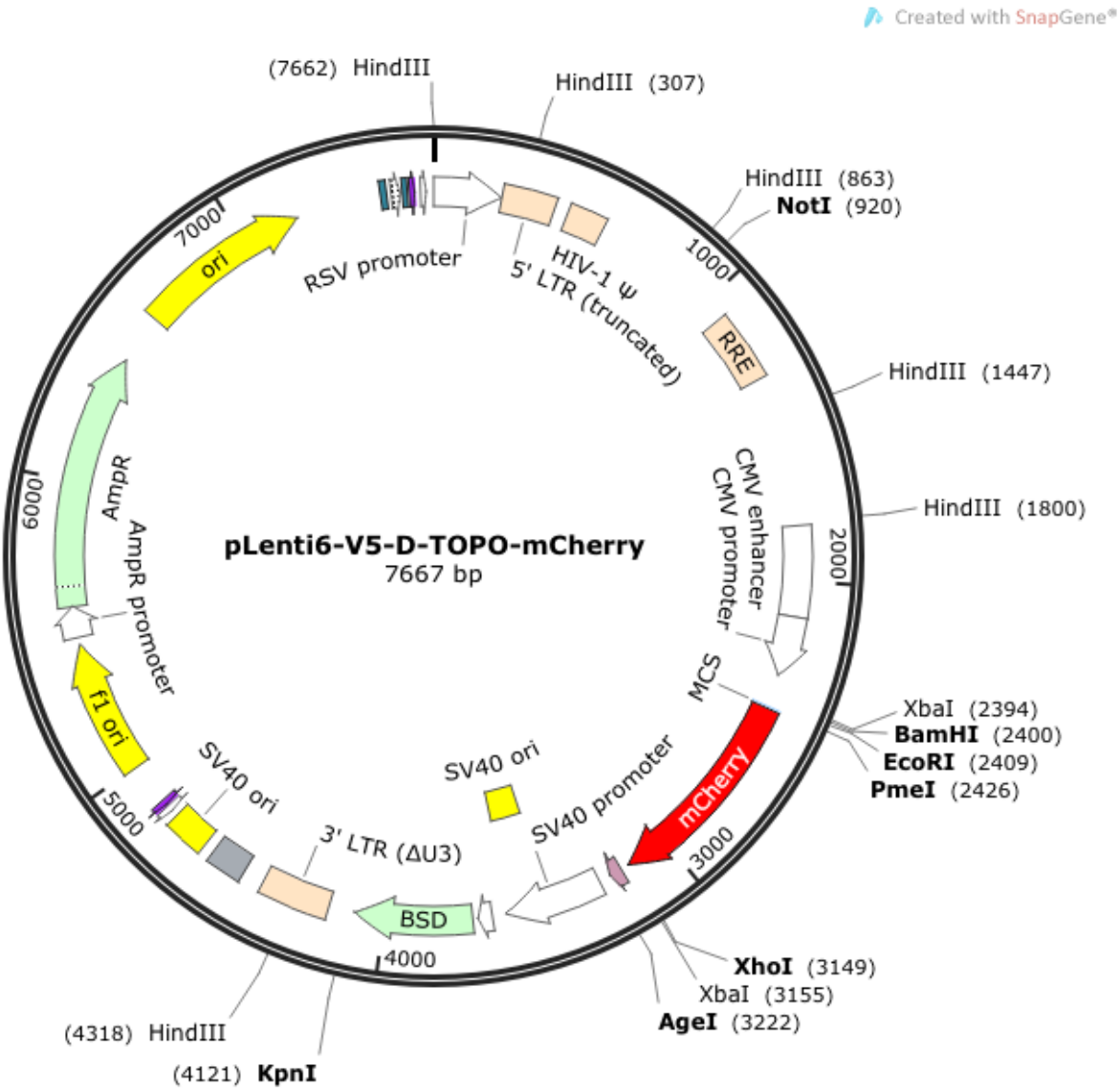

The LentiCRISPRv2 plasmid was digested with *BsmB*I and annealed oligonucleotides with complementary overhangs targeting EGFP, CD81, PI4KA, RACK1, EMC1 and EMC6 (Appendix I) were ligated.

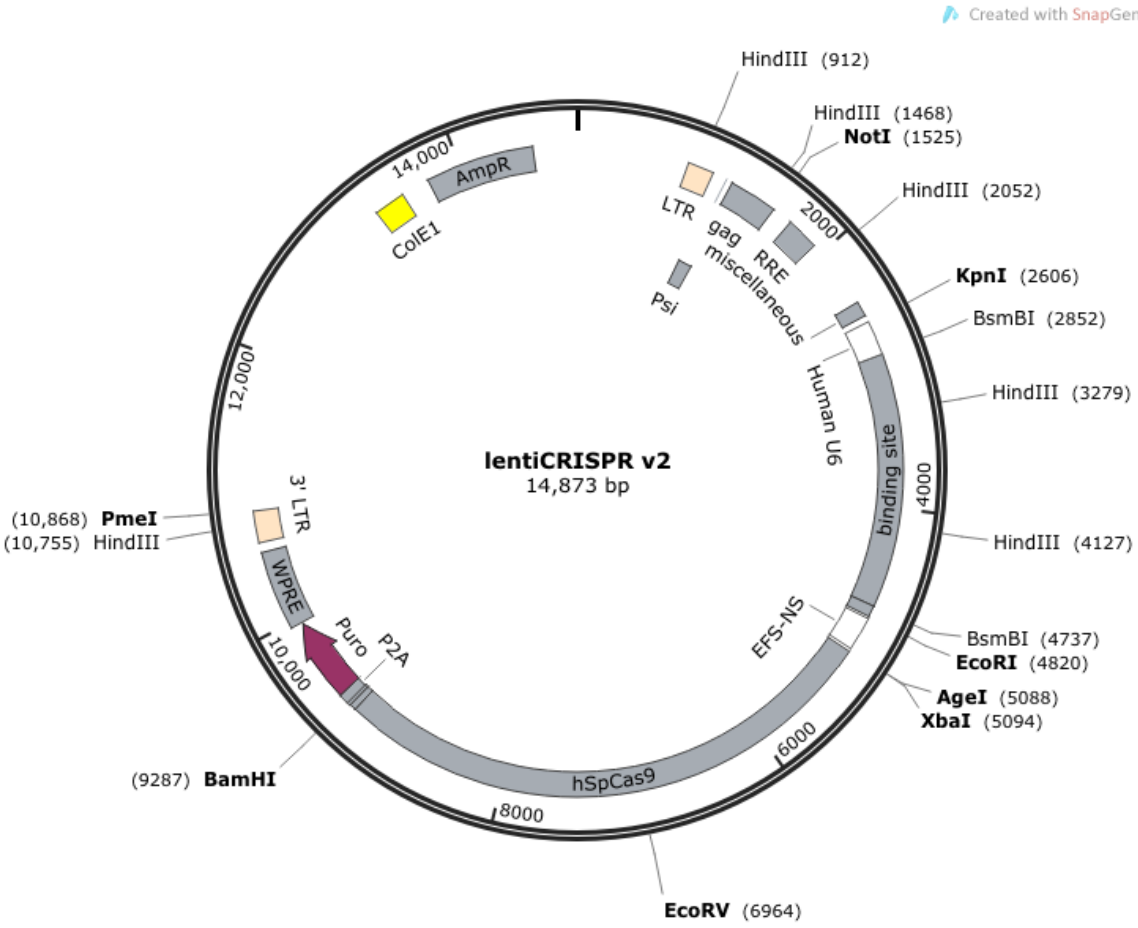

psPAX2

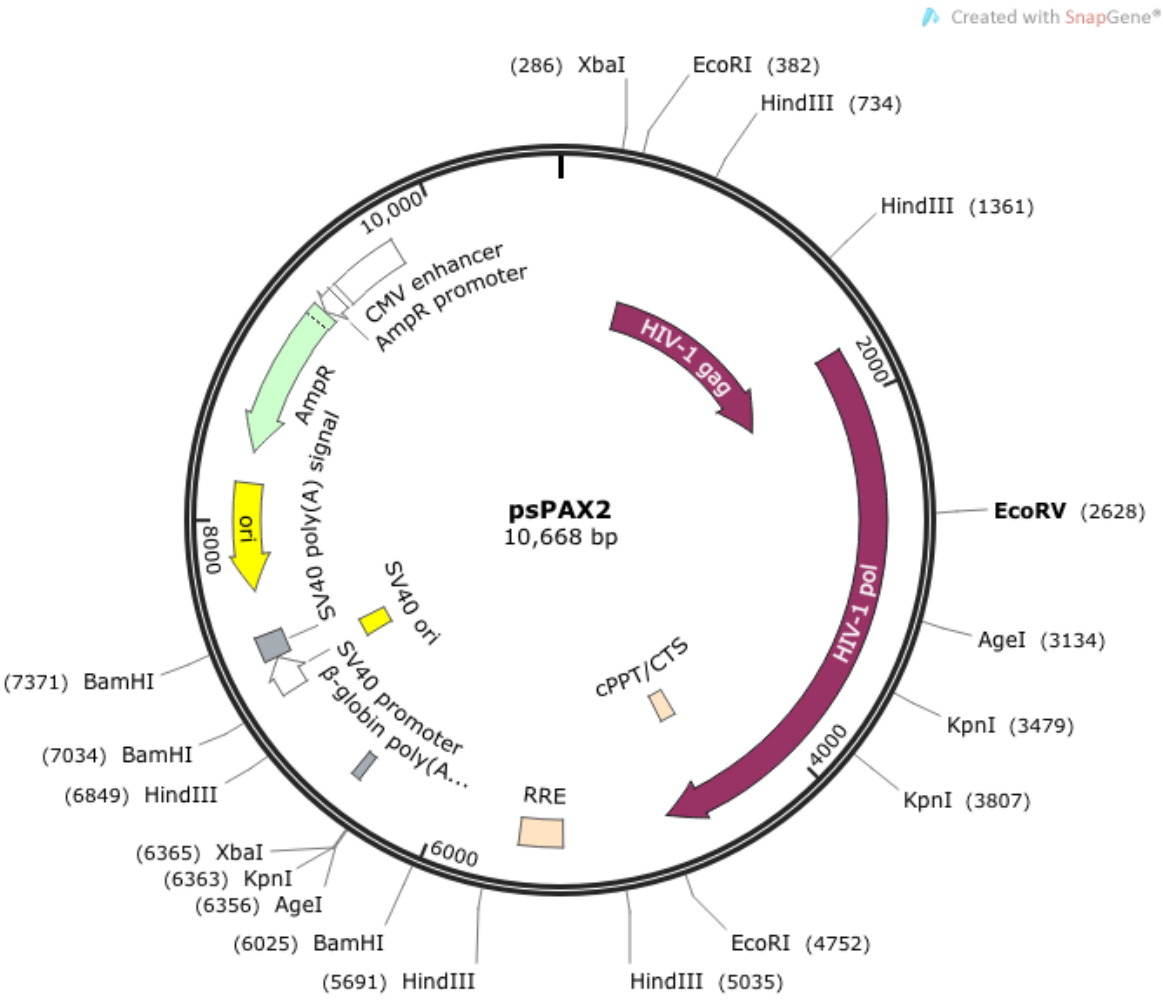
Created with SnapGene®
(286) XbaI
EcoRI (382)
HindIII (734)
HindIII (1361)
EcoRV (2628)
AgeI (3134)
KpnI (3479)
KpnI (3807)
EcoRI (4752)
HindIII (5035)
(5691) HindIII
(6025) BamHI
(6356) AgeI
(6363) KpnI
(6365) XbaI
(6849) HindIII
(7034) BamHI
(7371) BamHI
10,000
2000
4000
6000
8000
psPAX2
10,668 bp
CMV enhancer
AmpR promoter
AmpR
SV40 poly(A) signal
ori
SV40 ori
SV40 promoter
β-globin poly(A...
HIV-1 gag
HIV-1 pol
cPPT/CTS
RRE

pMD2.G

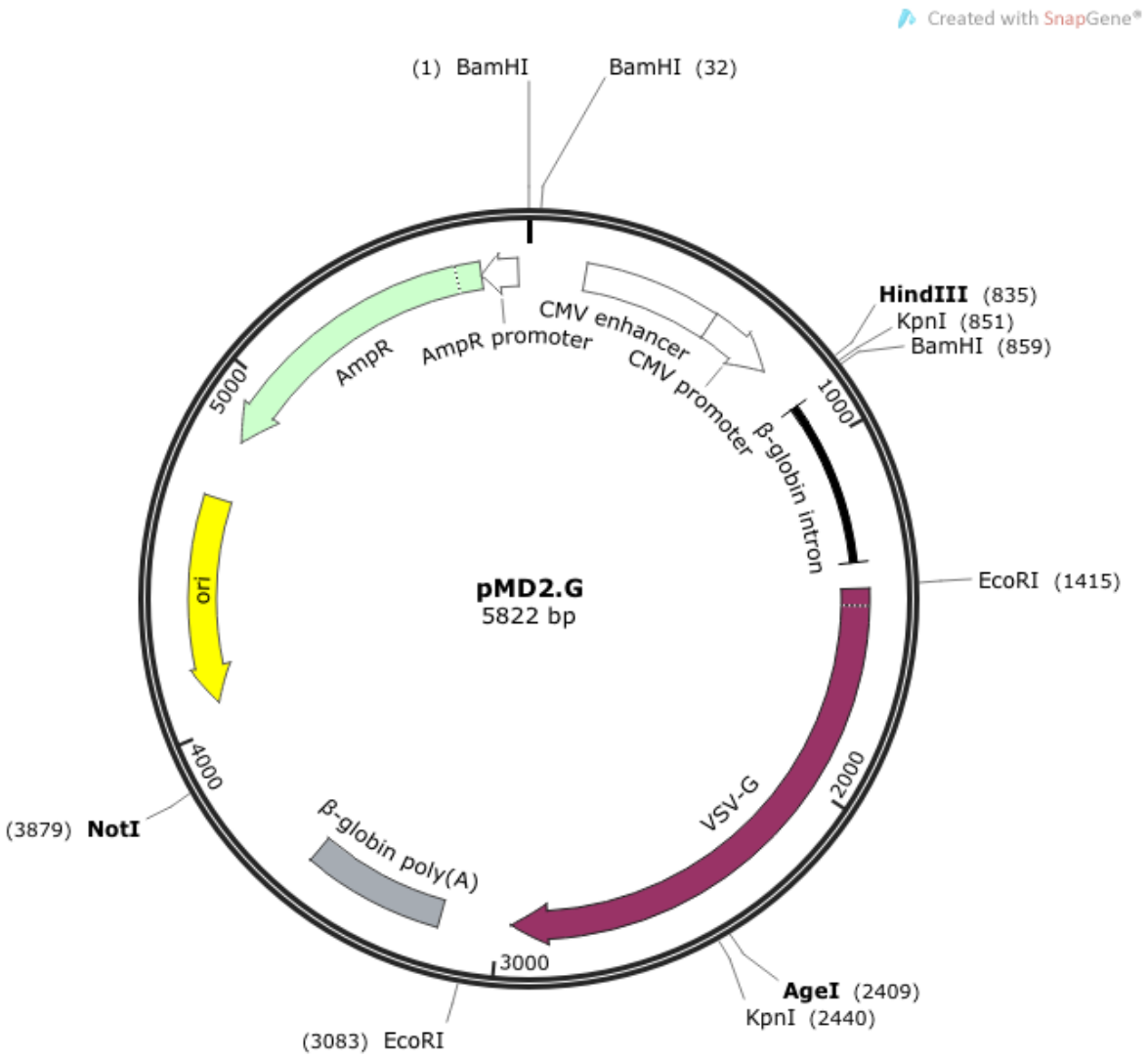
Created with SnapGene®
(1) BamHI
BamHI (32)
HindIII (835)
KpnI (851)
BamHI (859)
EcoRI (1415)
AgeI (2409)
KpnI (2440)
(3083) EcoRI
(3879) NotI
AmpR
AmpR promoter
CMV enhancer
CMV promoter
β-globin intron
ori
β-globin poly(A)
VSV-G
pMD2.G
5822 bp
1000
2000
3000
4000
5000

pFK-sgDVs-R2A

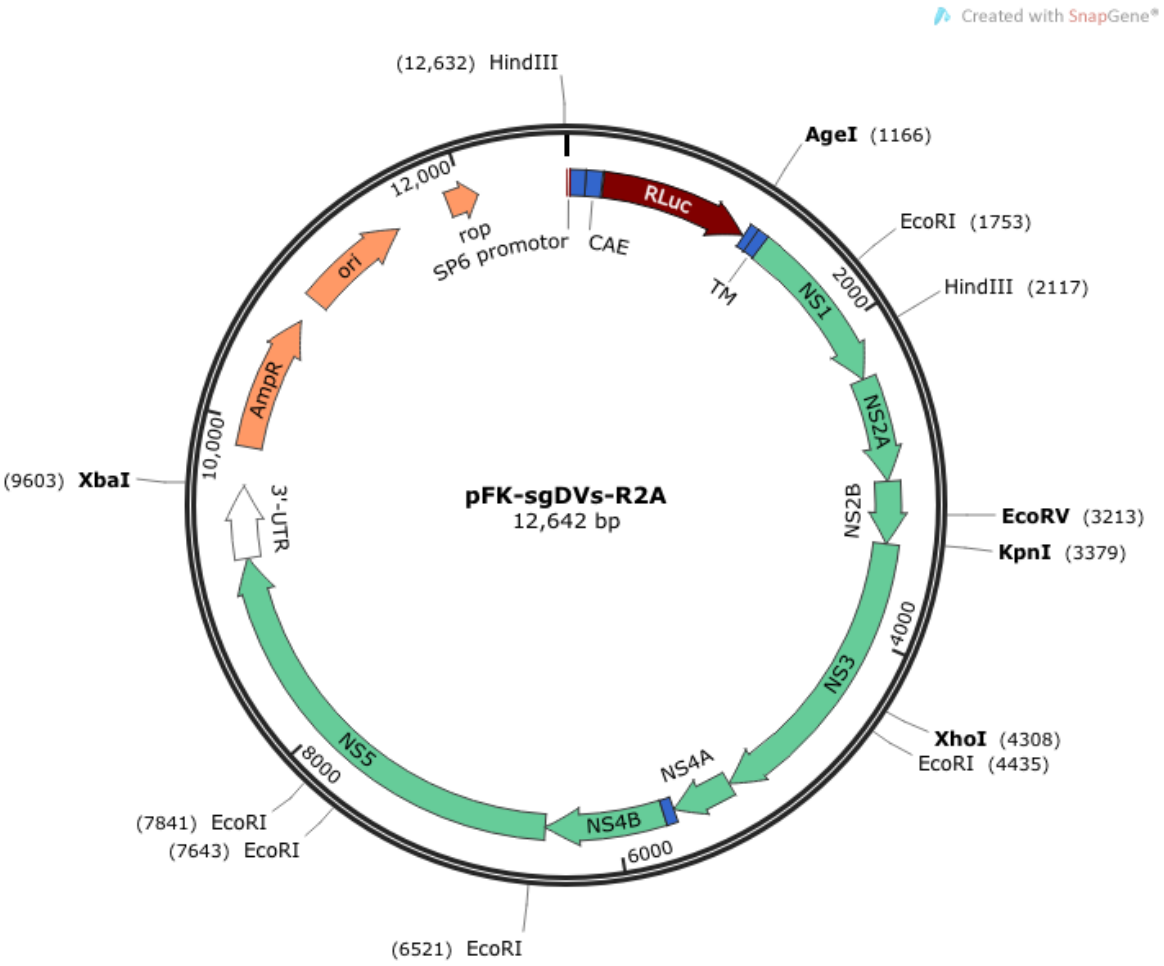

pFK-sgDVs-R2A-GND

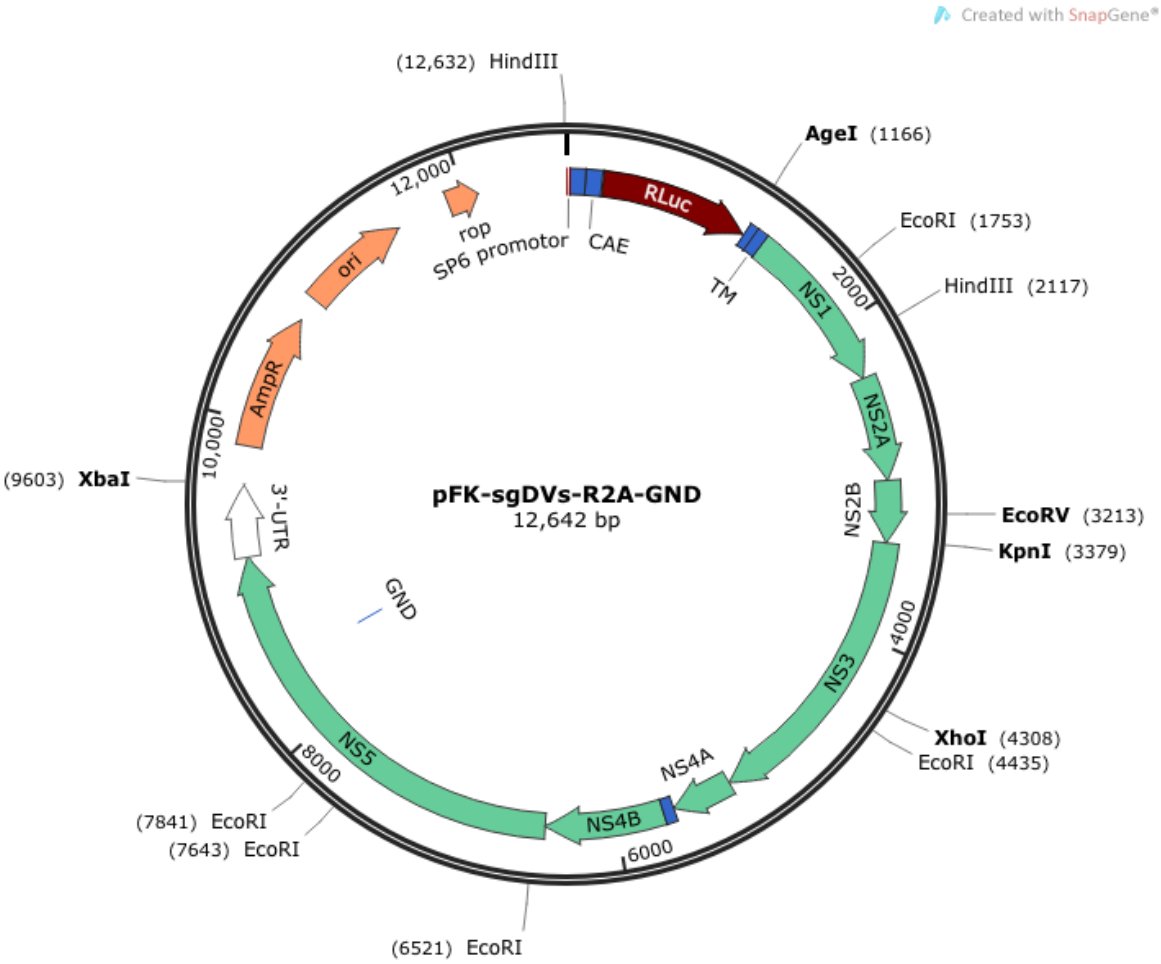

References

Acosta EG, Castilla V, Damonte EB (2012) Differential requirements in endocytic trafficking for penetration of dengue virus. PLoS ONE 7:e44835. doi: 10.1371/journal.pone.0044835

Adams DR, Ron D, Kiely PA (2011) RACK1, A multifaceted scaffolding protein: Structure and function. Cell Commun Signal 9:22–24. doi: 10.1186/1478-811X-9-22

Aguirre S, Luthra P, Sanchez-Aparicio MT, et al (2017) Dengue virus NS2B protein targets cGAS for degradation and prevents mitochondrial DNA sensing during infection. Nat Microbiol 2:17037–11. doi: 10.1038/nmicrobiol.2017.37

Aguirre S, Maestre AM, Pagni S, et al (2012) DENV inhibits type I IFN production in infected cells by cleaving human STING. PLoS Pathog 8:e1002934. doi: 10.1371/journal.ppat.1002934

Aid M, Abbink P, Larocca RA, et al (2017) Zika Virus Persistence in the Central Nervous System and Lymph Nodes of Rhesus Monkeys. Cell 169:610–620.e14. doi: 10.1016/j.cell.2017.04.008

Akey DL, Brown WC, Jose J, et al (2015) Structure-guided insights on the role of NS1 in flavivirus infection. Bioessays 37:489–494. doi: 10.1002/bies.201400182

Akira S, Uematsu S, Takeuchi O (2006) Pathogen recognition and innate immunity. Cell 124:783–801. doi: 10.1016/j.cell.2006.02.015

Aktepe TE, Liebscher S, Prier JE, et al (2017) The Host Protein Reticulon 3.1A Is Utilized by Flaviviruses to Facilitate Membrane Remodelling. Cell Rep 21:1639–1654. doi: 10.1016/j.celrep.2017.10.055

Aktepe TE, Mackenzie JM (2018) Shaping the flavivirus replication complex: It is curvaceous! Cell Microbiol 20:e12884. doi: 10.1111/cmi.12884

Aktepe TE, Pham H, Mackenzie JM (2015) Differential utilisation of ceramide during replication of the flaviviruses West Nile and dengue virus. Virology 484:241–250. doi: 10.1016/j.virol.2015.06.015

Albulescu L, Bigay J, Biswas B, et al (2017) Uncovering oxysterol-binding protein (OSBP) as a target of the anti-enteroviral compound TTP-8307. Antiviral Res 140:37–44. doi: 10.1016/j.antiviral.2017.01.008

Allison SL, Schalich J, Stiasny K, et al (2001) Mutational evidence for an internal fusion peptide in flavivirus envelope protein E. J Virol 75:4268–4275. doi: 10.1128/JVI.75.9.4268-4275.2001

Alvarez DE, Lodeiro MF, Ludueña SJ, et al (2005) Long-range RNA-RNA interactions circularize the dengue virus genome. J Virol 79:6631–6643. doi: 10.1128/JVI.79.11.6631-6643.2005

Alvisi G, Madan V, Bartenschlager R (2011) Hepatitis C virus and host cell lipids: an intimate connection. RNA Biol 8:258–269. doi: 10.4161/rna.8.2.15011

Amako Y, Sarkeshik A, Hotta H, et al (2009) Role of oxysterol binding protein in hepatitis C virus infection. J Virol 83:9237–9246. doi: 10.1128/JVI.00958-09

Angleró-Rodríguez YI, Pantoja P, Sariol CA (2014) Dengue virus subverts the interferon induction pathway via NS2B/3 protease-IκB kinase epsilon interaction. Clin Vaccine Immunol 21:29–38. doi: 10.1128/CVI.00500-13

Appel N, Pietschmann T, Bartenschlager R (2005) Mutational analysis of hepatitis C virus nonstructural protein 5A: potential role of differential phosphorylation in RNA replication and identification of a genetically flexible domain. J Virol 79:3187–3194. doi: 10.1128/JVI.79.5.3187-3194.2005

Ashour J, Laurent-Rolle M, Shi PY, Garcia-Sastre A (2009) NS5 of Dengue Virus Mediates STAT2 Binding and Degradation. J Virol 83:5408–5418. doi: 10.1128/JVI.02188-08

Assenberg R, Mastrangelo E, Walter TS, et al (2009) Crystal structure of a novel conformational state of the flavivirus NS3 protein: implications for polyprotein processing and viral replication. J Virol 83:12895–12906. doi: 10.1128/JVI.00942-09

Atoom AM, Taylor NGA, Russell RS (2014) The elusive function of the hepatitis C virus p7 protein. Virology 462-463:377–387. doi: 10.1016/j.virol.2014.04.018

Bai Y, Zhou K, Doudna JA (2013) Hepatitis C virus 3'UTR regulates viral translation through direct interactions with the host translation machinery. Nucleic Acids Res 41:7861–7874. doi: 10.1093/nar/gkt543

Bailey CC, Zhong G, Huang I-C, Farzan M (2014) IFITM-Family Proteins: The Cell's First Line of Antiviral Defense. Annu Rev Virol 1:261–283. doi: 10.1146/annurev-virology-031413-085537

Barrangou R, Marraffini LA (2014) CRISPR-Cas systems: Prokaryotes upgrade to adaptive immunity. Mol Cell 54:234–244. doi: 10.1016/j.molcel.2014.03.011

Barrows NJ, Anglero-Rodriguez Y, Kim B, et al (2019) Dual roles for the ER membrane protein complex in flavivirus infection: viral entry and protein biogenesis. Scientific Reports 9:9711–16. doi: 10.1038/s41598-019-45910-9

Baumann M, Gires O, Kolch W, et al (2000) The PKC targeting protein RACK1 interacts with the Epstein-Barr virus activator protein BZLF1. Eur J Biochem 267:3891–3901. doi: 10.1046/j.1432-1327.2000.01430.x

Beatty PR, Puerta-Guardo H, Killingbeck SS, et al (2015) Dengue virus NS1 triggers endothelial permeability and vascular leak that is prevented by NS1 vaccination. Sci Transl Med 7:304ra141–304ra141. doi: 10.1126/scitranslmed.aaa3787

Beck A, Tesh RB, Wood TG, et al (2014) Comparison of the live attenuated yellow fever vaccine 17D-204 strain to its virulent parental strain Asibi by deep sequencing. J Infect Dis 209:334–344. doi: 10.1093/infdis/jit546

Berger KL, Cooper JD, Heaton NS, et al (2009) Roles for endocytic trafficking and phosphatidylinositol 4-kinase III alpha in hepatitis C virus replication. Proc Natl Acad Sci USA 106:7577–7582. doi: 10.1073/pnas.0902693106

Berger KL, Kelly SM, Jordan TX, et al (2011) Hepatitis C virus stimulates the phosphatidylinositol 4-kinase III alpha-dependent phosphatidylinositol 4-phosphate production that is essential for its replication. J Virol 85:8870–8883. doi: 10.1128/JVI.00059-11

Best SM (2013) Viruses PLAY DEAD to TAMe interferon responses. Cell Host Microbe 14:117–118. doi: 10.1016/j.chom.2013.07.014

Best SM (2017) The Many Faces of the Flavivirus NS5 Protein in Antagonism of Type I Interferon Signaling. J Virol. doi: 10.1128/JVI.01970-16

Bi J, Zhao Q, Zhu L, et al (2018) RACK1 is indispensable for porcine reproductive and respiratory syndrome virus replication and NF-κB activation in Marc-145 cells. Scientific Reports 8:2985–12. doi: 10.1038/s41598-018-21460-4

Bi Y, Sun L, Gao D, et al (2014) High-efficiency targeted editing of large viral genomes by RNA-guided nucleases. PLoS Pathog 10:e1004090. doi: 10.1371/journal.ppat.1004090

Bindels DS, Haarbosch L, van Weeren L, et al (2017) mScarlet: a bright monomeric red fluorescent protein for cellular imaging. Nat Methods 14:53–56. doi: 10.1038/nmeth.4074

Biswas A, Treadaway J, Tellinghuisen TL (2016) Interaction between Nonstructural Proteins NS4B and NS5A Is Essential for Proper NS5A Localization and Hepatitis C Virus RNA Replication. J Virol 90:7205–7218. doi: 10.1128/JVI.00037-16

Blight KJ, McKeating JA, Rice CM (2002) Highly permissive cell lines for subgenomic and genomic hepatitis C virus RNA replication. J Virol 76:13001–13014. doi: 10.1128/jvi.76.24.13001-13014.2002

Blomstrom DC, Fahey D, Kutny R, et al (1986) Molecular characterization of the interferon-induced 15-kDa protein. Molecular cloning and nucleotide and amino acid sequence. J Biol Chem 261:8811–8816.

Bluyssen HA, Vlietstra RJ, van der Made A, Trapman J (1994) The interferon-stimulated gene 54 K promoter contains two adjacent functional interferon-stimulated response elements of different strength, which act synergistically for maximal interferon-alpha inducibility. Eur J Biochem 220:395–402. doi: 10.1111/j.1432-1033.1994.tb18636.x

Bojjireddy N, Botyanszki J, Hammond G, et al (2014) Pharmacological and genetic targeting of the PI4KA enzyme reveals its important role in maintaining plasma

membrane phosphatidylinositol 4-phosphate and phosphatidylinositol 4,5-bisphosphate levels. J Biol Chem 289:6120–6132. doi: 10.1074/jbc.M113.531426

Borawski J, Troke P, Puyang X, et al (2009) Class III phosphatidylinositol 4-kinase alpha and beta are novel host factor regulators of hepatitis C virus replication. J Virol 83:10058–10074. doi: 10.1128/JVI.02418-08

Botos I, Segal DM, Davies DR (2011) The structural biology of Toll-like receptors. Structure 19:447–459. doi: 10.1016/j.str.2011.02.004

Botta L, Rivara M, Zuliani V, Radi M (2018) Drug repurposing approaches to fight Dengue virus infection and related diseases. Front Biosci (Landmark Ed) 23:997–1019. doi: 10.2741/4630

Brass V, Berke JM, Montserret R, et al (2008) Structural determinants for membrane association and dynamic organization of the hepatitis C virus NS3-4A complex. Proc Natl Acad Sci USA 105:14545–14550. doi: 10.1073/pnas.0807298105

Brès PL (1986) A century of progress in combating yellow fever. Bull World Health Organ 64:775–786.

Brubaker SW, Bonham KS, Zanoni I, Kagan JC (2015) Innate immune pattern recognition: a cell biological perspective. Annu Rev Immunol 33:257–290. doi: 10.1146/annurev-immunol-032414-112240

Byk LA, Iglesias NG, De Maio FA, et al (2016) Dengue Virus Genome Uncoating Requires Ubiquitination. MBio 7:504. doi: 10.1128/mBio.00804-16

Carlin AF, Vizcarra EA, Branche E, et al (2018) Deconvolution of pro- and antiviral genomic responses in Zika virus-infected and bystander macrophages. Proc Natl Acad Sci USA 115:E9172–E9181. doi: 10.1073/pnas.1807690115

Carpentier A, Sheldon J, Vondran FWR, et al (2020) Efficient acute and chronic infection of stem cell-derived hepatocytes by hepatitis C virus. Gut 69:1659–1666. doi: 10.1136/gutjnl-2019-319354

Carrère-Kremer S, Montpellier C, Lorenzo L, et al (2004) Regulation of hepatitis C virus polyprotein processing by signal peptidase involves structural determinants at the p7 sequence junctions. J Biol Chem 279:41384–41392. doi: 10.1074/jbc.M406315200

Castillo Ramirez JA, Urcuqui-Inchima S (2015) Dengue Virus Control of Type I IFN Responses: A History of Manipulation and Control. J Interferon Cytokine Res 35:421–430. doi: 10.1089/jir.2014.0129

Cathey JT, Marr JS (2014) Yellow fever, Asia and the East African slave trade. Trans R Soc Trop Med Hyg 108:252–257. doi: 10.1093/trstmh/tru043

Ceballos-Olvera I, Chávez-Salinas S, Medina F, et al (2010) JNK phosphorylation, induced during dengue virus infection, is important for viral infection and requires the presence of cholesterol. Virology 396:30–36. doi: 10.1016/j.virol.2009.10.019

Cerikan B, Goellner S, Neufeldt CJ, et al (2020) A Non-Replicative Role of the 3' Terminal Sequence of the Dengue Virus Genome in Membranous Replication Organelle Formation. Cell Rep 32:107859. doi: 10.1016/j.celrep.2020.107859

Chan JFW, Choi GKY, Yip CCY, et al (2016) Zika fever and congenital Zika syndrome: An unexpected emerging arboviral disease. J Infect 72:507–524. doi: 10.1016/j.jinf.2016.02.011

Chang BY, Harte RA, Cartwright CA (2002) RACK1: a novel substrate for the Src protein-tyrosine kinase. Oncogene 21:7619–7629. doi: 10.1038/sj.onc.1206002

Chatel-Chaix L, Bartenschlager R (2014) Dengue virus- and hepatitis C virus-induced replication and assembly compartments: the enemy inside--caught in the web. J Virol 88:5907–5911. doi: 10.1128/JVI.03404-13

Chen B, Gilbert LA, Cimini BA, et al (2013) Dynamic imaging of genomic loci in living human cells by an optimized CRISPR/Cas system. Cell 155:1479–1491. doi: 10.1016/j.cell.2013.12.001

Chen S, Sanjana NE, Zheng K, et al (2015) Genome-wide CRISPR screen in a mouse model of tumor growth and metastasis. Cell 160:1246–1260. doi: 10.1016/j.cell.2015.02.038

Cheriyath V, Glaser KB, Waring JF, et al (2007) G1P3, an IFN-induced survival factor, antagonizes TRAIL-induced apoptosis in human myeloma cells. J Clin Invest 117:3107–3117. doi: 10.1172/JCI31122

Chiramel AI, Best SM (2018) Role of autophagy in Zika virus infection and pathogenesis. Virus Res 254:34–40. doi: 10.1016/j.virusres.2017.09.006

Chiramel AI, Meyerson NR, McNally KL, et al (2019) TRIM5α Restricts Flavivirus Replication by Targeting the Viral Protease for Proteasomal Degradation. Cell Rep 27:3269–3283.e6. doi: 10.1016/j.celrep.2019.05.040

Chiu W-W, Kinney RM, Dreher TW (2005) Control of translation by the 5“- and 3-”terminal regions of the dengue virus genome. J Virol 79:8303–8315. doi: 10.1128/JVI.79.13.8303-8315.2005

Choo QL, Kuo G, Weiner AJ, et al (1989) Isolation of a cDNA clone derived from a blood-borne non-A, non-B viral hepatitis genome. Science 244:359–362. doi: 10.1126/science.2523562

Chu L-W, Yang C-J, Peng K-J, et al (2019) TIM-1 As a Signal Receptor Triggers Dengue Virus-Induced Autophagy. Int J Mol Sci 20:4893. doi: 10.3390/ijms20194893

Chuang Y-C, Lin Y-S, Liu C-C, et al (2013) Factors contributing to the disturbance of coagulation and fibrinolysis in dengue virus infection. J Formos Med Assoc 112:12–17. doi: 10.1016/j.jfma.2012.10.013

Chuansumrit A, Chaiyaratana W (2014) Hemostatic derangement in dengue hemorrhagic fever. Thromb Res 133:10–16. doi: 10.1016/j.thromres.2013.09.028

Chukkapalli V, Randall G (2014) Hepatitis C virus replication compartment formation: mechanism and drug target. Gastroenterology 146:1164–1167. doi: 10.1053/j.gastro.2014.03.017

Ci Y, Liu Z-Y, Zhang N-N, et al (2020) Zika NS1-induced ER remodeling is essential for viral replication. J Cell Biol 219:881. doi: 10.1083/jcb.201903062

Clements AN, Harbach RE (2017) History of the discovery of the mode of transmission of yellow fever virus. J Vector Ecol 42:208–222. doi: 10.1111/jvec.12261

Coldbeck-Shackley RC, Eyre NS, Beard MR (2020) The Molecular Interactions of ZIKV and DENV with the Type-I IFN Response. Vaccines (Basel) 8:530. doi: 10.3390/vaccines8030530

Coller KE, Berger KL, Heaton NS, et al (2009) RNA interference and single particle tracking analysis of hepatitis C virus endocytosis. PLoS Pathog 5:e1000702. doi: 10.1371/journal.ppat.1000702

Colpitts TM, Barthel S, Wang P, Fikrig E (2011) Dengue virus capsid protein binds core histones and inhibits nucleosome formation in human liver cells. PLoS ONE 6:e24365. doi: 10.1371/journal.pone.0024365

Counihan NA, Rawlinson SM, Lindenbach BD (2011) Trafficking of hepatitis C virus core protein during virus particle assembly. PLoS Pathog 7:e1002302. doi: 10.1371/journal.ppat.1002302

Crosse KM, Monson EA, Dumbrepatil AB, et al (2020) Viperin binds STING and enhances the type-I interferon response following dsDNA detection. Immunol Cell Biol imcb.12420. doi: 10.1111/imcb.12420

Cui S, Eisenächer K, Kirchhofer A, et al (2008) The C-terminal regulatory domain is the RNA 5'-triphosphate sensor of RIG-I. Mol Cell 29:169–179. doi: 10.1016/j.molcel.2007.10.032

D'Angelo G, Vicinanza M, Di Campli A, De Matteis MA (2008) The multiple roles of PtdIns(4)P -- not just the precursor of PtdIns(4,5)P2. J Cell Sci 121:1955–1963. doi: 10.1242/jcs.023630

Daep CA, Muñoz-Jordán JL, Eugenin EA (2014) Flaviviruses, an expanding threat in public health: focus on dengue, West Nile, and Japanese encephalitis virus. J Neurovirol 20:539–560. doi: 10.1007/s13365-014-0285-z

Daffis S, Szretter KJ, Schriewer J, et al (2010) 2'-O methylation of the viral mRNA cap evades host restriction by IFIT family members. Nature 468:452–456. doi: 10.1038/nature09489

Dalrymple NA, Cimica V, Mackow ER (2015) Dengue Virus NS Proteins Inhibit RIG-I/MAVS Signaling by Blocking TBK1/IRF3 Phosphorylation: Dengue Virus Serotype 1 NS4A Is a Unique Interferon-Regulating Virulence Determinant. MBio 6:e00553–15. doi: 10.1128/mBio.00553-15

Dang J, Tiwari SK, Lichinchi G, et al (2016) Zika Virus Depletes Neural Progenitors in Human Cerebral Organoids through Activation of the Innate Immune Receptor TLR3. Cell Stem Cell 19:258–265. doi: 10.1016/j.stem.2016.04.014

Dawes BE, Smalley CA, Tiner BL, et al (2016) Research and development of Zika virus vaccines. NPJ Vaccines 1:16007–7. doi: 10.1038/npjvaccines.2016.7

de Weerd NA, Nguyen T (2012) The interferons and their receptors--distribution and regulation. Immunol Cell Biol 90:483–491. doi: 10.1038/icb.2012.9

Decroly E, Ferron F, Lescar J, Canard B (2011) Conventional and unconventional mechanisms for capping viral mRNA. Nat Rev Microbiol 10:51–65. doi: 10.1038/nrmicro2675

Deen J (2016) The Dengue Vaccine Dilemma: Balancing the Individual and Population Risks and Benefits. PLoS Med 13:e1002182. doi: 10.1371/journal.pmed.1002182

DeFilippis VR, Robinson B, Keck TM, et al (2006) Interferon regulatory factor 3 is necessary for induction of antiviral genes during human cytomegalovirus infection. J Virol 80:1032–1037. doi: 10.1128/JVI.80.2.1032-1037.2006

Dejarnac O, Hafirassou ML, Chazal M, et al (2018) TIM-1 Ubiquitination Mediates Dengue Virus Entry. Cell Rep 23:1779–1793. doi: 10.1016/j.celrep.2018.04.013

Dejnirattisai W, Supasa P, Wongwiwat W, et al (2016) Dengue virus sero-cross-reactivity drives antibody-dependent enhancement of infection with zika virus. Nat Immunol 17:1102–1108. doi: 10.1038/ni.3515

Del Campo M, Feitosa IML, Ribeiro EM, et al (2017) The phenotypic spectrum of congenital Zika syndrome. Am J Med Genet A 173:841–857. doi: 10.1002/ajmg.a.38170

Demirov D, Gabriel G, Schneider C, et al (2012) Interaction of influenza A virus matrix protein with RACK1 is required for virus release. Cell Microbiol 14:774–789. doi: 10.1111/j.1462-5822.2012.01759.x

Denolly S, Mialon C, Bourlet T, et al (2017) The amino-terminus of the hepatitis C virus (HCV) p7 viroporin and its cleavage from glycoprotein E2-p7 precursor determine specific infectivity and secretion levels of HCV particle types. PLoS Pathog 13:e1006774. doi: 10.1371/journal.ppat.1006774

Doench JG, Fusi N, Sullender M, et al (2016) Optimized sgRNA design to maximize activity and minimize off-target effects of CRISPR-Cas9. Nat Biotechnol 34:184–191. doi: 10.1038/nbt.3437

Dong C, Qu L, Wang H, et al (2015) Targeting hepatitis B virus cccDNA by CRISPR/Cas9 nuclease efficiently inhibits viral replication. Antiviral Res 118:110–117. doi: 10.1016/j.antiviral.2015.03.015

Du X, Shen X, Dai L, et al (2020) PSMD12 promotes breast cancer growth via inhibiting the expression of pro-apoptotic genes. Biochem Biophys Res Commun. doi: 10.1016/j.bbrc.2020.03.095

Dukhovny A, Lamkiewicz K, Chen Q, et al (2019) A CRISPR Activation Screen Identifies Genes That Protect against Zika Virus Infection. J Virol 93:707. doi: 10.1128/JVI.00211-19

Duschene KS, Broderick JB (2010) The antiviral protein viperin is a radical SAM enzyme. FEBS Lett 584:1263–1267. doi: 10.1016/j.febslet.2010.02.041

Dutra HLC, Rocha MN, Dias FBS, et al (2016) Wolbachia Blocks Currently Circulating Zika Virus Isolates in Brazilian Aedes aegypti Mosquitoes. Cell Host Microbe 19:771–774. doi: 10.1016/j.chom.2016.04.021

Dutta D, Clevers H (2017) Organoid culture systems to study host-pathogen interactions. Curr Opin Immunol 48:15–22. doi: 10.1016/j.coi.2017.07.012

Dzimianski JV, Scholte FEM, Bergeron É, Pegan SD (2019) ISG15: It's Complicated. J Mol Biol 431:4203–4216.

Echavarria-Consuegra L, Smit JM, Reggiori F (2019) Role of autophagy during the replication and pathogenesis of common mosquito-borne flavi- and alphaviruses. Open Biol 9:190009. doi: 10.1098/rsob.190009

Edgil D, Polacek C, Harris E (2006) Dengue virus utilizes a novel strategy for translation initiation when cap-dependent translation is inhibited. J Virol 80:2976–2986. doi: 10.1128/JVI.80.6.2976-2986.2006

Erbil S, Oral O, Mitou G, et al (2016) RACK1 Is an Interaction Partner of ATG5 and a Novel Regulator of Autophagy. J Biol Chem 291:16753–16765. doi: 10.1074/jbc.M115.708081

Estes JD, Wong SW, Brenchley JM (2018) Nonhuman primate models of human viral infections. Nat Rev Immunol 18:390–404.

Eyre NS, Aloia AL, Joyce MA, et al (2017a) Sensitive luminescent reporter viruses reveal appreciable release of hepatitis C virus NS5A protein into the extracellular environment. Virology 507:20–31. doi: 10.1016/j.virol.2017.04.003

Eyre NS, Fiches GN, Aloia AL, et al (2014) Dynamic imaging of the hepatitis C virus NS5A protein during a productive infection. J Virol 88:3636–3652. doi: 10.1128/JVI.02490-13

Eyre NS, Johnson SM, Eltahla AA, et al (2017b) Genome-Wide Mutagenesis of Dengue Virus Reveals Plasticity of the NS1 Protein and Enables Generation of Infectious Tagged Reporter Viruses. J Virol 91:504. doi: 10.1128/JVI.01455-17

Eyre NS, Kirby EN, Anfiteatro DR, et al (2020) Identification of Estrogen Receptor Modulators as Inhibitors of Flavivirus Infection. Antimicrob Agents Chemother 64:504. doi: 10.1128/AAC.00289-20

Farquhar MJ, Hu K, Harris HJ, et al (2012) Hepatitis C virus induces CD81 and claudin-1 endocytosis. J Virol 86:4305–4316. doi: 10.1128/JVI.06996-11

Fatima K, Syed NI (2018) Dengvaxia controversy: impact on vaccine hesitancy. J Glob Health 8:010312. doi: 10.7189/jogh.08-020312

Faustino AF, Martins AS, Karguth N, et al (2019) Structural and Functional Properties of the Capsid Protein of Dengue and Related Flavivirus. Int J Mol Sci 20:3870. doi: 10.3390/ijms20163870

Felmlee DJ, Hafirassou ML, Lefevre M, et al (2013) Hepatitis C virus, cholesterol and lipoproteins--impact for the viral life cycle and pathogenesis of liver disease. Viruses 5:1292–1324. doi: 10.3390/v5051292

Fernandez-Garcia MD, Meertens L, Chazal M, et al (2016) Vaccine and Wild-Type Strains of Yellow Fever Virus Engage Distinct Entry Mechanisms and Differentially Stimulate Antiviral Immune Responses. MBio 7:e01956–15. doi: 10.1128/mBio.01956-15

Feroldi E, Pancharoen C, Kosalaraksa P, et al (2012) Single-dose, live-attenuated Japanese encephalitis vaccine in children aged 12-18 months: randomized, controlled phase 3 immunogenicity and safety trial. Hum Vaccin Immunother 8:929–937. doi: 10.4161/hv.20071

Ferreira AR, Magalhães AC, Camões F, et al (2016) Hepatitis C virus NS3-4A inhibits the peroxisomal MAVS-dependent antiviral signalling response. J Cell Mol Med 20:750–757. doi: 10.1111/jcmm.12801

Fiches GN, Eyre NS, Aloia AL, et al (2016) HCV RNA traffic and association with NS5A in living cells. Virology 493:60–74. doi: 10.1016/j.virol.2016.02.016

Fischl W, Bartenschlager R (2013) High-throughput screening using dengue virus reporter genomes. Methods Mol Biol 1030:205–219. doi: 10.1007/978-1-62703-484-5_17

Flipse J, Diosa-Toro MA, Hoornweg TE, et al (2016) Antibody-Dependent Enhancement of Dengue Virus Infection in Primary Human Macrophages; Balancing Higher Fusion against Antiviral Responses. Scientific Reports 6:29201–13. doi: 10.1038/srep29201

Ford SA, Allen SL, Ohm JR, et al (2019) Selection on Aedes aegypti alters Wolbachia-mediated dengue virus blocking and fitness. Nat Microbiol 11:e0005625–8. doi: 10.1038/s41564-019-0533-3

Foster TL, Gallay P, Stonehouse NJ, Harris M (2011) Cyclophilin A interacts with domain II of hepatitis C virus NS5A and stimulates RNA binding in an isomerase-dependent manner. J Virol 85:7460–7464. doi: 10.1128/JVI.00393-11

Fraser CS, Hershey JWB, Doudna JA (2009) The pathway of hepatitis C virus mRNA recruitment to the human ribosome. Nat Struct Mol Biol 16:397–404. doi: 10.1038/nsmb.1572

Fujita T, Reis LF, Watanabe N, et al (1989) Induction of the transcription factor IRF-1 and interferon-beta mRNAs by cytokines and activators of second-messenger pathways. Proc Natl Acad Sci USA 86:9936–9940. doi: 10.1073/pnas.86.24.9936

Gack MU, Diamond MS (2016) Innate immune escape by Dengue and West Nile viruses. Curr Opin Virol 20:119–128. doi: 10.1016/j.coviro.2016.09.013

Gack MU, Shin YC, Joo C-H, et al (2007) TRIM25 RING-finger E3 ubiquitin ligase is essential for RIG-I-mediated antiviral activity. Nature 446:916–920. doi: 10.1038/nature05732

Gaj T, Gersbach CA, Barbas CF (2013) ZFN, TALEN, and CRISPR/Cas-based methods for genome engineering. Trends Biotechnol 31:397–405. doi: 10.1016/j.tibtech.2013.04.004

Gallay PA (2012) Cyclophilin inhibitors: a novel class of promising host-targeting anti-HCV agents. Immunol Res 52:200–210. doi: 10.1007/s12026-011-8263-5

Gallina A, Rossi F, Milanesi G (2001) Rack1 binds HIV-1 Nef and can act as a Nef-protein kinase C adaptor. Virology 283:7–18. doi: 10.1006/viro.2001.0855

Gallo S, Ricciardi S, Manfrini N, et al (2018) RACK1 Specifically Regulates Translation through Its Binding to Ribosomes. Mol Cell Biol 38:555. doi: 10.1128/MCB.00230-18

Gao L, Aizaki H, He J-W, Lai MMC (2004) Interactions between viral nonstructural proteins and host protein hVAP-33 mediate the formation of hepatitis C virus RNA replication complex on lipid raft. J Virol 78:3480–3488. doi: 10.1128/jvi.78.7.3480-3488.2004

Geddawy A, Ibrahim YF, Elbahie NM, Ibrahim MA (2017) Direct Acting Anti-hepatitis C Virus Drugs: Clinical Pharmacology and Future Direction. J Transl Int Med 5:8–17. doi: 10.1515/jtim-2017-0007

Gilbert LA, Larson MH, Morsut L, et al (2013) CRISPR-mediated modular RNA-guided regulation of transcription in eukaryotes. Cell 154:442–451. doi: 10.1016/j.cell.2013.06.044

Gillespie LK, Hoenen A, Morgan G, Mackenzie JM (2010) The endoplasmic reticulum provides the membrane platform for biogenesis of the flavivirus replication complex. J Virol 84:10438–10447. doi: 10.1128/JVI.00986-10

Gizzi AS, Grove TL, Arnold JJ, et al (2018) A naturally occurring antiviral ribonucleotide encoded by the human genome. Nature 558:610–614. doi: 10.1038/s41586-018-0238-4

Goffard A, Dubuisson J (2003) Glycosylation of hepatitis C virus envelope proteins. Biochimie 85:295–301. doi: 10.1016/s0300-9084(03)00004-x

Goh P-Y, Tan Y-J, Lim SP, et al (2004) Cellular RNA helicase p68 relocalization and interaction with the hepatitis C virus (HCV) NS5B protein and the potential role of

p68 in HCV RNA replication. J Virol 78:5288–5298. doi: 10.1128/jvi.78.10.5288-5298.2004

Gottwein JM, Jensen TB, Mathiesen CK, et al (2011) Development and application of hepatitis C reporter viruses with genotype 1 to 7 core-nonstructural protein 2 (NS2) expressing fluorescent proteins or luciferase in modified JFH1 NS5A. J Virol 85:8913–8928. doi: 10.1128/JVI.00049-11

Gouttenoire J, Penin F, Moradpour D (2010) Hepatitis C virus nonstructural protein 4B: a journey into unexplored territory. Rev Med Virol 20:117–129. doi: 10.1002/rmv.640

Grabowski JM, Hill CA (2017) A Roadmap for Tick-Borne Flavivirus Research in the "Omics" Era. Front Cell Infect Microbiol 7:519–519.

Grant A, Ponia SS, Tripathi S, et al (2016) Zika Virus Targets Human STAT2 to Inhibit Type I Interferon Signaling. Cell Host Microbe 19:882–890. doi: 10.1016/j.chom.2016.05.009

Grebely J, Dalgard O, Conway B, et al (2018) Sofosbuvir and velpatasvir for hepatitis C virus infection in people with recent injection drug use (SIMPLIFY): an open-label, single-arm, phase 4, multicentre trial. Lancet Gastroenterol Hepatol 3:153–161. doi: 10.1016/S2468-1253(17)30404-1

Guy B, Briand O, Lang J, et al (2015) Development of the Sanofi Pasteur tetravalent dengue vaccine: One more step forward. Vaccine 33:7100–7111. doi: 10.1016/j.vaccine.2015.09.108

Hafirassou ML, Meertens L, Umaña-Diaz C, et al (2018) A Global Interactome Map of the Dengue Virus NS1 Identifies Virus Restriction and Dependency Host Factors. Cell Rep 22:1364. doi: 10.1016/j.celrep.2018.01.038

Haller O, Arnheiter H, Gresser I, Lindenmann J (1979) Genetically determined, interferon-dependent resistance to influenza virus in mice. J Exp Med 149:601–612. doi: 10.1084/jem.149.3.601

Halstead SB (2015) Reappearance of chikungunya, formerly called dengue, in the Americas. Emerging Infect Dis 21:557–561. doi: 10.3201/eid2104.141723

Hamamoto I, Nishimura Y, Okamoto T, et al (2005) Human VAP-B is involved in hepatitis C virus replication through interaction with NS5A and NS5B. J Virol 79:13473–13482. doi: 10.1128/JVI.79.21.13473-13482.2005

Hamel R, Dejarnac O, Wichit S, et al (2015) Biology of Zika Virus Infection in Human Skin Cells. J Virol 89:8880–8896. doi: 10.1128/JVI.00354-15

Han P, Dai Q, Fan L, et al (2019) Genome-Wide CRISPR Screening Identifies JAK1 Deficiency as a Mechanism of T-Cell Resistance. Front Immunol 10:251. doi: 10.3389/fimmu.2019.00251

Hase T, Summers PL, Eckels KH (1989) Flavivirus entry into cultured mosquito cells and human peripheral blood monocytes. Arch Virol 104:129–143. doi: 10.1007/bf01313814

Heaton BE, Kennedy EM, Dumm RE, et al (2017) A CRISPR Activation Screen Identifies a Pan-avian Influenza Virus Inhibitory Host Factor. Cell Rep 20:1503–1512. doi: 10.1016/j.celrep.2017.07.060

Heaton NS, Perera R, Berger KL, et al (2010) Dengue virus nonstructural protein 3 redistributes fatty acid synthase to sites of viral replication and increases cellular fatty acid synthesis. Proc Natl Acad Sci USA 107:17345–17350. doi: 10.1073/pnas.1010811107

Helbig KJ, Beard MR (2014) The role of viperin in the innate antiviral response. J Mol Biol 426:1210–1219. doi: 10.1016/j.jmb.2013.10.019

Helbig KJ, Lau DT-Y, Semendric L, et al (2005) Analysis of ISG expression in chronic hepatitis C identifies viperin as a potential antiviral effector. Hepatology 42:702–710. doi: 10.1002/hep.20844

Henke JI, Goergen D, Zheng J, et al (2008) microRNA-122 stimulates translation of hepatitis C virus RNA. EMBO J 27:3300–3310. doi: 10.1038/emboj.2008.244

Hermance ME, Thangamani S (2017) Powassan Virus: An Emerging Arbovirus of Public Health Concern in North America. Vector Borne Zoonotic Dis 17:453–462. doi: 10.1089/vbz.2017.2110

Hertzog PJ, Williams BRG (2013) Fine tuning type I interferon responses. Cytokine Growth Factor Rev 24:217–225. doi: 10.1016/j.cytogfr.2013.04.002

Hinten SR, Beckett GA, Gensheimer KF, et al (2008) Increased recognition of Powassan encephalitis in the United States, 1999-2005. Vector Borne Zoonotic Dis 8:733–740. doi: 10.1089/vbz.2008.0022

Hoenen A, Liu W, Kochs G, et al (2007) West Nile virus-induced cytoplasmic membrane structures provide partial protection against the interferon-induced antiviral MxA protein. J Gen Virol 88:3013–3017. doi: 10.1099/vir.0.83125-0

Holden KL, Harris E (2004) Enhancement of dengue virus translation: role of the 3“ untranslated region and the terminal 3” stem-loop domain. Virology 329:119–133. doi: 10.1016/j.virol.2004.08.004

Holden P, Horton WA (2009) Crude subcellular fractionation of cultured mammalian cell lines. BMC Res Notes 2:243–10. doi: 10.1186/1756-0500-2-243

Honda M, Kaneko S, Matsushita E, et al (2000) Cell cycle regulation of hepatitis C virus internal ribosomal entry site-directed translation. Gastroenterology 118:152–162. doi: 10.1016/s0016-5085(00)70424-0

Hopfer H, Herzig MC, Gosert R, et al (2020) Hunting coronavirus by transmission electron microscopy - a guide to SARS-CoV-2-associated ultrastructural

pathology in COVID-19 tissues. Histopathology 150:w20203. doi: 10.1111/his.14264

Hsu M, Zhang J, Flint M, et al (2003) Hepatitis C virus glycoproteins mediate pH-dependent cell entry of pseudotyped retroviral particles. Proc Natl Acad Sci USA 100:7271–7276. doi: 10.1073/pnas.0832180100

Hsu PD, Scott DA, Weinstein JA, et al (2013) DNA targeting specificity of RNA-guided Cas9 nucleases. Nat Biotechnol 31:827–832. doi: 10.1038/nbt.2647

Hughes M, Griffin S, Harris M (2009) Domain III of NS5A contributes to both RNA replication and assembly of hepatitis C virus particles. J Gen Virol 90:1329–1334. doi: 10.1099/vir.0.009332-0

Hutvágner G, Simard MJ, Mello CC, Zamore PD (2004) Sequence-specific inhibition of small RNA function. PLoS Biol 2:E98. doi: 10.1371/journal.pbio.0020098

Ikeda M, Abe K-I, Dansako H, et al (2005) Efficient replication of a full-length hepatitis C virus genome, strain O, in cell culture, and development of a luciferase reporter system. Biochem Biophys Res Commun 329:1350–1359. doi: 10.1016/j.bbrc.2005.02.138

Ivashkiv LB, Donlin LT (2014) Regulation of type I interferon responses. Nat Rev Immunol 14:36–49. doi: 10.1038/nri3581

Iversen MB, Paludan SR (2010) Mechanisms of type III interferon expression. J Interferon Cytokine Res 30:573–578. doi: 10.1089/jir.2010.0063

Iwasaki A, Medzhitov R (2015) Control of adaptive immunity by the innate immune system. Nat Immunol 16:343–353. doi: 10.1038/ni.3123

Jiang D, Weidner JM, Qing M, et al (2010) Identification of five interferon-induced cellular proteins that inhibit west nile virus and dengue virus infections. J Virol 84:8332–8341. doi: 10.1128/JVI.02199-09

Jirasko V, Montserret R, Lee JY, et al (2010) Structural and functional studies of nonstructural protein 2 of the hepatitis C virus reveal its key role as organizer of virion assembly. PLoS Pathog 6:e1001233. doi: 10.1371/journal.ppat.1001233

John SP, Chin CR, Perreira JM, et al (2013) The CD225 domain of IFITM3 is required for both IFITM protein association and inhibition of influenza A virus and dengue virus replication. J Virol 87:7837–7852. doi: 10.1128/JVI.00481-13

Jones CT, Ma L, Burgner JW, et al (2003) Flavivirus capsid is a dimeric alpha-helical protein. J Virol 77:7143–7149. doi: 10.1128/jvi.77.12.7143-7149.2003

Joung J, Konermann S, Gootenberg JS, et al (2017) Genome-scale CRISPR-Cas9 knockout and transcriptional activation screening. Nat Protoc 12:828–863. doi: 10.1038/nprot.2017.016

Judge AD, Sood V, Shaw JR, et al (2005) Sequence-dependent stimulation of the mammalian innate immune response by synthetic siRNA. Nat Biotechnol 23:457–462. doi: 10.1038/nbt1081

Kasai F, Hirayama N, Ozawa M, et al (2018) HuH-7 reference genome profile: complex karyotype composed of massive loss of heterozygosity. Hum Cell 31:261–267. doi: 10.1007/s13577-018-0212-3

Kato F, Nio Y, Yagasaki K, et al (2019) Identification of inhibitors of dengue viral replication using replicon cells expressing secretory luciferase. Antiviral Res 172:104643. doi: 10.1016/j.antiviral.2019.104643

Kaul A, Stauffer S, Berger C, et al (2009) Essential role of cyclophilin A for hepatitis C virus replication and virus production and possible link to polyprotein cleavage kinetics. PLoS Pathog 5:e1000546. doi: 10.1371/journal.ppat.1000546

Kawasaki T, Kawai T (2014) Toll-like receptor signaling pathways. Front Immunol 5:461. doi: 10.3389/fimmu.2014.00461

Ke P-Y (2018) The Multifaceted Roles of Autophagy in Flavivirus-Host Interactions. Int J Mol Sci 19:3940. doi: 10.3390/ijms19123940

Kell AM, Gale M (2015) RIG-I in RNA virus recognition. Virology 479-480:110–121. doi: 10.1016/j.virol.2015.02.017

Kemenesi G, Bányai K (2019) Tick-Borne Flaviviruses, with a Focus on Powassan Virus. Clin Microbiol Rev 32:437. doi: 10.1128/CMR.00106-17

Kerr IM, Brown RE, Hovanessian AG (1977) Nature of inhibitor of cell-free protein synthesis formed in response to interferon and double-stranded RNA. Nature 268:540–542. doi: 10.1038/268540a0

Kessler DS, Veals SA, Fu XY, Levy DE (1990) Interferon-alpha regulates nuclear translocation and DNA-binding affinity of ISGF3, a multimeric transcriptional activator. Genes Dev 4:1753–1765. doi: 10.1101/gad.4.10.1753

Khromykh AA, Meka H, Guyatt KJ, Westaway EG (2001) Essential role of cyclization sequences in flavivirus RNA replication. J Virol 75:6719–6728. doi: 10.1128/JVI.75.14.6719-6728.2001

Khromykh AA, Westaway EG (1994) Completion of Kunjin virus RNA sequence and recovery of an infectious RNA transcribed from stably cloned full-length cDNA. J Virol 68:4580–4588.

Khumthong R, Angsuthanasombat C, Panyim S, Katzenmeier G (2002) In vitro determination of dengue virus type 2 NS2B-NS3 protease activity with fluorescent peptide substrates. J Biochem Mol Biol 35:206–212. doi: 10.5483/bmbrep.2002.35.2.206

Kieft JS, Zhou K, Jubin R, Doudna JA (2001) Mechanism of ribosome recruitment by hepatitis C IRES RNA. RNA 7:194–206. doi: 10.1017/s1355838201001790

Kiely PA, Baillie GS, Barrett R, et al (2009) Phosphorylation of RACK1 on tyrosine 52 by c-Abl is required for insulin-like growth factor I-mediated regulation of focal adhesion kinase. J Biol Chem 284:20263–20274. doi: 10.1074/jbc.M109.017640

Kim S-J, Kim J-H, Kim Y-G, et al (2004) Protein kinase C-related kinase 2 regulates hepatitis C virus RNA polymerase function by phosphorylation. J Biol Chem 279:50031–50041. doi: 10.1074/jbc.M408617200

Kimura T, Katoh H, Kayama H, et al (2013) Ifit1 inhibits Japanese encephalitis virus replication through binding to 5“ capped 2-”O unmethylated RNA. J Virol 87:9997–10003. doi: 10.1128/JVI.00883-13

King AMQ, Adams MJ, Carstens EB, Lefkowitz EJ (eds) (2012) Family - Flaviviridae. In: Virus Taxonomy. Elsevier, San Diego, pp 1003–1020

Kistler KE, Vosshall LB, Matthews BJ (2015) Genome engineering with CRISPR-Cas9 in the mosquito Aedes aegypti. Cell Rep 11:51–60. doi: 10.1016/j.celrep.2015.03.009

Knight E, Korant BD (1979) Fibroblast interferon induces synthesis of four proteins in human fibroblast cells. Proc Natl Acad Sci USA 76:1824–1827. doi: 10.1073/pnas.76.4.1824

Kohler PO, Bridson WE (1971) Isolation of hormone-producing clonal lines of human choriocarcinoma. J Clin Endocrinol Metab 32:683–687. doi: 10.1210/jcem-32-5-683

Koike-Yusa H, Li Y, Tan E-P, et al (2014) Genome-wide recessive genetic screening in mammalian cells with a lentiviral CRISPR-guide RNA library. Nat Biotechnol 32:267–273. doi: 10.1038/nbt.2800

Kondoh T, Letko M, Munster VJ, et al (2018) Single-Nucleotide Polymorphisms in Human NPC1 Influence Filovirus Entry Into Cells. J Infect Dis 218:S397–S402. doi: 10.1093/infdis/jiy248

Konermann S, Brigham MD, Trevino AE, et al (2015) Genome-scale transcriptional activation by an engineered CRISPR-Cas9 complex. Nature 517:583–588. doi: 10.1038/nature14136

Kou Z, Wu Q, Kou X, et al (2015) CRISPR/Cas9-mediated genome engineering of the ferret. Cell Res 25:1372–1375. doi: 10.1038/cr.2015.130

Koutsoudakis G, Kaul A, Steinmann E, et al (2006) Characterization of the early steps of hepatitis C virus infection by using luciferase reporter viruses. J Virol 80:5308–5320. doi: 10.1128/JVI.02460-05

Krauer F, Riesen M, Reveiz L, et al (2017) Zika Virus Infection as a Cause of Congenital Brain Abnormalities and Guillain-Barré Syndrome: Systematic Review. PLoS Med 14:e1002203. doi: 10.1371/journal.pmed.1002203

Kubota T, Yokosawa N, Yokota S-I, Fujii N (2002) Association of mumps virus V protein with RACK1 results in dissociation of STAT-1 from the alpha interferon

receptor complex. J Virol 76:12676–12682. doi: 10.1128/jvi.76.24.12676-12682.2002

Kuno G, Chang GJ, Tsuchiya KR, et al (1998) Phylogeny of the genus Flavivirus. J Virol 72:73–83. doi: 10.1128/JVI.72.1.73-83.1998

Kurreck J (2006) siRNA efficiency: structure or sequence-that is the question. J Biomed Biotechnol 2006:83757–7. doi: 10.1155/JBB/2006/83757

Kweon J, Kim Y (2018) High-throughput genetic screens using CRISPR-Cas9 system. Arch Pharm Res 41:875–884. doi: 10.1007/s12272-018-1029-z

Kwon Y-J, Heo J, Wong HEE, et al (2014) Kinome siRNA screen identifies novel cell-type specific dengue host target genes. Antiviral Res 110:20–30. doi: 10.1016/j.antiviral.2014.07.006

Kyono K, Miyashiro M, Taguchi I (2002) Human eukaryotic initiation factor 4AII associates with hepatitis C virus NS5B protein in vitro. Biochem Biophys Res Commun 292:659–666. doi: 10.1006/bbrc.2002.6702

LaFontaine E, Miller CM, Permaul N, et al (2020) Ribosomal protein RACK1 enhances translation of poliovirus and other viral IRESs. Virology 545:53–62. doi: 10.1016/j.virol.2020.03.004

Lai CJ, Zhao BT, Hori H, Bray M (1991) Infectious RNA transcribed from stably cloned full-length cDNA of dengue type 4 virus. Proc Natl Acad Sci USA 88:5139–5143. doi: 10.1073/pnas.88.12.5139

Lamken P, Lata S, Gavutis M, Piehler J (2004) Ligand-induced assembling of the type I interferon receptor on supported lipid bilayers. J Mol Biol 341:303–318. doi: 10.1016/j.jmb.2004.05.059

Lang J, Cheng Y, Rolfe A, et al (2018) An hPSC-Derived Tissue-Resident Macrophage Model Reveals Differential Responses of Macrophages to ZIKV and DENV Infection. Stem Cell Reports 11:348–362. doi: 10.1016/j.stemcr.2018.06.006

Larrubia JR, Moreno-Cubero E, Lokhande MU, et al (2014) Adaptive immune response during hepatitis C virus infection. World J Gastroenterol 20:3418–3430. doi: 10.3748/wjg.v20.i13.3418

Laureti M, Narayanan D, Rodriguez-Andres J, et al (2018) Flavivirus Receptors: Diversity, Identity, and Cell Entry. Front Immunol 9:2180. doi: 10.3389/fimmu.2018.02180

Ledur PF, Karmirian K, Pedrosa CDSG, et al (2020) Zika virus infection leads to mitochondrial failure, oxidative stress and DNA damage in human iPSC-derived astrocytes. Scientific Reports 10:1218–14. doi: 10.1038/s41598-020-57914-x

Lee C-J, Liao C-L, Lin Y-L (2005) Flavivirus activates phosphatidylinositol 3-kinase signaling to block caspase-dependent apoptotic cell death at the early stage of virus infection. J Virol 79:8388–8399. doi: 10.1128/JVI.79.13.8388-8399.2005

Lee JS, Tabata K, Twu W-I, et al (2019) RACK1 mediates rewiring of intracellular networks induced by hepatitis C virus infection. PLoS Pathog 15:e1008021. doi: 10.1371/journal.ppat.1008021

Lei S, Ryu J, Wen K, et al (2016) Increased and prolonged human norovirus infection in RAG2/IL2RG deficient gnotobiotic pigs with severe combined immunodeficiency. Scientific Reports 6:25222–12. doi: 10.1038/srep25222

Lenschow DJ, Giannakopoulos NV, Gunn LJ, et al (2005) Identification of interferon-stimulated gene 15 as an antiviral molecule during Sindbis virus infection in vivo. J Virol 79:13974–13983. doi: 10.1128/JVI.79.22.13974-13983.2005

Lewin AR, Reid LE, McMahon M, et al (1991) Molecular analysis of a human interferon-inducible gene family. Eur J Biochem 199:417–423. doi: 10.1111/j.1432-1033.1991.tb16139.x

Li H, Clum S, You S, et al (1999) The serine protease and RNA-stimulated nucleoside triphosphatase and RNA helicase functional domains of dengue virus type 2 NS3 converge within a region of 20 amino acids. J Virol 73:3108–3116.

Li K, Foy E, Ferreon JC, et al (2005) Immune evasion by hepatitis C virus NS3/4A protease-mediated cleavage of the Toll-like receptor 3 adaptor protein TRIF. Proc Natl Acad Sci USA 102:2992–2997. doi: 10.1073/pnas.0408824102

Li L, Lok S-M, Yu I-M, et al (2008) The flavivirus precursor membrane-envelope protein complex: structure and maturation. Science 319:1830–1834. doi: 10.1126/science.1153263

Li Q, Brass AL, Ng A, et al (2009) A genome-wide genetic screen for host factors required for hepatitis C virus propagation. Proc Natl Acad Sci USA 106:16410–16415. doi: 10.1073/pnas.0907439106

Li Y, Masaki T, Yamane D, et al (2013) Competing and noncompeting activities of miR-122 and the 5' exonuclease Xrn1 in regulation of hepatitis C virus replication. Proc Natl Acad Sci USA 110:1881–1886. doi: 10.1073/pnas.1213515110

Li Y, Muffat J, Omer Javed A, et al (2019) Genome-wide CRISPR screen for Zika virus resistance in human neural cells. Proc Natl Acad Sci USA 116:9527–9532. doi: 10.1073/pnas.1900867116

Liang Y, Cao X, Ding Q, et al (2018) Hepatitis C virus NS4B induces the degradation of TRIF to inhibit TLR3-mediated interferon signaling pathway. PLoS Pathog 14:e1007075. doi: 10.1371/journal.ppat.1007075

Lieber MR (2010) The mechanism of double-strand DNA break repair by the nonhomologous DNA end-joining pathway. Annu Rev Biochem 79:181–211. doi: 10.1146/annurev.biochem.052308.093131

Lin DL, Inoue T, Chen Y-J, et al (2019a) The ER Membrane Protein Complex Promotes Biogenesis of Dengue and Zika Virus Non-structural Multi-pass

Transmembrane Proteins to Support Infection. Cell Rep 27:1666–1674.e4. doi: 10.1016/j.celrep.2019.04.051

Lin J-P, Fan Y-K, Liu HM (2019b) The 14-3-3η chaperone protein promotes antiviral innate immunity via facilitating MDA5 oligomerization and intracellular redistribution. PLoS Pathog 15:e1007582. doi: 10.1371/journal.ppat.1007582

Lingala S, Ghany MG (2015) Natural History of Hepatitis C. Gastroenterol Clin North Am 44:717–734. doi: 10.1016/j.gtc.2015.07.003

Liu HM, Loo Y-M, Horner SM, et al (2012a) The mitochondrial targeting chaperone 14-3-3ε regulates a RIG-I translocon that mediates membrane association and innate antiviral immunity. Cell Host Microbe 11:528–537. doi: 10.1016/j.chom.2012.04.006

Liu N (2015) Insecticide resistance in mosquitoes: impact, mechanisms, and research directions. Annu Rev Entomol 60:537–559. doi: 10.1146/annurev-ento-010814-020828

Liu S, Xiao L, Nelson C, et al (2012b) A cell culture adapted HCV JFH1 variant that increases viral titers and permits the production of high titer infectious chimeric reporter viruses. PLoS ONE 7:e44965. doi: 10.1371/journal.pone.0044965

Liu T, Zhang L, Joo D, Sun S-C (2017) NF-κB signaling in inflammation. Signal Transduct Target Ther 2:a000034–9. doi: 10.1038/sigtrans.2017.23

Liu WJ, Chen HB, Wang XJ, et al (2004) Analysis of adaptive mutations in Kunjin virus replicon RNA reveals a novel role for the flavivirus nonstructural protein NS2A in inhibition of beta interferon promoter-driven transcription. J Virol 78:12225–12235. doi: 10.1128/JVI.78.22.12225-12235.2004

Liu Y, Wang W, Zou Z, et al (2019) Hepatitis C Virus Entry into Macrophages/Monocytes Mainly Depends on the Phagocytosis of Macrophages. Dig Dis Sci 64:1226–1237. doi: 10.1007/s10620-018-5401-0

Lodeiro MF, Filomatori CV, Gamarnik AV (2009) Structural and functional studies of the promoter element for dengue virus RNA replication. J Virol 83:993–1008. doi: 10.1128/JVI.01647-08

Lohmann V (2019) Hepatitis C virus cell culture models: an encomium on basic research paving the road to therapy development. Med Microbiol Immunol 208:3–24. doi: 10.1007/s00430-018-0566-x

Lohmann V, Körner F, Herian U, Bartenschlager R (1997) Biochemical properties of hepatitis C virus NS5B RNA-dependent RNA polymerase and identification of amino acid sequence motifs essential for enzymatic activity. J Virol 71:8416–8428.

Lohmann V, Körner F, Koch J, et al (1999) Replication of subgenomic hepatitis C virus RNAs in a hepatoma cell line. Science 285:110–113. doi: 10.1126/science.285.5424.110

Long L, Deng Y, Yao F, et al (2014) Recruitment of phosphatase PP2A by RACK1 adaptor protein deactivates transcription factor IRF3 and limits type I interferon signaling. Immunity 40:515–529. doi: 10.1016/j.immuni.2014.01.015

Loo Y-M, Gale M (2011) Immune signaling by RIG-I-like receptors. Immunity 34:680–692. doi: 10.1016/j.immuni.2011.05.003

Lopez Sambrooks C, Baro M, Quijano A, et al (2018) Oligosaccharyltransferase Inhibition Overcomes Therapeutic Resistance to EGFR Tyrosine Kinase Inhibitors. Cancer Res 78:5094–5106. doi: 10.1158/0008-5472.CAN-18-0505

López-Bergami P, Habelhah H, Bhoumik A, et al (2005) RACK1 mediates activation of JNK by protein kinase C [corrected]. Mol Cell 19:309–320. doi: 10.1016/j.molcel.2005.06.025

Lundberg R, Melén K, Westenius V, et al (2019) Zika Virus Non-Structural Protein NS5 Inhibits the RIG-I Pathway and Interferon Lambda 1 Promoter Activation by Targeting IKK Epsilon. Viruses 11:1024. doi: 10.3390/v11111024

Ma H, Dang Y, Wu Y, et al (2015) A CRISPR-Based Screen Identifies Genes Essential for West-Nile-Virus-Induced Cell Death. Cell Rep 12:673–683. doi: 10.1016/j.celrep.2015.06.049

Ma J, Ketkar H, Geng T, et al (2018) Zika Virus Non-structural Protein 4A Blocks the RLR-MAVS Signaling. Front Microbiol 9:1350. doi: 10.3389/fmicb.2018.01350

Ma Y, Anantpadma M, Timpe JM, et al (2011) Hepatitis C virus NS2 protein serves as a scaffold for virus assembly by interacting with both structural and nonstructural proteins. J Virol 85:86–97. doi: 10.1128/JVI.01070-10

Mackenzie JM, Khromykh AA, Jones MK, Westaway EG (1998) Subcellular localization and some biochemical properties of the flavivirus Kunjin nonstructural proteins NS2A and NS4A. Virology 245:203–215. doi: 10.1006/viro.1998.9156

Mahmoudvand S, Shokri S, Taherkhani R, Farshadpour F (2019) Hepatitis C virus core protein modulates several signaling pathways involved in hepatocellular carcinoma. World J Gastroenterol 25:42–58. doi: 10.3748/wjg.v25.i1.42

Majzoub K, Hafirassou ML, Meignin C, et al (2014) RACK1 controls IRES-mediated translation of viruses. Cell 159:1086–1095. doi: 10.1016/j.cell.2014.10.041

Marceau CD, Puschnik AS, Majzoub K, et al (2016) Genetic dissection of Flaviviridae host factors through genome-scale CRISPR screens. Nature 535:159–163. doi: 10.1038/nature18631

Markoff L (1989) In vitro processing of dengue virus structural proteins: cleavage of the pre-membrane protein. J Virol 63:3345–3352.

Martins IC, Gomes-Neto F, Faustino AF, et al (2012) The disordered N-terminal region of dengue virus capsid protein contains a lipid-droplet-binding motif. Biochem J 444:405–415. doi: 10.1042/BJ20112219

Martín-Acebes MA, Blázquez A-B, Jiménez de Oya N, et al (2011) West Nile virus replication requires fatty acid synthesis but is independent on phosphatidylinositol-4-phosphate lipids. PLoS ONE 6:e24970. doi: 10.1371/journal.pone.0024970

Masaki T, Suzuki R, Murakami K, et al (2008) Interaction of hepatitis C virus nonstructural protein 5A with core protein is critical for the production of infectious virus particles. J Virol 82:7964–7976. doi: 10.1128/JVI.00826-08

McCartney EM, Eyre NS, Beard MR (2011) Border patrol intensifies for hepatitis C virus entry. Hepatology 54:1472–1475. doi: 10.1002/hep.24586

McDougall WM, Perreira JM, Reynolds EC, Brass AL (2018) CRISPR genetic screens to discover host-virus interactions. Curr Opin Virol 29:87–100. doi: 10.1016/j.coviro.2018.03.007

McLauchlan J, Lemberg MK, Hope G, Martoglio B (2002) Intramembrane proteolysis promotes trafficking of hepatitis C virus core protein to lipid droplets. EMBO J 21:3980–3988. doi: 10.1093/emboj/cdf414

Meertens L, Carnec X, Lecoin MP, et al (2012) The TIM and TAM families of phosphatidylserine receptors mediate dengue virus entry. Cell Host Microbe 12:544–557. doi: 10.1016/j.chom.2012.08.009

Meister G, Tuschl T (2004) Mechanisms of gene silencing by double-stranded RNA. Nature 431:343–349. doi: 10.1038/nature02873

Messina JP, Humphreys I, Flaxman A, et al (2015) Global distribution and prevalence of hepatitis C virus genotypes. Hepatology 61:77–87. doi: 10.1002/hep.27259

Meurs E, Chong K, Galabru J, et al (1990) Molecular cloning and characterization of the human double-stranded RNA-activated protein kinase induced by interferon. Cell 62:379–390. doi: 10.1016/0092-8674(90)90374-n

Meylan E, Curran J, Hofmann K, et al (2005) Cardif is an adaptor protein in the RIG-I antiviral pathway and is targeted by hepatitis C virus. Nature 437:1167–1172. doi: 10.1038/nature04193

Miller S, Kastner S, Krijnse-Locker J, et al (2007) The non-structural protein 4A of dengue virus is an integral membrane protein inducing membrane alterations in a 2K-regulated manner. J Biol Chem 282:8873–8882. doi: 10.1074/jbc.M609919200

Miyanari Y, Atsuzawa K, Usuda N, et al (2007) The lipid droplet is an important organelle for hepatitis C virus production. Nat Cell Biol 9:1089–1097. doi: 10.1038/ncb1631

Modhiran N, Watterson D, Muller DA, et al (2015) Dengue virus NS1 protein activates cells via Toll-like receptor 4 and disrupts endothelial cell monolayer integrity. Sci Transl Med 7:304ra142–304ra142. doi: 10.1126/scitranslmed.aaa3863

Moradpour D, Brass V, Bieck E, et al (2004) Membrane association of the RNA-dependent RNA polymerase is essential for hepatitis C virus RNA replication. J Virol 78:13278–13284. doi: 10.1128/JVI.78.23.13278-13284.2004

Moradpour D, Penin F, Rice CM (2007) Replication of hepatitis C virus. Nat Rev Microbiol 5:453–463. doi: 10.1038/nrmicro1645

Morchang A, Lee RCH, Yenchitsomanus P-T, et al (2017) RNAi screen reveals a role of SPHK2 in dengue virus-mediated apoptosis in hepatic cell lines. PLoS ONE 12:e0188121. doi: 10.1371/journal.pone.0188121

Morrison J, Laurent-Rolle M, Maestre AM, et al (2013) Dengue virus co-opts UBR4 to degrade STAT2 and antagonize type I interferon signaling. PLoS Pathog 9:e1003265. doi: 10.1371/journal.ppat.1003265

Motwani M, Pesiridis S, Fitzgerald KA (2019) DNA sensing by the cGAS-STING pathway in health and disease. Nat Rev Genet 20:657–674. doi: 10.1038/s41576-019-0151-1

Mulkey SB, Arroyave-Wessel M, Peyton C, et al (2020) Neurodevelopmental Abnormalities in Children With In Utero Zika Virus Exposure Without Congenital Zika Syndrome. JAMA Pediatr 174:269–276. doi: 10.1001/jamapediatrics.2019.5204

Muller DA, Young PR (2013) The flavivirus NS1 protein: molecular and structural biology, immunology, role in pathogenesis and application as a diagnostic biomarker. Antiviral Res 98:192–208. doi: 10.1016/j.antiviral.2013.03.008

Murray JM, Aaskov JG, Wright PJ (1993) Processing of the dengue virus type 2 proteins prM and C-prM. J Gen Virol 74 (Pt 2):175–182. doi: 10.1099/0022-1317-74-2-175

Musso D, Nilles EJ, Cao-Lormeau V-M (2014) Rapid spread of emerging Zika virus in the Pacific area. Clin Microbiol Infect 20:O595–6. doi: 10.1111/1469-0691.12707

Nakabayashi H, Taketa K, Miyano K, et al (1982) Growth of human hepatoma cells lines with differentiated functions in chemically defined medium. Cancer Res 42:3858–3863.

Narayana SK, Helbig KJ, McCartney EM, et al (2015) The Interferon-induced Transmembrane Proteins, IFITM1, IFITM2, and IFITM3 Inhibit Hepatitis C Virus Entry. J Biol Chem 290:25946–25959. doi: 10.1074/jbc.M115.657346

Nasirudeen AMA, Wong HH, Thien P, et al (2011) RIG-I, MDA5 and TLR3 synergistically play an important role in restriction of dengue virus infection. PLoS Negl Trop Dis 5:e926. doi: 10.1371/journal.pntd.0000926

Neasta J, Kiely PA, He D-Y, et al (2012) Direct interaction between scaffolding proteins RACK1 and 14-3-3ζ regulates brain-derived neurotrophic factor (BDNF) transcription. J Biol Chem 287:322–336. doi: 10.1074/jbc.M111.272195

Nelles DA, Fang MY, O'Connell MR, et al (2016) Programmable RNA Tracking in Live Cells with CRISPR/Cas9. Cell 165:488–496. doi: 10.1016/j.cell.2016.02.054

Neufeldt CJ, Cortese M, Scaturro P, et al (2019) ER-shaping atlastin proteins act as central hubs to promote flavivirus replication and virion assembly. Nat Microbiol 4:2416–2429. doi: 10.1038/s41564-019-0586-3

Ng KT, Takebe Y, Chook JB, et al (2015) Co-infections and transmission networks of HCV, HIV-1 and HPgV among people who inject drugs. Scientific Reports 5:15198–11. doi: 10.1038/srep15198

Ng TI, Mo H, Pilot-Matias T, et al (2007) Identification of host genes involved in hepatitis C virus replication by small interfering RNA technology. Hepatology 45:1413–1421. doi: 10.1002/hep.21608

Ngueyen TTN, Kim S-J, Lee JY, Myoung J (2019) Zika Virus Proteins NS2A and NS4A Are Major Antagonists that Reduce IFN-β Promoter Activity Induced by the MDA5/RIG-I Signaling Pathway. J Microbiol Biotechnol 29:1665–1674. doi: 10.4014/jmb.1909.09017

Niepmann M (2013) Hepatitis C virus RNA translation. Curr Top Microbiol Immunol 369:143–166. doi: 10.1007/978-3-642-27340-7_6

Oishi I, Yoshii K, Miyahara D, et al (2016) Targeted mutagenesis in chicken using CRISPR/Cas9 system. Scientific Reports 6:23980–10. doi: 10.1038/srep23980

Oliveira ERA, de Alencastro RB, Horta BAC (2017) New insights into flavivirus biology: the influence of pH over interactions between prM and E proteins. J Comput Aided Mol Des 31:1009–1019. doi: 10.1007/s10822-017-0076-8

Ong SH, Li Y, Koike-Yusa H, Yusa K (2018) Author Correction: Optimised metrics for CRISPR-KO screens with second-generation gRNA libraries. Scientific Reports 8:6136–1. doi: 10.1038/s41598-018-24092-w

Orchard RC, Sullender ME, Dunlap BF, et al (2019) Identification of Antinorovirus Genes in Human Cells Using Genome-Wide CRISPR Activation Screening. J Virol 93:668. doi: 10.1128/JVI.01324-18

Osuna-Ramos JF, Reyes-Ruiz JM, Del Ángel RM (2018) The Role of Host Cholesterol During Flavivirus Infection. Front Cell Infect Microbiol 8:388. doi: 10.3389/fcimb.2018.00388

Otto GA, Puglisi JD (2004) The pathway of HCV IRES-mediated translation initiation. Cell 119:369–380. doi: 10.1016/j.cell.2004.09.038

Panayiotou C, Lindqvist R, Kurhade C, et al (2018) Viperin Restricts Zika Virus and Tick-Borne Encephalitis Virus Replication by Targeting NS3 for Proteasomal Degradation. J Virol 92:500. doi: 10.1128/JVI.02054-17

Pang X, Zhang M, Dayton AI (2001) Development of Dengue virus type 2 replicons capable of prolonged expression in host cells. BMC Microbiol 1:18–7. doi: 10.1186/1471-2180-1-18

Pantoja P, Pérez-Guzmán EX, Rodríguez IV, et al (2017) Zika virus pathogenesis in rhesus macaques is unaffected by pre-existing immunity to dengue virus. Nat Commun 8:15674–13. doi: 10.1038/ncomms15674

Parnas O, Jovanovic M, Eisenhaure TM, et al (2015) A Genome-wide CRISPR Screen in Primary Immune Cells to Dissect Regulatory Networks. Cell 162:675–686. doi: 10.1016/j.cell.2015.06.059

Patkar CG, Larsen M, Owston M, et al (2009) Identification of inhibitors of yellow fever virus replication using a replicon-based high-throughput assay. Antimicrob Agents Chemother 53:4103–4114. doi: 10.1128/AAC.00074-09

Paul D, Bartenschlager R (2015) Flaviviridae Replication Organelles: Oh, What a Tangled Web We Weave. Annu Rev Virol 2:289–310. doi: 10.1146/annurev-virology-100114-055007

Paul D, Romero-Brey I, Gouttenoire J, et al (2011) NS4B self-interaction through conserved C-terminal elements is required for the establishment of functional hepatitis C virus replication complexes. J Virol 85:6963–6976. doi: 10.1128/JVI.00502-11

Paul LM, Carlin ER, Jenkins MM, et al (2016) Dengue virus antibodies enhance Zika virus infection. Clin Transl Immunology 5:e117. doi: 10.1038/cti.2016.72

Perera R, Khaliq M, Kuhn RJ (2008) Closing the door on flaviviruses: entry as a target for antiviral drug design. Antiviral Res 80:11–22. doi: 10.1016/j.antiviral.2008.05.004

Perez-Pinera P, Kocak DD, Vockley CM, et al (2013) RNA-guided gene activation by CRISPR-Cas9-based transcription factors. Nat Methods 10:973–976. doi: 10.1038/nmeth.2600

Perng Y-C, Lenschow DJ (2018) ISG15 in antiviral immunity and beyond. Nat Rev Microbiol 16:423–439. doi: 10.1038/s41579-018-0020-5

Pérard J, Rasia R, Medenbach J, et al (2009) Human initiation factor eIF3 subunit b interacts with HCV IRES RNA through its N-terminal RNA recognition motif. FEBS Lett 583:70–74. doi: 10.1016/j.febslet.2008.11.025

Platanias LC (2005) Mechanisms of type-I- and type-II-interferon-mediated signalling. Nat Rev Immunol 5:375–386. doi: 10.1038/nri1604

Ponting CP, Oliver PL, Reik W (2009) Evolution and functions of long noncoding RNAs. Cell 136:629–641. doi: 10.1016/j.cell.2009.02.006

Preugschat F, Yao CW, Strauss JH (1990) In vitro processing of dengue virus type 2 nonstructural proteins NS2A, NS2B, and NS3. J Virol 64:4364–4374.

Priyamvada L, Quicke KM, Hudson WH, et al (2016) Human antibody responses after dengue virus infection are highly cross-reactive to Zika virus. Proc Natl Acad Sci USA 113:7852–7857. doi: 10.1073/pnas.1607931113

Puschnik AS, Majzoub K, Ooi YS, Carette JE (2017a) A CRISPR toolbox to study virus-host interactions. Nat Rev Microbiol 15:351–364. doi: 10.1038/nrmicro.2017.29

Puschnik AS, Marceau CD, Ooi YS, et al (2017b) A Small-Molecule Oligosaccharyltransferase Inhibitor with Pan-flaviviral Activity. Cell Rep 21:3032–3039. doi: 10.1016/j.celrep.2017.11.054

Płaszczyca A, Scaturro P, Neufeldt CJ, et al (2019) A novel interaction between dengue virus nonstructural protein 1 and the NS4A-2K-4B precursor is required for viral RNA replication but not for formation of the membranous replication organelle. PLoS Pathog 15:e1007736. doi: 10.1371/journal.ppat.1007736

Qi Y, Li Y, Zhang Y, et al (2015) IFI6 Inhibits Apoptosis via Mitochondrial-Dependent Pathway in Dengue Virus 2 Infected Vascular Endothelial Cells. PLoS ONE 10:e0132743. doi: 10.1371/journal.pone.0132743

Rabl J, Leibundgut M, Ataide SF, et al (2011) Crystal structure of the eukaryotic 40S ribosomal subunit in complex with initiation factor 1. Science 331:730–736. doi: 10.1126/science.1198308

Randall G, Panis M, Cooper JD, et al (2007) Cellular cofactors affecting hepatitis C virus infection and replication. Proc Natl Acad Sci USA 104:12884–12889. doi: 10.1073/pnas.0704894104

Rastogi M, Sharma N, Singh SK (2016) Flavivirus NS1: a multifaceted enigmatic viral protein. Virol J 13:131–10. doi: 10.1186/s12985-016-0590-7

Razali K, Amin J, Dore GJ, et al (2009) Modelling and calibration of the hepatitis C epidemic in Australia. Stat Methods Med Res 18:253–270. doi: 10.1177/0962280208094689

Rehwinkel J, Gack MU (2020) RIG-I-like receptors: their regulation and roles in RNA sensing. Nat Rev Immunol 20:537–551. doi: 10.1038/s41577-020-0288-3

Reiss S, Rebhan I, Backes P, et al (2011) Recruitment and activation of a lipid kinase by hepatitis C virus NS5A is essential for integrity of the membranous replication compartment. Cell Host Microbe 9:32–45. doi: 10.1016/j.chom.2010.12.002

Ren Q, Li C, Yuan P, et al (2015) A Dual-reporter system for real-time monitoring and high-throughput CRISPR/Cas9 library screening of the hepatitis C virus. Scientific Reports 5:8865–7. doi: 10.1038/srep08865

Rice CM, Grakoui A, Galler R, Chambers TJ (1989) Transcription of infectious yellow fever RNA from full-length cDNA templates produced by in vitro ligation. New Biol 1:285–296.

Richard AS, Shim B-S, Kwon Y-C, et al (2017) AXL-dependent infection of human fetal endothelial cells distinguishes Zika virus from other pathogenic flaviviruses. Proc Natl Acad Sci USA 114:2024–2029. doi: 10.1073/pnas.1620558114

Richardson RB, Ohlson MB, Eitson JL, et al (2018) A CRISPR screen identifies IFI6 as an ER-resident interferon effector that blocks flavivirus replication. Nat Microbiol 3:1214–1223. doi: 10.1038/s41564-018-0244-1

Riedl W, Acharya D, Lee J-H, et al (2019) Zika Virus NS3 Mimics a Cellular 14-3-3-Binding Motif to Antagonize RIG-I- and MDA5-Mediated Innate Immunity. Cell Host Microbe 26:493–503.e6. doi: 10.1016/j.chom.2019.09.012

Robbiani DF, Bozzacco L, Keeffe JR, et al (2017) Recurrent Potent Human Neutralizing Antibodies to Zika Virus in Brazil and Mexico. Cell 169:597–609.e11. doi: 10.1016/j.cell.2017.04.024

Rodriguez KR, Bruns AM, Horvath CM (2014) MDA5 and LGP2: accomplices and antagonists of antiviral signal transduction. J Virol 88:8194–8200. doi: 10.1128/JVI.00640-14

Romero-Brey I, Berger C, Kallis S, et al (2015) NS5A Domain 1 and Polyprotein Cleavage Kinetics Are Critical for Induction of Double-Membrane Vesicles Associated with Hepatitis C Virus Replication. MBio 6:e00759. doi: 10.1128/mBio.00759-15

Romero-Brey I, Merz A, Chiramel A, et al (2012) Three-dimensional architecture and biogenesis of membrane structures associated with hepatitis C virus replication. PLoS Pathog 8:e1003056. doi: 10.1371/journal.ppat.1003056

Roosendaal J, Westaway EG, Khromykh A, Mackenzie JM (2006) Regulated cleavages at the West Nile virus NS4A-2K-NS4B junctions play a major role in rearranging cytoplasmic membranes and Golgi trafficking of the NS4A protein. J Virol 80:4623–4632. doi: 10.1128/JVI.80.9.4623-4632.2006

Rothan HA, Kumar M (2019) Role of Endoplasmic Reticulum-Associated Proteins in Flavivirus Replication and Assembly Complexes. Pathogens 8:148. doi: 10.3390/pathogens8030148

Saeedi BJ, Geiss BJ (2013) Regulation of flavivirus RNA synthesis and capping. Wiley Interdiscip Rev RNA 4:723–735. doi: 10.1002/wrna.1191

Sainz B, Barretto N, Uprichard SL (2009) Hepatitis C virus infection in phenotypically distinct Huh7 cell lines. PLoS ONE 4:e6561. doi: 10.1371/journal.pone.0006561

Saito T, Gale M (2007) Principles of intracellular viral recognition. Curr Opin Immunol 19:17–23. doi: 10.1016/j.coi.2006.11.003

Saito T, Hirai R, Loo Y-M, et al (2007) Regulation of innate antiviral defenses through a shared repressor domain in RIG-I and LGP2. Proc Natl Acad Sci USA 104:582–587. doi: 10.1073/pnas.0606699104

Saitoh T, Satoh T, Yamamoto N, et al (2011) Antiviral protein Viperin promotes Toll-like receptor 7- and Toll-like receptor 9-mediated type I interferon production in plasmacytoid dendritic cells. Immunity 34:352–363. doi: 10.1016/j.immuni.2011.03.010

Sall AA, Faye O, Diallo M, et al (2010) Yellow fever virus exhibits slower evolutionary dynamics than dengue virus. J Virol 84:765–772. doi: 10.1128/JVI.01738-09

Sanjana NE, Shalem O, Zhang F (2014) Improved vectors and genome-wide libraries for CRISPR screening. Nat Methods 11:783–784. doi: 10.1038/nmeth.3047

Sanson KR, Hanna RE, Hegde M, et al (2018) Optimized libraries for CRISPR-Cas9 genetic screens with multiple modalities. Nat Commun 9:5416–15. doi: 10.1038/s41467-018-07901-8

Sato M, Hata N, Asagiri M, et al (1998) Positive feedback regulation of type I IFN genes by the IFN-inducible transcription factor IRF-7. FEBS Lett 441:106–110. doi: 10.1016/s0014-5793(98)01514-2

Savidis G, McDougall WM, Meraner P, et al (2016a) Identification of Zika Virus and Dengue Virus Dependency Factors using Functional Genomics. Cell Rep 16:232–246. doi: 10.1016/j.celrep.2016.06.028

Savidis G, Perreira JM, Portmann JM, et al (2016b) The IFITMs Inhibit Zika Virus Replication. Cell Rep 15:2323–2330. doi: 10.1016/j.celrep.2016.05.074

Scaturro P, Cortese M, Chatel-Chaix L, et al (2015) Dengue Virus Non-structural Protein 1 Modulates Infectious Particle Production via Interaction with the Structural Proteins. PLoS Pathog 11:e1005277. doi: 10.1371/journal.ppat.1005277

Schaller T, Appel N, Koutsoudakis G, et al (2007) Analysis of hepatitis C virus superinfection exclusion by using novel fluorochrome gene-tagged viral genomes. J Virol 81:4591–4603. doi: 10.1128/JVI.02144-06

Scherer WF, Syverton JT, Gey GO (1953) Studies on the propagation in vitro of poliomyelitis viruses. IV. Viral multiplication in a stable strain of human malignant epithelial cells (strain HeLa) derived from an epidermoid carcinoma of the cervix. J Exp Med 97:695–710. doi: 10.1084/jem.97.5.695

Schilling M, Bridgeman A, Gray N, et al (2020) RIG-I Plays a Dominant Role in the Induction of Transcriptional Changes in Zika Virus-Infected Cells, which Protect from Virus-Induced Cell Death. Cells 9:1476. doi: 10.3390/cells9061476

Schoggins JW (2019) Interferon-Stimulated Genes: What Do They All Do? Annu Rev Virol 6:567–584. doi: 10.1146/annurev-virology-092818-015756

Schoggins JW, Dorner M, Feulner M, et al (2012) Dengue reporter viruses reveal viral dynamics in interferon receptor-deficient mice and sensitivity to interferon effectors in vitro. Proc Natl Acad Sci USA 109:14610–14615. doi: 10.1073/pnas.1212379109

Schoggins JW, Wilson SJ, Panis M, et al (2011) A diverse range of gene products are effectors of the type I interferon antiviral response. Nature 472:481–485. doi: 10.1038/nature09907

Schöbel A, Rösch K, Herker E (2018) Functional innate immunity restricts Hepatitis C Virus infection in induced pluripotent stem cell-derived hepatocytes. Scientific Reports 8:3893–12. doi: 10.1038/s41598-018-22243-7

Scutigliani EM, Kikkert M (2017) Interaction of the innate immune system with positive-strand RNA virus replication organelles. Cytokine Growth Factor Rev 37:17–27. doi: 10.1016/j.cytogfr.2017.05.007

Seo J-Y, Yaneva R, Hinson ER, Cresswell P (2011) Human cytomegalovirus directly induces the antiviral protein viperin to enhance infectivity. Science 332:1093–1097. doi: 10.1126/science.1202007

Shalem O, Sanjana NE, Hartenian E, et al (2014) Genome-scale CRISPR-Cas9 knockout screening in human cells. Science 343:84–87. doi: 10.1126/science.1247005

Shang Z, Song H, Shi Y, et al (2018) Crystal Structure of the Capsid Protein from Zika Virus. J Mol Biol 430:948–962. doi: 10.1016/j.jmb.2018.02.006

Shao Q, Herrlinger S, Zhu Y-N, et al (2017) The African Zika virus MR-766 is more virulent and causes more severe brain damage than current Asian lineage and dengue virus. Development 144:4114–4124. doi: 10.1242/dev.156752

Shaw AE, Hughes J, Gu Q, et al (2017) Fundamental properties of the mammalian innate immune system revealed by multispecies comparison of type I interferon responses. PLoS Biol 15:e2004086. doi: 10.1371/journal.pbio.2004086

Shi ST, Polyak SJ, Tu H, et al (2002) Hepatitis C virus NS5A colocalizes with the core protein on lipid droplets and interacts with apolipoproteins. Virology 292:198–210. doi: 10.1006/viro.2001.1225

Shimakami T, Hijikata M, Luo H, et al (2004) Effect of interaction between hepatitis C virus NS5A and NS5B on hepatitis C virus RNA replication with the hepatitis C virus replicon. J Virol 78:2738–2748. doi: 10.1128/jvi.78.6.2738-2748.2004

Shiryaev SA, Chernov AV, Aleshin AE, et al (2009) NS4A regulates the ATPase activity of the NS3 helicase: a novel cofactor role of the non-structural protein NS4A from West Nile virus. J Gen Virol 90:2081–2085. doi: 10.1099/vir.0.012864-0

Singh PK, Singh S, Farr D, Kumar A (2019) Interferon-stimulated gene 15 (ISG15) restricts Zika virus replication in primary human corneal epithelial cells. Ocul Surf 17:551–559. doi: 10.1016/j.jtos.2019.03.006

Smith I, Greenside PG, Natoli T, et al (2017) Evaluation of RNAi and CRISPR technologies by large-scale gene expression profiling in the Connectivity Map. PLoS Biol 15:e2003213. doi: 10.1371/journal.pbio.2003213

Somnuke P, Hauhart RE, Atkinson JP, et al (2011) N-linked glycosylation of dengue virus NS1 protein modulates secretion, cell-surface expression, hexamer stability, and interactions with human complement. Virology 413:253–264. doi: 10.1016/j.virol.2011.02.022

Steinmann E, Penin F, Kallis S, et al (2007) Hepatitis C virus p7 protein is crucial for assembly and release of infectious virions. PLoS Pathog 3:e103. doi: 10.1371/journal.ppat.0030103

Stocks CE, Lobigs M (1998) Signal peptidase cleavage at the flavivirus C-prM junction: dependence on the viral NS2B-3 protease for efficient processing requires determinants in C, the signal peptide, and prM. J Virol 72:2141–2149.

Subramani C, Nair VP, Anang S, et al (2018) Host-Virus Protein Interaction Network Reveals the Involvement of Multiple Host Processes in the Life Cycle of Hepatitis E Virus. mSystems 3:860. doi: 10.1128/mSystems.00135-17

Sumiyoshi H, Hoke CH, Trent DW (1992) Infectious Japanese encephalitis virus RNA can be synthesized from in vitro-ligated cDNA templates. J Virol 66:5425–5431.

Sumpter R, Loo Y-M, Foy E, et al (2005) Regulating intracellular antiviral defense and permissiveness to hepatitis C virus RNA replication through a cellular RNA helicase, RIG-I. J Virol 79:2689–2699. doi: 10.1128/JVI.79.5.2689-2699.2005

Sun L, Wu J, Du F, et al (2013) Cyclic GMP-AMP synthase is a cytosolic DNA sensor that activates the type I interferon pathway. Science 339:786–791. doi: 10.1126/science.1232458

Sun M, Kraus WL (2015) From discovery to function: the expanding roles of long noncoding RNAs in physiology and disease. Endocr Rev 36:25–64. doi: 10.1210/er.2014-1034

Sun W, He B, Yang B, et al (2018) Genome-wide CRISPR screen reveals SGOL1 as a druggable target of sorafenib-treated hepatocellular carcinoma. Lab Invest 98:734–744. doi: 10.1038/s41374-018-0027-6

Supekova L, Supek F, Lee J, et al (2008) Identification of human kinases involved in hepatitis C virus replication by small interference RNA library screening. J Biol Chem 283:29–36. doi: 10.1074/jbc.M703988200

Suzuki T, Okamoto T, Katoh H, et al (2018) Infection with flaviviruses requires BCLXL for cell survival. PLoS Pathog 14:e1007299. doi: 10.1371/journal.ppat.1007299

Tai AW, Benita Y, Peng LF, et al (2009) A functional genomic screen identifies cellular cofactors of hepatitis C virus replication. Cell Host Microbe 5:298–307. doi: 10.1016/j.chom.2009.02.001

Tai AW, Salloum S (2011) The role of the phosphatidylinositol 4-kinase PI4KA in hepatitis C virus-induced host membrane rearrangement. PLoS ONE 6:e26300. doi: 10.1371/journal.pone.0026300

Takagi H, Arimura K, Uto T, et al (2016) Plasmacytoid dendritic cells orchestrate TLR7-mediated innate and adaptive immunity for the initiation of autoimmune inflammation. Scientific Reports 6:24477–18. doi: 10.1038/srep24477

Tan S-L, Ranjith-Kumar CT, Kao CC (2006) Biochemical Activities of the HCV NS5B RNA-Dependent RNA Polymerase.

Tassaneetrithep B, Burgess TH, Granelli-Piperno A, et al (2003) DC-SIGN (CD209) mediates dengue virus infection of human dendritic cells. J Exp Med 197:823–829. doi: 10.1084/jem.20021840

Tay MYF, Saw WG, Zhao Y, et al (2015) The C-terminal 50 amino acid residues of dengue NS3 protein are important for NS3-NS5 interaction and viral replication. J Biol Chem 290:2379–2394. doi: 10.1074/jbc.M114.607341

Theiler M, Smith HH (1937) THE USE OF YELLOW FEVER VIRUS MODIFIED BY IN VITRO CULTIVATION FOR HUMAN IMMUNIZATION. J Exp Med 65:787–800. doi: 10.1084/jem.65.6.787

Thompson JM, Iwasaki A (2008) Toll-like receptors regulation of viral infection and disease. Adv Drug Deliv Rev 60:786–794.

Tomicic MT, Thust R, Kaina B (2002) Ganciclovir-induced apoptosis in HSV-1 thymidine kinase expressing cells: critical role of DNA breaks, Bcl-2 decline and caspase-9 activation. Oncogene 21:2141–2153. doi: 10.1038/sj.onc.1205280

Trotard M, Lepère-Douard C, Régeard M, et al (2009) Kinases required in hepatitis C virus entry and replication highlighted by small interference RNA screening. FASEB J 23:3780–3789. doi: 10.1096/fj.09-131920

Tsai Y-T, Chang S-Y, Lee C-N, Kao C-L (2009) Human TLR3 recognizes dengue virus and modulates viral replication in vitro. Cell Microbiol 11:604–615. doi: 10.1111/j.1462-5822.2008.01277.x

Tsutsumi T, Suzuki T, Shimoike T, et al (2002) Interaction of hepatitis C virus core protein with retinoid X receptor alpha modulates its transcriptional activity. Hepatology 35:937–946. doi: 10.1053/jhep.2002.32470

Tu H, Gao L, Shi ST, et al (1999) Hepatitis C virus RNA polymerase and NS5A complex with a SNARE-like protein. Virology 263:30–41. doi: 10.1006/viro.1999.9893

Uchil PD, Satchidanandam V (2003) Architecture of the flaviviral replication complex. Protease, nuclease, and detergents reveal encasement within double-layered membrane compartments. J Biol Chem 278:24388–24398. doi: 10.1074/jbc.M301717200

Upadhyay AS, Vonderstein K, Pichlmair A, et al (2014) Viperin is an iron-sulfur protein that inhibits genome synthesis of tick-borne encephalitis virus via radical SAM domain activity. Cell Microbiol 16:834–848. doi: 10.1111/cmi.12241

Usacheva A, Smith R, Minshall R, et al (2001) The WD motif-containing protein receptor for activated protein kinase C (RACK1) is required for recruitment and activation of signal transducer and activator of transcription 1 through the type I interferon receptor. J Biol Chem 276:22948–22953. doi: 10.1074/jbc.M100087200

Vaillancourt FH, Pilote L, Cartier M, et al (2009) Identification of a lipid kinase as a host factor involved in hepatitis C virus RNA replication. Virology 387:5–10. doi: 10.1016/j.virol.2009.02.039

van der Schaar HM, Rust MJ, Chen C, et al (2008) Dissecting the cell entry pathway of dengue virus by single-particle tracking in living cells. PLoS Pathog 4:e1000244. doi: 10.1371/journal.ppat.1000244

van Diemen FR, Kruse EM, Hooykaas MJG, et al (2016) CRISPR/Cas9-Mediated Genome Editing of Herpesviruses Limits Productive and Latent Infections. PLoS Pathog 12:e1005701. doi: 10.1371/journal.ppat.1005701

Vanwalscappel B, Gadea G, Desprès P (2019) A Viperin Mutant Bearing the K358R Substitution Lost its Anti-ZIKA Virus Activity. Int J Mol Sci 20:1574. doi: 10.3390/ijms20071574

Virreira Winter S, Zychlinsky A, Bardoel BW (2016) Genome-wide CRISPR screen reveals novel host factors required for Staphylococcus aureus α-hemolysin-mediated toxicity. Scientific Reports 6:24242–9. doi: 10.1038/srep24242

Vonderstein K, Nilsson E, Hubel P, et al (2018) Viperin Targets Flavivirus Virulence by Inducing Assembly of Noninfectious Capsid Particles. J Virol 92:498. doi: 10.1128/JVI.01751-17

Wakita T (2009) Isolation of JFH-1 strain and development of an HCV infection system. Methods Mol Biol 510:305–327. doi: 10.1007/978-1-59745-394-3_23

Wakita T, Pietschmann T, Kato T, et al (2005) Production of infectious hepatitis C virus in tissue culture from a cloned viral genome. Nat Med 11:791–796. doi: 10.1038/nm1268

Wang B, Thurmond S, Zhou K, et al (2020) Structural basis for STAT2 suppression by flavivirus NS5. Nat Struct Mol Biol 27:875–885. doi: 10.1038/s41594-020-0472-y

Wang H, Perry JW, Lauring AS, et al (2014) Oxysterol-binding protein is a phosphatidylinositol 4-kinase effector required for HCV replication membrane integrity and cholesterol trafficking. Gastroenterology 146:1373–85.e1–11. doi: 10.1053/j.gastro.2014.02.002

Wang T, Birsoy K, Hughes NW, et al (2015) Identification and characterization of essential genes in the human genome. Science 350:1096–1101. doi: 10.1126/science.aac7041

Wang W, Xu L, Su J, et al (2017) Transcriptional Regulation of Antiviral Interferon-Stimulated Genes. Trends Microbiol 25:573–584. doi: 10.1016/j.tim.2017.01.001

Watterson D, Kobe B, Young PR (2012) Residues in domain III of the dengue virus envelope glycoprotein involved in cell-surface glycosaminoglycan binding. J Gen Virol 93:72–82. doi: 10.1099/vir.0.037317-0

Watterson D, Modhiran N, Young PR (2016) The many faces of the flavivirus NS1 protein offer a multitude of options for inhibitor design. Antiviral Res 130:7–18. doi: 10.1016/j.antiviral.2016.02.014

Welbourn S, Green R, Gamache I, et al (2005) Hepatitis C virus NS2/3 processing is required for NS3 stability and viral RNA replication. J Biol Chem 280:29604–29611. doi: 10.1074/jbc.M505019200

Welsch S, Miller S, Romero-Brey I, et al (2009) Composition and three-dimensional architecture of the dengue virus replication and assembly sites. Cell Host Microbe 5:365–375. doi: 10.1016/j.chom.2009.03.007

Wengler G (1989) Cell-associated West Nile flavivirus is covered with E+pre-M protein heterodimers which are destroyed and reorganized by proteolytic cleavage during virus release. J Virol 63:2521–2526.

Werren JH, Baldo L, Clark ME (2008) Wolbachia: master manipulators of invertebrate biology. Nat Rev Microbiol 6:741–751. doi: 10.1038/nrmicro1969

Wheeler LJ, Watson ZL, Qamar L, et al (2019) Multi-Omic Approaches Identify Metabolic and Autophagy Regulators Important in Ovarian Cancer Dissemination. iScience 19:474–491. doi: 10.1016/j.isci.2019.07.049

WHO World Health Organisation - ZIKV Epidemiology Update 2019. In: WHO. https://www.who.int/emergencies/diseases/zika/zika-epidemiology-update-july-2019.pdf?ua=1. Accessed 10 Feb 2020

Williams CL (2016) Ralf Bartenschlager, Charles Rice, and Michael Sofia are honored with the 2016 Lasker~DeBakey Clinical Medical Research Award. J Clin Invest 126:3639–3644.

Winkler G, Maxwell SE, Ruemmler C, Stollar V (1989) Newly synthesized dengue-2 virus nonstructural protein NS1 is a soluble protein but becomes partially hydrophobic and membrane-associated after dimerization. Virology 171:302–305. doi: 10.1016/0042-6822(89)90544-8

Winter J, Breinig M, Heigwer F, et al (2016) caRpools: an R package for exploratory data analysis and documentation of pooled CRISPR/Cas9 screens. Bioinformatics 32:632–634. doi: 10.1093/bioinformatics/btv617

Wolff G, Melia CE, Snijder EJ, Bárcena M (2020) Double-Membrane Vesicles as Platforms for Viral Replication. Trends Microbiol 28:1022–1033. doi: 10.1016/j.tim.2020.05.009

Wong G, Qiu X-G (2018) Type I interferon receptor knockout mice as models for infection of highly pathogenic viruses with outbreak potential. Zool Res 39:3–14. doi: 10.24272/j.issn.2095-8137.2017.052

Wu Q, Wu W, Fu B, et al (2019a) JNK signaling in cancer cell survival. Med Res Rev 39:2082–2104. doi: 10.1002/med.21574

Wu Y, Liu Q, Zhou J, et al (2017) Zika virus evades interferon-mediated antiviral response through the co-operation of multiple nonstructural proteins in vitro. Cell Discov 3:17006. doi: 10.1038/celldisc.2017.6

Wu Z, Zhang W, Wu Y, et al (2019b) Binding of the Duck Tembusu Virus Protease to STING Is Mediated by NS2B and Is Crucial for STING Cleavage and for Impaired Induction of IFN-β. J Immunol 203:3374–3385. doi: 10.4049/jimmunol.1900956

Xia H, Luo H, Shan C, et al (2018) An evolutionary NS1 mutation enhances Zika virus evasion of host interferon induction. Nat Commun 9:414–13. doi: 10.1038/s41467-017-02816-2

Xie T, Chen T, Li C, et al (2019a) RACK1 attenuates RLR antiviral signaling by targeting VISA-TRAF complexes. Biochem Biophys Res Commun 508:667–674. doi: 10.1016/j.bbrc.2018.11.203

Xie X, Gayen S, Kang C, et al (2013) Membrane topology and function of dengue virus NS2A protein. J Virol 87:4609–4622. doi: 10.1128/JVI.02424-12

Xie X, Zou J, Puttikhunt C, et al (2015) Two distinct sets of NS2A molecules are responsible for dengue virus RNA synthesis and virion assembly. J Virol 89:1298–1313. doi: 10.1128/JVI.02882-14

Xie X, Zou J, Zhang X, et al (2019b) Dengue NS2A Protein Orchestrates Virus Assembly. Cell Host Microbe 26:606–622.e8. doi: 10.1016/j.chom.2019.09.015

Xing H, Xu S, Jia F, et al (2020) Zika NS2B is a crucial factor recruiting NS3 to the ER and activating its protease activity. Virus Res 275:197793. doi: 10.1016/j.virusres.2019.197793

Yamamoto M, Sato S, Hemmi H, et al (2003) Role of adaptor TRIF in the MyD88-independent toll-like receptor signaling pathway. Science 301:640–643. doi: 10.1126/science.1087262

Yang L, Yang JL, Byrne S, et al (2014) CRISPR/Cas9-Directed Genome Editing of Cultured Cells. Curr Protoc Mol Biol 107:31.1.1–17. doi: 10.1002/0471142727.mb3101s107

Yao N, Reichert P, Taremi SS, et al (1999) Molecular views of viral polyprotein processing revealed by the crystal structure of the hepatitis C virus bifunctional protease-helicase. Structure 7:1353–1363. doi: 10.1016/s0969-2126(00)80025-8

Yin X, Zhong X, Pan S (2016) VERTICAL TRANSMISSION OF DENGUE INFECTION: THE FIRST PUTATIVE CASE REPORTED IN CHINA. Rev Inst Med Trop Sao Paulo 58:90. doi: 10.1590/S1678-9946201658090

Yoneyama M, Kikuchi M, Matsumoto K, et al (2005) Shared and unique functions of the DExD/H-box helicases RIG-I, MDA5, and LGP2 in antiviral innate immunity. J Immunol 175:2851–2858. doi: 10.4049/jimmunol.175.5.2851

Yu C-Y, Liang J-J, Li J-K, et al (2015) Dengue Virus Impairs Mitochondrial Fusion by Cleaving Mitofusins. PLoS Pathog 11:e1005350. doi: 10.1371/journal.ppat.1005350

Yuan M, Zhang W, Wang J, et al (2015) Efficiently editing the vaccinia virus genome by using the CRISPR-Cas9 system. J Virol 89:5176–5179. doi: 10.1128/JVI.00339-15

Zevini A, Olagnier D, Hiscott J (2017) Crosstalk between Cytoplasmic RIG-I and STING Sensing Pathways. Trends Immunol 38:194–205. doi: 10.1016/j.it.2016.12.004

Zhang R, Miner JJ, Gorman MJ, et al (2016) A CRISPR screen defines a signal peptide processing pathway required by flaviviruses. Nature 535:164–168. doi: 10.1038/nature18625

Zhang Y, Corver J, Chipman PR, et al (2003) Structures of immature flavivirus particles. EMBO J 22:2604–2613. doi: 10.1093/emboj/cdg270

Zhang Y, Zhang W, Ogata S, et al (2004) Conformational changes of the flavivirus E glycoprotein. Structure 12:1607–1618. doi: 10.1016/j.str.2004.06.019

Zhao X, Li J, Winkler CA, et al (2018) IFITM Genes, Variants, and Their Roles in the Control and Pathogenesis of Viral Infections. Front Microbiol 9:3228. doi: 10.3389/fmicb.2018.03228

Zheng Y, Liu Q, Wu Y, et al (2018) Zika virus elicits inflammation to evade antiviral response by cleaving cGAS via NS1-caspase-1 axis. EMBO J 37:747. doi: 10.15252/embj.201899347

Zhou Y, Ray D, Zhao Y, et al (2007) Structure and function of flavivirus NS5 methyltransferase. J Virol 81:3891–3903. doi: 10.1128/JVI.02704-06

Zhou Z, Wang N, Woodson SE, et al (2011) Antiviral activities of ISG20 in positive-strand RNA virus infections. Virology 409:175–188. doi: 10.1016/j.virol.2010.10.008

Zona L, Tawar RG, Zeisel MB, et al (2014) CD81-receptor associations--impact for hepatitis C virus entry and antiviral therapies. Viruses 6:875–892. doi: 10.3390/v6020875